Apoptosis, redox stress and cancer

by

Thunicia Moodley

B.Sc. (Natal), B.Sc.Hons (*cum laude*) (Natal)

Submitted in fulfilment of the academic requirements for the degree

Master of Science

in the

School of Molecular and Cellular Biosciences

University of Natal

Pietermaritzburg

2000

PREFACE

The experimental work described in this thesis was carried out in the Department of Biochemistry, University of Natal, Pietermaritzburg from March 1999 to June 2000, under the supervision of Dr Edith Elliott.

These studies represent original work by the author and have not been submitted in any other form to another university. Where use was made of the work of others, it has been duly acknowledged in the text.

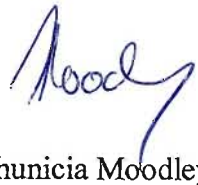

Thunicia Moodley
December 2000

ABSTRACT

Apoptosis is a regulated "programme" by which cells are induced to die in a manner which does not result in pathological inflammatory reactions, and involves dismantling of the cell into membrane-bound fragments that are removed by phagocytosis. This process is induced in order to remodel tissues and maintain homeostasis in cell numbers. Apoptosis may be induced via many pathways, many of which are redox-regulated, and is dysregulated in cancer cells, mainly due to mutational inactivation of certain pathways. Cancer cells also have a non-linear response to redox imbalance, a potentially exploitable characteristic for the therapeutic selective induction of apoptosis in cancer cells in mixed cell populations.

Model cell culture systems are required for the selective toxicity testing of anti-cancer drugs, many of which work by inducing redox stress. In the current study, hydrogen peroxide was selected as the redox stress-inducing agent, and the test cells were an immortal, non-invasive breast epithelial cell line (MCF10A) and its *ras*-transfected, pre-malignant derivative (MCF10AneoT). A reliable, sensitive, cost-effective and least time-consuming system for detection of apoptosis in such a system was sort and two novel methods, cytochrome c release and caspase-3 activity assays, were finally selected and compared with results seen by conventional DNA laddering and morphological examination at the light and electron microscopic level. No single procedure was found to be reliable individually. For the model system used, a combination of electron microscopy and DNA laddering was sufficient for simply detecting apoptotic cell death and necrosis. The caspase activity assay distinguished between apoptosis and necrosis, and cytochrome c release proved the most sensitive indicator of cell response. However, since cytochrome c release may be reversible and may not necessarily proceed to the downstream events of apoptosis in the time frame used in the current assays, it is not certain that cytochrome c release ultimately leads to apoptosis. However, three forms of cytochrome c were observed on western blots, the nature and significance of which remains to be determined. A comparison of the results of different methods allowed a model for the sequence of specific apoptotic events to be proposed.

ACKNOWLEDGEMENTS

My gratitude goes to the following people for their contribution towards my thesis:

My mother and grandparents, who constantly encouraged me and provided the means to pursue my studies.

My supervisor, Dr Edith Elliott, for allowing me to pursue this route of study even though it was not her field of expertise, and for thorough reading of this manuscript.

Dr Theresa Coetzer, for organising chickens for immunisation, and initial help with injections.

The staff of the Centre for Electron Microscopy, UNP. To Vijay Bandu, Priscilla Donnelly, Helen Roberts, Belinda White and Tony Bruton, for their help with all the technical matters of microscopes, photographs, and computers.

Ms Lesley Brown and Ms Jenny Schwartz, for prompt ordering of chemicals, and administrative matters, respectively, Ms Mel Webber for technical matters, and Agnes Zondi and Richard Shabalala, for a clean working environment.

The University of Natal and the former Foundation for Research Development (FRD), for bursaries and scholarships for my post-graduate studies.

To "Lab 44" - Brendon, Ché and Lizette for providing a great working atmosphere and for enormous support and encouragement in times of great distress. Especially to Brendon for constant help and inspiration.

Fellow post-graduates, Jonathan, Eric, Natasha, Elise, Brendan, Janine, Megan and AJ for making the department a fun place.

Chantal, Preshnee, Thirusha and Meshentha, my closest friends throughout my university years.

Divagaran, for all times.

LIST OF TABLES

LIST OF FIGURES

LIST OF ABBREVIATIONS AND SYMBOLS

A_{280}	absorbance at 280 nm
A_{595}	absorbance at 595 nm
ABTS	2,2'-azino-di-(3-ethyl)-benzthiozoline sulfonic acid
AE1	monoclonal antibodies to acidic human epithelial keratins
AE3	monoclonal antibodies to basic human epithelial keratins
AFC	7-amino-4-trifluoromethyl coumarin
AIDS	acquired immuno-deficiency syndrome
AIF	apoptosis–inducing factor
~	approximately
AMC	7-amido-4-methylcoumarin
ANT	adenine nucleotide translocase
Apaf-1	apoptosis protease activating factor-1
APC	antigen presenting cell
ATP	adenosine 5'-triphosphate
BCIP	5-bromo-4-chloro-3-indolyl phosphate
Bcl-2	B-cell lymphoma/leukemia-2
BH	Bcl-2 homology domain
bp	base pairs
BSA	bovine serum albumin
CAD	caspase-activated DNase
CAPE	caffeic phenethyl ester
CARD	caspase recruitment domain
Caspases	cysteine aspartate-specific proteases
Cdks	cycling dependent kinases
CD95	cluster determinant 95
CFA	complete Freund's adjuvant
CHAPS	3-[(3-Cholamidopropyl)-dimethylammonio]-1-propane sulfonate
CIFA	cytochrome c inactivating factor of apoptosis
CO_2	carbon dioxide
COOH	carboxyl terminus
CoQ	coenzyme Q
CTL	cytotoxic T lymphocytes
CyP-D	cyclophilin-D
cyt c	cytochrome c
Da	daltons
dATP	di-adenosine-5'-triphosphosphate
DED	death effector domain
DEF	death effector filament
DEVD-AFC	Asp-Glu-Val-Asp-7-amino-4-trifluoromethyl coumarin
DEVD-AMC	Asp-Glu-Val-Asp-7-amido-4-methylcoumarin
DFF	DNA fragmentation factor
ϕ	diameter
DIG	digoxygenin
dist.H_2O	distilled water
DMEM	Dulbecco's modified Eagle's medium
DMF	dimethylformamide

DMSO	dimethyl sulfoxide
DNA	deoxyribonucleic acid
DNAse	deoxyribonuclease
DTT	dithiothreitol
dUTP	deoxyuridine triphosphate
ECM	extracellular matrix
EDTA	ethylene diamine tetraacetic acid
ECL	enhanced chemiluminescence
EGF	epidermal growth factor
EGTA	ethylene glycol-bis(β-aminoethyl ether) N,N,N',N'-tetraacetic acid
ELISA	enzyme-linked immunosorbent assay
EMA	epithelial membrane antigen
FA	focal ahesion
FAD(H_2)	flavin adenine dinucleotide
FADD	Fas-associated death domain
FAK	focal adhesion kinase
g	relative centrifugal force
GDP	guanosine 5'-diphosphate
GSH	reduced glutathione
GSSG	oxidised glutathione
GTP	guanosine 5'-triphosphate
GTPase	guanosine 5'-triphosphate hydrolase
h	hours
HBSS	Hanks balanced salt solution
HEPES	*N*-2-hydroxy-piperazine-*N*'-2 ethane sulfonic acid
HP-1	histone protein 1
HSPs	heat shock proteins
HMEC	human mammary epithelial cells
HRPO	horseradish peroxidase
HMW	high molecular weight
H_2O_2	hydrogen peroxide
IAP	inhibitor of apoptosis
ICAD	inhibitor of caspase-activated DNase
IFA	incomplete Freund's adjuvant
IgY	immunoglobulin Y
ISNT	*in situ* nick translation
JNK	jun N-terminal kinase
KA-4	monoclonal antibody to human keratins 14, 15, 16, 19
kbp	kilo base pairs
kDa	kilodaltons
kV	kilovolts
l	litres
LBR	lamin B receptor
LMW	low molecular weight
mA	milliamperes
MAPK	mitogen-activated protein kinase
mbp	mega base pairs
MC-5	monoclonal antibody to epithelial sialomucins
MCF	Michigan Cancer Foundation

MFA breast	monoclonal antibody to epithelial sialomucins
MHC	major histocompatibility complex
min	minutes
ml	millilitres
ψ_m	mitochondrial membrane potential
MLCK	myosin light chain kinase
mM	millimolar
MNAse	Micrococcal nuclease
MQH_2O	ultrapure milliQ water
mRNA	messenger ribonucleic acid
MT	microtubule
M_r	molecular weight
mV	millivolts
MWM	molecular weight markers
NAD(H)	nicotinamide adenine dinucleotide
NADP(H)	nicotinamide adenine dinucleotide phosphate
NBT	nitroblue tetrazolium
NEM	N-ethylmaleimide
NF-κβ	nuclear factor κβ
NK	natural killer
nM	nanometres
NP40	nonylphenoxy polyethoxy ethanol
NuMa	nuclear matrix protein
N_2	nitrogen gas
O_2^-	superoxide anion
•OH	hydroxyl free radical
ORP 150	150 kDa oxygen-regulated protein
PARP	poly ADP ribose polymerase
PBS	phosphate buffered saline
PCD	programmed cell death
PEF	permeability enhancing factor
PEG	polyethylene glycol
PFA	paraformaldehyde
PFGE	pulse field gel electrophoresis
pH_i	intracellular pH
P_i	inorganic phosphate
pHo6	plasmid homer 6
PKC	protein kinase C
PI	propidium iodide
PMSF	phenylmethylsulfonyl fluoride
Ponceau S	3-hydroxy-4-[2-sulfo-4(sulfo-phenylazo)phenylazo]2,7-napthalene disulfonic acid
PS	phosphatidylserine
PT	permeability transition
$p21^{ras}$	21 kDa *ras*-encoded protein
RNA	ribonucleic acid
ROIs	reactive oxygen intermediates
ROS	reactive oxygen species
RT	room temperature
sarkosyl	N-Lauroylsarcosine

SAPK	stress-activated protein kinase
-S-As(OH)-S	arsenite-activated thiol
SDS	sodium dodecyl sulfate
SDS-PAGE	sodium dodecyl sulfate polyacrylamide gel electrophoresis
TAAs	tumour associated antigens
TAE	tris-acetate-EDTA
TATAs	tumour associated transplantation antigens
TBS	Tris buffered saline
TCA	tricarboxylic acid
TE	Tris-EDTA
TEMED	*N,N,N',N'*,-tetramethyl ethylene diamine
TEN	Tris-EDTA-NaCl
TGF	tumour growth factor
TN	Tris-NaCl
TNC	Tris-tergitol NP40-calcium chloride
TNF	tumour necrosis factor
TNFR	tumour necrosis factor receptor
Tricine	*N*-[2-hydroxy-1,1-bis(hydroxymethyl)ethyl]glycine
Tris	2-amino-2-(hydroxymethyl)-1,3-propandiol
Triton X-100	polyoxyethylene (9-10) *p-t*-octyl phenol
TSAs	tumour specific antigens
TUNEL	Tdt-mediated X-dUTP nick end labelling, X = biotin, fluorescein or digoxygenin
μm	micrometer (10^{-6} meter)
μM	micromolar
UV	ultraviolet
V	volts
VDAC	voltage-dependent anion channel
VEGF	vascular endothelial growth factor

TABLE OF CONTENTS

CHAPTER 1

INTRODUCTION

1.1 Apoptosis – an introduction

Apoptosis, or programmed cell death (PCD), is a highly conserved and regulated "programme" by which cells commit suicide under a variety of internal and external controls. It is the most common form of cell death, present physiologically from development through adult life, and in pathological conditions such as autoimmune and neurodegenerative diseases, AIDS and vascular diseases (Allen *et al.*, 1998). It occurs under a wide range of primarily physiological processes, including the removal of interdigital cells during embryonic digit formation, the elimination of massive numbers of neurons generated in early development to ensure refinement of connections at later stages, the deletion of autoreactive T and B cell clones during maturation, the formation of diverse immune cells from progenitor cells, the involution or self-renewal of epithelial tissues or glands, and in tumour regression. In these cases the purpose of apoptosis is to actively remove superfluous cells, cells with inappropriate specificity or developmental capacity, or cells that have already served their purpose. This removal of cells is triggered by hormones and growth factors in the cellular environment (Borner *et al.*, 1994).

Since homeostasis within developing and adult multicellular organisms is highly dependent on rates of cell proliferation relative to cell death, even slight alterations in the rate of cell death can result in dire clinical consequences, e.g., increased proliferation or increased removal of cells may lead to such conditions as neoplasia or degenerative conditions. The prevalence of apoptosis in human disease, and the question of whether apoptosis is central to disease etiology or pathogenesis, has led to extensive investigations of the molecular mechanisms by which it is induced and regulated. Understanding the molecular components and mechanisms of the death machinery may lead to the development of drugs which may alter the fate of a cell in many pathological conditions. Although many are optimistic about the potential of this unexplored therapeutic avenue, it has been difficult to assess the precise function of genes and signalling molecules in mammalian cells as the cascade of events leading ultimately to

cell death are complex (Allen *et al.*, 1998). Although the morphological hallmarks of apoptosis have been extensively documented, the molecular participants in the process have only recently begun to be unravelled (Evans *et al.*, 1997).

1.2 Differences between apoptosis and necrosis

Apoptosis is a morphologically and biochemically distinct form of cell death and can be distinguished by several criteria from cell death due to necrosis (Leist *et al.*, 1997). It is an active, energy-dependent process of cellular self-destruction (Lee *et al.*, 1997) characterised by controlled autodigestion of the cell. This involves cytoskeletal disruption, cell shrinkage (due to water loss), membrane blebbing, nuclear condensation, oligonucleosomal DNA fragmentation (DNA "ladder") and loss of mitochondrial function. Eventually, the whole cell fragments into membrane-bound cell fragments that are rapidly ingested by neighbouring cells or phagocytes (Fraser and Evan, 1996). Plasma membrane integrity around cell fragments is maintained, and surface opsonins are expressed to ensure phagocytic clearance of apoptotic bodies, to prevent an inflammatory response. In contrast, necrotic cell death, resulting from acute cellular injury, is typified by rapid cell swelling (due to influx of water) and lysis, random DNA degradation, and early loss of cell membrane integrity, resulting in leakage of cytoplasmic contents and the induction of an inflammatory response (Thompson, 1995) (Fig. 1.1). These two types of cell death can occur simultaneously in tissues or cell cultures exposed to the same stimulus, the intensity of the initial insult deciding the induction of apoptosis or necrosis. This suggests that, while some early events may be common to both types of cell death, a downstream controller may be required to direct cells toward the more organised apoptotic cell death (Leist *et al.*, 1997).

In drug therapy, the induction of non-inflammatory cell death is the desired outcome. Therefore, the induction of apoptosis rather than necrosis is required. Before the apoptotic process is described in detail, physiological factors that prevent cells from spontaneously undergoing apoptosis (i.e., a "default death pathway"), thus eliciting cell survival, will be discussed.

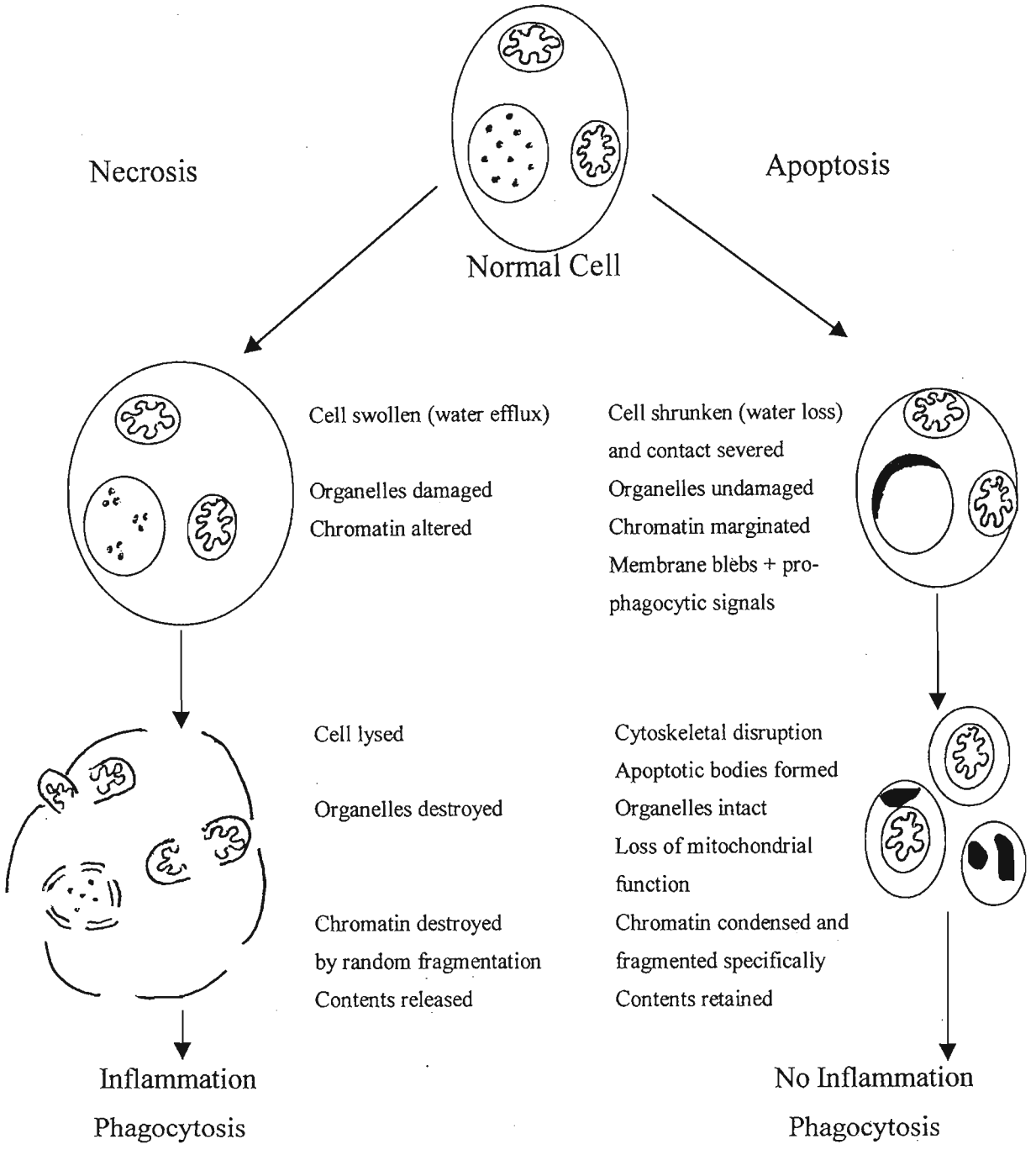

Figure 1.1 Distinction between necrosis and apoptosis.

Degeneration by necrosis is usually the result of cell damage. Apoptosis, on the other hand, is an active, energy-dependent process of self-destruction. The maintenance of plasma membrane integrity, and surface expression of opsonins, to ensure phagocytic clearance of apoptotic bodies, prevents an inflammatory response. Necrosis, however, results in leakage of cytoplasmic contents and induction of an inflammatory response. Adapted from Williams *et al.* (1992).

1.3 Cell survival

It has been proposed that cells require survival signals to avoid the engagement of apoptosis (Raff, 1992). Growth, as well as cellular life and death, are under the continuous influence of both intracellular and extracellular signals. The specific features of such signals would likely be determined by cell type, the presence of other cells, cell shape, tissue topology, and the types of adhesive interaction with surrounding extracellular matrix (ECM) molecules (Boudreau *et al.*, 1995; Ruoslahti and Reed, 1994). The type and consequences of cell adhesion may be more important than adhesion itself (Rak *et al.*, 1995). The "default" death pathway is suppressed by extracellular survival factors such as cytokines and hormones, direct cellular interactions with neighbours or ECM, and synaptic connections. For example, many cells require integrin-mediated adhesion, either to each other or to ECM proteins, for their survival. This important mechanism restricts the location and mobility of cells whose viability depends on direct physical contact with their source of survival signal (Meier and Evan, 1998). Integrins are receptor αβ heterodimers with overlapping specificity toward ECM components. Integrin-mediated cell-ECM interactions promote the assembly of cytoskeletal and signalling molecule complexes at sites called focal adhesions (Ilic *et al.*, 1998), which may involve the cooperation of integrins with soluble factors. The role of integrins and the cytoskeleton in signal transduction may be to provide a scaffold whereupon components of growth factor cassettes are assembled into discrete domains within the cell, so that they can propagate signals efficiently. A modular nature for membrane signalling complexes has been proposed, which may explain the recruitment of signalling proteins to cytoskeletal structures such as adhesion plaques (Farrelly *et al.*, 1999). When these adhesion plaques are disrupted, through cleavage by certain proteases, survival signals are not received by the cell, which subsequently dies by apoptosis (Frisch *et al.*, 1996).

1.4 The apoptotic process – initiation, effector and execution phases

The process of apoptosis is complex, but can be divided into three functionally distinct phases. These are the initiator, effector and execution phases (Fig. 1.2). During

the heterogenous initiator phase, cells receive the death-inducing stimulus. The inducers of apoptosis may either be extrinsic (such as anti-neoplastic therapies or oxidative stress) or intrinsic (i.e., naturally occurring such as naturally generated H_2O_2 and hormones or ligation of death ligands). The biochemical events participating in the initiation phase induce the activation of distinct pathways, as the pathway induced depends on the lethal stimulus, as well as on resident signal transduction machinery, and is cell-type specific (Mills *et al.*, 1998a). The effector/intermediate phase seems to be specific for various inducers, but may also converge on a common signalling molecule, ceramide, and generally results in caspase-8 and -9 activation (Mills *et al.*, 1998a). During this phase, the "central executioner of apoptosis" is still subject to regulatory mechanisms (Susin *et al.*, 1997). During the execution/final degradation phase, the morphology and characteristic biochemistry of an apoptotic cell (e.g., discrete DNA fragmentation and fragmentation of the cell into membrane-bound components) become manifest (Susin *et al.*, 1997). Execution occurs through the activation and action of caspases, a highly conserved family of cysteine proteases with specificity for aspartic acid-containing substrates. It is the cleavage of certain key substrates that orchestrates the death and packaging of the cell fragments, containing intact organelles, for clearance (Green, 1998). This phase appears to be similar in all cells regardless of inducer or cell-type specificities (Fig. 1.2), and once this phase has been initiated, cells are committed to die.

An alternate view is held by Mathias *et al.* (1998), who argue that the effector and final phases of apoptosis are characterised by a commitment phase, in which alteration of mitochondrial function and recruitment of a cascade of effector caspases occurs, and an effector phase, during which key cellular proteins are inactivated by cleavage, and organelles are degraded and packaged. Here, the cell loses viability (Mills *et al.*, 1998a). This, however, may be a view biased by specific inducers and cell types. As can be seen from the scheme illustrated in Fig. 1.2, not all pathways to apoptosis occur via the mitochondrion.

Apoptosis may not occur as it usually does if certain proteins in the effector phase, such as Ras, Bcl-2 and p53, are mutated or overexpressed, such as occurs frequently in various types of cancers. Such mutations and their consequences are discussed in Section 1.5.

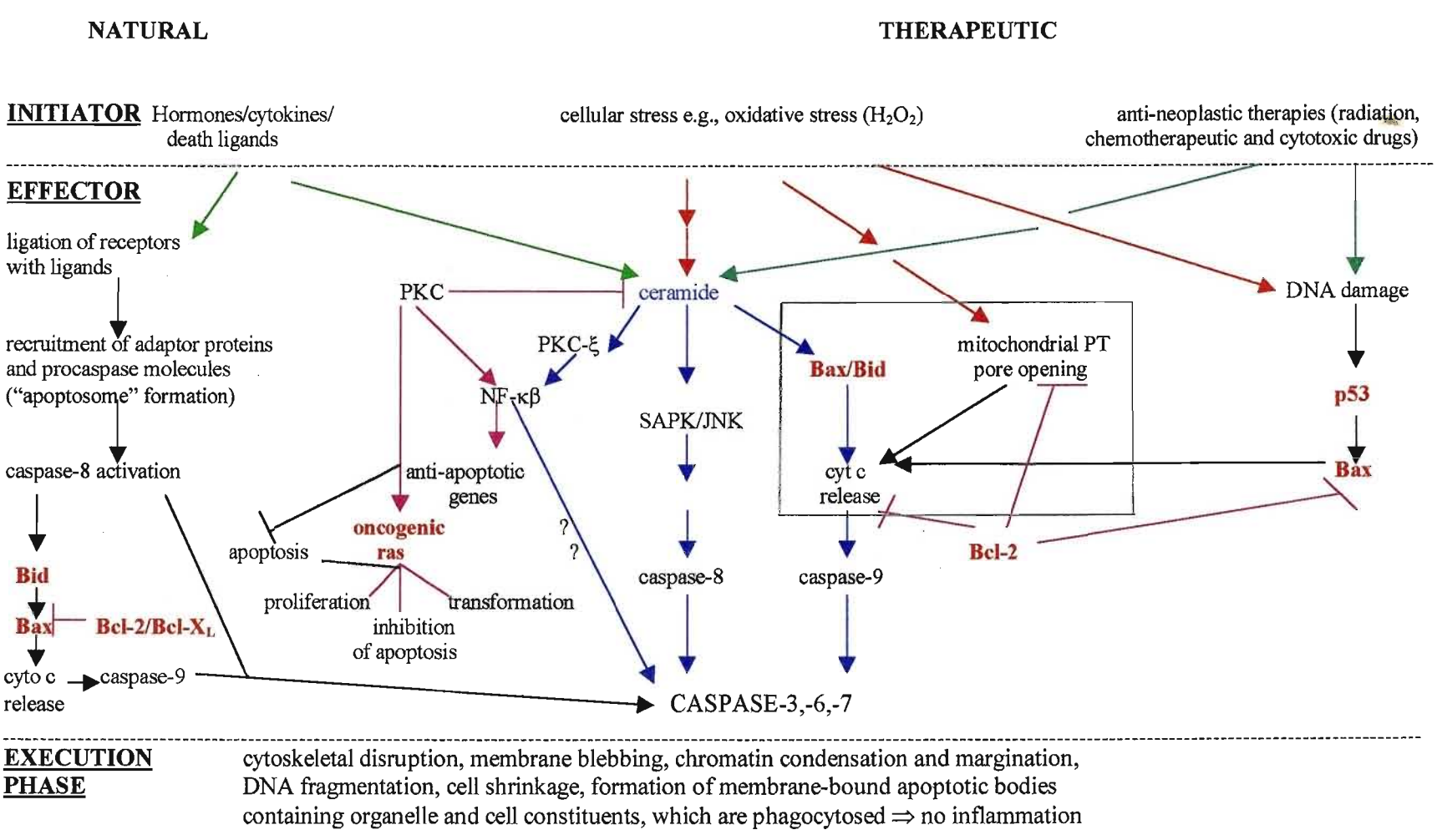

Figure 1.2 Various pathways of apoptosis – the phases and their areas of convergence.
Effector phase pathways of the apoptotic process may differ between various inducers and cell types, but they may also converge on a common path of ceramide signalling. The pathway may diverge after ceramide signalling, depending on other signals, upstream and downstream of ceramide, which may also be cell-type specific. See text for details of pathway.

Key: bright green, dark green and red arrows = diverging pathways of initiators; blue arrows = central common pathway of ceramide signalling; red text = important factors discussed in literature, grey box = mitochondrial pathway; pink lines = anti-apoptotic paths. **Abbr.**: PT, permeability transition; PKC, protein kinase C; SAPK, stress-activated protein kinase; JNK, Jun N-terminal kinase; cyt c, cytochrome c; NF-κβ, nuclear factor κβ.

1.4.1 The initiation phase

The initiation of apoptosis is carefully regulated. Many different signals originating either from within or outside the cell have been shown to influence the decision between life and death (Steller, 1995). Generally, the lethal stimulus and subsequent effector phase pathway induced may be grouped under the headings of therapeutic stimulae, such as oxidative stress, radiation or chemotherapeutic drugs, or natural stimulae, such as cytokines and cell-cell interactions which often involve hormones or specific death receptor ligation (TNF or Fas/APO1/CD95) (Steller, 1995). The latter are soluble factors secreted upon stimulation of cells by certain initiators and bind to their respective receptors on cell surfaces. Ligation of these receptors leads to signal transduction resulting in apoptosis.

The effector pathways induced by various stimuli occur either via the mitochondrion or central ceramide pathway. Cell-cell interactions via death receptor ligation may occur, in addition to the latter paths mentioned, by formation of protein complexes and direct caspase recruitment. However, most paths eventually lead to the activation of caspases (Fig. 1.2) (Coppola and Ghibelli, 2000; Green, 1998).

1.4.1.1 Apoptosis induced by cell-cell interactions and natural factors (intrinsic)

Included amongst the bewildering diversity of extracellular and intracellular factors that modulate apoptosis are cytokines, oncogenes, tumour suppressor genes and cell cycle components, as well as the presence of conflicting signals and unscheduled proliferation (Evan *et al.*, 1995). These diverse signals may act to either suppress or promote the activation of the death program, and the same signal may have the opposite effect on diverse cell types, the outcome depending on the relative amounts, activities, and stabilities of promoter or suppressor proteins (Steller, 1995). Physiologically, it is advantageous to have such differences to be able to induce cell-specific apoptosis, in order to selectively eliminate specific cells in a heterogeneous tissue (Wertz and Hanley, 1996) (e.g., selective elimination of tumour cells in a population of normal and tumour cells).

In the immune system cell elimination and lysis is mediated by dedicated, professional killer cells, i.e., cells which actively kill other cells. For example, cytotoxic T lymphocytes (CTLs) or natural killer (NK) cells induce apoptosis in their targets, such as virus-infected cell or tumour cells. In these cases, an effector molecule expressed at the surface of CTLs or NK cells, such as Fas which binds Fas-ligand on the target cell, or a soluble cytokine produced by the effector cells, is thought to be responsible for target cell death (Nagata and Golstein, 1995). The other pathways used by killer cells employs perforin and granzymes and causes "involuntary suicide" in target cells, as the presence of death receptors and their signalling machinery in the target cell are not required (Podak *et al.*, 1999).

1.4.1.2 Apoptosis induced by stress/infection/therapeutic damage (extrinsic)

Anti-neoplastic drugs (Stennicke and Salvesen, 1997), shortage of obligatory growth factors, oxygen or metabolic supply, or subnecrotic or chemical damage (Susin *et al.*, 1997) all induce apoptosis in cells. Anti-neoplastic drugs are often metabolised to produce H_2O_2, which is a source of oxidative stress to cells, via the process of redox cycling. The chemical accepts an electron, forming a free radical which reacts rapidly with oxygen to generate the superoxide anion radical ($O^{\bullet}_2^-$) and other active oxygen species. Superoxide dismutase catalyses the dismutation of $O^{\bullet}_2^-$ to H_2O_2, which reacts with metal ions, such as Fe^{2+} and Cu^{2+} (Fenton reaction) in the cell, or with $O^{\bullet}_2^-$ (Haber-Weiss reaction), to produce the highly reactive •OH which causes additional, and more severe, damage to cells (Cohen and d'Arcy Doherty, 1987).

1.4.1.3 The pre-effector phase

While much is understood about the machinery of the apoptotic pathway, comparatively less is known about the regulation of mechanisms by which the cell commits to PCD (Bates and Vousden, 1999). Acidification of the cytosol may serve as a global switch that facilitates the activity of enzymes that dismantle the cell during apoptosis. Cytoplasmic alkalinisation in cells retards the apoptotic response (Froelich *et al.*, 1996). Recent studies have provided increasing evidence implicating a role for

mitochondria in the effector phase of this process. By understanding the role that some major regulators of apoptosis play either at the commitment or execution phases of cell death in a given tissue and pathology, we will be in a better position to design and explore new therapeutic modalities (Schmitt *et al.*, 1997).

1.4.2 The effector phase

During the effector phase, i.e., post-damage and receptor-ligation, after survival signals have been overcome, various pathways of signal transduction are activated, depending on the stimulus and cell type. Despite these differences, an intensive review of the literature reveals a possible common pathway involving ceramide signalling, and most often, the mitochondria (Fig. 1.2) (Bissonette *et al.*, 1997; Chen and Faller, 1995; Chou *et al.*, 1999; Clark *et al.*, 1996; Coopersmith *et al.*, 1997; Froesch *et al.*, 1999; Gilmore *et al.*, 2000; Green, 1998; Li *et al.*, 1998; Luo *et al.*, 1998; Mathias *et al.*, 1998; Miyashita and Reed, 1995).

1.4.2.1 The ceramide pathway

The signal of cellular stress is transduced via a sphingolipid found in various cellular membranes, ceramide, which is the central molecule of the sphingomyelin pathway, and serves as a second messenger for cellular functions ranging from proliferation and differentiation to growth arrest and apoptosis. The pleiotropic nature of ceramide signalling may be due to the fact that, in different cell types, it is linked to a variety of receptors. Further, ceramide engages different downstream effectors, depending on the cellular microenvironment, the concomitant activation of other second messengers and the activity of enzymes that convert ceramide into other metabolites. The magnitude of ceramide generation, the site and source of its generation, the phase of the cell cycle, and the state of activation of transmodulating signals all appear to play a role in the final outcome (Mathias *et al.*, 1998).

The mechanisms by which ceramide mediates apoptosis have not yet been fully addressed, however, it is known that mitochondria are targets (Ghafourifar *et al.*, 1999) (Fig. 1.2). Resultant release of cytochrome c (a mitochondrial protein found in the

intermembrane space, and which participates in the respiratory chain) from mitochondria, leads to the activation of caspases. These are the cysteine proteases that are responsible for majority of the protein cleavage and, thus, for the morphology changes induced during apoptosis (Mathias *et al.*, 1998). In addition to the involvement of mitochodria in ceramide signalling, this sphingolipid may also transcriptionally activate the JNK (Jun N-terminal kinase) pathway, which also results in caspase activation (Fig. 1.2).

Protein kinase C (PKC) may influence ceramide-induced apoptosis by a mechanism involving Ras, depending on the state of the protein and factors found upstream or downstream. Ras proteins are GTPases and function as regulated molecular switches, which control signal transduction pathways that mediate cell growth and differentiation (Clark *et al.*, 1996). Ras, which depends on PKC and ceramide levels, sits at the apex of multiple effectors, each of which presides over its own suite of diverging and multifunctional signalling pathways (Fig. 1.2). In such a network of pleotropic effectors, no single cell fate is ever really controlled by any single effector. Rather, the predominant outcome of Ras signalling is a result of a network of interactions between differing signalling pathways, wherein some signals are reinforced while others are gated (Meier and Evan, 1998).

1.4.2.2 The alternate pathways

Aside from the common ceramide pathway, each inducer may follow separate effector pathways (Fig. 1.2), depending on the cell type being studied.

The effector phase, after ligation of death receptors, e.g. binding of Fas to Fas ligand, involves the formation of protein complexes and procaspase recruitment, resulting in caspase activation.

The signalling pathways of both oxidative stress (e.g., H_2O_2) and anti-neoplastic drugs (which are frequently metabolised to H_2O_2 and other reactive oxygen species), overlap not only in the ceramide pathway but also in their alternative paths. The latter is a path of DNA damage, and involves p53, a tumour suppressor which participates in genome surveillance and DNA repair. The specific roles played by p53 in this process includes the arrest of cycling cells before S-phase, to allow for repair of damaged DNA prior to DNA replication, and the induction of apoptosis for cases in which the DNA

damage is too severe to be properly repaired (Miyashita and Reed, 1995). In the case of apoptosis induction, mitochondria are induced to release cytochrome c, with consequent caspase activation (Fig. 1.2). Additionally, oxidative stress may affect mitochondria directly by opening of the permeability transition pore, resulting in cytochrome c release and subsequent apoptotic events (Fig. 1.2).

The *bcl-2* gene family is composed of proteins that play a pivotal role in apoptosis. Some proteins within this family such as Bcl-2 and Bcl-X_L inhibit apoptosis, while others including Bax, Bak, Bad and Bid promote apoptosis (Yang and Korsmeyer, 1996; Kroemer, 1997; Reed, 1997). Bcl-2 family members are involved in the effector phase pathways of all the inducers discussed (Fig. 1.2).

It has been proposed that Bcl-2 may inhibit cell death by interfering with the function of pro-apoptotic Bcl-2 homologues, by repressing the release of cytochrome c from mitochondria, by the sequestration of caspase activators, by interfering with the production of free radicals by cytotoxic agents, or by regulating intracellular calcium homeostasis, all of which take part in the apoptotic program (Froesch *et al.*, 1999). Bcl-2 is also a highly efficient inhibitor of mitochondrial alterations including large amplitude swelling, mitochondrial transmembrane potential (ψ_m) collapse and release of apoptosis-inducing factor (AIF), a mitochondrial protein which, upon stimulation, is released into the cytosol, where it activates caspase-3, facilitating entry into the execution phase (Susin *et al.*, 1997).

The participation of the tumour suppressors (p53 and Bax) and promoters (Ras and Bcl-2) in apoptosis is significant since the genes encoding these factors are frequently mutated in cancers. Thus, it is important to understand their function/relevance in cells, and these will be considered in the section on cancer (Section 1.5.2).

1.4.3 The execution/degradation phase

The execution/degradation phase, which is responsible for the protein cleavage resulting in the morphological characteristics of apoptosis, occurs after caspases have been activated, manifesting as membrane blebbing, chromatin condensation and margination, DNA laddering, and the presence of membrane-bound apoptotic bodies.

These features may occur almost universally amongst different cell types and in the presence of various inducers.

1.5 Cancer (carcinogenesis/tumourigenesis)

Apoptosis directly regulates tumourigenesis (Fisher, 1994). Carcinogenesis is associated with an imbalance between the regulation of cell proliferation and apoptotic cell death, which is an essential part of normal tissue development (Raff, 1992). Tumour growth depends on the ability of tumour cells to ignore the normal homeostatic mechanisms that regulate cell turnover within tissues (Ashwell *et al.*, 1994). Tumours require anti-apoptotic mutations in addition to inappropriate proliferation in order to survive and propagate (Evan *et al.*, 1995). Preneoplastic cells maintain the ability to undergo apoptosis as a mechanism of tumour growth suppression, but this critical control of apoptosis is lost as these lesions progress to carcinomas (Shibata *et al.*, 1996).

Elucidation of the nature of the molecular links between cell proliferation and apoptosis is of key importance in cancer biology and therapy (Evan *et al.*, 1995). Cycling cells often encounter a crossroads of apoptosis and mitosis where the decision for the subsequent fate is made. If anti-apoptotic survival factors act at this point, cells are rescued from apoptosis. Alternatively, survival factors may actively promote cell proliferation and, hence, diminish the chance of the cell undergoing apoptosis (Borner, 1996). Numerous common factors are involved in apoptosis and cell cycle regulation, suggesting that these could be related or even coupled (Simm *et al.*, 1997).

Because the selective induction of apoptosis in cancerous tissue is an important therapeutic aim, the elucidation of factors involved in the regulation of normal pathways leading to apoptosis, as well as the effect of mutations in such pathways and the altered physiology of neoplastic cells, are of importance for cancer treatment (Cejna *et al.*, 1994). The success of cancer therapy requires the destruction of each and every cancer cell within a tumour, without undue toxicity to surrounding normal cells. This daunting task may be facilitated by secondary *in vivo* effects, including immunological responses and the so-called "bystander effect" (the death of normal cells adjacent to transformed cells). However, true success is likely to come from an improved understanding of critical targets that distinguish cancer cells from surrounding normal cells, including both

molecular alterations within cancer cells themselves and essential supportive elements such as tumour vasculature (Haber, 1999).

1.5.1 Differences between normal cells and cancer cells

Cancer cells differ from normal cells in several aspects. These are listed in Table 1.

In cancer cells, a chronic imbalance of the redox status exists, eliciting excessive reactive oxygen intermediate (ROI) production and tumour promotion. Excessive ROIs cause maximal growth promotion when cells are protected from excessive ROI toxicity, as ROIs are inducers of gene expression. In addition, ROIs interfere with the complex signalling mechanisms regulating mitosis and differentiation, and a deregulation of these processes may also increase cell transformation (Morel and Barouki, 1999). Constitutive generation of H_2O_2 and other ROIs by tumour cells could potentially enhance neoplastic behaviour by augmenting both genetic instability of a tumour, and its capacity to injure and penetrate host tissues (Szatrowski and Nathan, 1991).

Cells found at the centre of solid tumours are subjected to hypoxic conditions, i.e., a lack of oxygen and nutrients (Young and Hill, 1990) due to limited and disordered vasculature (Schmaltz *et al.*, 1998). If hypoxia does not injure the tissue irreversibly, large scale DNA over-replication and gene amplification occurs when cells are deprived of oxygen (Rice *et al.*, 1986), allowing non-specific genome amplification, and promoting tumour progression (Sager *et al.*, 1985). Hypoxia also selects for cells with defects in apoptosis, i.e., hypoxia provides a physiological selective pressure in tumours for the expansion of variants that have lost their apoptotic potential, and in particular for cells acquiring *p53* mutations. Genetic alterations, such as loss of the *p53* tumour suppressor gene, over-expression of the apoptosis-inhibitor protein Bcl-2, or mutation of the *ras* oncogene, substantially reduce hypoxia-induced cell death (Graeber *et al.*, 1996).

To overcome cell death in tumours under prolonged hypoxic conditions, angiogenesis, the formation of new blood vessels from the existing vasculature, occurs after the expression of angiogenesis-inducing proteins such as VEGF (vascular endothelial growth factor) (Scott *et al.*, 1998) and ORP-150 (150 kDa oxygen-regulated

Table 1. Altered features reported for tumour cells[a]

1. Loss of normal growth control
2. Growth to high density *in vitro*, i.e., a relatively high nuclear overlap index (>0.5 versus <0.2 for normal versus transformed cells)
3. Reduced heterotypic contact inhibition *in vitro*
4. Decreased cell-surface fibronectin
5. Expression of TATAs, TAAs and TSAs, including oncofetal antigens and viral determinants
6. General alterations in cell surface components (proteins, glycoproteins, proteoglycans, sialic acid)
7. Altered glycosylation
8. Increased plasma membrane shedding
9. Increased sensitivity to lectin agglutination
10. Increased receptor mobility
11. Altered permeability and transport of nutrients
12. Decreased mitochondrial content
13. Unregulated autocrine secretion of growth factors
14. Decreased requirements for serum and exogenous growth factors
15. Altered cell junctions
16. Altered cell communication
17. Increased deformability
18. Changes in cell surface projections
19. Altered cell motility (including chemotactic behaviour)
20. Changes in enzyme content and secretion
21. Altered production and secretion of hormones, and changes in hormone dependency
22. Increased histological heterogeneity (e.g., cytoplasmic basophilia, nuclear pleomorphism)
23. Altered adhesiveness
24. Decreased anchorage dependence
25. Altered ploidy
26. Increased chromosomal aberrations, i.e., genetic instability
27. Changes in intracellular signalling activity
28. Presence of activated oncogene products
29. Excessive production of proto-oncogene products
30. Altered nuclear DNA organisation[b]
31. Altered cytoskeletal organisation and altered expression of cytoskeletal proteins[c]
32. Raised intracellular polyamine concentrations[d]
33. Alterations in the glycolytic pathway, by increased lactate dehydrogenase activity[e]

Many of these changes reflect alterations in cell metabolism/behaviour without any readily obvious direction of change (i.e., as to whether the alteration is increased or decreased). Even where a general trend may be apparent, there exist many specific exceptions so that it is difficult to define any universal tumour cell characteristic.

[a] From Evans (1991), [b] Samuel *et al.* (1997), [c] Hunter (1997), [d] Lindsay and Wallace (1999), [e] Shim *et al.* (1997).

protein) (Ozawa *et al.*, 1999). Oxidative stress, defined as situations which augment oxidant exposure, or compromise anti-oxidant capacity (Pacifici and Davies, 1990), may arise as a result of reoxygenation after hypoxia. Tumour cell populations that have been reoxygenated, by angiogenesis, have increased metastatic potential (Young and Hill, 1990), due to sudden oxidative reperfusion and generation of ROIs causing accumulating DNA damage, leading to mutations (Morel and Barouki, 1999). Even if hypoxia had not selected for variants with *p53* mutations, oxidative inhibition of p53 function also prevents the activation of genes necessary to induce apoptosis or DNA repair. The roles of mutated proteins in cancer and apoptosis will now be discussed.

1.5.2 Tumour suppressor genes and oncogenes as regulators of apoptosis

Much attention has focussed on gene products found to act as intracellular regulators of the cell death machinery. These include p53, Bcl-2 and Ras. Mutated or dysregulated forms of all of these genes are found in association with many cancers (Martin *et al.*, 1995). They are discussed here because of their importance in both apoptosis and cancer, as well as the cellular response to chemotherapy (Fig. 1.2).

1.5.2.1 p53

Wild-type p53 limits cellular proliferation by inducing either a transient cell cycle block, apoptosis, or senescence, depending on the cellular context (Levine, 1997). It may regulate the cell cycle via cyclin-dependent kinases, and the action of Bax, a pro-apoptotic pore-forming protein of mitochondrial membranes, which may contribute to the release of apoptogenic proteins, such as AIF and cytochrome c, from the intermembrane space. p53 participates in a cellular system involved in genome surveillance and DNA repair. As many of the p53 functions play important roles in monitoring, preventing or eliminating tumour cells (Miyashita and Reed, 1995), disruption of any one of these processes might promote tumour progression (Wallace-Brodeur and Lowe, 1999). Loss of p53 function, which occurs in over half of all human tumours, may contribute to the genomic instability in tumour cells, both by allowing tumour cells to replicate damaged

DNA, which would cause errors in the genome, and by promoting the survival of cells so that genome alterations accumulate with time (Miyashita and Reed, 1995).

While wild-type p53 has a growth suppressive action that may be mediated by transcriptional activation of the *p21/WAF1/CIP1* gene, the product of which is a potent inhibitor of cyclin-dependent kinases, the mechanism by which elevated p53 levels leads to apoptosis is unknown, but is believed to involve transcriptional activation of apoptotic genes such as *bax* (Bissonette *et al.*, 1997).

There is some evidence that p53 probably does not commit the cell to apoptosis, rather, it adjusts the relative sensitivity of cells so that apoptosis can be triggered more easily in response to stimuli that activate the endogenous cell death pathway, or when cells are confronted with clashes in their signals for cell cycle control (Wu and Levine, 1994). As p53 pre-disposes a cell to death, tumours harbouring *p53* mutations are inherently more aggressive and, in many instances, more resistant to traditional therapies, which are drugs that either directly or indirectly damage DNA (Wallace-Brodeur and Lowe, 1999).

Heat shock proteins (HSPs), which function as molecular chaperones, may control the conformation and inactivation of p53. The dysregulation of molecular chaperone function and protein folding pathways have been linked to key events in tumourigenesis, and one such example may be the elevated stability of the HSP-mutant p53 complex (Hupp, 1999).

1.5.2.2 Bcl-2

Bcl-2 is the acronym for B-cell lymphoma/leukemia-2 gene, and is an anti-apoptotic protein involved in B-cell malignancies (Reed, 1994). Some Bcl-2 family members are associated with intracellular membranes including the nuclear envelope, the endoplasmic reticulum and the outer mitochondrial membrane, membrane attachment being presumably due to a hydrophobic amino acid sequence present at the COOH terminus (Eskes *et al.*, 1998). Bcl-2 appears to be restricted to tissues in which apoptosis shapes developing structures or accounts for cell turnover (Hockenbery *et al.*, 1991). Bcl-2 family proteins can form both homodimers and heterodimers, and, as a consequence of this, they can function either independently or in concert to regulate apoptosis, e.g., Bax functions to promote apoptosis, but Bcl-2 may bind to Bax, changing

its conformation, thus preventing apoptosis. Dimerisation of Bcl-2 family members involve interactions between conserved amino acid sequences known as Bcl-2 homology (BH) domains (Desagher *et al.*, 1999).

Bcl-2 is over-expressed in most breast carcinomas (Allen *et al.*, 1998), and its expression is altered in a variety of other cancers through various mechanisms, including loss of p53 tumour suppressor, which downregulates *bcl-2* expression in some tissues (Miyashita and Reed, 1995). Bcl-2 facilitates a prolonged, stable, metabolically dormant state from which cells recover with high efficiency (Garland and Halestrap, 1997), possibly facilitating drug resistance. Bcl-2 also functions as an inhibitor of cell death induced by many agents in a variety of cell types, thus contributing to cell expansion by inhibiting physiological cell turnover (Miyashita and Reed, 1995), and to resistance to anti-cancer therapies (Froesch *et al.*, 1999). It cannot, however, protect against every type of apoptosis-inducing stimulus (Allen *et al.*, 1998).

1.5.2.3 Ras

Promotion as well as suppression of cell death by oncogenic forms of Ras have been reported (Coopersmith *et al.*, 1997). The three human *ras* genes (H-, N-, and K-*ras*) encode closely related 21 kDa proteins ($p21^{ras}$) that function as regulated molecular switches that control signal transduction pathways which mediate cell growth and differentiation (Clark *et al.*, 1996) (Fig. 1.2). Wild-type Ras proteins function by cycling between inactive GDP-bound and active GTP-bound forms, i.e., they are regulated by an on-off mechanism in normal cells (Bollag *et al.*, 1996), *ras* mutations leading to chronic stimulation of growth regulatory pathways and cellular transformation (Clark *et al.*, 1996). Mutations of *ras* proto-oncogenes are among the most common alterations in cancer cells (Bollag *et al.*, 1996), being present in approximately 30% of all human cancers (Barbacid, 1987). Frequency of *ras* mutations, arising by point mutation, as well as the specific *ras* gene involved, varies significantly between different types of tumours (Clark *et al.*, 1996).

Oncogenic mutant proteins show defective intrinsic GTP hydrolysis and, therefore, accumulate elevated levels of Ras•GTP, resulting in chronic stimulation of growth regulatory pathways (Bollag *et al.*, 1996). Hence, mutant *ras* oncogenes may

contribute to tumourigenesis through their ability to promote cell proliferation, as well as by inhibiting apoptosis, but only when mutations in other pro-apoptotic proteins are present (Coopersmith *et al.*, 1997). Ras activation leads to increased flux through a number of effector pathways (Bollag *et al.*, 1996). Oncogenic Ras normally promotes apoptosis, especially after PKC decreases (Chen and Faller, 1995), but Ras may inhibit apoptosis by regulating members of the Bcl-2 family, including Bcl-2 itself, by the stimulatory effect on transcription and function of these survival proteins (Kinoshita *et al.*, 1995). Oncogenic Ras promotes apoptosis in "uninitiated" cells (cells without other mutations of oncogenes or tumour suppressor genes). However, it facilitates the progression of "initiated" cells with a proliferative abnormality to a more neoplastic state, i.e., additional mutations (e.g., in p53) may be needed to suppress the pro-apoptotic response of oncogenic Ras (Coopersmith *et al.*, 1997).

Ha-*ras* leads to activation of the Na^+/H^+anti-port (Maly *et al.*, 1989), which causes efflux of protons and, thus, intracellular alkalinisation. As cytoplasmic alkalinisation retards the apoptotic process (Froelich *et al.*, 1996), this may further contribute to the anti-apoptotic function of *ras*. These opposing effects of Ras may be attributed to the pleotropic nature of Ras signalling, as discussed in Section 1.4.2.1, and the numerous upstream and downstream effectors.

1.5.3 Cancer therapy, redox status and oxidative stress

All of the anti-cancer treatments are aimed at selectively inducing cell death in cancer cells (Hickman, 1996). Oncogenically transformed cells usually do not have totally functional pathways for induction of apoptosis, because transformation blocks apoptosis signalling pathways via mutations in pro-apoptotic proteins, and upregulates anti-apoptotic proteins. Therefore, transformed cells must be killed by therapies that do not depend on pro-apoptotic systems which may be mutated by transformation (Podak *et al.*, 1999).

Well-established treatment modalities such as irradiation, cytotoxic chemotherapy, heating and hormone therapies ultimately enhance apoptosis (Kerr *et al.*, 1994). It is important to emphasise that although tumours that are resistant to certain therapies may not undergo apoptosis following treatment with the particular therapy,

these cells retain the ability to undergo apoptosis in response to other agents, e.g., hormone therapies for breast cancers, which depend on the binding of oestrogen to its receptor for survival. Failure of current anti-hormonal therapies is commonly associated with emergence of hormone-independent cells in which the apoptotic pathway is no longer coupled to hormone-dependent pathways. At this point, cells no longer respond to anti-oestrogen therapies and tumour growth accelerates. Therefore, agents that induce apoptosis in oestrogen-independent cells, or augment cellular sensitivity to anti-oestrogens, represent important adjuncts to existing therapies for breast cancer patients (Welsh, 1994).

Cancer cells often have an immature phenotype representing a block in the normal differentiation pathway. Treatments capable of inducing differentiation have been discovered for cancer cell lines *in vitro* and have, in some cases, been developed as anti-cancer therapies (Beere and Hickman, 1993). Restoration of a normal differentiation program in cancer cells thus appears to reactivate an apoptotic mechanism (Mancini *et al.*, 1997). However, the mechanisms by which these treatments activate PCD are just beginning to be examined.

Many chemotherapeutic agents induce DNA damage or cause disruptions in DNA metabolism (Lowe *et al.*, 1993). Signals emerging from DNA-damaging agents are influenced by a series of cellular checkpoints, and induce complex cellular responses involving DNA repair and transcription regulation, which are related to specific gene expression and activation. Ordered balance within the ratio of effector and repressor proteins regulating the decision of a cell to survive or die, has already been suggested to form an important checkpoint for cell death (Oltvai and Korsmeyer, 1994). Even slight differences in expression among these proteins influence apoptosis induced by cancer chemotherapy (Schmitt *et al.*, 1997). As wild-type p53 regulates the cell cycle and transcription of the pro-apoptotic protein, Bax, tumours harbouring *p53* mutations are more aggressive and more resistant to traditional therapies, as they are able to by-pass Bax-mediated apoptosis. Hence, they represent a tumour subpopulation the treatment for which is desperately in need of new approaches (Wallace-Brodeur and Lowe, 1999).

Many chemicals require metabolic activation to ROIs in order to exert their toxicity. These include active or potential anti-tumour agents such as Adriamycin, Daunomycin A, Mitomycin C, Bleomycin and Neocarzinostatin, which are all capable of

redox-cycling, a process which produces hydroxyl radicals, superoxide and hydrogen peroxide (Cohen and d'Arcy Doherty, 1987). Treatment with such compounds induces oxidative stress, and normal cells handle oxidative stress better than transformed cells, due to the loss of normal redox state regulation in transformed cells. As seen in studies of reduction with caffeic acid phenethyl ester (CAPE), as well as oxidation with H_2O_2, the transformed cells are often killed via apoptosis whereas the normal cells are more resistant (Chiao *et al.*, 1995). In cases of *p53* mutation, such therapies may be preferable to those inducing DNA damage, therefore. Sensitivity of cells to oxidative stress may be cell type-specific, however and, therefore, needs to be confirmed in a specific model system.

1.5.3.1 Control of redox state of cells

As mentioned above, cancer cells exhibit loss of normal redox state regulation (Chiao *et al.*, 1995). Normal eukaryotic cells have developed efficient mechanisms to counteract the detrimental effects of oxidative stress, which result mainly in DNA and lipid damage. Any perturbation of ROI homeostasis is sensed by regulatory molecules in normal cells, and triggers reactions re-establishing physiological levels of ROIs. This is achieved by anti-oxidants such as glutathione (GSH) and vitamins C and E, as well as a multitude of enzymes specialised in interconverting or eliminating ROIs and repairing damaged protein, DNA, and lipids (Schreck and Baeuerle, 1994). Anti-oxidant compounds can be grouped with respect to their mode of action. In living cells, they can be anti-oxidants by chelating transition metals, by directly scavenging ROIs, by increasing the GSH level, by stimulating the activity or new synthesis of anti-oxidant enzymes, or by inhibiting the activity of ROI-producing enzymes (Muller *et al.*, 1997). This anti-oxidative apparatus is used to establish a "normoxic" condition in the cell (Schreck and Baeuerle, 1994).

GSH is a tripeptide consisting of glycine, cysteine and glutamic acid moieties, and occurs in millimolar concentrations in the cytosol (Meister, 1994). It is the major intracellular redox buffer in almost all cell types. Furthermore, it has recently been implicated in protection against the induction of apoptotic and necrotic cell death in a variety of cell types (Staal *et al.*, 1993). Since it is the most prevalent constituent in the

cellular pool of reducing equivalents, even modest variations in GSH concentrations can strongly modulate redox status (Allen, 1991). Additionally, a number of anti-oxidant enzymes use GSH as a co-substrate to counteract ROIs, and to catalyse repair and reducing reactions (Muller *et al.*, 1997). The intracellular redox state, which is expressed as the ratio of the concentration of oxidising equivalents to the concentration of reducing equivalents (Meister, 1983), is coupled to the oxidation state of cysteine residues in proteins by complex thiol/disulfide exchange mechanisms, through which redox status influences the activity of a variety of redox-sensitive enzymes (Staal *et al.*, 1993). A change in glutathione redox status (ΔGSH/GSSG/both), if coupled to changes in the redox states of thiols and disulfides in specific proteins, could provide a regulatory signal that affects the biological activity of not only enzymes, but also receptors, transporters, and transcription factors (Gilbert, 1995). The intracellular GSH redox status has been suggested to play an important role in metabolic regulation, cellular activation and proliferation, gene expression and mRNA stability, and protein folding (Hwang *et al.*, 1995).

The process of apoptosis is also regulated by cellular redox status (Sato *et al.*, 1995). Redox modification of critical cellular proteins, by reversible interaction(s) of selected cysteines with GSH, particularly during oxidative stress, plays an important role in the mechanisms by which oxidative stress affects the cell cycle, and as a result influence mitogenesis and apoptosis (Cotgreave and Gerdes, 1998).

Cellular transformation in humans is often associated with large increases in GSH concentration (Mitchell and Russo, 1987), but produces patterns of cellular response to oxidative stress that are uncharacteristic of normal tissues. Whereas GSH concentration in normal tissues is directly proportional to ambient oxygen tension, transformed cells exhibit a non-linear response to oxidative stress (Allen, 1991). The sensitivity of transformed cells to anti-tumour drugs may be determined by the inability of transformed cells to synthesise GSH in response to oxidative stress (Meister, 1994). The concentrations of GSH and GSSG in cells change considerably in response to oxidative stress (Gilbert, 1995). Therefore, cancer cells may be more sensitive to oxidative stress, as shown in studies with CAPE and H_2O_2 (Chiao *et al.*, 1995). Thus, the induction of oxidative stress in cancer cells may be exploited therapeutically to selectively target cancer cells.

1.5.3.2 Oxidative stress in physiological and pathological conditions

Oxidative stress can result from exogenous sources (i.e., redox-active xenobiotics), or from increases in endogenous oxidative metabolism (i.e., mitochondrial electron transport, reperfusion of hypoxic tissue, and the oxidative burst reaction of neutrophils during inflammatory processes) (Schreck and Baeuerle, 1994).

Situations that augment oxidant exposure, or compromise anti-oxidant capacity, are commonly referred to as oxidative stress (Pacifici and Davies, 1990). Such stress, resulting from the deleterious effects of ROIs, is an important phenomenon in many biological systems (Gidrol *et al.*, 1996). Oxygen radicals and other activated oxygen species are known to participate in numerous physiological and pathological processes (Pacifici and Davies, 1990).

As a by-product of normal aerobic metabolism, molecular oxygen undergoes successive single electron transfers that result in the generation of ROIs such as superoxide radical (O_2^-), hydroxyl radical (•OH), and hydrogen peroxide (H_2O_2) (Gidrol *et al.*, 1996). Moderate oxidative stress may selectively alter sensitive physiological processes, including cell signalling and gene activation, as well as the balance between DNA damage and repair. Radicals can modulate the activity of kinases, promoting cell growth and directly interact with protooncogenes. Thus, sustained exposure to moderate pro-oxidant levels may play an important role at several stages in carcinogenesis. When radical generation overwhelms cell anti-oxidant defense, lethal mechanisms are activated and cell death ensues (Dypbukt *et al.*, 1994).

The role of oxidative stress in apoptosis has generated considerable debate since anti-oxidants as well as well as pro-oxidants were shown to inhibit this form of cell death. There is a growing consensus that reactive oxidants play a key role in the control of apoptosis, although the precise nature of this control is unclear (Goldkorn *et al.*, 1998).

In pathological conditions, excessive generation of free radicals can lead to various degrees of oxidative stress. ROIs are involved in lipid peroxidation, protein denaturation, and DNA damage, which eventually results in various mutations. These cellular damages can lead to a range of pathological symptoms observed, both through apoptosis and necrosis, in diseases like cancer and arthritis (Gidrol *et al.*, 1996).

Lipid peroxidation, one of the best-known manifestations of oxidative cell injury (Farber *et al.*, 1990), is a complex process whereby unsaturated lipid material undergoes free radical chain reactions, leading to the formation of lipid hydroperoxides. The latter decompose to many secondary products, amongst which is a three-carbon dialdehyde, malonaldehyde, which readily reacts with free amino groups on biological compounds such as amino acids, proteins, amino phospholipids and nucleic acids (DNA, RNA) (Dillard and Tappel, 1984). Products of peroxidation are identical, regardless of the method of initiation (Porter, 1984). Membrane peroxidation leads to modifications of membrane fluidity, decreases in membrane potential, increased permeability to H^+ and other ions, fragility and altered membrane integrity (Foote *et al.*, 1984). This may lead to increased calcium permeability, integral protein failure and cell death (Sun *et al.*, 1997). Extensive peroxidation leads to eventual rupture of membranes, and subsequent release of cell and organelle contents, such as lysosomal hydrolytic enzymes (Halliwell and Gutteridge, 1990).

Mitochondrial damage may also occur as a result of oxidative cell injury by •OH and other ROIs. Cell killing is correlated with a loss of mitochondrial energisation, rather than with the depletion of ATP alone (Farber *et al.*, 1990). Exposure of proteins to •OH represents a relatively indiscriminate damaging system, as most amino acids are good targets for modification. Proteins that contain transition metals may suffer "site-specific" damage when H_2O_2 or O_2^- is added. The increased proteolytic susceptibility of oxidatively modified proteins is thought to result from increased denaturation/hydrophobicity (Pacifici and Davies, 1990). The production of •OH close to DNA potentially leads to modifications of purines and pyrimidines or strand breakage. The reaction of •OH with a biomolecule may produce another radical, usually of lower reactivity. Such less reactive molecules may cause their own problems, since they can sometimes diffuse away from the site of formation and attack specific biomolecules (Halliwell and Gutteridge, 1990).

When cells are subjected to high external concentrations of H_2O_2, DNA strand breakage usually occurs. This could occur because the oxidant stress leads to activation of some specific DNA-cleaving mechanism, such as a calcium-dependent endonuclease. An alternative mechanism may be seen if H_2O_2 survives in sufficient concentrations to reach the nucleus and react with intracellular metal ions to give •OH. This may fragment

the DNA by site-specific attack, or H_2O_2 may react with Fe^{2+} (to form •OH) which might already be present on the DNA *in vivo*. Alternatively, the oxidant stress might liberate iron ions from their sites of sequestration within the cell so that they can bind to DNA (Halliwell and Gutteridge, 1990).

Radicals of lipids, proteins, fatty and amino acids, vitamins, hormones, and other compounds may also be formed after reactions of primary radicals with biological substrates (Popov and Lewin, 1999).

Depending on the intensity of insult, cell death may occur via apoptosis or necrosis.

1.6 Model systems and methodologies for studying apoptosis

Many therapies function via the induction of oxidative stress, defined as situations which augment oxidant exposure, or compromise anti-oxidant capacity (Pacifici and Davies, 1990), and aim to exploit the redox imbalance in tumour cells, to selectively induce apoptosis in these cells. In order to test chemotherapeutic agents, a model test system is required. Usually such models are cell cultures systems. The most desirable cell culture system would consist of the normal and malignant equivalent of the particular cell type to be subjected to treatment. Such a system would allow the assessment of both toxicity and selective toxicity of the test substances on that cell type. Such a model system does exist for breast epithelial cells, and is described in depth in Section 1.6.1. The main aim of the current study was to establish which were the most sensitive detection systems for early detection of apoptotic events for use in drug trials.

At the time of commencement of this study, apoptosis and early detection of this phenomenon were the focus of much research, and different detection systems were constantly being promoted as being the most sensitive. The model system finally used in the study consisted of a unique breast epithelial cell line, which was described as being immortal, and without viral and mutational basis for such immortality, and its c-Ha-*ras* transformed, pre-malignant counterpart (containing a Val-17 c-Ha-*ras* mutation) (Basolo *et al.*, 1991). The agent used to induce oxidative stress was H_2O_2, the latter often being the catabolic product of many chemotherapeutic agents (Cohen and d'Arcy Doherty, 1987).

The detection systems available at the commencement of the study were reviewed and evaluated on the basis of cost, sensitivity, and specificity for apoptosis as opposed to necrosis. Two morphological, one enzymatic, and two electrophoretic methods were finally selected. The basis for this selection is described in the following sections.

1.6.1 A model system - the parental MCF10A cell line and its pre-malignant derivative, MCF10AneoT

The immortal human mammary epithelial cell (HMEC) line, the MCF10A cell line, is unique as it was established from tissues of non-malignant origin (Soule *et al.*, 1990).

1.6.1.1 Origin

A decreasing in the Ca^{2+} concentration in culture media usually increases the *in vitro* cultural longevity of normal epithelial cells. The MCF10A cell line, however, is an immortal cell line that arose spontaneously, without viral or chemical intervention, from mortal human diploid mammary epithelial cells cultured under such conditions. The diploid mortal cells, MCF10M, senesce when transferred serially in 1.05 mM Ca^{2+}, whereas the immortal cell line, designated MCF10A (attached cells) and MCF10F (floating cells), proliferates for years in medium either with the normal Ca^{2+} concentrations used (1.05 mM) or in low Ca^{2+} medium (0.04 mM) (Soule *et al.*, 1990). None of the known oncogenic mutations which could be responsible for immortilisation (c-*erbB*-1/*HER*-2/*neu*, c-*erbA*-1, *int*-2, and c-Ha-*ras*-1) could be detected (Basolo *et al.*, 1991). The parental line contains functionally active p53 (Shekhar *et al.*, 1997).

The MCF10A cell line originated from breast tissue obtained from a mastectomy performed on a 36-year-old parous, pre-menopausal woman with no family history of breast malignancy. The breast histopathological diagnosis was extensive fibrocystic disease, consisting of increased mammary fibrous stroma containing numerous dilated mammary ducts, benign apocrine metaplasia, and small confocal areas of intraductal hyperplasia with no evidence of atypia. The patient was free of disease (Soule *et al.*, 1990).

1.6.1.2 Characteristics

The immunocytochemical characteristics of the MCF10A and MCF10F include positive reactivity with antibodies against keratins (i.e., KA-4 and AE1/AE-3 Mabs) and epithelial sialomucins (i.e., MFA-breast, MC-5 and EMA antibodies) (Tait *et al.*, 1990).

MCF10A has the characteristics of normal breast epithelium by the following criteria: (a) lack of tumorigenicity in nude mice; (b) three-dimensional growth in collagen; (c) growth in culture that is controlled by hormones and growth factors; (d) lack of anchorage-independent growth; and (e) dome formation in confluent cultures. Cytogenetic analysis prior to immortalisation showed normal diploid cells. Although later passages showed minimal rearrangement and near-diploidy, the immortal cells were not karyotypically normal (Soule *et al.*, 1990).

This cell line was then transformed to a pre-malignant derivative by transfection with the mutationally activated c-Ha-*ras*.

1.6.1.3 The pre-malignant cell line derivative of MCF10A

A significant event in cancer research has been the identification and subsequent characterisation of mutated oncogenes; in particular, mutational activation of the *ras* gene has been found. In some cancers, *ras* oncogene insertion initiates a cascade of phenotypical abnormalities leading to pre-malignant cell transformation. By transfection of the MCF10A cells with the plasmid Homer 6 (pHo6) containing the human T24-mutated c-Ha-*ras* oncogene and a neomycin resistance gene, NeoT, the pre-malignant equivalent of the MCF10A cell line, the MCF10AneoT cell line, was produced (Basolo *et al.*, 1991). Though the parental cell line contains wild type, functionally active p53, the *ras*-transfected equivalent possesses p53 which is not mutated, but which was found to exist predominantly in a conformationally altered state, when cells are confluent. This is defective in its ability to bind DNA in a sequence-specific manner and to induce transcriptional activation from the WAF-1 promoter, which is responsible for β-galactosidase expression (Shekhar *et al.*, 1997). The physiological differences between MCF10A and its *ras*-transfected equivalent (Basolo *et al.*, 1991) are listed in Table 2, and the morphological differences (Russo *et al.*, 1991) are seen in Table 3.

Table 2. Physiological comparison of MCF10A and MCF10ANeoT [a1]

MCF10A	MCF10ANeoT
average colony size	much larger colonies
poor colony-forming efficiency in agar-Methocel	good colony-forming efficiency in agar-Methocel
significant growth reduction in the absence of hormones/growth factors	no growth reduction in the absence of hormones/growth factors
no invasiveness	high invasiveness
no collagenolytic activity	high collagenolytic activity
low locomotion	high locomotion
high chemotaxis	high chemotaxis
negative tumourigenicity	positive tumourigenicity
lysosomal pH 5.0 [a2]	lysosomal pH 6.1 [a2]
normal TGFα-protein secretion	increased TGFα-protein secretion
normal amounts of c-Ha-*ras* RNA transcripts	increased amounts of c-Ha-*ras* RNA transcripts
no activated p21 (*ras* gene related protein products)	activated p21 expressed

[a1] from Basolo *et al.* (1991).

[a2] from Sloane *et al.* (1994).

Table 3. Morphological comparison of MCF10A and MCF10ANeoT [b]

MCF10A	MCF10ANeoT
monolayers interrupted by the formation of domes, present at confluence	at confluence they pile up, forming solid colonies (Zone B) surrounded either by isolated cells or by cells forming a continuous layer (Zone A)
cells regular in size, slightly polyhedral, monolayers form cobblestone pattern	disorganised pattern, loss of contact inhibition, Zone A cells polyhedral, stratified multilayer 2-3 cells thick; Zone B cells pleomorphic (spherical/elongated), clumps 12-13 layers thick
adjacent cells closely apposed forming a ridge between the cells	Zone A lacks intercellular ridge, Zone B intercellular spaces widened and irregular
number, length and diameter of microvilli small	number, length and diameter of microvilli much larger
multiple interdigitations of the plasma membrane, which were joined by well-formed desmosomes	Zone A cells joined by small desmosomes, and forms intracellular lumina lined by small blunt projections, no desmosomes in Zone B cells
small fragments of smooth and rough ER	numerous stacks of ER (more prominent in Zone A)
inconspicuous golgi	coated vesicles associated with golgi
scanty, small round/slightly elongated mitochondria	mitochondria large, round/elongated with swollen matrix
scanty primary and secondary lysosomes	numerous lysosomes
bundles of filaments connecting desmosomes or free in cytoplasm	lacks bundles of tonofilaments
nuclei oval, slightly elongated with smooth nuclear membrane showing occasional indentations, finely dispersed heterochromatin with inconspicuous nucleolus	nuclear size uniformly enlarged, nuclear shape varies from oval with a smooth membrane to irregular with deep indentations, prominent large nucleolus
Additional features : numerous ribosomes and polyribosomes	Additional features : secretory electron-dense material in lumen, numerous coated vesicles scattered throughout the cytoplasm, near cell surface or in contact with the lumen, pools of glycogen which varied from cell to cell, lipid droplets present

[b] from Russo *et al.* (1991).

Though the exact basis for the immortality of the MCF10A cell line is not known, MCF10 cell lines have several advantages over other breast cell lines currently available for studies of the aetiology and effects of malignant transformation, and for testing the possible selectivity of anti-cancer drugs on variously transformed derivatives. The cells are (a) not treated with a pro-carcinogen, (b) do not harbour SV40 genetic information, and (c) the karyotype is near diploid with minimal rearrangement (Soule *et al.*, 1990). Moreover, the *ras*-transformed cell line constitutes a model of a pre-malignant, invasive cell, the acquisition of full carcinogenic transformation usually requiring three or more mutations (Kinzler and Vogelstein, 1996). Studies on such a system could give insight into the effect of transfection with a single oncogene (mutationally activated c-Ha *ras*) and the susceptibility of cells to a particular treatment or drug.

1.7 Induction of oxidative stress

As mentioned, oxidative stress is induced by many chemotherapeutic agents. Intact cells can be subjected to oxidative stress by the direct addition of oxidants, e.g., H_2O_2. H_2O_2 is a convenient reagent as it is commercially available in high purity and is easy to quantify (Pacifici and Davies, 1990). It is also a representative ROI, and has been shown to induce permanent growth arrest and apoptosis in a number of cell types. H_2O_2, while relatively inactive, can be reduced to the highly reactive hydroxyl radical (•OH) by a metal ion through the Fenton reaction (Yakes and van Houten, 1997). The Fenton reaction is represented by :

$$Fe^{2+} + H_2O_2 \rightarrow \text{intermediate complex} \rightarrow Fe^{3+} + \bullet OH + OH^-$$

Traces of Fe^{3+} might be able to react further with H_2O_2, although this is very slow at physiological pH :

$$Fe^{3+} + H_2O_2 \rightarrow \text{intermediate complex} \rightarrow Fe^{2+} + O_2^- + 2H^+$$

Even more reactions are possible :

$$\bullet OH + H_2O_2 \rightarrow H_2O + H^+ + O_2^-$$

$$O_2^- + Fe^{3+} \rightarrow Fe^{2+} + O_2$$

$$\bullet OH + Fe^{2+} \rightarrow Fe^{3+} + HO^-$$

The overall sum of these, unless some other reagent is added, is an iron-catalysed decomposition of H_2O_2 :

$2\ H_2O_2 \rightarrow O_2 + 2\ H_2O$ (Halliwell and Gutteridge, 1990).

•OH has a short lifetime, and is one of the most powerful oxidants in aqueous solution (Dypbukt *et al.*, 1994). Pure H_2O_2 has no unpaired electrons, contains no free radicals, and has limited reactivity, but it can cross biological membranes (Halliwell and Gutteridge, 1990). H_2O_2 is often used in cell culture experiments to induce oxidative stress, as it can potentially be detoxified by the cell, and is produced in increasing amounts in response to many physiological stimuli (Muller *et al.*, 1997). The toxicity of H_2O_2 to cells has been reported to be variable. The variability can be accounted for both by the activity of H_2O_2-removing enzymes, and by the rate of conversion of H_2O_2 into more highly reactive radicals (Halliwell and Gutteridge, 1990).

A prerequisite for studies of induction of apoptosis by H_2O_2 is the unequivocal detection of the apoptotic type of cell death. Unfortunately, at the commencement of this study, no single detection system has emerged as being totally reliable and universally applicable.

1.8 Methods for the detection of apoptosis

There are several methods for the detection of apoptosis, each with their own advantages and disadvantages. The most commonly used and trusted methods have been assessment of morphological characteristics and DNA fragmentation assays. For completeness, a brief overview of available methods will be given, as well as some details of those chosen for use in this project.

1.8.1 Assessment of morphological characteristics

Morphological assessment is still the most reliable method of quantifying apoptosis, but this is both subjective and laborious (Martin *et al.*, 1994). The apoptotic process involves a sequence of cell shrinkage, increased cytoplasmic density, nuclear membrane convolution, chromatin compaction and segregation, and the formation of membrane-bound apoptotic bodies, while necrotic cells have smooth nuclear membranes, swollen cytoplasm and organelles, and a ruptured plasma membrane. These morphological changes can be detected using the electron microscope. Membrane

blebbing and apoptotic bodies can only be seen by simple phase-contrast light microscopy with difficulty. Another versatile tool is confocal laser scanning microscopy, powerful for both morphological analysis and macromolecular localisation, but unavailable for this study. These techniques all have the same disadvantage in that they are qualitative, but not quantitative. Changes in size and granularity of apoptotic cells can also be observed using flow cytometry. Apoptosis is accompanied by water loss, cell shrinkage and DNA fragmentation, whereas necrosis is not. Thus, apoptotic and necrotic cells differ in light scatter patterns. Flow cytometric analysis is a very rapid and objective way of enumerating apoptotic cells, but these changes are not consistent in all cell types (Sgonc and Wick, 1994). This apparatus was also not available for this study, however.

For this study, both light microscopy and electron microscopic examination were selected as the reference methods for detection of apoptotic cell death. As apoptotic DNA fragmentation is said to be distinctive, and an inexpensive method for detection of apoptosis, this assay was also carried out.

1.8.2 Analysis of DNA degradation

There are several methods for analysing DNA degradation, including agarose gel electrophoresis, pulse field gel electrophoresis, labelling of DNA strand breaks visualised either by fluorescence or light microscopy or by a colorimetric assay (i.e., an ELISA), and DNA stains.

1.8.2.1 Agarose gel electrophoresis

The most striking biochemical event in apoptosis is the DNA cleavage between nucleosomes that produces fragments in multiples of approximately 180 base pairs (bp). This phenomenon is most often analysed by agarose gel electrophoresis, which shows DNA fragmentation in nuclear extracts and the typical "DNA ladder" of DNA cleavage products produced by apoptosis. Necrotic cells show "smears" of DNA, due to random DNA fragmentation, on such gels. An improved method for the detection of DNA fragmentation visualises the DNA after Southern blotting with a radiolabelled total

cellular DNA probe, instead of ethidium bromide staining. This increases the sensitivity. This technique is time-consuming, however, requires a great number of cells, involves radioactivity in the more sensitive assays, and is unable to define the percentage of apoptotic nuclei or recognise the apoptotic cell populations in a heterogeneous cell population (Sgonc and Wick, 1994). Internucleosomal DNA fragmentation is only a qualitative measure of apoptotic cell death and, most importantly, does not occur in all cases of apoptosis. In addition, this type of cleavage might be a late and dispensible step in apoptosis. However, it is still one of the most useful tests for apoptosis currently available, but it is fairly technically demanding as high molecular weight (HMW) DNA is easily sheared if not handled very carefully, giving false results of DNA fragmentation (Martin *et al.*, 1994).

1.8.2.2 Pulse field gel electrophoresis

An alternative to agarose gel electrophoresis is pulse field gel electrophoresis (PFGE). Prior to internucleosomal DNA cleavage, DNA is fragmented into HMW fragments, which are not detected by conventional agarose gels (Weaver *et al.*, 1993). PFGE, which is a specialised form of electrophoresis in which the direction and duration of the electrical field are changed periodically, permits the separation of DNA fragments as large as 5 Mbp, allowing DNA fragments in apoptosis to be examined at whole new levels. Under appropriate conditions, DNA fragments from <100 bp to 1 Mbp can be resolved on a single gel, as opposed to the resolution of 100bp-30kbp on conventional agarose gels (Walker and Sikorska, 1997). As equipment for carrying out such investigations was unavailable, this method of analysing the DNA of test cells was also not considered.

1.8.2.3 Detection of DNA strand breaks

Alternative methods used to assess DNA strand breaks are based on labelling the cellular DNA for such breaks, and subsequently analysing these using flow cytometry, fluorescence microscopy or light microscopy. These methods could potentially have been used because light and fluorescent microscopes were available, and individual fixed,

permeabilised cells or tissue sections could have been labelled (Sgonc and Wick, 1994). Cleavage of DNA induced by application of the test substance may yield double-stranded, LMW DNA fragments (mono- and oligonucleosomes) as well as single strand breaks ("nicks") in HMW DNA. These strand breaks would be detected by enzymatic labelling of the free 3'-OH termini with modified nucleotides (X-dUTP, X = biotin, DIG or fluorescein). Suitable labelling enzymes which may be used in this system include DNA polymerase (for *in situ* nick translation or ISNT) and terminal deoxynucleotidyl transferase (for TdT-mediated X-dUTP nick end labelling or TUNEL, fluorescein-dUTP allowing direct detection by fluorescence microscopy or flow cytometry). Alternatively, if DNA is labelled with biotin- or DIG-dUTP, the incorporated nucleotides may be incubated with streptavidin or an anti-DIG antibody, which can be viewed by light microscopy, if conjugated to a reporter molecule, e.g., alkaline phosphatase or peroxidase. TUNEL is more sensitive and faster than the ISNT method. These methods have been reported to be useful for the detection of apoptosis before any morphological changes occur. However, both detect not only apoptotic DNA, but also the random fragmentation of DNA that may occur during necrosis due to the multiple endonucleases that are released at this time.

There are also rare situations when apoptosis is induced without DNA degradation (Eisel *et al.*, 1998). Hypercondensation of DNA during apoptosis and the protein environment may also limit the penetration of labelling molecules, so that there are blank areas even though the cell exhibits apoptotic DNA cleavage. Furthermore, without pretreatments, TUNEL sensitivity is too low, and pretreatments easily induce areas of general labelling in normal nuclei (Negoescu *et al.*, 1998). Thus, another independent assay must be used to confirm apoptosis (Eisel *et al.*, 1998).

An alternative method which circumvents the isolation and electrophoretic analysis of DNA is the immunological detection of LMW DNA (histone-complexed DNA fragments) by an immunoassay, ELISA. This can be used to distinguish apoptosis from necrosis, by measuring the DNA fragments either in the cell culture lysates (apoptosis) or supernatants (leakage occurs in necrosis). It is very sensitive, requiring as few as 500 cells, 1000-fold fewer cells than required by the traditional DNA ladder method. Accurate numerical measurement of oligonucleosomal particles have been reported, and this is a quick and convenient test system, facilitating high sample

thoroughput (Eisel *et al.*, 1998). Test kits were extremely expensive, however, and hence, this test option was eliminated.

1.8.2.4 DNA stains

There are three methods for studying cell death that use DNA stains: a dye exclusion method, profile of DNA content and visualisation of morphological changes using staining techniques.

(a) Dye exclusion. Viable and dead cells can be distinguished by differential staining. Cells with disturbed plasma membrane permeability are stained, whereas undamaged (viable) cells are not stained with "exclusion dyes" (dyes that do not penetrate the normal intact plasma membrane). The most frequently used dye is trypan blue, visualised by light microscopy. The fluorescent dye, propidium iodide (PI) which becomes highly fluorescent after binding to DNA, can be used in the same manner.

(b) Profile of DNA content. If cells are permeabilised, the LMW DNA inside the cytoplasm of apoptotic cells leaks out during the subsequent rinsing and staining procedure. The lower DNA content of these cells means they contain less DNA stained by a fluorochrome. This can be measured by flow cytometry. The major disadvantage of this technique is that apoptotic G_2-phase cells exhibit a reduced DNA content, which could represent the DNA content of a G_1-cell. Therefore, such cells may not be detected as apoptotic, resulting in an underestimation of the apoptotic population. Necrotic cells will also be detected using this method, as necrotic cells become leaky and DNA may be lost, allowing no distinction between apoptotic and necrotic cells. The option of using such a test system was, therefore, eliminated.

(c) Morphological changes. The bisbenzimidazole dye, Hoechst 33342, and also acridine orange, penetrates the plasma membrane and stains DNA in unpermeabilised cells. The nuclei of apoptotic cells stain uniformly with Hoechst 33342 and have highly condensed chromatin. This can take the form of crescents around the periphery of the nucleus, or the entire nucleus can appear to be one or a group of featureless, bright spherical beads. These morphological changes in the nuclei of apoptotic cells can be visualised by fluorescence microscopy, and may be

distinguished from normal, non-apoptotic cells by the stronger blue fluorescence of the apoptotic cells. Co-staining of the cells with PI allows the discrimination of dead cells from apoptotic cells. Necrotic cells would be stained with both Hoescht 33342 and PI, while apoptotic cells remain impermeable to PI, allowing entrance of only Hoescht 33342 into the cells.

One drawback of using vital staining methods for measuring apoptosis is the variability of dye penetration in different cells, and its variability of uptake under certain treatment conditions. Therefore, the ability of vital dyes to discriminate apoptotic cells from normal cells by increased uptake of dye has to be tested for each new cell system (Eisel *et al.*, 1998).

1.8.3 Annexin V binding

In normal cells, the distribution of phospholipids is asymmetric, with phosphatidylserine (PS) being limited to the inner cytoplasmic leaflet of the membrane. However, in apoptotic cells the PS is translocated to the outer surface of the cell membrane. Annexin V, a calcium-dependent phospholipid-binding protein, has a high affinity for PS. Annexin V binds to the PS exposed on cell surfaces of apoptotic cells, but will not bind the surface of non-apoptotic viable cells where PS is not exposed. However, because PS is also exposed on necrotic cells, annexin V will bind to both apoptotic and necrotic cells. Thus, to distinguish between apoptotic and necrotic cells, they must be stained simultaneously with annexin V and a vital dye such as PI, which will only enter necrotic cells with a leaky or permeable membrane (Eisel *et al.*, 1998). Annexin V can be detected by fluorescence microscopy or flow cytometry, and can be applied to both adherent cells grown on coverslips and cells in suspension. These kits were extremely expensive, however, and allowed limited numbers of analyses to be performed per kit. For this reason, the annexin assay was also not considered.

1.8.4 Caspase activity assays

Caspases are activated specifically during apoptosis, and are responsible for most of the extensive protein cleavage observed during this process. Thus, a measurement of

their activity is suggested to be an adequate indicator of apoptosis. During necrotic cell death, however, caspases are either not activated or leak out of the cell. Caspase activity is, therefore, not usually seen during necrosis. Caspase activity is usually measured in cell lysates by incubation of the lysates with a caspase-specific, fluorometric substrate, such as the Asp-Glu-Val-Asp-7-amido-4-methylcoumarin (DEVD-AMC) or Asp-Glu-Val-Asp-7-amino-4-trifluoro-methylcoumarin (DEVD-AFC) substrates. Active caspase-3, -6, and -7 cleave the AFC or AMC leaving group off the peptide, and this can be measured using a fluorimeter (Miller *et al.*, 1997). Caspase-3 was chosen for assessment of caspase activation as it was considered one of the major effector caspases, after the activation of caspases-8 and-9, its activity manifesting in the morphological changes associated with apoptosis. At the time of commencement of this study, there were variable reports, some suggesting that caspase-8 was the initiator caspase that activates downstream effector caspases, while others suggested that caspase-9 was the initiator caspase. It has recently become evident that the initiator caspase activated depends on whether apoptosis is initiated by ligation of death receptors to their ligands, or by cellular damage, e.g, oxidative stress (Coppola and Ghibelli, 2000). At the time the caspase assay was conducted in this study, it was not known which initiator caspase would be activated in such a system, therefore, an effector caspase (caspase-3), which would be activated in response to either of the initiator caspases, was selected for assessment. The use of multiwell plates facilitated the processing and analysing of a large number of samples for apoptosis simultaneously, allowing rapid and quantitative screening. The assay was also specific and sensitive, and was reported to be an early indicator of apoptosis, activation of caspase-3 occurring prior to nuclear and membrane permeability changes (Eisel *et al.*, 1998). Assessment of caspase activity was, thus, considered a good option.

1.8.5 Protein degradation assays

Several proteins have been reported to be cleaved during apoptosis, including poly(ADP-ribose)polymerase (PARP), a DNA repair enzyme, actin, fodrin, keratins in epithelial cells, as well as caspases, which must undergo proteolytic cleavage of the inactive precursors to produce active enzyme. Cell lysates can be separated by

electrophoresis, western blotted, probed with specific antibodies for the cleavage of specific proteins, and detected using a suitable system, which may be alkaline phosphatase or enhanced chemiluminescence. The products can subsequently be identified by their corresponding molecular weights. During necrosis, no such specific cleavage products have been reported. Therefore, such a system seems specific, but different proteins may be cleaved in different cell types, and as it was not known which proteins would be cleaved in the system to be used in the present study, the protein degradation assay was also eliminated.

1.8.6 Cytochrome c release from mitochondria

From 1996 onwards, increasing attention was being directed toward the role of cytochrome c in apoptotic processes. Following exposure to apoptotic stimuli, cytochrome c was shown to be rapidly released from mitochondria into the cytosol, an event which was reported to be required for the progression towards apoptosis in some systems, while in necrosis cytochrome c would not be anticipated to be present in either the mitochondria or cytoplasm due to the extensive cellular damage and leakage associated with necrosis. Cytochrome c release may be detected by western blotting and probing of cell fractions with antibodies to cytochrome c. Although the mechanism by which cytochrome c is released from mitochondria is still under investigation, cytosolic cytochrome c was thought to activate procaspases (Liu *et al.*, 1996). Thus, it was proposed to be one of the earliest markers for apoptosis, giving an indication of the induction of apoptosis even earlier than indicated by caspase-3. Cytochrome c release as an early marker for apoptosis was chosen for investigation in the present study.

1.8.7 Methods of choice for experimental work

Based on the advantages and disadvantages reported for the methods available for the detection of apoptosis, the following methods were chosen for investigation in this study (three execution phase and two effector phase):

(a) Morphological observation by light microscopy for an overview of cell rounding, and electron microscopy, to view ultrastructural changes, such as convolution of the

nuclear membrane, chromatin fragmentation, apposition to the nuclear membrane, and membrane blebbing, due to the apparent reliability and almost universal expression of such morphological features during apoptosis.

(b) Agarose gel electrophoresis for detection of DNA laddering.

(c) Caspase activity for its reported rapidity, specificity and sensitivity.

(d) Cytochrome c release was chosen as it was the focus of most of the recent research at the time of the commencement of this study. As this was a novel approach on which little definitive data was available, an attempt was made to raise universally applicable polyclonal antibodies to cytochrome c, and to determine whether cytochrome c is released during apoptosis, in the system studied. Cytochrome release has been shown to be cell-type specific but, due to the novelty of the approach and the potential for novel findings, this system was selected as the final detection system. Also, taking into consideration Fig. 1.2, it seems that all apoptotic pathways induced by oxidative stress, i.e., DNA damage, ceramide signalling and permeability transition pore opening, all result in cytochrome c release, so this seemed the best but other confirmatory tests, such as detection of DNA laddering and apoptotic morphology, were included.

The ease of interpretation of results, reliability and sensitivity, and cost in terms of time and effort, of these systems was assessed on the MCF10A and MCF10AneoT model system exposed to a range of concentrations of H_2O_2 for various lengths of time.

CHAPTER 2
MORPHOLOGY/ULTRASTRUCTURE

2.1 Introduction

The execution phase or the "active" phase of apoptosis occurs immediately after a cell commits to apoptosis. As discussed in Chapter 1, a series of apoptotic events culminates in the execution phase, during which the characteristic morphological features of apoptosis become evident, culminating in disassembly and packaging of the cell into membrane-bound apoptotic bodies for phagocytosis (Mills *et al.*, 1999). These features are visible by light microscopy, which gives an overview as many cells are viewed at any one time. Electron microscopy, however, allows sub-cellular details such as changes in the mitochondria, membranes and nucleus to be seen. These features are the most commonly exhibited during apoptosis, but they are not all always seen in all circumstances, and may perhaps not be seen concurrently, e.g., although nuclear changes, including chromatin condensation might occur, membrane blebbing and loss of microvilli may not be visible at all, or may only be visible much later. Since apoptotic changes occurring in the execution phase may vary from cell to cell, the phenotypic changes were examined in detail in the cells studied.

2.1.1 Apoptotic morphology : distinction from necrosis

As previously mentioned, apoptosis and necrosis have distinct ultrastructural features. The earliest recognisable morphological changes in cells undergoing apoptosis are condensation and fragmentation of the nuclear chromatin, with the formation of sharply delineated, uniformly finely granular masses of chromatin that become marginated against the nuclear envelope. The cytoplasm also becomes condensed. Progression of apoptosis is accompanied by convolution of the nuclear and cell outlines, and this is followed by breaking up of the nucleus into discrete fragments that are surrounded by a double-layered nuclear envelope, and by fragmentation of the cell as a whole to produce membrane-bound apoptotic bodies. The size and composition of the apoptotic bodies vary considerably. Many contain several nuclear fragments whereas

others lack a nuclear component. In addition, the extent of the nuclear and cellular budding varies with cell type, often being relatively restricted in small cells with a high nucleocytoplasmic to cytoplasmic ratio, such as lymphocytes. The cytoplasmic organelles of newly formed apoptotic bodies generally remain well-preserved (Kerr *et al.*, 1994).

The distinction between apoptosis and necrosis is unequivocal at electron microscopy level, and with practice, the two processes can be distinguished using light microscopic study alone (Kerr *et al.*, 1994). Condensation of nuclear chromatin occurs in the early stages of necrosis, but the chromatin is not radically redistributed, as it is in apoptosis. The edges of the chromatin aggregates tend to be irregular and poorly defined. In addition, the nucleus of the necrotic cell never separates into discrete, membrane-enclosed fragments. Late in necrosis, the chromatin disappears. The cytoplasm of the necrotic cell becomes grossly swollen, and plasma and organelle membranes progressively disintegrate. Despite this, the overall configuration of the cell is preserved until it is removed by mononuclear phagocytes. *In vivo*, the involvement of groups of contiguous cells and the presence of an inflammatory exudate usually provide additional confirmatory evidence that the cell death present, in a particular circumstance, is necrosis (Kerr *et al.*, 1994).

The execution phase in apoptosis is more distinctive and can be subdivided into several stages (Mills *et al.*, 1999).

2.1.2 The mitochondrial phase of execution

Recent evidence contradicts Kerr's observations (1994) that mitochondrial morphology is unaltered in apoptosis. Mitochondrial proliferation, which is likely to be governed by a redox-sensitive factor, is associated with condensation of the mitochondrial matrix and total mitochondrial volume reduction, and occurs during apoptosis in Colo-205 epithelial cells (Mancini *et al.*, 1997). The condensed appearance occurs before apoptotic changes in the nucleus. The degree of mitochondrial condensation subsequently increases in concert with the appearance of chromatin and cytoplasmic condensation. At later time points, signs of mitochondrial degeneration are apparent (Mancini *et al.*, 1997).

A reversible transition of mitochondrial morphology from an orthodox to a condensed conformation is associated with high and low energy states of mitochondria, respectively. The condensed conformation is characterised by a reduction in the inner mitochondrial compartment due to increased folding of the inner membrane, with a consequent increase of the outer compartment and intracristal space, and hence, without significant reduction of the total mitochondrial volume. In addition, there is loss of water and ions from the mitochondrial inner compartment, decreased ATP synthesis, and either maintained or decreased respiration. When the degree of mitochondrial condensation is advanced, the outer and inner mitochondrial membranes appear closely associated and the intracristal space is not enlarged. This is described as "mitochondrial pyknosis", is characterised by hyperdensity of the matrix and reduction in mitochondrial size, and may represent a more extensive and pathological degree of mitochondrial condensation, with contraction of the outer mitochondrial membrane. The condensed conformation, which is reversible before the "point of no return" is reached, is unstable and in situations of continued injury, the mitochondrial membrane becomes permeable and the organelle swells, with eventual rupture of the outer membrane and destruction of the different components. The swollen conformation represents a more advanced state of damage to the inner mitochondrial membrane and is usually associated with cellular necrosis. A transitional morphology characterised by increased intracristal space can also be observed between the condensed and the swollen configuration. (Mancini *et al.*, 1997).

Apoptotic cells also show a convergence of highly polarised mitochondria into an extremely packed mass at one side of the nucleus, in a stage correlated with the retraction of cell-cell contacts (i.e., the release stage, Section 2.1.4.1 below), but preceding nuclear condensation (Diaz *et al.*, 1999).

2.1.3 The nuclear phase of execution

Chromatin condensation and apposition to the nuclear envelope is an important feature of the execution phase (Duband-Goulet *et al.*, 1998). The nuclear lamina forms a protein mesh that underlies the nuclear membrane. Lamins are intermediate filament proteins that serve to organise the chromatin and they form part of the nuclear periphery, as well as part of a diffuse skeleton that ramifies throughout the interior of the nucleus

(Hozak *et al.*, 1995). Proteolytic degradation of lamins facilitates the nuclear events of apoptosis, perhaps by facilitating nuclear breakdown (Mckeon, 1991). Caspase-3 cleaves A- and B-type lamins (Duband-Goulet *et al.*, 1998) at a conserved aspartic acid residue at position 230 (Rao *et al.*, 1996). There are various models of how lamin cleavage facilitates apoptosis. Since lamins serve to anchor and to organise chromatin at the nuclear periphery, lamin proteolysis may allow detachment of DNA at the site where it contacts the lamina, and chromatin condensation into discrete packages. Inhibition of lamin degradation causes the DNA to "marginate", i.e, collapse against the periphery of the nucleus, causing hollowing of the nucleus and, thus, the lamina may involute along with the nuclear membranes. Lamin proteolysis may facilitate nuclear breakdown by permitting entrance of cytoplasmic proteases into the nucleus, allowing degradation of other nuclear substrates, as well as rendering the nucleases accessible to activation by cytoplasmic factors. Thus, lamins may represent a key substrate for the proteases activated during apoptosis (Rao *et al.*, 1996).

Lamin B receptor (LBR), a transmembrane protein of the inner nuclear membrane, interacts through its nucleoplasmic amino-terminal domain with both heterochromatin and B-type lamins, and is phosphorylated throughout the cell cycle but on different sites in interphase and mitosis. It is reported that (i) the amino-terminal domain of LBR is specifically cleaved during apoptosis; (ii) the proteolysis of LBR is a late event of apoptosis and occurs after lamin B cleavage; (iii) the phosphorylation of LBR during apoptosis is similar to that occurring during interphase. As condensed chromatin associates with the inner nuclear membrane until the late stages of apoptosis, it was suggested that the LBR plays a major role in maintaining this association (Soullam and Worman, 1993).

LBR has an amino-terminal domain of approximately 200 amino acids followed by a hydrophobic, carboxy-terminal domain with eight putative transmembrane segments. The amino-terminal domain of LBR contains three domains, each of them interacting with a nuclear component, B-type lamins, DNA, and histone protein 1 (HP1) chromatin proteins, respectively (Soullam and Worman, 1993). Due to the modular structure of its amino-terminal domain, the binding of LBR to chromatin is multivalent. Thus, chromatin-membrane association may persist, even after the processing of one or two of these components, and it has been suggested that a factor that may contribute to the

permanent association with the nuclear membrane may be the resistance of LBR to proteolysis until the late stages of apoptosis. During the ultimate stages of apoptosis, LBR proteolysis may be a cause or a consequence of nuclear envelope breakdown, releasing the chromatin-membrane association (Duband-Goulet *et al.*, 1998).

Other structural proteins of the nuclear matrix, such as nuclear matrix (NuMa) protein and topoisomerase II, are also key substrates for caspases (Duband-Goulet *et al.*, 1998).

2.1.4 The cytoplasmic phases of execution

By subdividing the execution phase into three sequential phases, almost all the data obtained on extra-mitochondrial and extra-nuclear execution phase events can be organised into a relatively coherent model (Fig. 2.1).

While it is still too early to generate a precise model of this critical aspect of apoptosis, it is possible to organise most of the results as they pertain to 3 distinct stages: release, blebbing and condensation (Fig. 2.1) (Mills *et al.*, 1999).

2.1.4.1 Release (actin reorganisation)

The process of "rounding up" is most dramatic in cells that are spread out, with firm matrix attachments and stress fibres, such as fibroblasts and epithelial cells (Brancolini *et al.*, 1997; Huot *et al.*, 1998), and requires actin rearrangement (Huot *et al.*, 1998). During anoikis (apoptosis due to detachment from the ECM), rounding up of cells results in disruption of focal adhesion kinase (FAK) signalling, leading to changes in a variety of key signal transduction pathways (Ilic *et al.*, 1998). The process of rounding up requires the cleavage or modification and involvement of several proteins:

(i) Intracellularly, FAK as well as three other focal adhesion (FA) structural proteins (α-actinin, talin and p130-CAS) that link actin to FAs are cleaved (van de Water *et al.*, 1999).

(ii) Another structural FA protein, paxillin, is dephosphorylated and dissociates from the FA (Bannerman *et al.*, 1998).

(iii) Hsp27 is critical for actin reorganisation (Huot *et al.*, 1998).

(iv) Gelsolin is also implicated in this phase (Kothakota *et al.*, 1997).

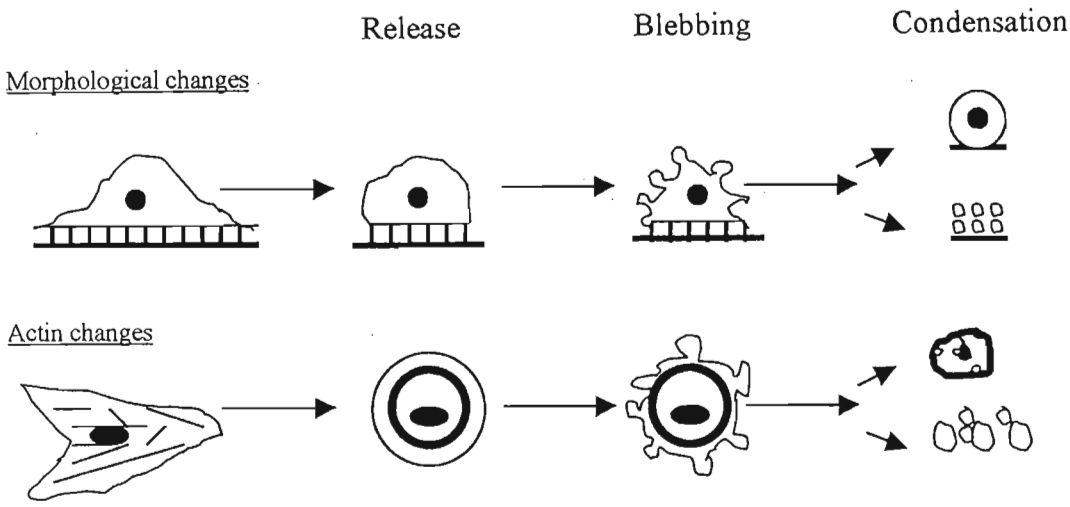

Figure 2.1 Scheme for temporal and mechanistic organisation of the cytoplasmic execution phase. In the model proposed, the first stage is release. As most cells enter the execution phase, they release ECM and cell-cell attachments and reorganise focal adhesions, adopting a more "rounded" morphology. This outward change correlates with the loss of stress fibres (if present) and a reorganisation of actin into a peripheral (cortical), membrane-associated ring. Microtubule disassembly also occurs in this stage. The blebbing stage begins with myosin II-dependent contraction of the actin ring followed by a period of sustained, dynamic plasma membrane protrusion and retraction. It continues until finally the cell enters the condensation stage, which is characterised by fragmentation into small apoptotic bodies or condensation into a single shrunken ball, correlating with the dissolution of polymerised actin. From Mills *et al.* (1999).

(v) Microtubule (MT) disassembly occurs early in the execution phase and may be necessary for cells to round up (Mills *et al.*, 1998a). Besides crippling intracellular transport, disassembly of MTs alters cellular compartments and releases a number of regulatory proteins that are normally bound to MTs (Reszka *et al.*, 1997).

(vi) Caspases, which cleave FA proteins, are implicated, but not all cell types require caspase activity for completion of this phase (Mills *et al.*, 1998b).

(vii) Calpains, which cleave α-actinin, fodrin and talin, structural proteins linking actin and the plasma membrane, are also implicated in release (Kneppler-Nicolai *et al.*, 1998).

2.1.4.2 Blebbing (actin-myosin II contraction)

After the cell rounding-up that occurs during release, the model proposed involves myosin II activation, which centripetally contracts the cortical actin ring (Fig. 2.2). The existence of a cellular checkpoint between release and blebbing has been suggested.

Plasma membrane blebbing and cellular fragmentation have been shown to depend upon actin polymerization. This could be dependent on fodrin integrity (Cotter *et al.*, 1992), since fodrin cleavage results in the reduced ability to cross-link actin filaments (Harris and Morrow, 1990), and has been implicated in blebbing, and fodrin is cleaved by caspases (Martin *et al.*, 1995). The ezrin, moesin, radixin family of actin membrane-linking proteins are also dephosphorylated and dissociated from the membrane (i.e., loss of microvilli) during the execution phase (Kondo *et al.*, 1997).

Myosin light chain kinase (MLCK), which activates nonmuscle myosin II by phoshorylating the regulatory light chain, is necessary for initiation and propagation of blebbing (Mills *et al.*, 1998b). Large amounts of ATP are required to maintain myosin contractility to allow blebbing to take place. Cellular energy generation needs, therefore, to be maintained during apoptosis (Nicotera and Leist, 1997).

2.1.4.3 Condensation (actin dissolution)

All cells eventually stop blebbing, usually after about an hour. Cessation of blebbing is followed by fragmentation into small apoptotic bodies, or condensation into a small ball with actin and MTs largely disassembled or degraded (Mills *et al.*, 1998a), both of which may represent a distinct stage of the execution phase, immediately downstream of blebbing. There may be a cellular checkpoint between blebbing and condensation, or perhaps cells can condense only after enough cytoskeleton has been dismantled/reorganised to allow cytoplasmic dissolution (Mills *et al.*, 1999).

It has been suggested that caspases are important in this process. The role of caspases in cell shrinkage events may be to limit blebbing and induce condensation (Mills *et al.*, 1999), as inhibition of caspases leads to either no morphological changes during apoptosis, or to cells trapped in a blebbing state, and unable to condense (McCarthy *et al.*, 1997), since morphological changes occur downstream of caspase activation (Fig. 1.2).

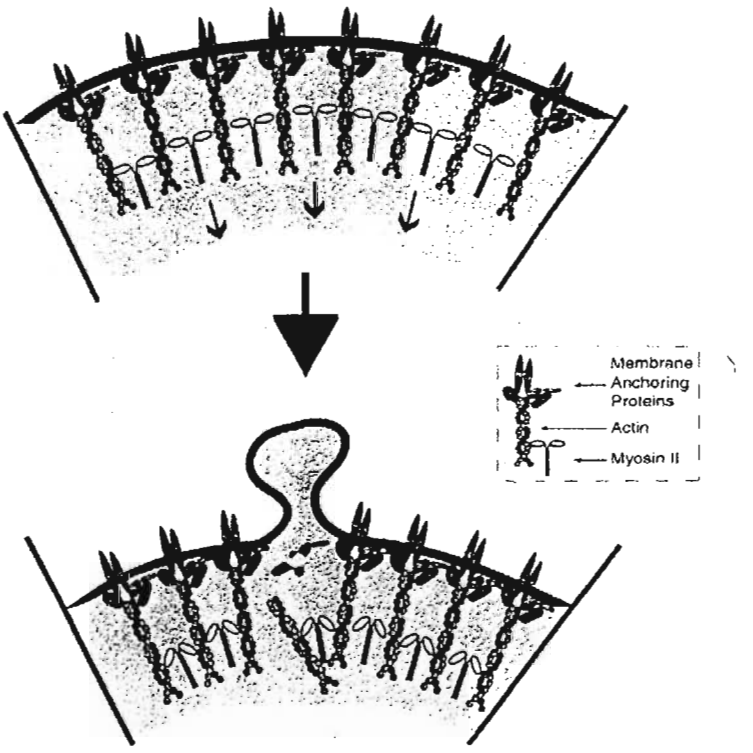

Figure 2.2 Model for bleb extrusion.

Contraction of cortical actin ring filaments by myosin II causes contraction of the plasma membrane, except in focal regions of weakness where the links that actin-membrane linking proteins provide between actin cytoskeleton and the plasma membrane may be broken focally, allowing blebs to protrude at foci where the plasma membrane is no longer anchored to the cytoskeleton. The combination of contraction and focal loss of membrane support leads to bleb formation. A counterforce (perhaps myosin I or VI) retracts the blebs and the cycle repeats. Actin and myosin may concentrate at the base of the blebs, and a thin rim of membrane-associated actin lines the blebs. From Mills *et al.* (1999).

In some cells, activation of the protein cross-linking enzyme, transglutaminase, has been implicated in cytoplasmic packaging during condensation (Fesus, 1993). It has been proposed that the transglutaminase activity leads to the formation of a highly cross-linked, rigid framework within apoptotic bodies, which aids in maintaining their integrity and, thus, in preventing leakage of their contents into the extracellular space (Kerr *et al.*, 1994).

Apoptosis is known to be a broadly conserved means of eliminating cells without damaging neighbouring cells or releasing potentially inflammatory free DNA and, hence, without inciting an immune response, as DNA remains packaged in discrete bodies

surrounded by membranes. The release, retraction and condensation stages result in the formation of a smaller cell or cell fragments for facilitated phagocytic clearance. For cells that maintain strong cell-cell contacts (such as epithelial cells), the cytoplasmic execution phase machinery may be very important, as the contraction of an apoptotic cell may occur to preserve an intact monolayer, by allowing neighbouring cells to move into the gap created by the dying cell. This is thought to be the case in epithelial monolayers as stretching of neighbouring cells towards the dying cell is seen to occur, and stress fibre formation is induced in the neighbouring cells, suggesting that they are being pulled into the spaces (Mills *et al.*, 1999).

The most important aspect of apoptosis is that death occurs without the release of potentially pathogenic or harmful macromolecules, such as free DNA and enzymes, and without the induction of inflammation or injury to surrounding cells. A primary role of the execution phase is to ensure that the dying cell is packaged to avoid these potentially devastating consequences (Mills *et al.*, 1999).

2.1.5 Phagocytosis

Recognition and removal is the final common event in most apoptotic cells (Fadok *et al.*, 1998). Apoptotic bodies arising in tissues are quickly ingested by nearby cells and degraded within their lysosomes. Phagocytes and various types of resident cells, including epithelial cells, participate in the removal of apoptotic bodies (Kerr *et al.*, 1994). The presence, on the phagocyte, of receptors capable of mediating the recognition and ingestion of dying cells is essential for apoptotic clearance (Platt *et al.*, 1998). In dying cells, changes to the cell surface occur before loss of plasma membrane integrity (Gregory *et al.*, 1998). These changes may be recognised by receptors on macrophages, and may facilitate uptake of apoptotic bodies or condensed cells.

Phosphatidylserine (PS) is usually present on the inner cytoplasmic leaflet of the membrane (Eisel *et al.*, 1998), and is actively confined to the inner cytosolic leaflet of the plasma membrane by aminophospholipid translocase. Inhibition of this enzyme leads to disruption of membrane phospholipid asymmetry and PS exposure at the outer surface, a process possibly requiring a second enzyme for transbilayer lipid scrambling (Vanags *et al.*, 1996). During apoptosis, potassium efflux, due to increased activity of potassium

channels, may also cause charge asymmetry on the plasma membrane, and this may also lead to PS translocation to the outer surface of the membrane. In addition, potassium efflux also leads to loss of plasma membrane potential, and cell volume reduction (Dallaporta *et al.*, 1999). Annexin V, a calcium-dependent phospholipid-binding protein, which has a high affinity for PS, is expressed by macrophages for recognition and phagocytosis of apoptotic cells (Eisel *et al.*, 1998).

Apoptotic changes on the cell membrane may be induced by many reagents, such as those inducing oxidative stress.

2.2 The effect of oxidative stress on cell morphology

Oxidative stress, produced by 20-200 μM H_2O_2-treatment, has previously been shown to induce the morphological changes characteristic of apoptosis, such as DNA degradation, nuclear fragmentation and membrane blebbing, in treated epithelial cells (Goldkorn *et al.*, 1998). This was thought to be triggered via a H_2O_2-induced ceramide signalling pathway. In other studies, on squamous cell carcinoma cells, 110-880 μM H_2O_2 was shown to decrease DNA synthesis, in a dose-dependent manner, while H_2O_2 levels >220 μM caused detachment of cells from the substratum, resulting in a dramatic decrease in the cell density (Ulukaya and Wood, 1998). These authors also showed that apoptosis occurred at 5-10 mM H_2O_2, while >10mM H_2O_2 resulted in necrosis. Studies of neuronal cells proved that mitochondrial membrane potential was unaffected by 25 μM H_2O_2, while 10-30 mM H_2O_2 depolarised mitochondria (Hoyt *et al.*, 1997). Thus, effects of various H_2O_2 concentrations may be cell-type specific, and should, therefore, be characterised for different cell types.

When the half-life of H_2O_2 in a specific cell culture is unknown, it has been recommended that the effect of H_2O_2 in a concentration range of 1 to 500 μM be tested (Muller *et al.*, 1997). Therefore, in the current study, the effects of 100, 250, 500 and 1000 μM H_2O_2 were assessed.

2.3 Characteristics and assessment of levels of H_2O_2

In this study, H_2O_2 was chosen to induce oxidative stress mainly because, as previously mentioned, it is easily available in a pure form, it is cheap, membrane-permeant, and forms a common ROS that has previously been shown to induce apoptosis in cell lines (Chiao *et al.*, 1995; Goldkorn *et al.*, 1998; Ulakaya and Wood, 1998; Hoyt *et al.*, 1997). In this study, Fe^{2+}, in the form of ferrous sulfate, was added to a final concentration of 3 μM (a physiological concentration) in order to increase the reactivity of H_2O_2 (Halliwell and Gutteridge, 1990). The reaction of H_2O_2 with Fe^{2+} is referred to as the Fenton reaction and results in the highly reactive •OH, which has a very short life. H_2O_2 also reacts with other transition metals, such as cobalt, copper, vanadium, chromium and nickel, which catalyse H_2O_2 breakdown to •OH (Halliwell and Gutteridge, 1990). H_2O_2, however, does not react with less reactive metals like potassium and phosphate, and is stable in their presence. It has been recommended that treatment with pro-oxidant stimuli, such as H_2O_2, should be performed in a simple, defined buffer, such as phosphate buffered saline (PBS), which contains phosphorus, sodium and potassium without serum, to avoid the possibility of the oxidant being lost by reaction with serum proteins in complex media (Muller *et al.*, 1997).

It is known that concentrated solutions of H_2O_2 disintegrate in solution upon standing for long periods of time, and are heat- and light-sensitive (Brown, 1974). However, intermediately dilute solutions like the stock solutions used in the experiments described here, are more stable provided they are stored in clean, smooth glass containers which are free of dust and transition metals (Brown, 1974).

As this study was a preliminary study, the actual levels of H_2O_2 used and ROS generated were not deemed critical, as long as they were adequate for the induction of apoptotic phenomena in the test cells used in this study. Thus, the amount of H_2O_2 present in the purchased solution of 30% (m/v), from which stock solutions were made, was assumed to be correct. It was considered more important that the relative amount of reactive species compared to the original undiluted stock solution was stable upon sterilisation and storage. To ensure that degradation of H_2O_2 did not occur upon such treatment of solutions, levels of H_2O_2 in the various stock solutions were determined prior and after such treatment, and periodically thereafter. This was done by a method

employing horseradish peroxidase (HRPO) to catalyse the breakdown of H_2O_2, and 2,2'-azino-di-(3-ethyl)-benzthiozoline sulfonic acid (ABTS) as an indicator system. The amount of HRPO to be used in this assay was optimised, and a standard curve of absorbance against H_2O_2 levels was generated, so that the relative amount of H_2O_2 in solutions could be monitored and assessed. These assays were done in 96-well ELISA plates.

2.3.1 Reagents

Phosphate buffered saline (PBS), pH 7.2. NaCl (8 g), KCl (0.2 g), $Na_2HPO_4.2H_2O$ (1.15 g) and KH_2PO_4 (0.2 g) were dissolved, adjusted to pH 7.2, and made up to 1 l with dist.H_2O.

1 mg/ml HRPO stock. HRPO (1 mg, Sigma) was dissolved in PBS (1 ml).

0.15 M Citrate-phosphate buffer, pH 5.0. A solution of citric acid (21 g/l) was titrated with a solution of $Na_2HPO_4.2H_2O$ (35.6 g/l) to pH 5.0.

ABTS indicator solution [0.05% (m/v) ABTS in citrate-phosphate buffer, pH 5.0]. ABTS (7.5 mg, Boehringer Mannheim) was dissolved in phosphate buffer, pH 5.0 (15 ml).

2.3.2 Procedure

For optimisation of HRPO levels, HRPO stock solution was serially diluted to give 1 μg HRPO/well to 1.2 x 10^{-4} μg HRPO/well, and was added, in quadruplicate, to an ELISA plate. The μM level of H_2O_2 used for this study was as indicated in Section 2.2 (100, 250, 500 and 1000 μM). An excess of the maximum amount of H_2O_2 required to be detected by the HRPO assay was chosen as the constant amount of H_2O_2 to be added to each well, i.e., the assay was required to give the maximum readable absorbance for the added amount of H_2O_2, and thereafter, a linear response to decreasing levels of H_2O_2. ABTS indicator solution (150 μl/well) and 150 mM H_2O_2 was added, the colour

developed for 15 min, and the absorbance at 405 nm was measured on a Titertek™ ELISA plate reader.

For the H_2O_2 calibration, 3.9×10^{-3} µg HRPO/well was added to an ELISA plate, serially diluted (untreated commercial) H_2O_2 was added (to a final concentration of 150 mM/well to 2.86×10^{-4} mM/well) to the ABTS indicator solution, in quadruplicate wells, the colour developed for 15 min, and the absorbance at 405 nm read. The relative amounts of H_2O_2 in autoclaved stored and diluted stock solutions were checked by reading the absorbance of a 1 µl sample. The concentration was calculated by linear regression analysis of the slope of the calibration curve.

2.3.3 Results

The level of HRPO to use for the H_2O_2 calibration curve (3.9×10^{-3} µg/well) was chosen on the basis of producing the maximum quantifiable signal at 405 nm and producing a linear calibration graph over the H_2O_2 test range. The 10 and 100 mM H_2O_2 stock solutions, which were tested prior and after autoclaving and periodically thereafter, were found to be stable upon autoclaving and storage, as evidenced by the constant absorbance values obtained in the above test system

2.4 Application of H_2O_2 in the current study

When cells were treated with H_2O_2, serum was omitted from the cell growth medium since it contains endogenous peroxidases, which may detoxify the H_2O_2. Untreated and H_2O_2-treated cells were observed using both light and electron microscopy, and checked for the induction of morphological signs of either apoptosis or necrosis.

2.4.1 Light microscopy

The effects of oxidative stress on cells can be determined by assessment of morphological changes, using light microscopy. H_2O_2-induced toxicity was observed as rounding-up of cells, and stretching of cells in an effort to cover gaps on the substratum

left by cells which have rounded-up and become detached. The latter phenomena are associated with apoptosis, while the appearance of cells with indistinct edges is associated with necrosis.

2.4.1.1 Reagents

Phosphate buffered saline (PBS), pH 7.2. See Section 2.3.1.

10 mM H_2O_2 Stock. An aliquot (114 µl) of H_2O_2 (30% (m/v)) was made up to 100 ml with PBS, autoclaved, and stored in a foil-covered bottle.

100 mM H_2O_2 Stock. An aliquot (1.14 ml) of H_2O_2 (30% (m/v)) was made up to 100 ml with PBS, autoclaved, and stored in a foil-covered bottle.

300 µM Ferrous sulfate stock. Immediately before use, $FeSO_4.7H_2O$ (0.0083 g) was dissolved in MilliQ H_2O (MQ, ultrapure water, 100ml).

DMEM-F12 Basal medium. DMEM-F12 mixture (1 bottle, Sigma) was dissolved in MQ H_2O (900 ml), with stirring. $NaHCO_3$ (1.2 g) was dissolved in a little MQ H_2O and added. The pH was adjusted to pH 7.2 using 1 M NaOH or HCl, and the solution was made up to 1 litre. The solution was filter-sterilised using a Sterivex 0.22 micron filter (Millipore) and stored as 200 ml aliquots at 4°C.

Hanks Balanced Salt Solution (HBSS). HBSS (1 bottle, Sigma) was dissolved in MQ H_2O (900 ml), with stirring. $NaHCO_3$ (0.35 g) was dissolved in a little MQ H_2O and added. The pH was adjusted to pH 7.2 using 1 M NaOH or HCl, and the solution was made up to 1 litre. The solution was filter-sterilised, and stored as 500 ml aliquots at 4°C.

50 µg/ml Epidermal growth factor (EGF) stock. EGF (100 µg, Upstate Biotechnology) was dissolved in sterile H_2O (2 ml) and frozen at -20°C.

600 µg/ml Insulin stock. Sterile HBSS (9.7 ml) was added to insulin (6 mg, Sigma). NaOH (0.3 ml, 0.1 M) was used to restore the pH to pH 7.2, and dissolve the insulin, and the solution was filtered with a 0.22 micron filter and stored at -20°C.

3.333 mg/ml Hydrocortisone stock. Hydrocortisone (10 mg, Sigma) was dissolved in absolute ethanol (3 ml) and stored at -20°C.

Complete medium. For the complete medium, EGF stock (80 µl), insulin stock (3.333 ml), and hydrocortisone stock (30 µl) were added to an aliquot of DMEM-F12 (200 ml). Horse serum (10 ml, GibcoBRL) and 100x antibiotic/antimycotic (2 ml, GibcoBRL) were added. Complete medium was also made up without serum for treatment of cells with H_2O_2.

Trypsin-EDTA working solution. Trypsin-EDTA (10 ml of a 10x solution, GibcoBRL) was diluted with HBSS (90 ml) and stored as 10 ml aliquots at -20°C.

2.4.1.2 Procedure

Cells stored in liquid nitrogen were re-established as a cell line by rapid thawing, and addition to a flask containing complete medium warmed to 37°C. Once cells were confluent, they were subcultured, and 25 cm^3 flasks seeded ($1x10^6$ cells/5ml medium) approximately 24 hours before treatment with H_2O_2. In all the experiments, cells were treated while they were growing exponentially (in subconfluent, 70-80% confluency). Medium was siphoned off, cells rinsed with HBSS, serum-free medium and varying volumes of H_2O_2 were added to final concentrations of 100, 250, 500 and 1000 µM (50 µl of 10 mM H_2O_2, and 12.5 µl, 25 µl and 50 µl of 100 mM H_2O_2, respectively). Fe^{2+} was added to all the flasks to a final concentration of 3 µM and cells exposed to H_2O_2 for various time periods (1, 4, 8 and 24 h). A range of H_2O_2 concentrations and times was tested to determine if the response in the two cell lines used might differ.

Cells were photographed using 100ASA film (1 sec, F8-11) prior to treatment and then at 1, 4, 8 and 24 hours after treatment, at 100x magnification on an Olympus CK2 inverted microscope.

2.4.1.3 Results

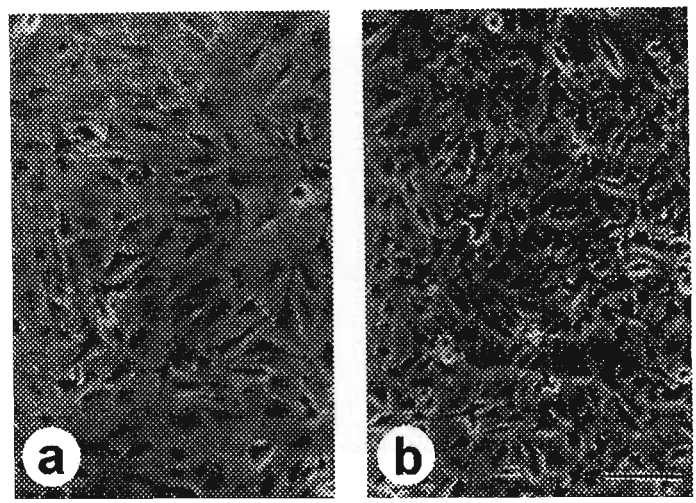

Figure 2.3 Morphology of untreated MCF10A and MCF10AneoT cells.
(a) MCF10A and (b) MCF10AneoT cells prior to treatment (controls). Bar = 100 μm.

Both the MCF10A and MCF10AneoT untreated cells, at 70-80% confluence, had a uniform distribution on the cell culture flasks. The cell peripheries were well-defined, and cells were of a high density, exhibiting only a few gaps, a moderate degree of stretching and a little rounding-up of cells (Fig. 2.3, a and b).

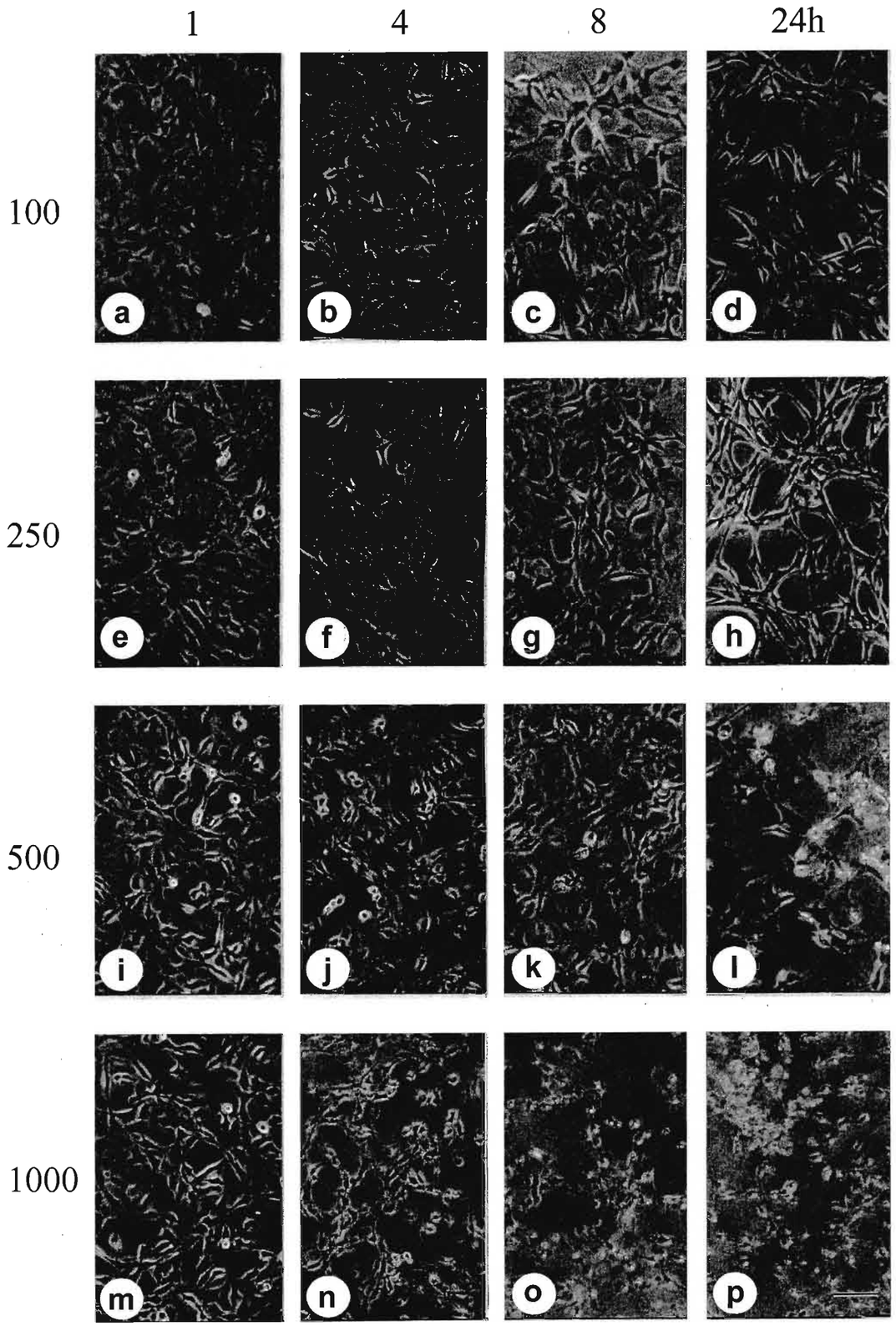

Figure 2.4 Morphological assessment of cell death of MCF10A cells by light microscopy. MCF10A cells treated with 3 μM Fe^{2+} in serum-free medium, and (a-d) 100 μM H_2O_2 after (a) 1 h, (b) 4 h, (c) 8 h, (d) 24 h; (e-h) 250 μM H_2O_2 after (e) 1 h, (f) 4 h, (g) 8 h, (h) 24 h; (i-l) 500 μM H_2O_2 after (i) 1 h, (j) 4 h, (k) 8 h, (l) 24 h; (m-p) 1000 μM H_2O_2 after (m) 1 h, (n) 4 h, (o) 8 h, (p) 24 h. Bar = 100 μm for all photographs.

A general trend of progressively increasing cell damage was noted in the MCF10A cells with increasing H_2O_2 concentration and time of treatment (Fig. 2.4). After 24 h of exposure to 100 μM H_2O_2 (Fig. 2.4, a-d) and 250 μM H_2O_2 (Fig. 2.4, e-h), the MCF10A cells appeared slightly more elongated or "stretched" and had more spaces between the cells (Fig. 2.4, d and h, respectively) than the untreated cells (Fig. 2.3, a). Stretching and loss of cells was less obvious during the exposure to 500 μM H_2O_2 (Fig. 2.4, i-l). However, after 24 h of exposure to 500 μM H_2O_2 (Fig. 2.4, l) cells became "rounded", as is characteristic of apoptotic morphology (Kerr *et al.*, 1994), damage being progressively more evident from 8 h onwards. Damage inflicted by treatment with 1000 μM H_2O_2 (Fig. 2.4, m-p) was more severe and damage was visible from 4 h of treatment, the cells becoming increasingly detached from the flask, less distinctly defined and possibly necrotic from 4 h onwards, with loss of cells by total detachment from the flask (or lysis) being clearly evident by 8-24 h (Fig. 2.4, o, p).

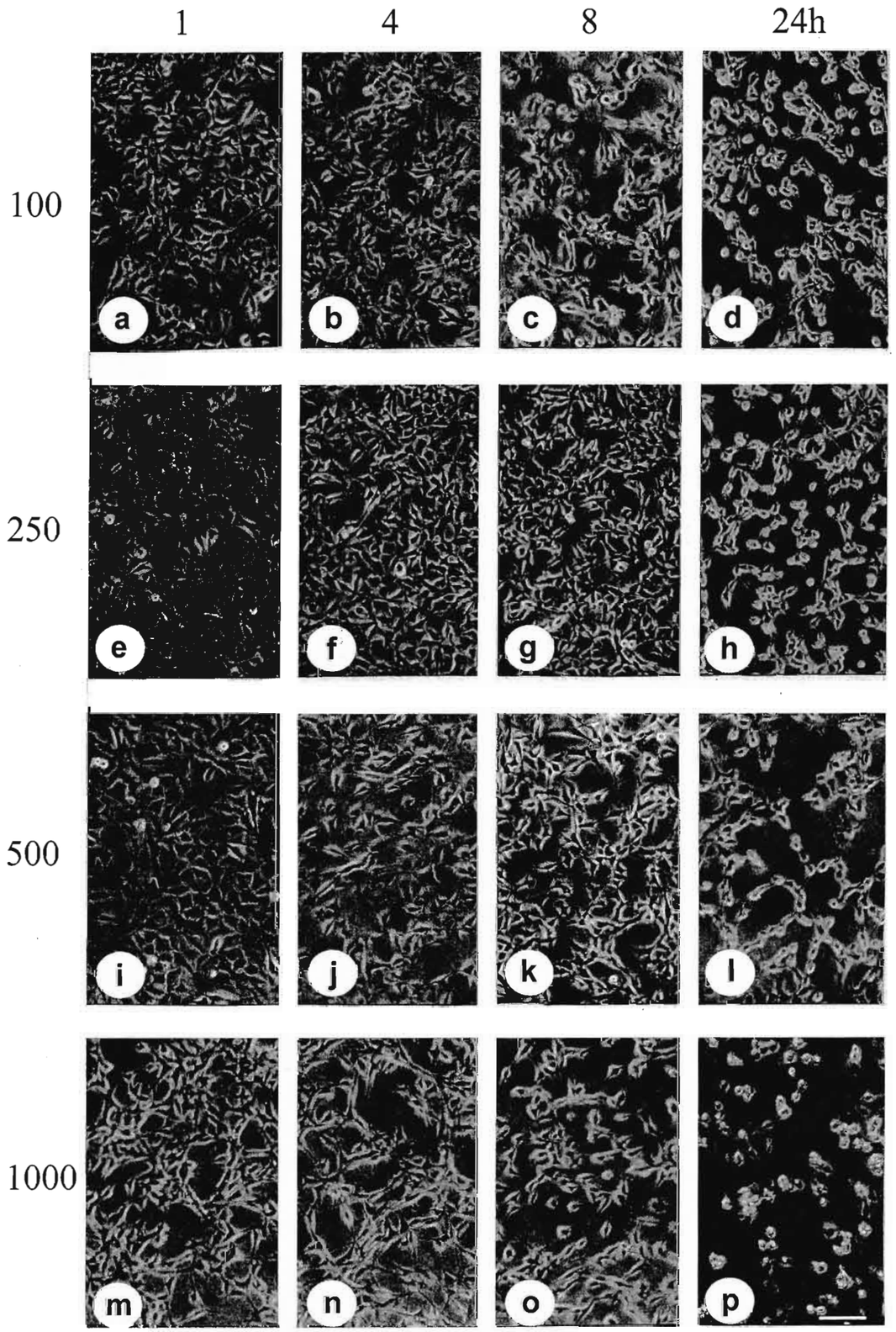

Figure 2.5 Morphological assessment of cell death of MCF10AneoT cells by light microscopy.
MCF10AneoT cells treated with 3 μM Fe^{2+} in serum-free medium, and (a-d) 100 μM H_2O_2 after (a) 1 h, (b) 4 h, (c) 8 h, (d) 24 h; (e-h) 250 μM H_2O_2 after (e) 1 h, (f) 4 h, (g) 8 h, (h) 24 h; (i-l) 500 μM H_2O_2 after (i) 1 h, (j) 4 h, (k) 8 h, (l) 24 h; (m-p) 1000 μM H_2O_2 after (m) 1 h, (n) 4 h, (o) 8 h, (p) 24 h.
Bar = 100 μm for all photographs.

As seen in the MCF10A cells, progressively increasing cell damage was visible with increased concentration and time of treatment, although at 250 and 500 μM H_2O_2, the cells seem more tolerant to the oxidative stress and for a greater time. The MCF10AneoT cells showed much greater sensitivity than the MCF10A cells to the lower H_2O_2 levels (100 and 250 μM, Fig. 2.5, a-d, e-h, respectively). At 100 μM H_2O_2 cell damage was visible within 8 h (Fig. 2.5, c), cells becoming visibly detached, while at 250 μM, damage was evident remarkably only at 24 h (Fig. 2.5, h). With 1000 μM H_2O_2, however, cells appeared "stretched" within 4 h, while rounding up was visible from 8 h onwards (Fig. 2.5, o-p). Although the MCF10AneoT cells displayed a visible response at 100 μM H_2O_2, while the MCF10A cells appeared normal at this concentration, the effect of redox stress on the MCF10AneoT cells did not seem as marked as in the MCF10A cells, as the MCF10A cells appeared to be necrotic (cells with indistinct boundaries) by 4 h at 1000 μM while the MCF10AneoT cells showed no obvious necrosis and fewer spaces between the cells, indicating that fewer cells were lost by detachment or lysis, except after 24 h of exposure (Fig. 2.5, d, h, l) possibly becoming necrotic after 24 h at 1000 μM H_2O_2 (Fig. 2.5, p).

2.4.1.4 Discussion

Differences in the susceptibility of the two cell types to the H_2O_2-induced oxidative stress manifest in the different extent of cell damage, determined by cellular rounding-up and detachment from the substratum, which in turn resulted in spaces between the adherent cells and floating dead cells in a different focal plane to that photographed.

Rounding-up of cells may be indicative of either cell division or apoptosis, and the rounding (without stretching) of the MCF10AneoT cells at 100 μM H_2O_2 may mean that there is an earlier onset of apoptosis in these cells. The MCF10AneoT cells appear to respond to 100 μM H_2O_2 in a much more uniform manner as they all appear simultaneously rounded, whereas the MCF10A cells seem to be a heterogenous population of cells, with some becoming rounded and detached, while others become stretched to fill the spaces left by dead cells, which have become detached and float in the medium. It also seems that the MCF10AneoT cells are more susceptible to oxidative stress-induced apoptosis (rounding-up) at the lower concentrations of H_2O_2, but are much more resistant to necrosis (their boundaries remaining distinct) than the MCF10A cells at the higher concentrations. The reported non-linear GSH response of tumour cells to oxidative stress (Allen, 1991) may explain why the MCF10AneoT cells appear more resistant to the higher concentrations of H_2O_2. Possibly when they do respond to the oxidative stress, it seems that they may over-respond and, thus, become marginally more resistant to necrosis.

As both cell lines were sub-confluent at all times, both should have been equally susceptible to the induction of apoptosis. The MCF10AneoT, however, appeared more sensitive to the apparent induction of apoptosis (i.e., were more rounded) and this is difficult to explain. The patterns of cellular response are difficult to interpret, as rounding-up of cells could signify either cell division or apoptosis. In addition, the point where cells cease to be apoptotic and become necrotic instead, is unclear from the light microscopic studies and were, therefore, confirmed by examining the ultrastructural details, by electron microscopy.

2.4.2 Electron microscopy

Electron microscopic examination was conducted, as the morphological features of apoptosis and necrosis are visible in much greater detail at this level. Cryoultramicrotomy is a low temperature method in which sucrose serves as a cryoprotectant, during freezing in liquid nitrogen, by replacing the majority of the water in cells. Rapid freezing allows the formation of vitreous ice, which is non-crystalline, and which does not disrupt cell membranes and cell integrity (Tokayasu, 1980). The cells, thus, maintain their structure, as they would in the fully hydrated state. This method was chosen for use instead of the conventional resin embedding procedures because it is much less labour-intensive and time-consuming, omitting hours of dehydration and days of resin infiltration and embedding, while still producing samples hard enough for ultrathin sectioning. Cyroultramicrotomy, however, requires considerable practice and skill.

Viewing of cells processed for electron microscopy allows the definitive features of apoptosis and necrosis to be distinguished, e.g., in necrotic cell death, extensive swelling of the cytoplasm and organelles, including mitochondria, occurs. However, in apoptosis, cellular shrinkage occurs, mitochondria may condense, chromatin is fragmented and closely apposed to the nuclear envelope, which becomes convoluted, and membrane blebbing takes place.

2.4.2.1 Reagents

0.4 M HEPES, pH 7.2. HEPES (23.8 g) was dissolved in MQ H_2O (230 ml). The pH was adjusted to pH 7.2 with NaOH, and the volume was made up to 250 ml.

0.2 M HEPES, pH 7.2. 0.4 M HEPES (125 ml) was diluted with MQ H_2O (120 ml). The pH was adjusted to pH 7.2 if necessary, and the volume made up to 250 ml.

Paraformaldehyde (PFA) stock solution (8% (m/v)). Paraformaldehyde (8 g) was dissolved in MQ H_2O (100 ml), heated (with stirring) to 60°C, and a minimum of concentrated NaOH was added to "clear" the solution, in a fume hood.

2% (m/v) Paraformaldehyde (PFA), 0.05% (v/v) glutaraldehyde in 0.2 M HEPES, pH 7.2. PFA (20 ml of 8% (m/v) stock solution) was added to a mixture of MQ H_2O (20 ml) and 0.4 M HEPES (40 ml). Glutaraldehyde (160 µl of a 25% (v/v) solution) was added to the solution, and the pH adjusted to pH 7.2 with HCl.

0.02 M Glycine in 0.2 M HEPES, pH 7.2. Glycine (0.15 g) was dissolved in 0.2 M HEPES (100 ml).

10% (m/v) Gelatin in 0.2 M HEPES, pH 7.2. Gelatin (10 g) was dissolved in 0.2 M HEPES with gentle heating.

10x PBS, pH 7.2. NaCl (8 g), KCl (0.2 g), $Na_2HPO_4.2H_2O$ (1.15 g) and KH_2PO_4 (0.2 g) were dissolved, the pH adjusted to pH 7.2, and the buffer made up to 100 ml with dist.H_2O.

2.1 M Sucrose in PBS, pH 7.2. Sucrose (71.88 g) was dissolved in a minimum of boiling MQ H_2O, the volume adjusted to 90 ml with MQ H_2O, and PBS (10 ml of a 10x solution) was added.

2.3 M Sucrose in PBS, pH 7.2. Sucrose (78.73 g) was dissolved in a minimum of boiling MQ H_2O, the volume adjusted to 90 ml with MQ H_2O, and PBS (10 ml of a 10x solution) was added.

2% (m/v) Methylcellulose. Methylcellulose (1 g) was dissolved in MQ H_2O (50 ml).

2% (m/v) Aqueous uranyl acetate. Uranyl acetate (1 g) was dissolved in MQ H_2O (50 ml), ethanol (1 ml, 95% (v/v)) added to lower the surface of tension, and stored in a foil-covered bottle at 4°C.

Uranyl acetate/methycellulose mixture. Immediately before use, uranyl acetate (100 µl, 2% (m/v)) was mixed with methylcellulose (900 µl, 2% (m/v)).

2.4.2.2 Procedure

Cells were grown to sub-confluence and treated as in Section 2.4.1.2. After treatment, cells were scraped into the medium with a rubber policeman. Floating rounded cells which had already detached from the substratum were, therefore, not lost. The cells were gently pelleted (460 x g, 3 min), the supernatant discarded, and the cell pellet rinsed with warm HBSS to remove H_2O_2. Cells were harvested in this manner in all future experiments. The harvested cells were fixed on ice (2% (m/v) PFA, 0.05% (v/v) glutaraldehyde, pH 7.2, 1 h), and then at 4°C (overnight). Excess aldehyde groups were quenched by the addition of glycine (0.02 M, 1 h, RT). The pellets were infiltrated with gelatin (10% (m/v), 1 h, 37°C) to facilitate easy handling of the pellet, and minimise cell loss. The cells were then incubated in sucrose cryoprotectant (2.3 M, 4°C, overnight). Cell pellets were cut into small blocks (~1mm^3), under a dissecting microscope, and mounted onto copper stubs (2 x 12 mm) . The excess sucrose was removed by blotting with filter paper, and stubs were frozen and stored in liquid nitrogen, in special cryo racks (Tokayasu, 1980).

Cells were sectioned, at -95°C using a glass knife, in an RMC MT6000XL ultramicrotome fitted with a CR2000 cryo attachment. Sections (~ 90 nm) were retrieved on a droplet of 2.1 M sucrose, using a wire loop, and placed onto formvar-coated hexagonal 100 mesh nickel grids (3 mm ϕ) which were carbon-coated, to support the section, and glow-discharged, to allow sections to "stick" to the carbon. The section-containing grids were floated onto PBS, pH 7.2, rinsed in 5 droplets of double dist.H_2O (1 min each), and stained in a uranyl acetate/methylcellulose mixture. Grids were picked up with a nichrome wire loop (4mm ϕ), and sealed in a thin film of uranyl

acetate/methylcellulose by dragging the edge of the loop along filter paper, thus removing the excess methycellulose mixture. Upon drying, the film sealing the grid should give a pink-blue interference colour in order to be of the correct thickness (Tokayasu, 1980). Grids were viewed in a Philips CW120 Biotwin transmission electron microscope, at 80-100 kV, and photographed.

2.4.2.3 Results

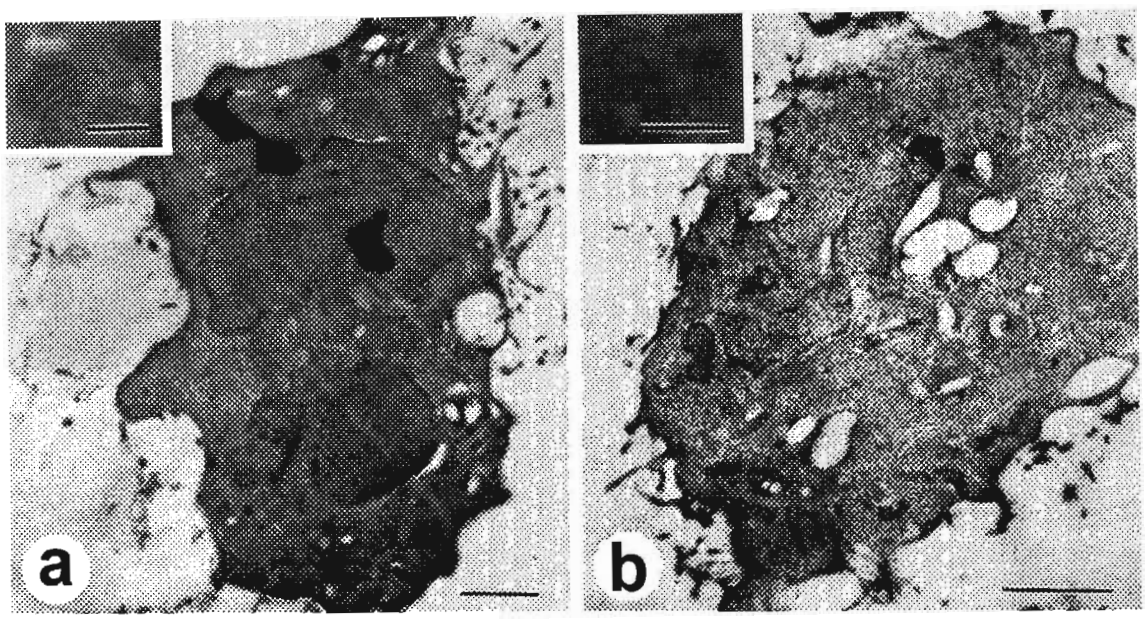

Figure 2.6 Ultrathin cryoultramicrotomy sections of untreated MCF10A and MCF10AneoT cells.
(a) MCF10A and (b) MCF10AneoT cells prior to treatment (controls).
Bar = 2 μm for micrographs of whole cells.
Bar = 500 nm for mitochondrial inserts.

In untreated cells there was no condensation or fragmentation of the chromatin, no apposition of chromatin to the nuclear membrane, a minimal loss of microvilli, a smooth, unconvoluted nuclear membrane and minimal cytoplasmic vacuolisation.

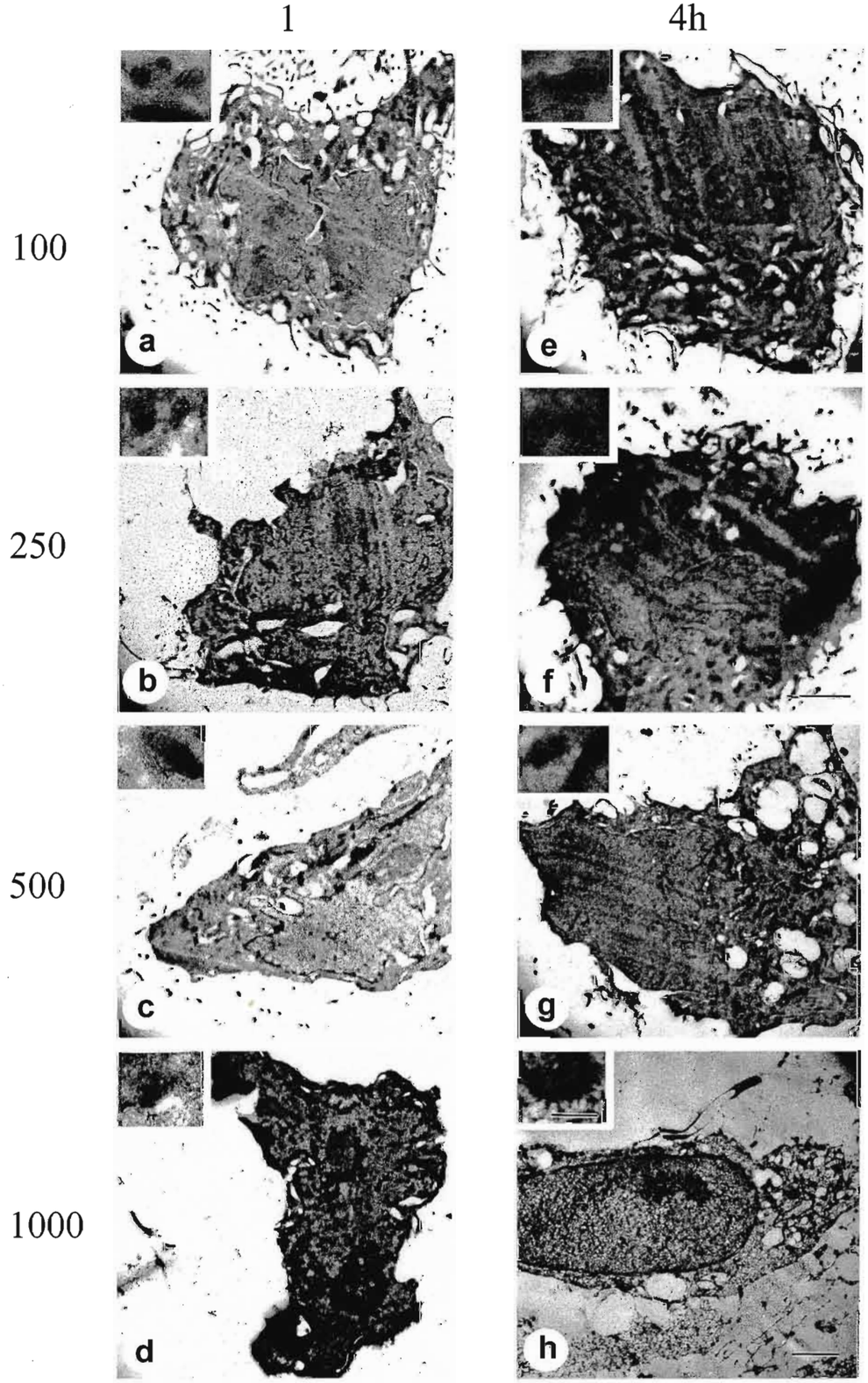

Figure 2.7 Ultrathin cryoultramicrotomy sections of MCF10A cells treated for 1 and 4 hours with H_2O_2 and Fe^{2+}.

MCF10A cells harvested 1 h after treatment with 3μM Fe^{2+} in serum-free medium and (a) 100 μM H_2O_2, (b) 250 μM H_2O_2, (c) 500 μM H_2O_2 (bar = 2 μM), (d) 1000 μM H_2O_2, and 4 h after treatment with 3 μM Fe^{2+} and (e) 100 μM H_2O_2, (f) 250 μM H_2O_2, (g) 500 μM H_2O_2, and (h) 1000 μM H_2O_2.

Bar = 2 μm for all micrographs of whole cells as per (h), unless otherwise shown.

Bar = 350 nm for all mitochondrial inserts.

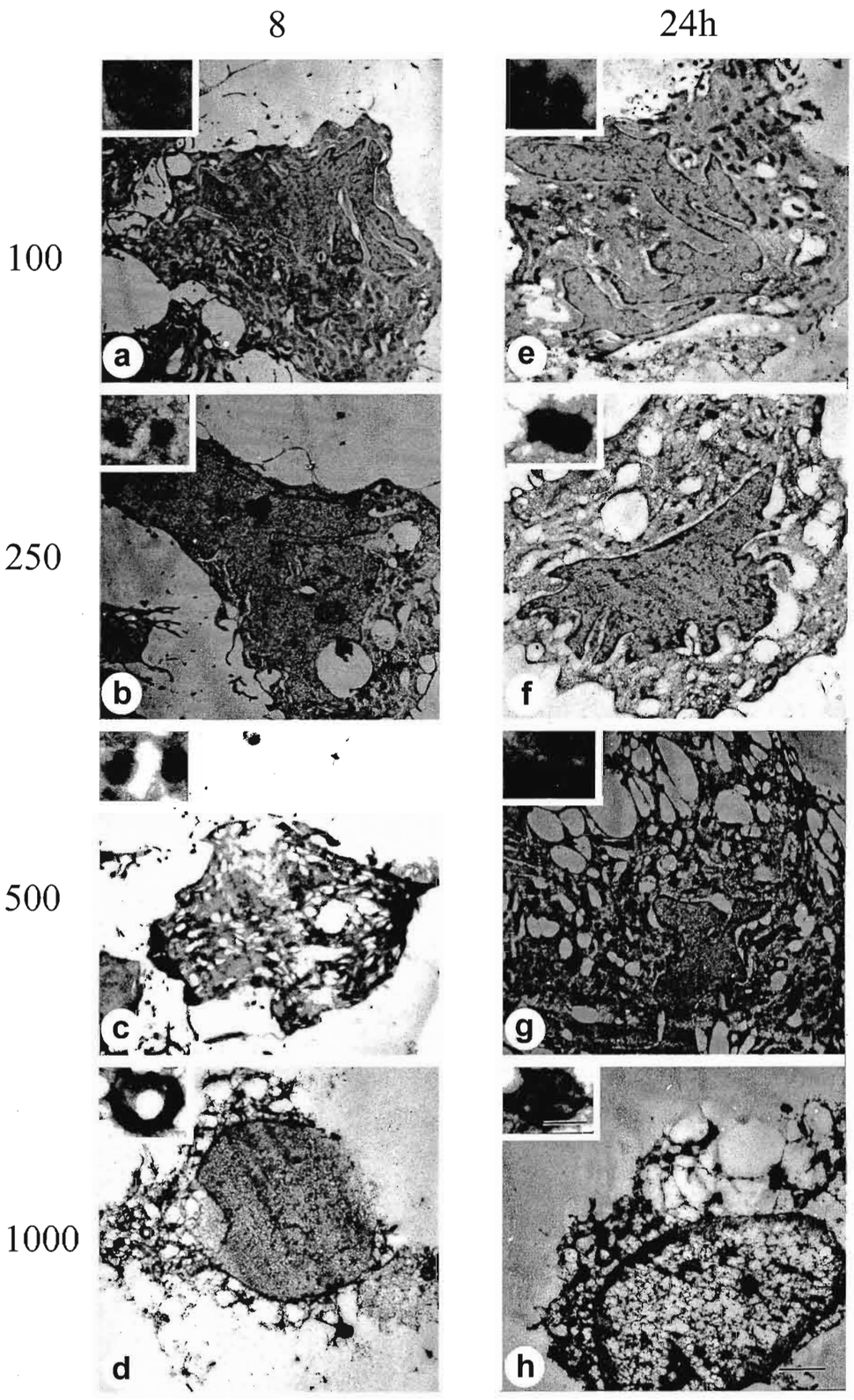

Figure 2.8 Ultrathin cryoultramicrotomy sections of MCF10A cells treated for 8 and 24 hours with H_2O_2 and Fe^{2+}.

MCF10A cells harvested 8 h after treatment with 3μM Fe^{2+} in serum-free medium and (a) 100 μM H_2O_2, (b) 250 μM H_2O_2, (c) 500 μM H_2O_2, (d) 1000 μM H_2O_2, and 24 h after treatment with 3 μM Fe^{2+} and (e) 100 μM H_2O_2, (f) 250 μM H_2O_2, (g) 500 μM H_2O_2, and (h) 1000 μM H_2O_2.

Bar = 2 μm for all micrographs of whole cells.

Bar = 350 nm for all mitochondrial inserts.

As was seen in the light microscopy experiments, an increase in cell damage was evident with increasing concentration and time of treatment. Apoptotic cells were identified by their loss of microvilli, nuclear convolution and apposition of chromatin to the nuclear membrane (chromatin margination), cytoplasmic vacuolisation, and condensed/hyperdense mitochondria. Necrotic cells were identified by the smooth nuclear membrane, plasma membrane rupture and organelle (mitochondria) swelling and lysis. With a few exceptions, all treated MCF10A cells showed some evidence of apoptosis such as loss of microvilli, nuclear convolution, chromatin margination, condensed mitochondria and progressive cytoplasmic vacuolisation with increased concentration and time (Figs 2.7, a-g, 2.8, a-c, e-g), except those treated with 1000 μM H_2O_2 which were apoptotic after 1 h (Fig. 2.7, d), but necrotic from 4 h onwards (Figs 2.7, h, 2.8, d, h), showing the characteristic smooth nuclear membrane, and mitochondrial swelling and rupture.

Mitochondrial proliferation, as reported by Mancini *et al.* (1997), was observed at random times and concentrations of treatment (Figs 2.7, a, c, f, g, 2.8, b, e, f, g).

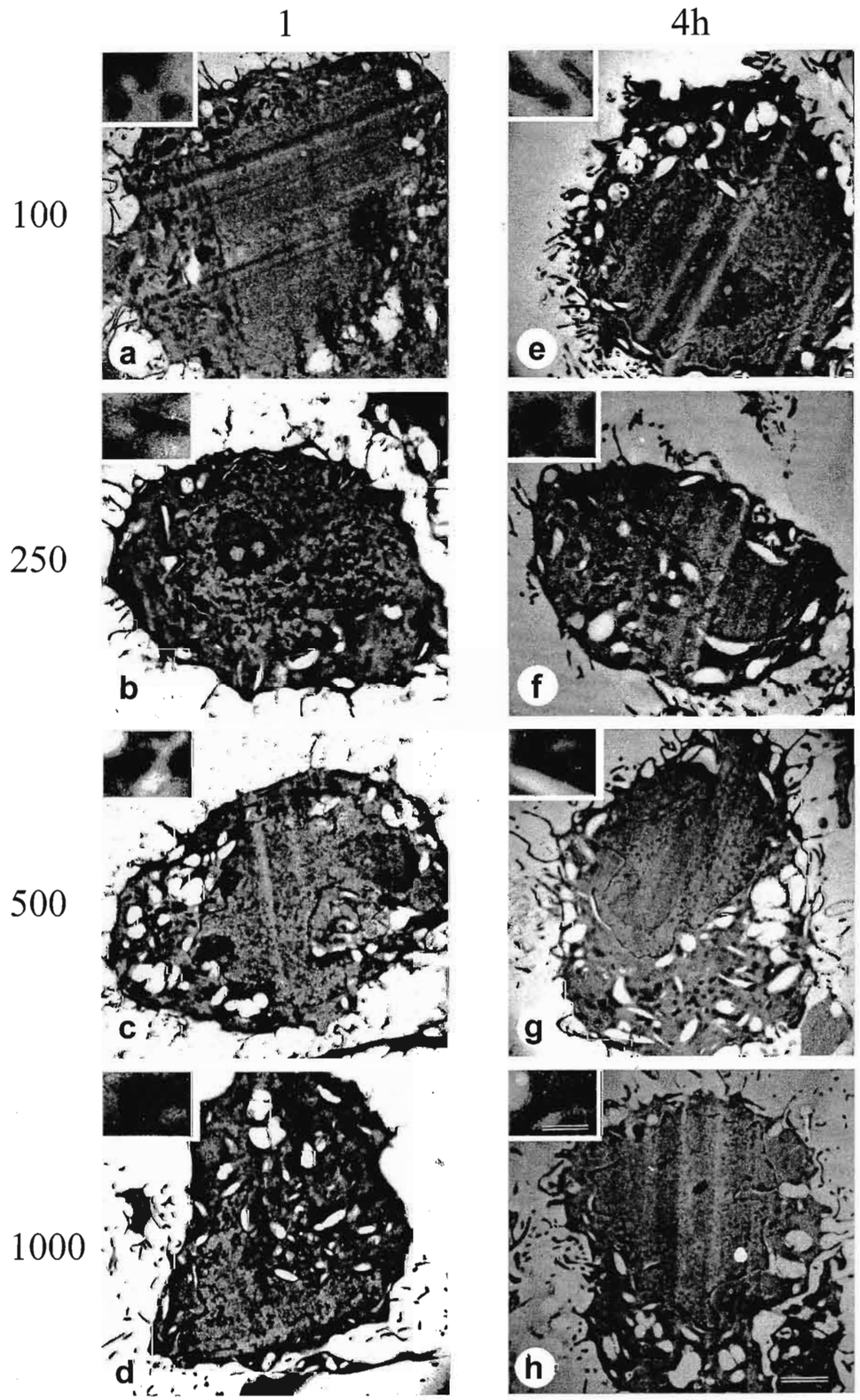

Figure 2.9 Ultrathin cryoultramicrotomy sections of MCF10AneoT cells treated for 1 and 4 hours with H_2O_2 and Fe^{2+}.

MCF10AneoT cells harvested 1 h after treatment with 3μM Fe^{2+} in serum-free medium and (a) 100 μM H_2O_2, (b) 250 μM H_2O_2, (c) 500 μM H_2O_2, (d) 1000 μM H_2O_2, and 4 h after treatment with 3 μM Fe^{2+} and (e) 100 μM H_2O_2, (f) 250 μM H_2O_2, (g) 500 μM H_2O_2, and (h) 1000 μM H_2O_2.

Bar = 2 μm for all micrographs of whole cells.

Bar = 350 nm for all mitochondrial inserts.

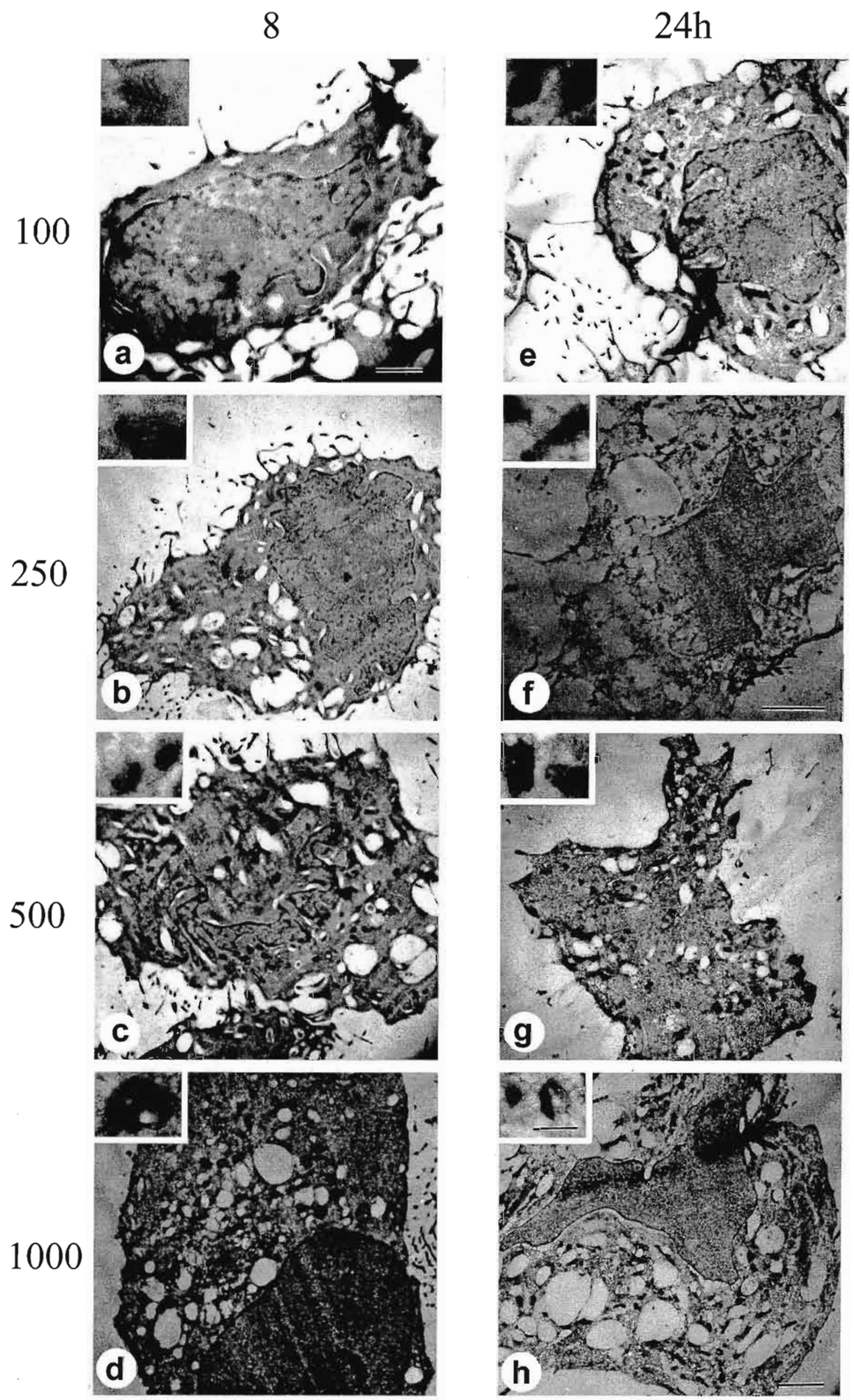

Figure 2.10 Ultrathin cryoultramicrotomy sections of MCF10AneoT cells treated for 8 and 24 hours with H_2O_2 and Fe^{2+}.

MCF10AneoT cells harvested 8 h after treatment with 3μM Fe^{2+} in serum-free medium and (a) 100 μM H_2O_2 (bar = 1 μm), (b) 250 μM H_2O_2, (c) 500 μM H_2O_2, (d) 1000 μM H_2O_2, and 24 h after treatment with 3 μM Fe^{2+} and (e) 100 μM H_2O_2, (f) 250 μM H_2O_2 (bar = 4 μm), (g) 500 μM H_2O_2, and (h) 1000 μM H_2O_2.

Bar = 2 μm for all micrographs of whole cells as per (h), unless otherwise shown.

Bar = 350 nm for all micrographs of mitochondrial inserts.

Besides those treated with 100 μM H_2O_2 for 1 h, most treated MCF10AneoT cells showed signs of apoptosis and showed progressive cytoplasmic vacuolisation with increased concentration and time (Figs 2.9, b-h, 2.10, a-c, e-g). Those treated with 1000 μM H_2O_2 were, however, apoptotic up to 4 h (Fig. 2.9, h), but necrotic from 8 h onwards (Fig. 2.10, d, h), with necrosis also occurring after 24 h of exposure to 250- and 500 μM H_2O_2. Fig. 2.10, d is an example of primary necrosis and Fig. 2.10, h, is an example of secondary necrosis. The latter refers to apoptotic cells in culture which appear very damaged, with a granular/vacuolar cytoplasm and ruptured mitochondria, but an intact and convoluted nucleus, indicating that the cells primary response was apoptosis, and not necrosis. MCF10AneoT cells treated with 500 and 1000 μM H_2O_2 were mixed populations of cells undergoing primary and secondary necrosis, while the MCF10A cells were all primarily necrotic at these concentrations.

As observed in the MCF10A cells, mitochondrial proliferation occurred at random times and concentrations (Figs 2.9, a, c, d, f, g, 2.10 c-h), but more frequently than in the MCF10A cells.

The trend of cellular damage in the form of necrosis corresponds with the light microscopic studies, showing that the MCF10AneoT cells appear to be more resistant than the MCF10A cells to necrosis at the higher levels of H_2O_2 (500 and 1000 μM). Although whole cell examination has proven to be a useful tool to distinguish necrotic cell death, electron microscopic analysis showed that it had little value for distinguishing variable stages of apoptotic cells. The mitochondria, due to their importance in apoptosis and reports of changes in their morphology during apoptotic cell death, were also examined. Enlargements of the inserts in Figs 2.7, 2.8, 2.9 and 2.10 were, therefore,

examined in greater detail in order to establish whether any additional information which could be used could be gathered.

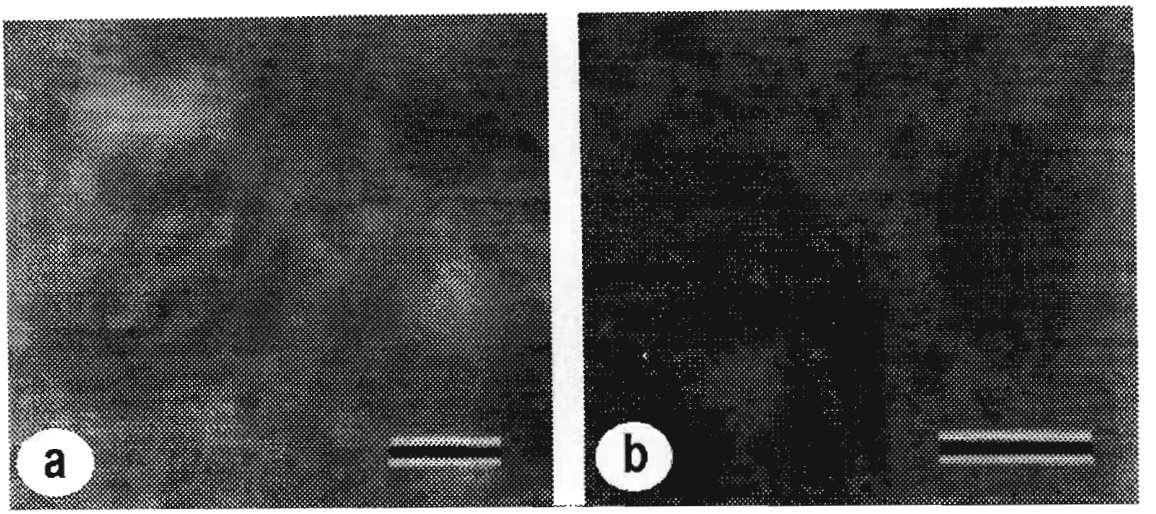

Figure 2.11 Mitochondria from ultrathin cryoultramicrotomy sections of untreated MCF10A and MCF10AneoT cells.

Mitochondria from (a) MCF10A and (b) MCF10AneoT cells prior to treatment (controls). Bar = 250 nm.

Untreated mitochondria of the MCF10A and MCF10AneoT cells appeared to be normal, the mitochondria of the MCF10AneoT cells being slightly elongated. In mitochondria of both cell types no condensation or hyperdensity was evident.

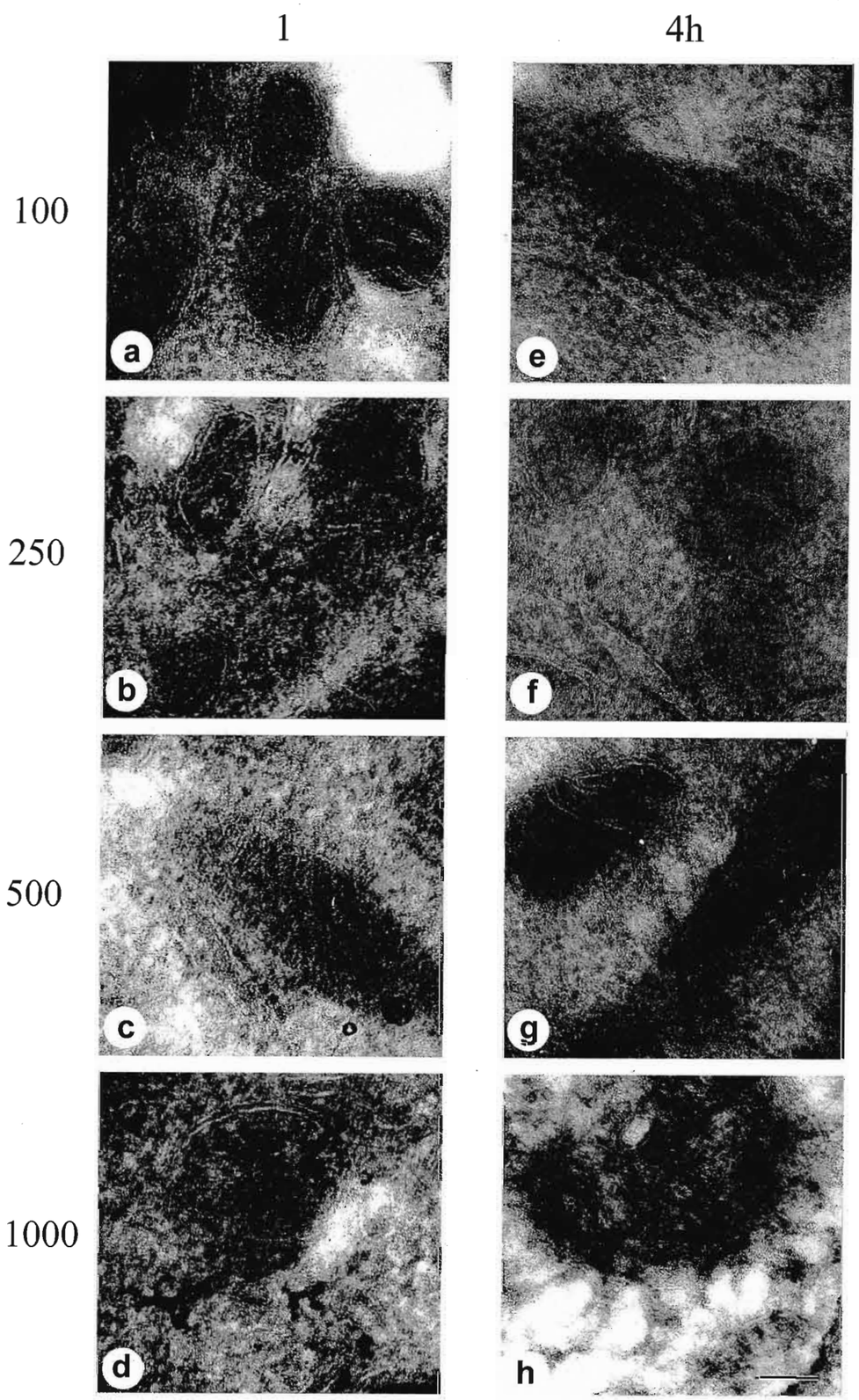

Figure 2.12 Mitochondria from ultrathin cryoultramicrotomy sections of MCF10A cells treated for 1 and 4 hours with H_2O_2 and Fe^{2+}.

Enlargements of mitochondria corresponding to the mitochondrial inserts of Fig. 2.7. Representative mitochondria from MCF10A cells harvested 1 h after treatment with 3μM Fe^{2+} in serum-free medium and (a) 100 μM H_2O_2, (b) 250 μM H_2O_2, (c) 500 μM H_2O_2, (d) 1000 μM H_2O_2, and 4 h after treatment with 3 μM Fe^{2+} and (e) 100 μM H_2O_2, (f) 250 μM H_2O_2, (g) 500 μM H_2O_2, and (h) 1000 μM H_2O_2.

Bar = 125 nm for all micrographs.

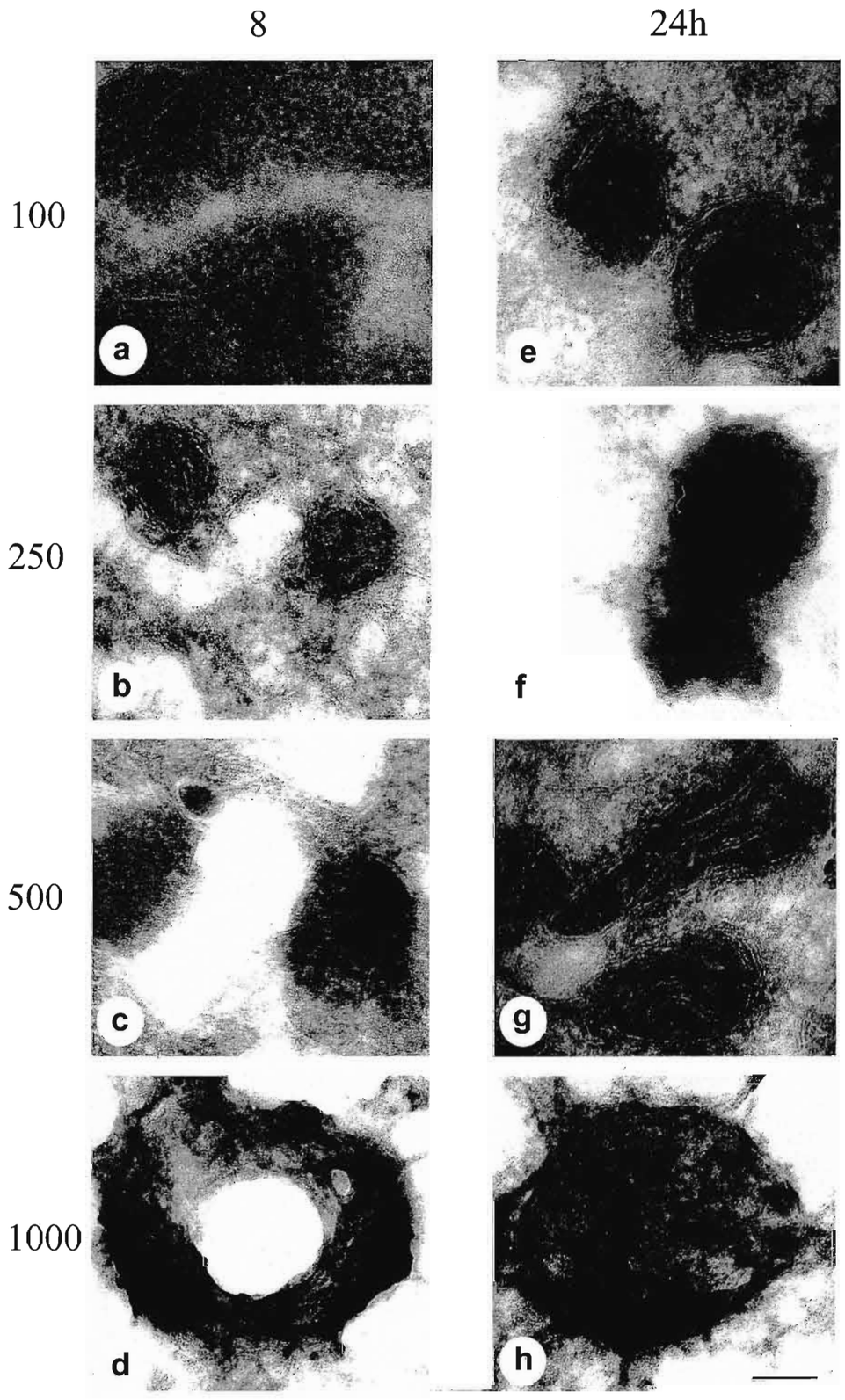

Figure 2.13 Mitochondria from ultrathin cryoultramicrotomy sections of MCF10A cells treated for 8 and 24 hours with H_2O_2 and Fe^{2+}.

Enlargements of mitochondria corresponding to the mitochondrial inserts of Fig. 2.8. Representative mitochondria from MCF10A cells harvested 8 h after treatment with 3μM Fe^{2+} in serum-free medium and (a) 100 μM H_2O_2, (b) 250 μM H_2O_2, (c) 500 μM H_2O_2, (d) 1000 μM H_2O_2, and 24 h after treatment with 3 μM Fe^{2+} and (e) 100 μM H_2O_2, (f) 250 μM H_2O_2, (g) 500 μM H_2O_2, and (h) 1000 μM H_2O_2.

Bar = 125 nm for all micrographs.

Mitochondria from all the treated MCF10A cells appeared to be condensed and very dense, as previously reported to have been seen in apoptotic cells (Mancini *et al.*, 1997), although their membranes seemed to be largely intact (Figs 2.12, a-g, 2.13, a-c, e-g), with the exception of mitochondria from cells treated with 1000 μM H_2O_2 for 4 h or more (Figs 2.12, h, 2.13, d, h), which appeared very swollen and/or ruptured, as seen in necrosis. These results verified the results of the other ultrastructural features observed in the treated MCF10A cells (Figs. 2.7, 2.8).

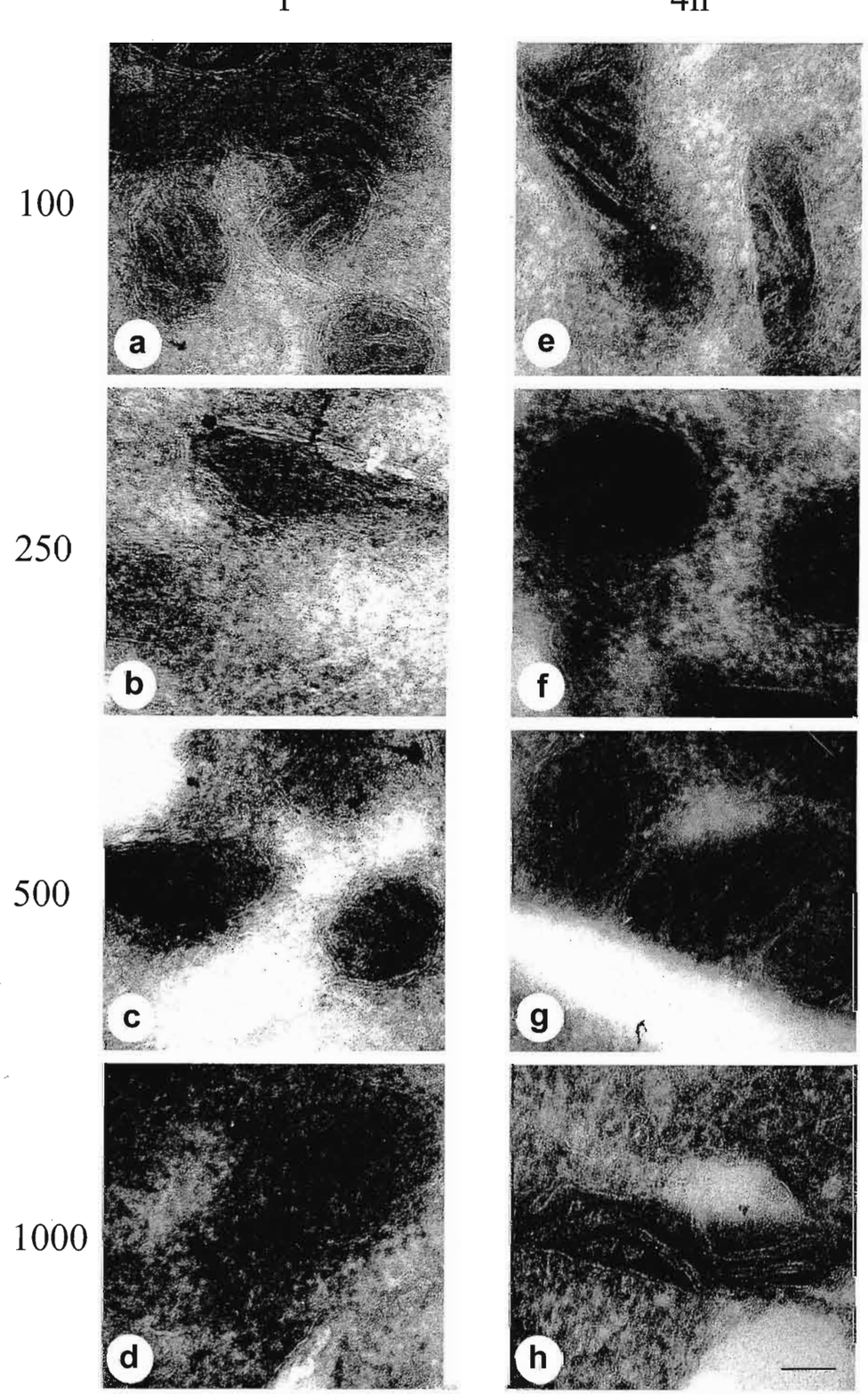

Figure 2.14 Mitochondria from ultrathin cryoultramicrotomy sections of MCF10AneoT cells treated for 1 and 4 hours with H_2O_2 and Fe^{2+}.

Enlargements of mitochondria corresponding to the mitochondrial inserts of Fig. 2.9. Representative mitochondria from MCF10AneoT cells harvested 1 h after treatment with 3μM Fe^{2+} in serum-free medium and (a) 100 μM H_2O_2, (b) 250 μM H_2O_2, (c) 500 μM H_2O_2, (d) 1000 μM H_2O_2, and 4 h after treatment with 3 μM Fe^{2+} and (e) 100 μM H_2O_2, (f) 250 μM H_2O_2, (g) 500 μM H_2O_2, and (h) 1000 μM H_2O_2.

Bar = 125 nm for all micrographs.

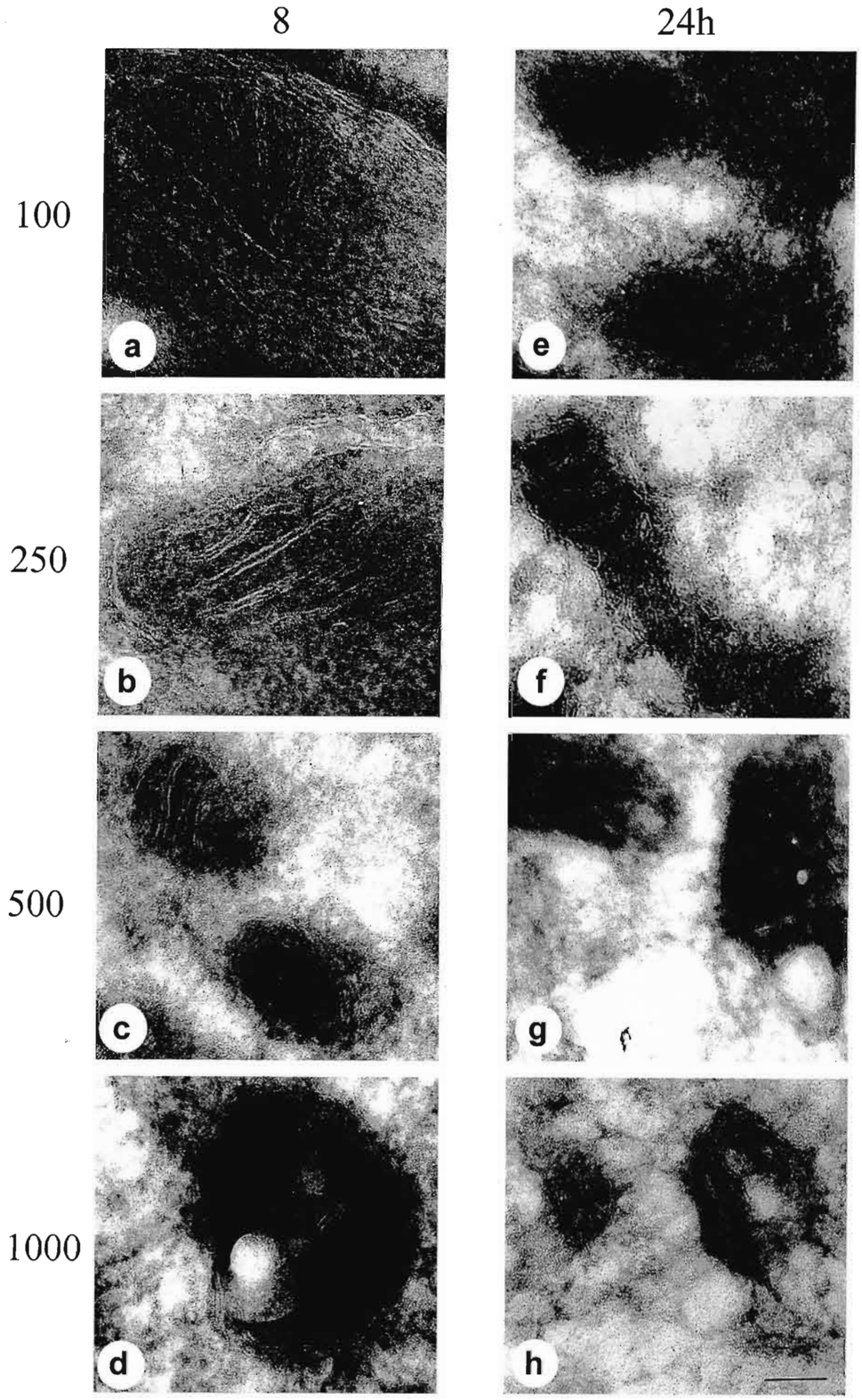

Figure 2.15 Mitochondria from ultrathin cryoultramicrotomy sections of MCF10AneoT cells treated for 8 and 24 hours with H_2O_2 and Fe^{2+}.

Enlargements of mitochondria corresponding to the mitochondrial inserts of Fig. 2.10. Representative mitochondria from MCF10AneoT cells harvested 8 h after treatment with 3μM Fe^{2+} in serum-free medium and (a) 100 μM H_2O_2, (b) 250 μM H_2O_2, (c) 500 μM H_2O_2, (d) 1000 μM H_2O_2, and 24 h after treatment with 3 μM Fe^{2+} and (e) 100 μM H_2O_2, (f) 250 μM H_2O_2, (g) 500 μM H_2O_2, and (h) 1000 μM H_2O_2.

Bar = 125 nm for all micrographs.

Mitochondria from the treated MCF10AneoT cells displayed various responses to the oxidative stress. After 1 h of treatment with 100 μM H_2O_2 (Fig. 2.14, a), there was a mixture of normal and condensed mitochondria in the cells, while at 4 (Fig. 2.14, e) and 8 h (Fig. 2.15, a), mitochondria appeared to be normal (slightly elongated), and at 24 h (Fig. 2.15, e) mitochondria appeared to be condensed. At 250 μM H_2O_2, mitochondria were condensed at 1 (Fig. 2.14, b), 4 (Fig. 2.14, f) and 24 h (Fig. 2.15, f) but were normal at 8 h (Fig. 2.15, b). At 500 μM, mitochondria were condensed at 1 (Fig. 2.14, c), 4 (Fig. 2.14, g) and 8 h (Fig. 2.15, c), although at 4 h there were also some normal mitochondria present (Fig. 2.14, g), while mitochondria at 24 h (Fig. 2.15, g) were swollen. At 1000 μM mitochondria were condensed at 1 (Fig. 2.14, d) and 4 h (Fig. 2.14, h), although at 4 h there were also normal mitochondria present, while they were swollen and/ruptured at 8 (Fig. 2.15, d) and 24 h (Fig. 2.15, h). These results appear to give additional data supporting the ultrastructural examination of the whole MCF10AneoT cells (Figs 2.9, 2.10).

2.4.2.4 Discussion

Electron microscopic examination of whole cells and mitochondria largely verified light microscopic studies, except that electron microscopic studies of both whole cells and mitochondria indicated that necrosis occurs much earlier in the MCF10AneoT cells than is evident by light microscopy. It seems that the MCF10A cells are more susceptible to cellular damage by high H_2O_2 concentrations than the MCF10AneoT cells.

It must be remembered that cells in a population may be at different stages of the cell cycle at any given time, and may be differentially susceptible to apoptosis and necrosis, and that apoptosis and necrosis are more easily induced in older cells. Thus, at any particular time in each cell type, while some cells are "blebbing" to form apoptotic bodies, others may have undergone this stage earlier, while others may already be experiencing secondary necrosis. The MCF10AneoT cells also divide much more rapidly than the MCF10A cell line and, hence, may also be less susceptible to the induction of apoptosis and necrosis, as they are generally a younger population at any one time. In this study, every effort was made to choose representative cells, but this is difficult and every precaution must be taken to avoid biased selection.

Since apoptosis is an energy-dependent process, ATP levels must be maintained throughout the apoptotic process, especially for the execution of morphological changes such as membrane blebbing. The MCF10AneoT cells seem to show the ability to manifest apoptotic characteristics, even when similar levels of H_2O_2 induce necrosis in the MCF10A cells. This implies that the transformed cell is able to maintain adequate levels of ATP for the apoptotic process to proceed. This also implies a functional mitochondrial oxidative phosphorylation system, as was shown in about 1972 to be the case for cancer cells (Weinhouse, 1972). Before this date, it was thought that aerobic glycolysis was required for the production of energy in cancer cells as they lost their respiratory capability, as a result of neoplastic transformation (Weinhouse, 1972). The present results seem to disprove this previous hypothesis, and confirm the more recent view, as the mitochondria of the transformed cell line seemed undamaged, intact and able to maintain adequate ATP levels for apoptosis to proceed under most treatment conditions.

While mitochondria from all the apoptotic MCF10A cells were condensed and very dense under most treatment conditions, mitochondria from the MCF10AneoT cells appeared to be more damage-resistant, as evidenced by the presence of normal, uncondensed mitochondria in treated MCF10AneoT cells at specific times of treatment and with different concentrations of H_2O_2. This pattern of response (as described in Section 2.4.2.3) may correspond with a "recovery phase", where mitochondria from treated cells initially appear damaged, but at later times of treatment appear normal (for a variable length of time), and subsequently appear to be damaged again, the latter possibly due to prolonged exposure to oxidative stress. The induction of this recovery phase seems to depend on the intensity of insult, as it comes into effect in these cells within 4 h of treatment with 100 μM H_2O_2, and within 8 h with 250 μM H_2O_2. The possible non-linear response to oxidative stress, and over-compensation by the pre-malignant cells is suggested by the even earlier appearance, at 4 h, of the recovery phase (as opposed to 8 h with 250 μM H_2O_2) in 500- and 1000 μM-treated MCF10AneoT cells, in which mitochondria are seen to proliferate.

The significance of the mitochondrial proliferation observed is unknown, but may be an attempt by the cells to maintain energy generation for avoidance or completion of the apoptotic process. However, the greater frequency of such proliferation observed in the MCF10AneoT cells seems to indicate that this proliferation may be linked to a greater resistance to oxidative stress-induced cell death, and may suggest that mitochondria proliferate in an attempt by the cells to recover from the induction of apoptosis.

It is of considerable significance that the pre-malignant cell line displayed a different pattern of mitochondrial responses compared to the normal cells, as mitochondria from cancer cells have been reported to differ from those of normal cells in factors such as membrane potential (Chen and Rivers, 1990). This impacts on respiration and mitochondrial fatty acid, pyruvate and ATP production and metabolism. Since mitochondria are the "powerhouses" of cells, as well as a storage facility for apoptogenic proteins (such as cytochrome c, AIF, caspases), the intrinsic differences in mitochondria of normal and cancer cells, as well as their differing responses to death-inducing stimuli can have important implications in cancer therapy.

2.5 Discussion

While the light microscopy gave a good overall picture of the cells, and is a very rapid method of visualising apoptotic cells, electron microscopy gave much greater detail of cellular structure. Cells that were apoptotic were identified at a much earlier stage by electron microscopy, although this technique is very time-consuming and technically difficult. Close examination of the mitochondria gave additional information and showed differences in the response patterns, which was not apparent by viewing of the whole cell, and which may be relevant to metabolism or the release of apoptogenic proteins during the apoptotic process.

The results of the light microscopic morphological and ultrastructural studies correlated well with each other, indicating the concentration and times of treatment where cells ceased to become apoptotic and became necrotic instead. In addition the differences in susceptibility of the normal MCF10A cells and the pre-malignant derivative were clearly evident. It seemed that the MCF10A cells were more susceptible to the H_2O_2-induced oxidative stress than the MCF10AneoT cells, with the threshhold to necrosis being 1000 μM at 4 h for the MCF10A cells, while that for the MCF10AneoT cells was 8-24 h at the equivalent concentration. In addition, the mitochondria from the latter cells also seemed to be more resistant to damage or able to recover, while those from the normal cells did not possess this characteristic.

Any form of mitochondrial damage is very important to the apoptotic process as it will affect energy production, as well as the release of cytochrome c and other apoptogenic proteins, from the intermembrane space, and thus, the downstream events of apoptosis. In this study, distinct areas of leakage in the mitochondrial membranes were not visible, but there may have been pores present which were too small to view, but which were large enough to allow release of cytochrome c and other proteins. Thus, while morphology and ultrastructure of cells appears to be a good indicator of apoptosis, morphological examination aims to look at many cells and to take an "average view". Such results should be confirmed by biochemical methods, such as detection of DNA laddering, caspase activity and/or cytochrome c release, which, by their nature, assay the sum product of many cells. These approaches are considered in the next chapters. Caspase activation would be anticipated to occur earlier than the morphological changes

(Mills *et al.*, 1999), as convolution of the nuclear membrane and chromatin condensation and apposition to the nuclear membrane, which were apparent from the electron microscopy studies, are a result of caspase activation (Duband-Goulet *et al.*, 1998). DNA laddering would also be expected to occur after caspase activation, as endonucleases may require activation by caspases (Enari *et al.*, 1998).

CHAPTER 3

BIOCHEMICAL CRITERIA

Although the assessment of morphological changes occurring during apoptosis have been widely used to distinguish apoptotic cells from necrotic cells, such changes may be subtle and difficult to definitively assess. Other biochemical detection of more average, quantifiable markers should, theoretically, assist the interpretation of morphological observations (Goping *et al.*, 1999). Two such marker systems, which could be used to detect the onset of apoptosis, are DNA fragmentation and caspase activation, both of which involve cell lysis and sampling of particular components.

3.1 DNA FRAGMENTATION

3.1.1 Introduction

Internucleosomal cleavage is considered to be the biochemical hallmark of apoptosis (Weaver *et al.*, 1993). Hundreds of papers have reported internucleosomal DNA cleavage during apoptosis in a wide variety of cells and tissues under many conditions (Bortner *et al.*, 1995). The purpose of DNA fragmentation during apoptosis may be to facilitate breakdown of the DNA upon uptake of apoptotic cells by phagocytes. Alternately, DNA degradation may serve to destroy the information content of the cell and, thus, act as an irreversible step in the process, or it may simply be a by-product of ion redistributions that occur during apoptosis (Martin *et al.*, 1994).

Chromatin cleavage is a multistep process, although the nature of the changes required to make the chromatin subunits progressively sensitive to degradation is still unclear (Zhivotovsky *et al.*, 1994). Chromatin is initially cleaved into high molecular weight (HMW) fragments, and subsequently into progressively lower molecular weight (LMW) fragments. A temporal correlation between the stages of DNA fragmentation and the appearance of nuclear morphological changes has been established. DNA fragments, >2 Mbp (mega base pairs), begin to accumulate in cells which are still adherent, prior to any observable nuclear morphological change. These large fragments are subsequently cleaved into 450-600 kbp (kilo base pairs) fragments (Rusnak *et al.*,

1996), and during this stage, the nuclei become more rounded, in the absence of any detectable chromatin condensation (Ghibelli *et al.*, 1995). Some smaller fragments of 30-50 kbp also begin to accumulate prior to detachment of the cells. Upon detachment, the largest fragments are completely degraded, and there is an increase in the amount of 30-50 kbp fragments (Rusnak *et al.*, 1996), accompanied by chromatin condensation (Ghibelli *et al.*, 1995). Subsequently, extensive internucleosomal DNA fragmentation correlates with complete nuclear fragmentation to apoptotic bodies (Ghibelli *et al.*, 1995). This pattern of DNA degradation occurs by activation of an endogenous endonuclease that cleaves the DNA in the linker region between histones on the chromosomes. Since the DNA wrapped around the histones consists of 180 to 200 base pairs (bp), multiples of this interval are characteristically observed and are commonly referred to as the "apoptotic ladder" (Bortner *et al.*, 1995).

DNA fragmentation, even at the earliest stages, occurs throughout the nucleus, including regions of already condensed chromatin (Ghibelli *et al.*, 1995). Early work suggested that degradation of DNA led to the collapse of chromatin structure. However, recent work suggests that these are actually separable events (Kass *et al.*, 1996). Nuclear degradation must occur at a relatively early stage of apoptosis when there is still sufficient ATP in the cell to drive chromatin condensation and the formation of apoptotic bodies (Walker and Sikorska, 1997). The appearance of large DNA fragments in the absence of internucleosomal DNA fragmentation also suggests that chromatin condensation may be independent of internucleosomal DNA fragmentation and that various types of DNA cleavage events may be cell-type specific (Bortner *et al.*, 1995).

Apoptotic DNA fragmentation is characterised by the generation of double-stranded breaks (Piperakis *et al.*, 1999). Single-strand breaks at higher levels of DNA organisation may not play an active role during apoptosis but perhaps can act as signals to induce the process (Bortner *et al.*, 1995).

There is an intimate relationship between DNA sequence, the structure of chromatin, and the ability of chromatin to be fragmented (see Fig. 3.1 for chromatin structure and sites of cleavage).

Cleavage sites include the linker region between nucleosomes and the stretches of DNA that attaches the chromatin to the nuclear matrix-lamina complex or nuclear scaffold (Laemmli *et al.*, 1992). Three classes of sites at which fragmentation occurs can

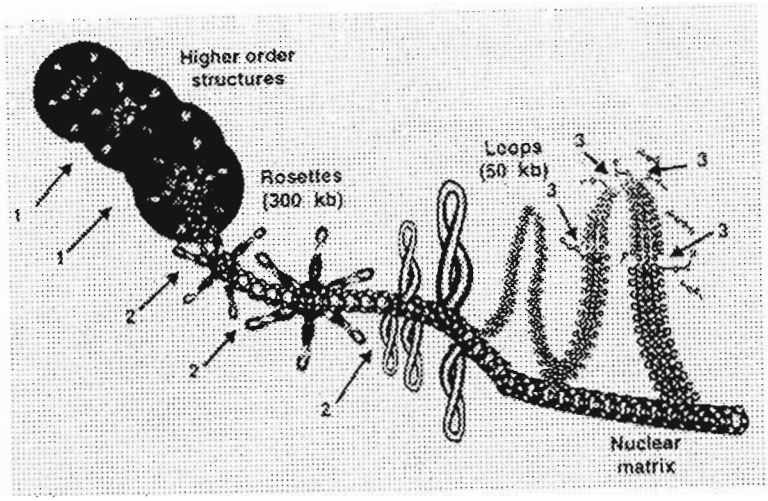

Figure 3.1. Chromatin structure and cleavage sites.

Higher order chromatin structures include the 30-nm fibre, the chromatin loop (50 kbp), and the rosette structures (300 kbp) of chromosomes. DNA is envisaged as being ordered into chromatin loops, which are wound into hexameric rosette structures, which, in turn, form the basic subunit of the coiled chromatid. As DNA is folded into these complex chromatin structures, certain regions of the molecule are more exposed to endonuclease cleavage. From Walker and Sikorska (1994).

be distinguished: (i) sites spaced throughout chromatin at intervals of >300 kbp, cleavable in the presence of Mg^{+}, (ii) a subset of sites (50 kbp) presumed to be at the base of some rosette structures, cleavable in the presence of Mg^{+} and a low concentration of Ca^{2+}, and (iii) sites (180 bp) within the linker regions of the nucleosomes in DNA loops, cleavable in the presence of Mg^{+} and higher levels of Ca^{2+}. Additional factors involved at this stage may make the final extent of DNA fragmentation highly variable in different cell types. There is evidence that cleavage depends on the availability of classes of sites, rather than altering the activity of an endonuclease that has free access to all of chromatin (Walker and Sikorska, 1994). DNA in the linker region may be predisposed to a structural alteration that renders it nuclease sensitive. Only a small percentage of linker regions are actually cleaved during apoptosis and these may be the only ones available for such a modification (Walker and Sikorska, 1997).

Various nucleases have been described. Attempts to find the enzyme responsible for DNA fragmentation has resulted in the isolation of different enzymes, suggesting that no single enzyme is responsible for all instances of apoptosis or for the complete process within a single cell type (Walker and Sikorska, 1994). Endonucleases differ in their ionic

and pH requirements. Among the Ca^{2+}/Mg^{+}-dependent endonucleases are DNaseI and NUC18. Endonucleases requiring acidic conditions for activation include DNaseII and a 40-45 kDa cation-independent enzyme which is inhibited by zinc, as well as two other acidic nucleases of 32 kDa which are not inhibited by zinc ions (Walker and Sikorska, 1997; Zhivotovsky *et al.*, 1994). DNA fragmentation factor (DFF), a heterodimeric protein that resides in the cytoplasm as an inactive precursor, is activated by caspase-3, and functions in the pathway leading to DNA fragmentation, following the induction of apoptosis. It is required for the activation of an endonuclease and DNA degradation. DFF is likely to be a non-caspase cysteine protease (Vaux *et al.*, 1997). During apoptosis a specific DNase, called caspase-activated DNase (CAD) is activated. CAD is found complexed with inhibitor of CAD (ICAD) and is, therefore, stored in an inactive form. Caspase-3 cleavage of this complex releases the CAD from its inhibitor and, hence, results in the DNase activity, causing DNA fragmentation in the nucleus (Enari *et al.*, 1998).

It has been suggested that the proteolytic degradation of lamins, which form a protein mesh underlying the nuclear membrane (Hozak *et* al., 1995) and serves to organise chromatin (McKeon, 1991), may facilitate the activation of nucleases responsible for DNA fragmentation, by allowing cytoplasmic proteases or other agents that bring about their activation, to enter the nucleus (Rao *et al.*, 1996). Actin cleavage, which results in the formation of apoptotic bodies, has also been suggested to activate endonucleases, as actin proteolysis occurs exactly at the site of interaction between actin and the endonuclease DNaseI, thus releasing DNaseI from its binding site and relieving the inhibition by actin (Villa *et al.*, 1998).

More than one endonuclease can affect DNA fragmentation even in the same cell type, and different inducers may activate different nucleases. There is great variation in the extent to which different cells degrade their DNA (Walker and Sikorska, 1997). Only a small percentage of the DNA is degraded all the way to oligonucleosomes and the bulk of the DNA remains in large fragments (50-300 kbp). However, this has not detracted from the usefulness of the DNA ladder as a biochemical marker for apoptosis (Walker and Sikorska, 1994).

3.1.2 The effect of oxidative stress on DNA

The ROIs, H_2O_2 and •OH, damage DNA by producing a broad spectrum of modified purines and pyrimidines in DNA, as well as strand breaks and sites of base loss. At least 11 different base products are induced, of which 35-50% of the total adducts are expected to result in strong blocks to polymerases, resulting in a decrease in amplification of the target sequence, since only those DNA templates that do not contain polymerase-blocking lesions will be amplified (Yakes and van Houten, 1997). Damaged lesions are processed in the cell by base excision repair enzymes. Ultimately, it is the efficiency of repair of a lesion, coupled with the interaction of an unrepaired lesion with the replicative DNA polymerase that determines the fate of the cell (Wallace, 1997).

Oxidative stress can induce apoptosis as detected by DNA "ladders" on agarose gels. This continues to be the most widely used method for detection of biochemical events in apoptosis, due to its simplicity and reproducibility.

3.1.3 Electrophoresis of isolated DNA from H_2O_2-treated cells

The method of DNA isolation and electrophoresis employed was essentially that of Douglas *et al.* (1992). It is a simple procedure, involving lysis of the cells in sodium dodecyl sulfate followed by extraction with saturated NaCl. This is a non-toxic method for DNA purification, as it does not involve conventional phenol-chloroform extraction. In addition, it overcomes the requirement for lengthy incubations in the presence of expensive proteinase K.

3.1.3.1 Reagents

TEN [10 mM Tris, 2 mM EDTA, 400 mM NaCl, pH 8.2]. Tris (0.303 g), EDTA (0.186 g) and NaCl (5.844 g) were dissolved in MQ H_2O (230 ml). The pH was adjusted to pH 8.2 with HCl, and the volume made up to 250 ml.

TE [10 mM Tris, 1 mM EDTA, pH 8.0]. Tris (0.121 g) and EDTA (0.037 g) were dissolved in MQ H_2O (80 ml). The pH was adjusted to pH 8.0 with HCl, and the volume made up to 100 ml.

10% (m/v) Sodium dodecyl sulfate (SDS). SDS (10 g) was dissolved in MQ H_2O (100 ml).

Saturated NaCl (6 M). NaCl (35.064 g) was dissolved in MQ H_2O, and the volume made up to 100 ml.

70% (v/v) Ethanol. MQ H_2O (30 ml) was added to ethanol (70 ml).

7.5 M Ammonium acetate, pH 7.5. Ammonium acetate (57.81 g) was dissolved in a minimum of MQ H_2O, the pH adjusted to pH 7.5 with acetic acid, and the volume made up to 100 ml.

0.5 M $MgCl_2.6H_2O$. $MgCl_2.6H_2O$ (2.541 g) was dissolved in MQ H_2O, and made up to 25 ml.

5x Loading buffer [0.25% (m/v) xylene cyanol, 0.25% (m/v) bromophenol blue, 30% (v/v) glycerol]. Xylene cyanol (0.125 g), bromophenol blue (0.125 g) and glycerol (15 ml) were dissolved in MQ H_2O (50 ml).

10x TAE (0.04 M Tris-acetate, 0.001 M EDTA). Tris (48.4 g), acetic acid (11.42 ml) and Na_2EDTA (7.44 g) were dissolved in MQ H_2O (900 ml). The pH was adjusted to pH 8.5 with acetic acid, and the volume made up to 1 l.

1x TAE. 10x TAE (100 ml) was diluted to 1 l with MQ H_2O.

1.8% (m/v) Agarose. Agarose (0.9 g) was dissolved in TAE buffer (50 ml), by heating.

10 mg/ml Ethidium bromide stock solution. Ethidium bromide (10 mg) was dissolved in MQ H_2O (1 ml).

All reagents used in DNA work (except agarose) were autoclaved and kept sterile for use.

3.1.3.2 Procedure

MCF10A and MCF10AneoT cells were grown, seeded, treated (Section 2.4.1.2), and harvested (Section 2.4.2.2) as previously described, and cell pellets were stored at -80°C until required. Each cell pellet was thawed in TEN buffer (900 µl), lysed by gentle vortexing, SDS (100 µl, 10% (m/v)) added, and pellets were incubated with very gentle shaking in a rotary shaker (55°C, 20 h). Saturated NaCl (250 µl) was added to precipitate proteins, the solution gently vortexed, and proteins pelleted by centrifugation (1400 x g, 10 min) and removed. $MgCl_2.6H_2O$ (2.1 µl) was added, to enhance the recovery of low molecular weight DNA fragments, two volumes of ice-cold ethanol (98-100%) added, lysates incubated (-80°C, 1 h) to precipitate the DNA, and centrifuged (12 000 x g, 15 min, 4°C). The DNA pellet was rinsed with 70% (v/v) ethanol, and centrifuged (12 000 x g, 5 min, 4°C). The excess ethanol was removed, and the DNA pellet was air-dried and re-dissolved in TE (50 µl).

The edges of a plastic agarose gel tray were sealed with masking tape to form a mould, and the tray was placed on a bench horizontally. The agarose mixture was heated until the agarose dissolved, and allowed to cool to about 60°C. Ethidium bromide stock (25 µl) was added to the solution to obtain a final concentration of 5 µg/ml, and the gel was poured, a comb placed in to form sample wells, and allowed to set (30 min). Loading buffer was added to the samples, which were then loaded into the wells of the gel. Gels were electrophoresed at 80V and maximum current until the bromophenol blue marker was about 1 cm from the bottom of the gel and examined by ultraviolet light.

3.1.3.3 Results

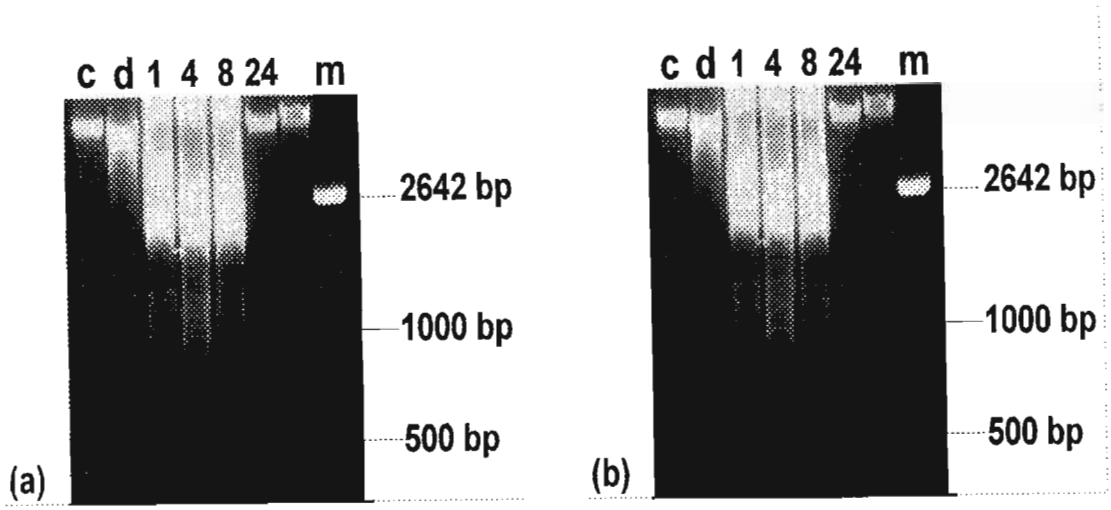

Figure 3.2 Electrophoresis of isolated DNA.

Isolated DNA from (a) MCF10A and (b) MCF10AneoT cells treated with 100 μM H_2O_2 and 3 μM Fe^{2+} in serum-free medium, was electrophoresed on a 1.8% agarose gel incoporating 5 μg/ml ethidium bromide. Lane c = control (untreated), lane d = MNase-digested sample, lane 1 = 1 h, lane 4 = 4 h, lane 8 = 8, lane 24 = 24 h, lane m = 100 bp MWM.

Bands of DNA (Fig. 3.2) are very pale and barely visible.

3.1.3.4 Discussion

Usually, DNA is re-precipitated during DNA isolations, to increase the purity. Although this was a modified method of DNA isolation in which the re-precipitation of DNA was eliminated to reduce loss of DNA, the amount of DNA isolated was very small as evidenced by the barely-visible UV-fluorescent bands. A much larger number of cells (and thus greater time and expense) would be required to obtain bands of greater intensity and visibility. Because of this, and the fact that pure DNA samples were not essential for this application, a method in which whole cell lysates are electrophoresed, was used for further studies. The fact that DNA ladders were not visible did not necessarily mean that the method was ineffective for sufficient DNA isolation; it could have been possible that DNA fragmentation only occurred at later stages or higher H_2O_2 concentrations.

However, using the whole cell lysate method saves a lot of time between experiments. A caspase assay was carried out on similarly treated (100 μM H_2O_2-treated) and lysed cells, in order to check that DNA fragmentation was induced, as majority of the studies to date have reported caspase activity to occur prior to DNA fragmentation, and DNA cleaving enzymes have been reported to be activated by caspases (Enari *et al.*, 1998; Vaux *et al.*, 1997). As this gave positive results, it is possible that DNA fragmentation did occur but was not detected.

3.1.4 Electrophoresis of whole cell lysates of H_2O_2-treated cells

It was not necessary to have pure DNA for this application, as it was merely the detection of DNA ladders that was important. Therefore, a method using whole cell lysates for electrophoresis was used (Zhu and Wang, 1997). This method involves lysis of the cells and a short incubation with proteinase K to degrade proteins, as there is no NaCl extraction as in the previous method (Section 3.1.3). The elimination of the actual DNA isolation procedure prevents the loss of low molecular weight fragments and considerably reduces the length of the assay.

3.1.4.1 Reagents

Lysis buffer [10 mM Tris, 100 mM NaCl, 25 mM EDTA, 1% (m/v) sarkosyl, pH 7.4]. Tris (0.121 g), NaCl (0.584 g), EDTA (0.931 g) and sarkosyl (1 g) were dissolved in MQ H_2O (80 ml), the pH adjusted to pH 7.4 with NaOH, and the volume made up to 100 ml.

10 mg/ml Proteinase K stock. Proteinase K (5 mg, Sigma) was dissolved in MQ H_2O (500 μl).

TN buffer [10 mM Tris, 10 mM NaCl, pH 7.4]. Tris (0.03 g) and NaCl (0.015 g) were dissolved in MQ H_2O (20 ml), the pH adjusted to pH 7.4 with HCl, and the volume made up to 25 ml.

60 mM EDTA. EDTA (0.223 g) was dissolved in MQ H_2O (10 ml).

Micrococcal nuclease (MNase). A stock solution of 150 units/ml (Boehringer Mannheim) was available.

All reagents except proteinase K and MNase were autoclaved.

3.1.4.2 Procedure

Cells were grown, seeded, treated (Section 2.4.1.2) and harvested (Section 2.4.2.2) as previously described, and cell pellets were stored at -80°C until required. Lysis buffer (30 µl) and proteinase K stock (4 µl) were added to each cell pellet, and the lysates were incubated (50°C, 1.5 h). As apoptotic DNA fragmentation can be mimicked by MNase digestion of nuclei (Arends *et al.*, 1990), a control using an MNase-digested sample was run. Untreated cells grown in serum-containing medium were lysed and incubated as described above. MNase (0.6 µl) was added, and the pellets incubated in a waterbath (37°C, 1 h). The reaction was stopped by the addition of EDTA (3 µl). Agarose gels were prepared as in Section 3.1.3.2, loading buffer was added to the samples, which were loaded and electrophoresed as described above (Section 3.1.3.2).

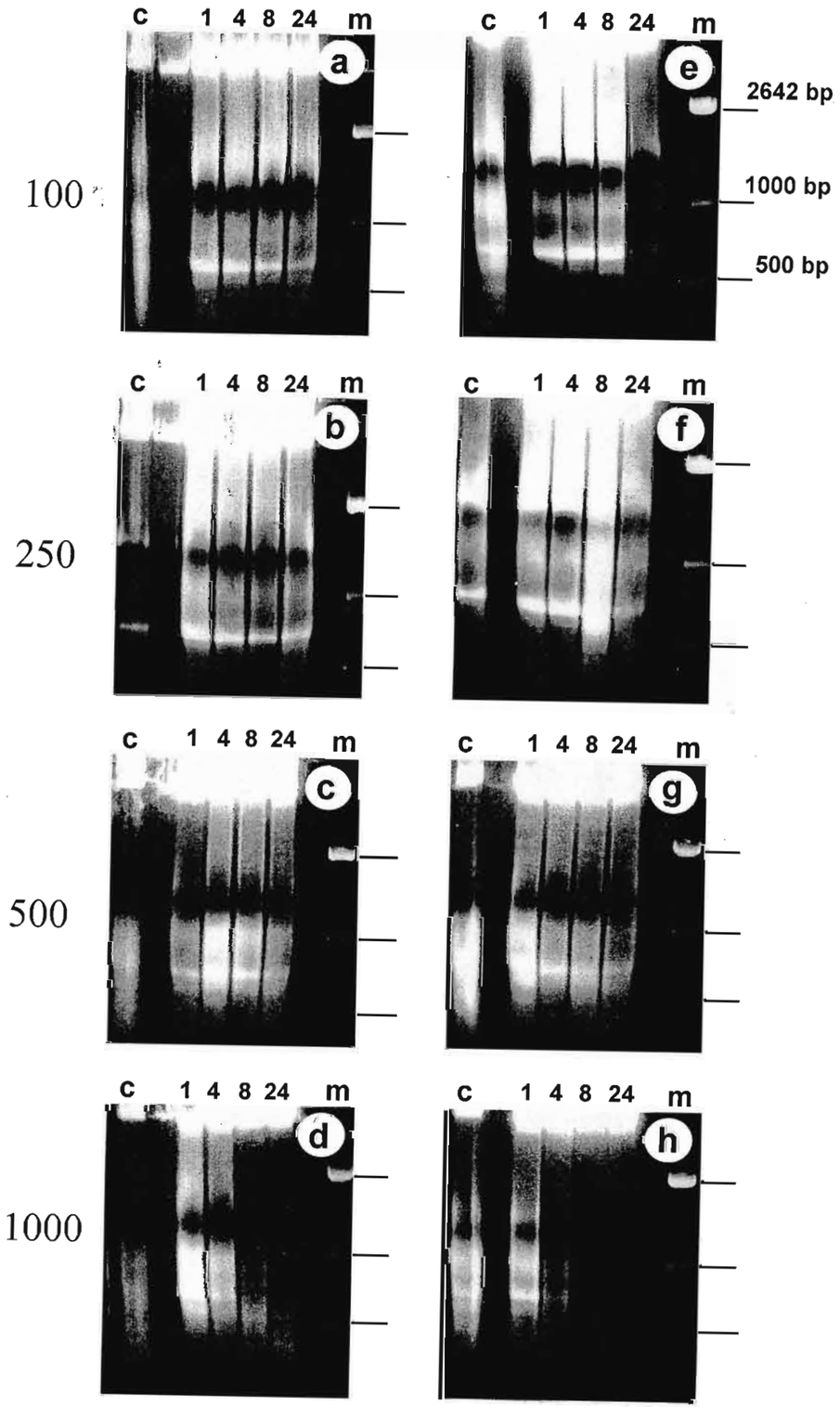

3.1.4.3 Results

Figure 3.3 Detection of apoptotic DNA degradation.

MCF10A cells, harvested after treatment with 3 μM Fe^{2+} in serum-free medium and (a) 100 μM H_2O_2, (b) 250 μM H_2O_2, (c) 500 μM H_2O_2, (d) 1000 μM H_2O_2, and MCF10AneoT$_8$ cells harvested after treatment with 3 μM Fe^{2+} in serum-free medium and (e) 100 μM H_2O_2, (f) 250 μM H_2O_2, (g) 500 μM H_2O_2, (h) 1000 μM H_2O_2, were electrophoresed on a 1.8% agarose gel incorporating 5 μg/ml ethidium bromide.

Lane c = control cells, lane 1 = 1 h, lane 4 = 4 h, lane 8 = 8 h, lane 24 = 24 h, lane m = molecular weight marker– bands are increments of 100 bp, with the bright bands representing 500, 1000, and 2642 bp.

The MCF10A cells treated with 100 μM (Fig. 3.3, a), 250 μM (Fig. 3.3, b), and 500 μM H_2O_2 (Fig. 3.3, c) all displayed similar patterns and degrees of DNA fragmentation which was indicative of apoptosis, while 1000 μM H_2O_2-treated cells (Fig. 3.3, d) showed "smearing" at 1 and 4 hours, and leakage of DNA at 8 and 24 h, both indicative of necrosis, in which there is random DNA fragmentation and permeabilisation of the membranes. The MCF10AneoT cells displayed a similar response to the MCF10A cells, except at 1000 μM, where the cells became necrotic resulting in leakage of fragmented DNA at 4 hours (Fig. 3.3, h, lane 4), instead of at 8 h when the MCF10A cells became leaky (Fig. 3.3, d, lane 8).

Some banding and streaking was also seen in control lanes (lanes c) but banding patterns were much less distinct than in test preparations.

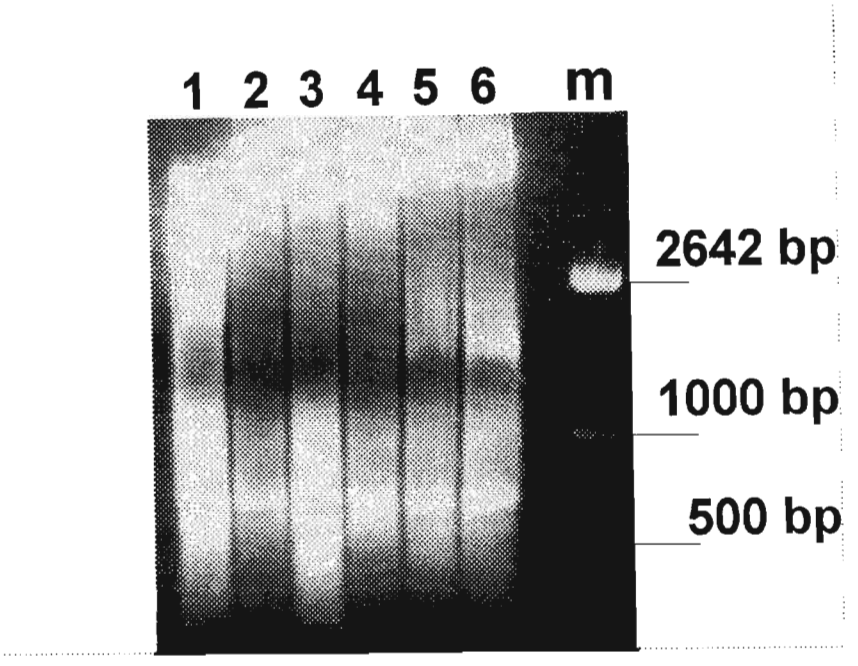

Figure 3.4 Confirmation of apoptotic DNA fragmentation.

MCF10A (lane 1) and MCF10AneoT cells (lane 2) irradiated with UVB light for 10 min; MCF10A (lane 3) and MCF10AneoT cells (lane 4) irradiated with UVB light for 30 min; MCF10A (lane 5) and MCF10AneoT (lane 6) cell lysates digested with MNase. Samples were electrophoresed on a 1.8% agarose gel incorporating 5 μg/ml ethidium bromide.

The pattern of DNA cleavage induced by irradiation with UVB light (Fig. 3.4, a, b) was similar to those obtained for the treated cells (Fig. 3.3, a-h).

3.1.4.4 Discussion

Non-apoptotic DNA extracts should ideally show a single high molecular weight band >2642 bp (i.e., genomic DNA). Some additional banding was seen in control extracts, however, as a proportion of the cells will inevitably undergo apoptosis during the test period. However, this was seen at a much lower level than the test cells. Some smearing was also seen, and was possibly generated during the preparation of extracts for electrophoresis. This too was at a lower level than seen in test lanes.

There did not seem to be any differences in the cleavage pattern of the MCF10A and MCF10AneoT cells, except at 1000 μM H_2O_2. At this concentration, the results of DNA fragmentation for the MCF10A cells correspond with that of the electron microscopic studies, which showed induction of necrosis from 4 h onwards. However, the results for the MCF10AneoT cells differ, as the results of DNA fragmentation showed

necrosis from 4 h onwards, while electron microscopic examination showed necrosis from 8 h. The leakage of DNA seen in the MCF10AneoT cells at 24 h after treatment with 100, 500 and 1000 μM H_2O_2 (and at 4 and 8 h with 1000 μM H_2O_2) may not really represent necrosis at these times and concentrations of H_2O_2, as there was some initial cell death in these cell populations, as is evident by examination of the untreated controls.

The controls using MNase and UV light were run because of the atypical DNA ladders obtained, i.e., internucleosomal fragmentation (bands of 180-200 bp) which is usually found in apoptotic cells, was not seen. H_2O_2 and •OH both cause DNA strand breaks. To ensure that the DNA pattern obtained was due to apoptotic cell death, and not due to oxidative stress breakage, cells were treated with UVB light which is known to induce apoptosis in epithelial cells (Aragane *et al.*, 1998), as well as with MNase, which produces 200 bp fragments and, thus, should give a ladder pattern identical to typical apoptotic DNA ladders. However, the pattern obtained in both controls was identical to those in all the test samples, proving that this is indeed the pattern of apoptotic DNA fragmentation characteristic of these cells.

These results are supported by Bortner *et al.* (1995) who observed that internucleosomal DNA cleavage seems to occur in immune cells, whereas in transformed or epithelial cells, it does not always occur. A difference in chromatin structure, rather than the availability or activity of endonuclease, determines the extent to which cells degrade their DNA (Walker and Sikorska, 1997).

When considering the role DNA fragmentation plays during the apoptotic process, it needs to be borne in mind that not all cultured cells *in vitro* may accurately reflect the processes occurring *in vivo*. Cell lines may be prevented from exhibiting certain apoptotic characteristics through the loss of signal transduction pathways or response to certain metabolic signals. While transformed cells still retain the ability to undergo mitosis, several features of apoptosis such as morphological characteristics or internucleosomal DNA cleavage may be inhibited during the immortalisation process. Adequate morphological studies are necessary to ascertain that apoptosis has occurred, particularly when different patterns of DNA degradation to those anticipated are observed (Bortner *et al.*, 1995).

The method used last (Zhu and Wang, 1997) saves much time and labour, and more of the LMW DNA is detected, due to lower loss, compared to the first method used

for isolation of DNA (Douglas *et al.*, 1992). DNA cleavage was apparent after just 1 h of apoptosis-induction, as opposed to reports of DNA fragmentation being a late event in apoptosis, occurring after caspase activation. This result correlated with the electron microscopic study, where nuclear convolution and chromatin condensation/fragmentation was apparent from 1 h onwards. As DNA fragmentation was visible within 1 h of treatment, which was the first time tested, these assays should have been conducted on cells treated for shorter periods of time, as DNA fragmentation may have occurred much earlier.

In most of the gels, the intensity of the bands did not increase with increasing time of treatment. Therefore, this extent of fragmentation may represent the maximum achievable during apoptosis, as reported in other studies (Cui *et al.*, 1994). Biochemical assays also require large numbers of cells more or less homogenously undergoing the biochemical events of interest. Apoptosis, however, is known to be an asynchronous process (Mills *et al.*, 1998a). Perhaps some cells undergo secondary necrosis after apoptosis, as time of treatment increases, and lose their DNA through the permeable nuclear and plasma membranes. Thus, an increase in DNA fragmentation is not noticed, or perhaps the method is too insensitive to detect small differences. Therefore, the DNA fragmentation assay appears to be qualitative, not quantitative.

To confirm these results, and to obtain additional information about which concentrations of H_2O_2 and times of exposure induce maximal observable biochemical changes between the two cell lines, quantitative caspase assays were conducted. As DNA fragmentation was apparent from 1 h, caspase activity was expected to be evident at an earlier time, as DNA fragmentation usually occurs after the activation of caspases, which activate nucleases.

3.2 CASPASE ACTIVITY

3.2.1 Introduction

Though several different types of biochemical events have been recognised as important in apoptosis, perhaps the most fundamental is the participation of members of the family of cysteine-dependent, Asp-specific proteases known as caspases. Caspases

cleave a number of cellular proteins, a process of limited proteolysis in which a small number of cuts, usually only one, are made in interdomain regions. Sometimes cleavage results in activation of the proteins, sometimes in inactivation, but never in degradation, because their substrate specificity distinguishes the caspases as among the most restricted of endopeptidases (Salvesen and Dixit, 1999).

Caspase family members participate in one of two distinct signalling pathways: (i) activation of proinflammatory cytokines, and (ii) promotion of apoptotic cell death (Salvesen and Dixit, 1997). Caspases function as the final executioner in apoptosis (Allen *et al.*, 1998), and the various caspases seem to have different substrate specificities (Vaux *et al.*, 1997). The primary recognition pocket (S_1) is well adapted to accept an aspartate side chain of the substrate, and additional pockets (S_2-S_4) distinguish the caspases from each other (Salvesen and Dixit, 1997).

The pH dependence of the caspases indicates that they are fully active within the pH range found in normal as well as apoptotic cells. It is possible that changes in pH during apoptosis may affect caspase activity indirectly by altering the structure of a particular set of natural substrates. However, this hypothetical event would change only the susceptibility of the substrate, not the activity of the caspases. The apparent stability to substantial changes in ionic strength indicates that this would not be limiting during commitment to apoptosis (Stennicke and Salvesen, 1997).

3.2.1.1 Classes of caspases

There are a variety of possible reasons why mammalian cells have multiple caspases, with different caspases being able to cleave the same protein substrates, in some cases. For example, caspases might be (i) activated in a tissue- or subcellular compartment-specific manner, (ii) specialised for proteolysis of particular substrates (in addition to general apoptotic substrates), (iii) ordered into a protease cascade, or (iv) responsive to different stimuli (Wilson, 1998).

There are two ways of classifying the caspases, by their resemblance to either caspase-1 or-3 cleavage specificities, or by their primary structures. The caspase-1-like proteases are caspase-1, -4, -5, and –13, and the caspase-3-like proteases are caspase-2, -3, -6, -7, -8, -9 and –10 (Thornberry and Lazebnik, 1998). The ability of certain

caspases to autoactivate or catalyse the processing of other caspase zymogens suggests the sequential activation of caspases in protease cascades (Salvesen and Dixit, 1997). The active caspases are promiscuous in cleaving other caspases, making it difficult to identify the initial triggering event in caspase activation (Li *et al.*, 1997). On the basis of their primary structures, caspases can be grouped into two classes: those that possess long N-terminal domains (class I caspases) and those that either possess short prodomains or lack prodomains (class II caspases). The prodomains in the class I caspases (caspase-8 and –9) contain protein-protein interaction domains that help recruit class I caspase precursors to specific death complexes. Activation of class II caspases such as caspase-3, -6 and –7, appears to require proteolytic processing by class I caspases (Thornberry and Lazebnik, 1998). Thus, the class II caspases are the downstream caspases that mediate proteolysis of a number of cellular proteins in a cell that is destined to die (Kumar and Colussi, 1999), whereas class I caspases are believed to be upstream or signalling caspases (Slee *et al.*, 1999).

3.2.1.2 Caspase substrates

The net effect of cleavage events is to: (1) halt cell cycle progression; (2) disable homeostatic and repair mechanisms; (3) initiate the detachment of the cell from its surrounding tissue structures; (4) disassemble structural components, and (5) mark the dying cell for engulfment by other cells such as macrophages (Nicholson and Thornberry, 1997).

Targets of caspases can be loosely categorised into structural proteins, signalling proteins, transcription-regulating proteins, and proteins and enzymes involved in DNA/RNA metabolism (Tan and Wang, 1998). Several structural proteins are cleaved by caspases, such as actin, lamin, fodrin, keratin, gelsolin and NuMa protein, consistent with the morphological events seen during apoptosis (Denis *et al.*, 1998). Caspases are also responsible for nuclear changes associated with apoptosis, including chromatin condensation (Hakem *et al.*, 1998) and DNA fragmentation, by activation of DFF (Liu *et al.*, 1998). Cells that are embedded in organised tissue structures need to be detached and this appears to be facilitated in part by the cleavage of focal adhesion kinase by caspases (Nicholson and Thornberry, 1997).

Caspase-dependent cell killing is not simply the result of protein destruction but also requires the activation of specific signalling pathways (Tan and Wang, 1998). Not only are they critical for correct morphological changes during apoptosis, but targeting substrates such as retinoblastoma protein, which control the cell cycle, proliferation and apoptosis, implies that they can effectively oppose any cellular attempt to redirect the cell death program (Allen *et al.*, 1998). Some of the substrates might not always be cleaved during cell death. Actin may only be cleaved in specific cell types by a subset of death inducers. Care should be taken not to generalise from any of the reported observations of protein cleavage by caspases. None of the cleavage events reported thus far has been proven to be absolutely required to kill cells. The "critical substrate" hypothesis predicts that a specific, single substrate (unidentified) must be cleaved to complete the cell death process. Alternatively, there might not be a single crucial substrate for the caspases, and death might require the cleavage of multiple substrates (but a limited number of key substrates), each contributing to a part of the apoptosis phenotype (Tan and Wang, 1998). The currently available evidence is consistent with the second hypothesis, which can be described as "death by a thousand cuts" (Martin and Green, 1995). Despite the apparent specificity of cleavage events that occur during apoptosis, it is also possible that some proteolytic victims are "innocent bystanders" and are of no substantial importance to the death process (Nicholson and Thornberry, 1997).

3.2.1.3 Caspase activation

Caspases are constitutively present in most cells, residing in the cytosol as a single chain proenzyme or zymogen. Upon receiving a death signal, these are activated to fully functional proteases by a first proteolytic cleavage to divide the chain into large and small caspase subunits and a second cleavage to remove the N-terminal domain (prodomain). The subunits assemble into a tetramer with two active sites (Green, 1998). The active enzyme is a heterotetramer that comprises two heterodimers derived from two precursor molecules (Thornberry and Lazebnik, 1998).

The events that lead to activation of caspases appears to follow the sequence outlined in Fig. 3.5: (1) conformational changes caused by upstream signalling events allow recruitment of adaptor molecules to a death complex; (2) this results in additional

changes that allow recruitment of caspases through specific domains; (3) once in close proximity, procaspase molecules form transient oligomers, which allows inter- or intra-molecular catalysis and activation (Kumar and Colussi, 1999).

The result in each case of caspase recruitment is the formation of a complex called an "apoptosome" that functions to mediate the activation of the caspase. Cells are committed to die even before caspases become active, although cell death induced by ligation of death receptors is an exception and commitment to apoptosis is dependent on caspases (Green, 1998).

A principal means of caspase activation is through transmembrane receptors, such as CD95/Fas or other members of the tumour necrosis factor receptor (TNFR) superfamily, which, in their cytoplasmic tail, contain a 60-amino acid death domain, necessary for apoptotic signalling and recruitment of adaptor proteins (Chinnaiyan and Dixit, 1997; Nagata and Golstein, 1995). The primary role of recruitment through adaptors is to bring procaspase molecules into close proximity, generating a high, localised concentration of procaspase molecules that is sufficient to induce their autoproteolytic processing, which generates active caspase (Kumar and Colussi, 1999). There are other forms of non-receptor apoptosis involving caspase activation, implying that additional cytoplasmic mechanisms of caspase activation must exist (Slee *et al.*, 1999). Although the death-effector domain (DED) is a critical protein interaction domain that recruits caspases into complexes with members of the TNFR superfamily, apoptosis can also be induced by expressing certain DED-containing proteins, but without surface receptor cross-linking. DED-containing proteins (FADD or caspase-8) mediate apoptosis by forming novel cytoplasmic filaments termed death effector filaments (DEFs), that recruit and activate procaspase zymogens. Thus, formation of DEFs allows a regulated intracellular assembly of apoptosis-signalling complexes that can initiate or amplify apoptotic stimuli intracellularly, as well as at the plasma membrane. Recruitment to the DEF is highly efficient, and would cause a dramatic increase in local concentration of procaspases, which causes autocatalytic processing and release of the active enzyme into the cytoplasm (Siegel *et al.*, 1998). The exact mechanism of autocatalytic processing of caspases is not fully understood but, for this to occur, either the caspase precursors carry some intrinsic activity, or proximity-induced dimerisation of precursors allows refolding, which generates a structure similar to that of an active, processed enzyme (Kumar and

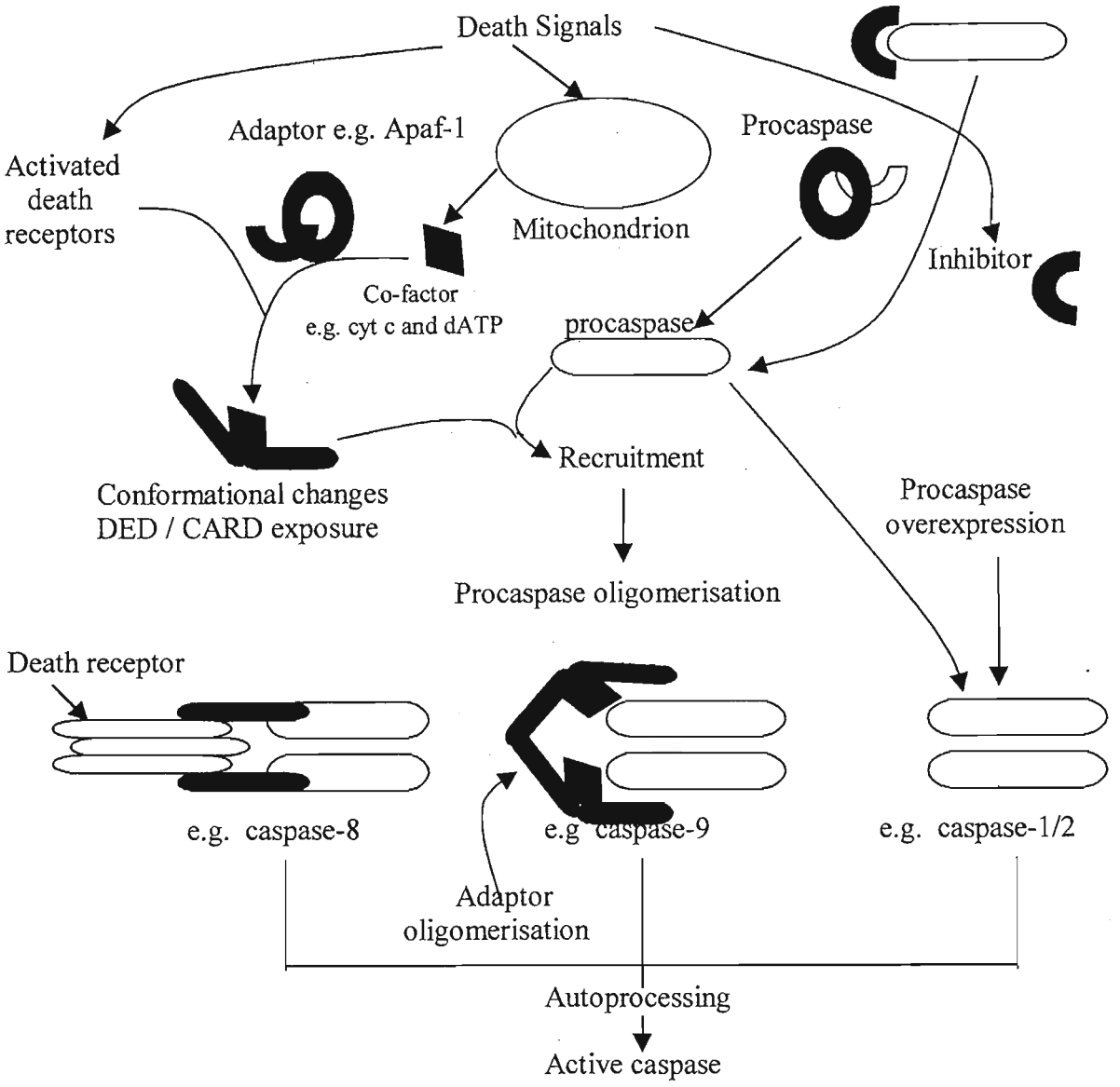

Figure 3.5 Models of caspase activation through oligomerisation.

Inactive procaspases undergo processing in response to apoptotic signals via two major pathways, involving death receptors and mitochondria. Activated death receptors interact with adaptors that recruit caspases, such as caspase-2, -8 and –10, to a membrane-associated death complex. Adaptor-mediated oligomerisation brings procaspase molecules into close proximity to allow autocatalytic activation. Many death signals lead to the release of cytochrome c (cyt c) from mitochondria which, along with dATP, binds to Apaf-1, which allows oligomerisation and recruitment of procaspase-9. Overexpression of some caspases presumably allows direct oligomerisation of procaspase molecules, independently of adaptors. Control of inappropriate activation of procaspases is likely to occur through inhibition of procaspase oligomerisation. This could be achieved by protein folding which might result in structural constraints, or by inhibitory proteins. From Kumar and Colussi (1999).

Colussi, 1999).

Despite many similarities, there are subtle differences in the mechanisms of the activation of the caspases studied so far. For instance, although procaspase-1 and -2 can oligomerise in a concentration-dependent manner without the need for an adaptor, caspase-8 and –9 require the adaptors Fas-associated death domain (FADD) and apoptosis protease activating factor-1 (Apaf-1), respectively, because they lack the intrinsic ability to form oligomers. Perhaps changes in conformation caused by death signalling, or removal of an inhibitory molecule, are sufficient to mediate oligomerisation of some caspases (Kumar and Colussi, 1999).

The activation of caspase-9, which is the upstream caspase activated in damage-induced apoptosis, requires Apaf-1, d-ATP and cytochrome c, which is released from the mitochondria in cells induced to undergo apoptosis. Binding of cytochrome c and d-ATP to Apaf-1 presumably causes conformational changes in the molecule that exposes the N-terminal caspase recruitment domain (CARD), enabling Apaf-1 to interact with the CARD domain in procaspase-9 (Srinivasula *et al.*, 1998). Binding leads to the cleavage of caspase-9, converting it to an active caspase, which then cleaves and activates caspase-3, thereby setting in motion the events that lead to DNA fragmentation and cell death (Li *et al.*, 1997).

3.2.1.4 Regulation of caspase activation

Activation of the initial caspase in an apoptotic pathway is the priming event in cell death and is, therefore, likely to be a tightly regulated process. Since caspase activation is achieved through oligomerisation of the precursor molecules, the regulation of oligomerisation must be important. As caspase activation is a complex process, requiring multiple protein-protein interactions and possibly resulting in conformational changes in various proteins, evolution of this multi-faceted activation mechanism possibly allows tighter control of apoptotic initiation through blocking of inappropriate oligomerisation of caspases. An inhibitor of apoptosis, ARC, contains a CARD domain and, thus, might function by blocking the interaction between specific CARD-containing molecules. Another level of regulation might be provided by direct binding of inhibitory

molecules to procaspases themselves, which would block inappropriate dimerisation and activation (Kumar and Colussi, 1999).

Single-chain zymogens of caspases-8 and -9 are partly active. Therefore, they should cause a slow production of active executioner caspases, but they are not dangerous to healthy cells. This may be explained by the presence of endogenous caspase inhibitors, members of the IAP (inhibitor of apoptotic protein) family, which inhibit executioner caspases-3 and -7, and possibly present a barrier to caspase activity that must be exceeded before the execution phase of apoptosis can occur. Thus, in the presence of IAPs, a little caspase activation is acceptable because it would be rapidly saturated by the inhibitors. In this hypothesis, the IAPs regulate the apoptotic threshold (Salvesen and Dixit, 1999).

Although it is widely accepted that caspases are obligatory for physiological cell death, it has been shown that other enzymes can act either upstream to activate caspases, or downstream to be activated as a consequence of proteolysis by caspases, i.e., other essential enzymes are involved in the intracellular apoptotic pathway (Vaux *et al.*, 1997). The involvement of the caspase family in cell death does not exclude a role for other families of protease, such as calpains or proteasome complex (Villa *et al.*, 1998). It has been suggested that vertebrate cells may have a caspase-independent death programme(s), which may serve as a back-up suicide mechanism (Weil *et al.*, 1998).

Caspases are, however, activated by most inducers of cell death and in most cell types. Oxidative stress, induced by H_2O_2, was shown to cause nuclear morphological changes (Goldkorn *et al.*, 1998) (as seen in Section 2.4.2.3) and DNA degradation (Hoyt *et al.*, 1997; Goldkorn *et al.*, 1998) (as seen in Section 3.1.4.3), both thought to be consequences of caspase activation, as cleavage of specific substrates by caspases has been proposed to either activate death effector molecules or trigger the structural changes characteristic of apoptotic cells (Bossy-Wetzel *et al.*, 1998). Thus, in the MCF10A and MCF10AneoT test cells, caspase activation and, hence, activity was anticipated to be detectable prior to these events.

3.2.2 The effect of oxidative stress on caspase activity

Caspase activity can be measured either by a fluorometric enzyme assay, or by western blot detection of caspase cleavage, by probing with specific caspase antibodies. The former was chosen, as it is much quicker, less costly, requires considerably smaller cell numbers, and is quantitative. Caspases-3 and -6 (executioner caspases) are the most active in apoptotic cells regardless of stimuli (Allen *et al.*, 1998), and their activation is an indication of a relatively early event in the signalling cascade, occurring prior to an increase in extranuclear/nuclear events (Vanags *et al.*, 1996). Thus, the substrate Ac-DEVD-AMC, which is cleaved by caspases-3 and -6, was used. The method employed was that of Miller *et al.* (1997).

3.2.2.1 Reagents

1 mg/ml Leupeptin stock. Leupeptin (0.5 mg, Sigma) was dissolved in MQ H_2O (500 µl), and stored as aliquots at -20°C.

200 mM Phenylmethylsulfonyl fluoride (PMSF) stock. PMSF (0.0174 g, Sigma) was dissolved in methanol (500 µl) and stored as aliquots at -20°C.

1 mM Dithiothreiotol (DTT) stock. DTT (4 mg, Sigma) was dissolved in dist.H_2O (26 µl) immediately before use.

2 mM Ac-DEVD-AMC Substrate stock. Substrate (5 mg, Sigma) was dissolved in dimethylsulfoxide (DMSO, 3.7 ml, Sigma) and stored as aliquots at -20°C.

Buffer A [10 mM HEPES, 42 mM KCl, 5 mM $MgCl_2$, 0.5% (m/v) CHAPS, 1 mM DTT, 1 mM PMSF, 1 µg/ml leupeptin, 0.02% (m/v) NaN_3, pH 7.4]. HEPES (0.238 g), KCl (0.313 g), $MgCl_2$ (0.048 g), CHAPS (0.5 g) and NaN_3 (0.02 g) were dissolved in MQ H_2O (80 ml), titrated with NaOH to pH 7.4, and made up to 100 ml. Immediately before use, leupeptin (2 µl), PMSF (10 µl) and DTT (2 µl) were added to the buffer (2 ml).

Buffer B [25 mM HEPES, 1 mM EDTA, 0.1% (m/v) CHAPS, 10% (m/v) sucrose, 3 mM DTT, 30 μM Ac-DEVD-AMC, 0.02% (m/v) NaN_3, pH 7.5]. HEPES (0.596 g), EDTA (0.037 g), CHAPS (0.1 g), sucrose (10 g) and NaN_3 (0.02 g) were dissolved in 80 ml MQ H_2O, titrated with NaOH to pH 7.5, and made up to 100 ml. Immediately before use, DTT (15 μl) and Ac-DEVD-AMC (75 μl) were added to the buffer (5 ml).

1 mM 7-amido-4-methylcoumarin (AMC) stock. AMC (0.001 g, Sigma) was dissolved in DMSO (5.714 ml) and stored at -20°C. This was diluted as required.

3.2.2.2 Procedure

Cells were grown, seeded (1 x 10^6 cells/5 ml in 35 mm cell culture petri dishes), treated (Section 2.4.1.2) and harvested (Section 2.4.2.2) as previously described. An additional treatment time (30 min) was included. The cell pellets were stored at -80°C until required for the assay.

Cell pellets were thawed in buffer A (100 μl), and lysed by vortexing. Thawing slowly after freezing aids in cell lysis due to the formation of ice crystals, which fracture cell membranes. Insoluble material was removed by gentle centrifugation (1400 x g, 1 min, RT), and the supernatant was assayed for enzyme activity. Each cell lysate was added as 50 μl aliquots to duplicate wells in a 96 multiwell plate, followed by addition of buffer B (150 μl) to each well. The plate was incubated (37°C, 1 h), with occasional mixing, and the fluorescence measured at the end of the incubation period, at excitation wavelength 370 nm and emission 460 nm, in a 7620 Microplate Fluorometer (Cambridge Technology, Inc.). The experiment was done in triplicate, and the results, which were calculated relative to the untreated control and were an average of all three experiments, were expressed as picomoles AMC released. These values were calculated using the equation obtained by linear regression analysis of the slope of a standard curve (picomoles AMC released against fluorescent units), generated by reading the fluorescence values, at excitation wavelength 370 nm and emission 460 nm, of dilutions of 1 mM AMC stock solution ranging from 0 to 120 picomoles.

3.2.2.3 Results

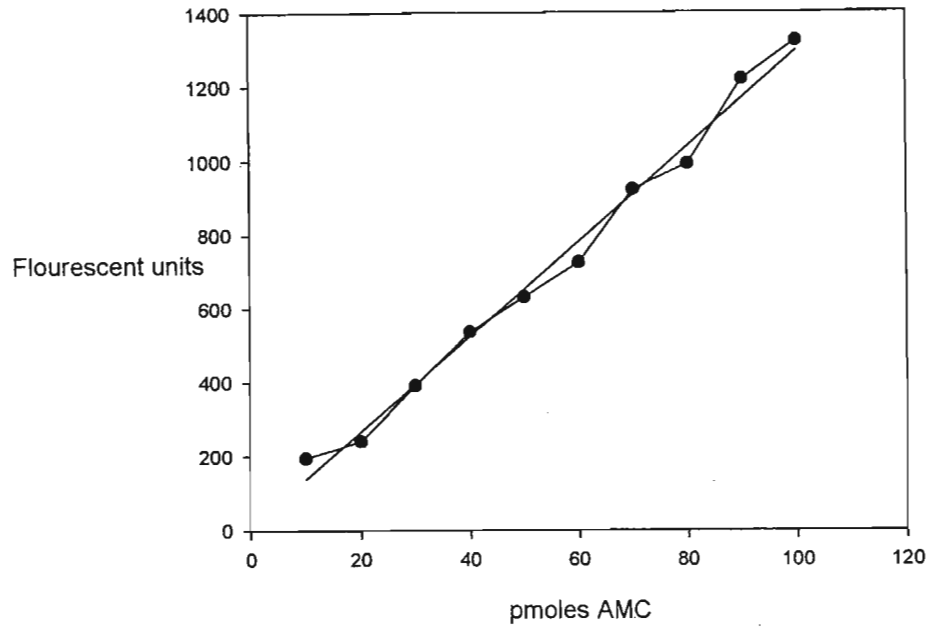

Figure 3.6 AMC calibration curve.

There was generally a time-dependent trend of increasing caspase activity, with activity generally increasing with increasing H_2O_2 concentrations up to a certain critical concentration, and decreasing thereafter (as summarised in Fig. 3.8, a, b). The caspase activity in the MCF10AneoT cells was much higher than that seen in the MCF10A cells (Fig. 3.7, a-d). Some initial interference with fluorescent readings of all cell lysates was observed between 0 and 1 h (Fig. 3.7, a-d), with readings dropping below baseline zero, in the case of the MCF10A cells, and being continued from 1-24 h at the highest concentration of H_2O_2 (1000 μM).

In the 100 μM and 250 μM H_2O_2-treated cells, increasing caspase activity was generally observed with increasing time of treatment, with the activity in the MCF10AneoT cell supernatants being higher than in MCF10A cells. However, the MCF10A caspase activity was much higher at 250 μM H_2O_2 (Fig. 3.7, b) than at 100 μM H_2O_2 (Figs 3.7, a, 3.8, a), whereas that of MCF10AneoT was only slightly higher (Figs 3.7, a, b, 3.8, b). In the MCF10AneoT cells there was a very sharp increase in enzyme activity from 4 to 8 h with exposure to 250 μM H_2O_2 (Fig. 3.7, b), whereas the

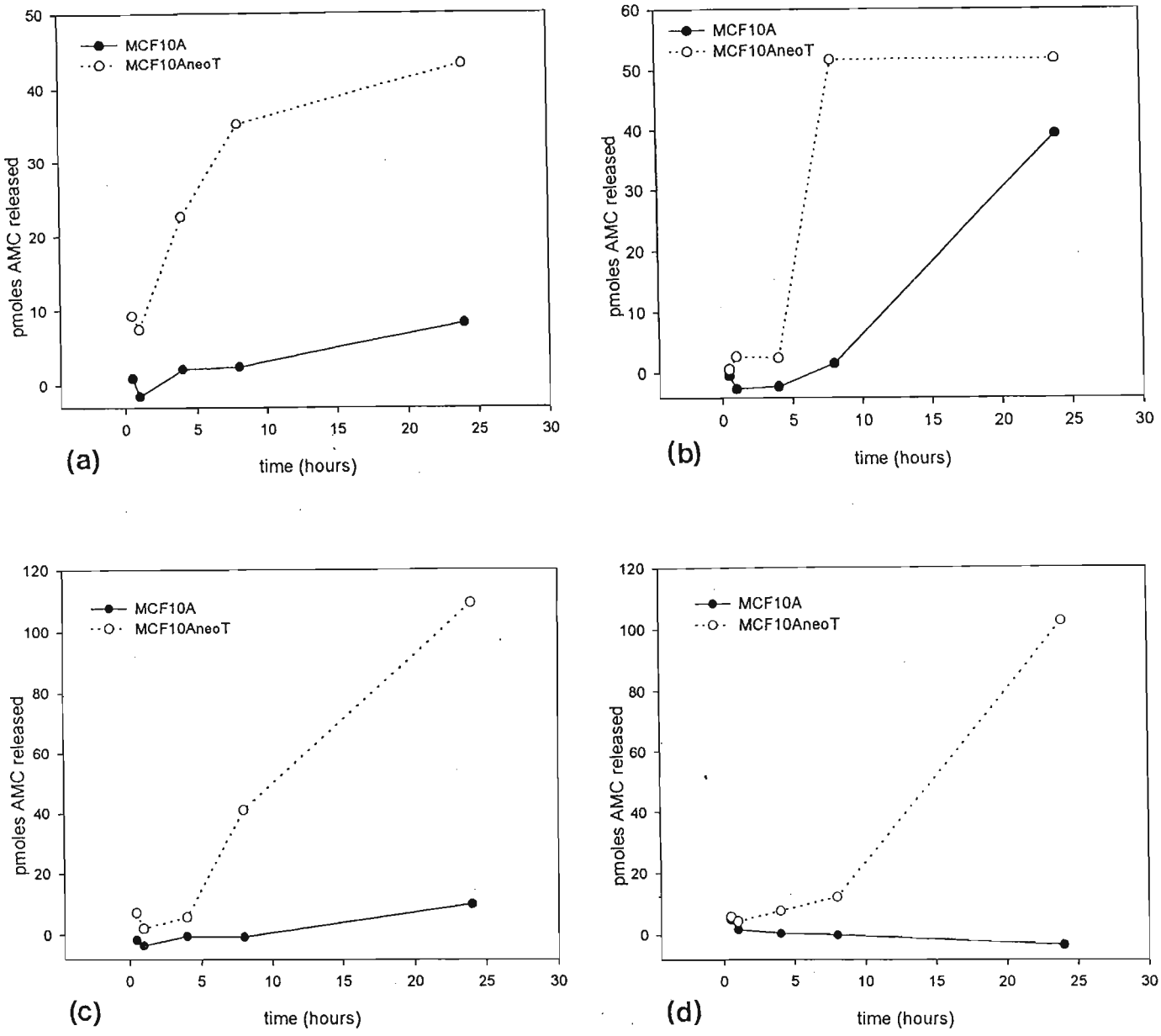

Figure 3.7 DEVD-AMC cleavage by H_2O_2-treated MCF10A and MCF10AneoT cells.

A comparison of DEVD-AMC cleavage, representative of caspase activity, by MCF10A and MCF10AneoT cells treated in serum-free medium with 3 μM Fe^{2+} and (a) 100 μM, (b) 250 μM, (c) 500 μM, and (d) 1000 μM H_2O_2.

activity in the MCF10A cells at this concentration increased from 8 h onwards (Fig. 3.7, b). The caspase activity of the MCF10A cells peaked at 250 μM H_2O_2 (Fig. 3.7, a), and decreased steadily after this with increasing levels of H_2O_2 (Figs 3.7, c, d, 3.8, a). The enzyme activity in MCF10AneoT cells, however, increased in a time- and dose-dependent manner (Fig. 3.7, a, b, c), peaking at 500 μM H_2O_2 (Figs 3.7, c, 3.8, b) and decreasing slightly upon exposure to 1000 μM H_2O_2 (Figs 3.7, d, 3.8, b).

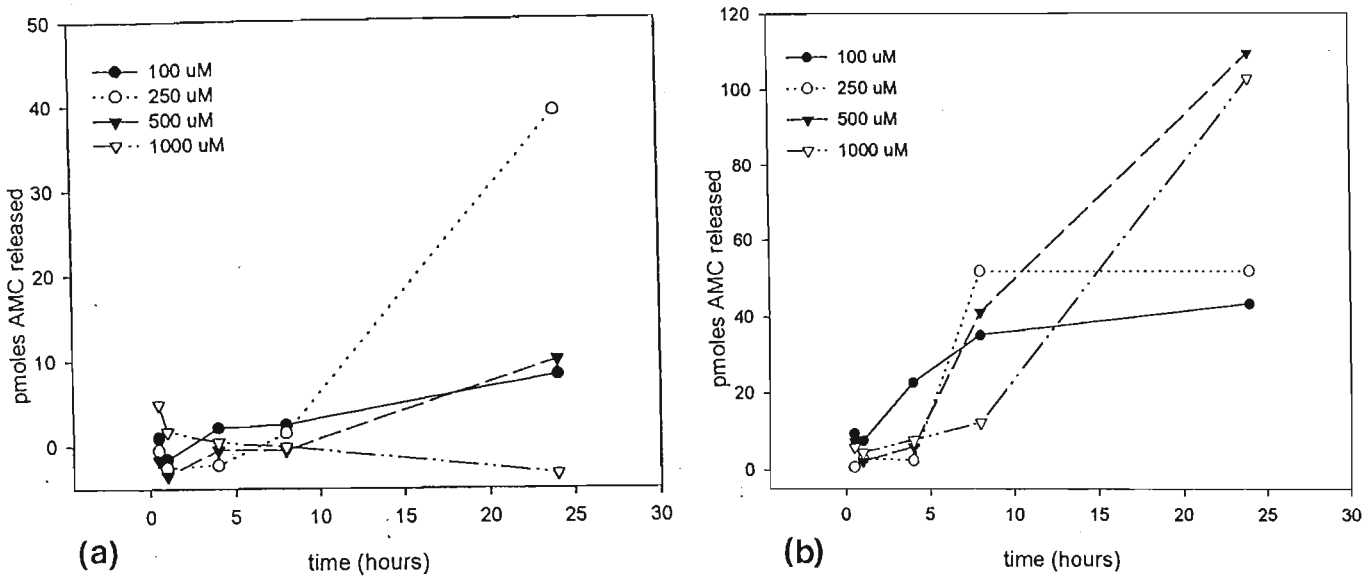

Figure 3.8 Composites of DEVD-AMC cleavage by MCF10A and MCF10AneoT cells at various H_2O_2 concentrations.

A comparison of DEVD-AMC cleavage, representative of caspase activity, by (a) MCF10A, and (b) MCF10AneoT cells, at various concentrations of H_2O_2.

3.2.2.4 Discussion

At all concentrations of treatment, there was an initial slight decrease in caspase activity from 30 min to 1 h in both cell lines, and significant caspase activity increases were only seen after 8 h in the MCF10A cells, and after 4 h in the MCF10AneoT cells. The possibility that this initial decrease was a result of quenching of the fluorescence by H_2O_2 remaining after treatment was eliminated, as cell pellets were rinsed with HBSS after harvesting. Such a decrease may be due to the fact that H_2O_2 can inhibit caspases (Boggs *et al.*, 1998), which would therefore only be activated much later, once the H_2O_2 was detoxified by the cells. The fact that caspases were activated earlier in the MCF10AneoT cells than in the MCF10A cells further supports the hypothesis of an inducible anti-oxidant by the cancer cells.

An interpretation of the sudden decrease in the induced caspase activity at higher levels of H_2O_2 is that necrosis, and the resultant permeability of the outer membrane of cells, allowed the release of caspases from the cells. The necrotic threshold of the

MCF10A cells, therefore, seems to occur at 250 μM H_2O_2, after which caspase activity decreases, possibly due to leakage as proposed. The necrosis threshold for the MCF10AneoT cells appeared to be 500 μM. The explanation that the activity decrease at higher levels of H_2O_2 seems to be due to leakage of membranes, as a result of necrosis, does not seem to fit the pattern of induction of necrosis as interpreted from light and electron microscopic studies, unless the caspase assay gives a much more sensitive detection of the necrotic process, detecting cellular leakage at an earlier time than necrotic morphology is visible.

The caspase activity in the MCF10AneoT cells was much higher than that in the MCF10A. This could mean that the MCF10AneoT cells are more susceptible to oxidative stress-induced apoptosis. However, this explanation does not correspond with the results from morphological studies and caspase activity at higher concentrations, although it does correlate with the light microscopic studies, in which the MCF10AneoT cells looked more affected and possibly more damaged than the MCF10A cells at the lower (100- and 250 μM) H_2O_2 concentrations. However, the finding that the concentration of H_2O_2 required to induce the highest caspase activity was 250 μM for the MCF10A cells, but 500 μM for the MCF10AneoT cells, indicates that the MCF10AneoT cells may be more resistant to oxidative stress-induced cell death and necrosis. This proposal is reinforced by the observation of greatly decreased caspase activity at 500 μM and 1000 μM H_2O_2 in the MCF10A cells, but a continued increase in activity at 500 μM H_2O_2 and only a slight decrease at 1000 μM in the MCF10AneoT cells, as well as by the results from the light and electron microscopic studies, which showed the onset of necrosis at an earlier time in the MCF10A cells than in the MCF10AneoT cells.

The results appear to be consistent with the hypothesis proposed, in Sections 2.4.1.4 and 2.4.2.4, of a non-linear response to oxidative stress and over-compensation, to redox stresses, by the pre-malignant cells so that they become more resistant to oxidative stress-induced damage at high concentrations of the stress-inducing agonist. Such a response may most likely involve the induction of GSH, which has previously been reported to be higher in tumour cells than in normal cells (Mitchell and Russo, 1987), or the activation of an enzyme with peroxidase activity. But the former is more likely, and

may possibly be induced via a *ras* activation, since the pre-malignant MCF10AneoT cells are transfected with mutationally activated *ras*.

GSH maintains the reducing environment in cells, and may regulate redox-controlled thiol proteins such as caspases, in addition to directly scavenging free radicals and other oxidants. If the levels of GSH are indeed higher in the MCF10AneoT cells, they would still possess sufficient levels of GSH for maintaining cell functioning and activity of redox-controlled proteins after GSH depletion by scavenging, whereas the MCF10A cells would be greatly depleted of GSH. The MCF10AneoT cells may, therefore, be able to overcome the oxidative stress or die by a controlled process (apoptosis), while the MCF10A cells may be unable to cope with the stress and die by necrosis. During necrosis, the cell membrane may become permeable due to uncontrolled H_2O_2 damage by lipid peroxidation and result in the leakage of cellular contents, including caspases, and this was possibly what was seen at 500- and 1000 μM H_2O_2.

Cleavage of cellular components by caspases have been reported to be responsible for the morphology characteristic of apoptosis. However, in the system under investigation, morphological changes were visible by 1 h, while significant caspase activity was seen much later. Therefore, it may be possible that other proteases, such as calpain proteases (Mills *et al.*, 1998a), are involved in the liberation of DNases and in generating the characteristic morphological features.

3.3 Discussion

It seems that necrosis, as evidenced by cellular leakage, was detected at a lower H_2O_2 concentration (500 μM) at the biochemical level, and only at a much higher level (1000 μM) in the morphological studies. The caspase fluorometric technique used, although not an earlier indicator than morphology of the progression towards apoptosis in the system tested, gives more valuable information. Quantitative rises in caspase activity are very clear, whereas no change in morphology (visualised by light microscopy) was seen in the MCF10A cells even after 24 h of treatment with 100 μM H_2O_2, and gives a clear indication of the onset of necrosis. Another advantage of this method is that it is quicker, easier to perform and more sensitive than agarose gel electrophoresis, as it gives

comparable, quantitative data. Also, the danger of harmful substances is eliminated as there is no use of UV light or ethidium bromide, which is very toxic and carcinogenic.

Caspase activity has been proven to be a relatively late (but useful) indicator of apoptosis in the system studied, as significant caspase activity was detected after morphological changes and apoptotic DNA fragmentation occurred. Therefore, cytochrome c release, which has been reported to be an early apoptotic event in other systems, was investigated, in an effort to determine the earliest detectable apoptotic events in the system under examination. Cytochrome c was anticipated to be released because, as mentioned in Section 2.5, although examination of mitochondria did not reveal any membrane disruption in apoptotic cells, pores may have been present. Also, caspases in damage-induced apoptosis have been reported to be activated after cytochrome c is released (Coppola and Ghibelli, 2000; Mathias *et al.*, 1998).

CHAPTER 4
MITOCHONDRIAL CHANGES IN APOPTOSIS

4.1 Introduction

The importance of the mitochondrion in the induction of apoptosis has recently become evident (Henkart and Grinstein, 1996). Emerging evidence suggests that mitochondria participate in the effector and execution phase of the cell death cascade (Newmeyer *et al.*, 1994; Petit *et al*, 1995; Krippner *et al.*, 1996; Murphy *et al.*, 1996; Yang *et al.*, 1997; Zou *et al.*, 1997). As previously described, cell death may be induced via various signals reaching the cell, ultimately leading to release, from the intermembrane mitochondrial compartment, of death-inducing factors such as cytochrome c, apoptosis inducing factor (AIF) and certain pro-caspases (Crompton, 1999). The exact mechanisms and sequence of events that lead to apoptosis remain unclear, but these will be discussed and interpreted for the particular cell line used, in light of results of the previous chapters, and the literature. It seems that a specialised pore, the permeability transition (PT) pore, which is made up of many components, is important in the normal functioning of mitochondria and for its role in the release of apoptogenic proteins, such as cytochrome c, during apoptosis. Before PT and the mitochondrial responses during apoptosis may be discussed, the structure and function of mitochondria (including resident proteins) and their role in the normal and apoptotic cell must be considered.

4.2 Structure and function of mitochondria

Mitochondria are the organelles that specialise in the rapid oxidation of a limited number of substrates (particularly pyruvate and fatty acids, NADH and $FADH_2$), with conservation of the resulting free energy in the form of ATP (Chen and Rivers, 1990) (Fig. 4.1). The mitochondria are enveloped by two separate lipid bilayer membranes, the outer and the inner membranes. These define two submitochondrial compartments, the intermembrane space between the two membranes, and the matrix or central compartment (Lodish *et al*, 1995). The outer membrane of the mitochondrion is pierced by simple,

single protein pores (Dihanich, 1990) that largely allow passage of charged and uncharged solutes up to 5 kDa in size (Chen and Rivers, 1990). The PT pore is made up of some of these proteins as well as components from the inner membrane and the matrix, and usually has an exclusion limit of 1.5 kDa (Crompton, 1999). The inner membrane is responsible for the production of energy via the generation of a proton gradient between the intermembrane space and the inner matrix (Chen and Rivers, 1990) and contains a number of transporters, the F_0F_1 ATPase pump and the electron transport chain responsible for the production of the proton gradient, and hence, ATP (Fig. 4.1).

4.2.1 Structure and function of transporter proteins of the outer membrane

Apart from hydrophobic molecules, only water and gases like CO_2, N_2, and O_2, may permeate phospholipid bilayers by simple diffusion. Most biological membranes, including those of the mitochondrion, however, maintain ion gradients between different compartments, and have highly specific transport systems, which allow molecules to selectively cross the membrane (Dihanich, 1990).

The outer mitochondrial membrane functions primarily as a permeability barrier with a defined exclusion limit for hydrophilic metabolites (Ha *et al.*, 1993). This is mainly due to the presence of pore-forming proteins, called porins or voltage-dependent anion channels (VDAC) (Dihanich, 1990), and possibly Bcl-2, Bcl-X_L, Bid and Bax proteins which either form permanent discrete pores, as depicted in Figure 4.1, or affect the permeability properties of the mitochondrial membrane, by being recruited from the cytosol during the induction of apoptosis (Nouraini *et al.*, 2000). In addition, Bcl-2 may interact with the VDAC component of the highly specialised PT pore in the mitochondrial membranes (Crompton, 1999), and thus, regulate its activity.

4.2.1.1 Voltage-dependent anion channel (VDAC) proteins

The outer mitochondrial membrane appears not to limit diffusion of respiratory substrates such as NADH and the adenine nucleotides, ADP and ATP. These have molecular weights in the range 0.1-0.4 kDa and are generally negatively charged. At the

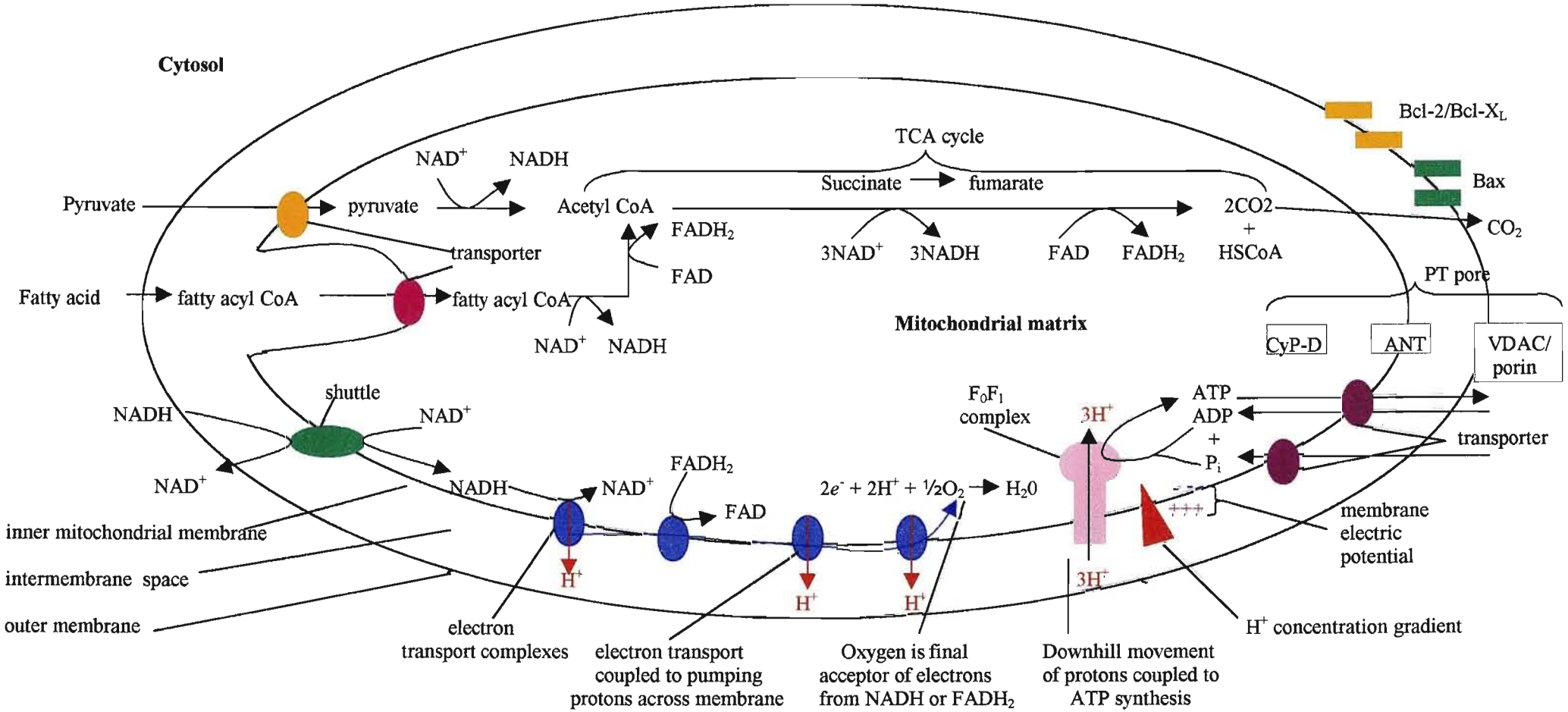

Figure 4.1 Outline of the major metabolic reactions, membrane transporters and pores of the mitochondria.

The substrates of oxidative phophorylation – pyruvate, fatty acids, ADP, and P_I – are transported to the matrix from the cytosol by transporters. O_2 diffuses into the matrix. NADH, which is generated in the cytosol during glycolysis, is not transported directly to the matrix because the inner membrane is impermeable to NAD^+ or NADH. Thus, a shuttle system transports electrons from cytosolic NADH to the electron transport chain. ATP is transported to the cytosol in exchange for ADP and P_i, CO_2 diffuses into the cytosol across the mitochondrial membranes. Fatty acids are linked to CoA on the outer mitochondrial membrane amd shuttled across the membrane by a translocase enzyme. The electron transfer carrier protein complexes that transfer electrons from NADH and $FADH_2$ to O_2 are depicted as blue oval structures. Bcl-2 family member proteins (Bcl-2, Bcl-X_L, Bax) are found in the outer membrane and may form pores. The permeability transition (PT) pore consists of an association between the voltage-dependent anion channel (VDAC), in the outer membrane, adenine nucleotide translocator (ANT), in the inner membrane, and cyclophilin-D (CyP-D), in the matrix. Adapted from Lodish *et al.* (1995).

other extreme of size and charge, the outer membrane is usually impermeable to cytochrome c in its mature form (holocytochrome c), a cationic polypeptide of 12 kDa (Dihanich, 1990).

Mitochondrial porins, or VDACs, are the outer membrane basic proteins with molecular masses between 30 and 35 kDa (Dihanich, 1990), which allow low-M_r solute access to the solute-specific transport systems of the inner membrane (Figs 4.1, 4.2) (Crompton, 1999). The VDAC proteins contain stretches of alternating hydrophobic and hydrophilic amino acids, arranged in a β-barrel containing 16 anti-parallel, amphiphilic β-strands, or 12 β-strands and the amphiphilic N-terminal α-helix. It has been suggested that the N-terminus is exposed to either the intermembrane space or the cytosol, and may play a role in stabilisation of the open state of the pore by interacting with the flexible loops, which perform the "gating" function (Popp *et al.*, 1996).

The VDAC channel is not ion-specific but it does display ion selectivity. It is generally more permeable to smaller than to larger solutes of like charge and is more permeable to anions than to cations of similar size. It is also voltage-gated, i.e., it switches to lower-conducting substrates when exposed to transmembrane potentials as low as 20 mV. Not only is the voltage-induced "closed" state less conducting than the "open" state, it is reported to have opposite selectivity, i.e., it is more permeable to cations than anions. The effect of the "open" to "closed" VDAC transition on mitochondrial metabolism may be profound (Dihanich, 1990), as it regulates the flux of hydrophilic metabolites (<5 kDa) across the outer membrane and, thus, affects pyruvate, fatty acid and ATP metabolism. Alternately, as part of the PT pore (Crompton, 1999), it may regulate the efflux of cytochrome c and other death-inducing factors (AIF, caspases) from the intermembrane space, via a mechanism requiring Bcl-2 family member participation and, thus, affect downstream events in the apoptotic cascade. The function of the individual simple pore-forming proteins, their interactions with each other, and their perceived role in apoptosis are considered before the PT pore, release of apoptogenic proteins and consequences thereof, are discussed.

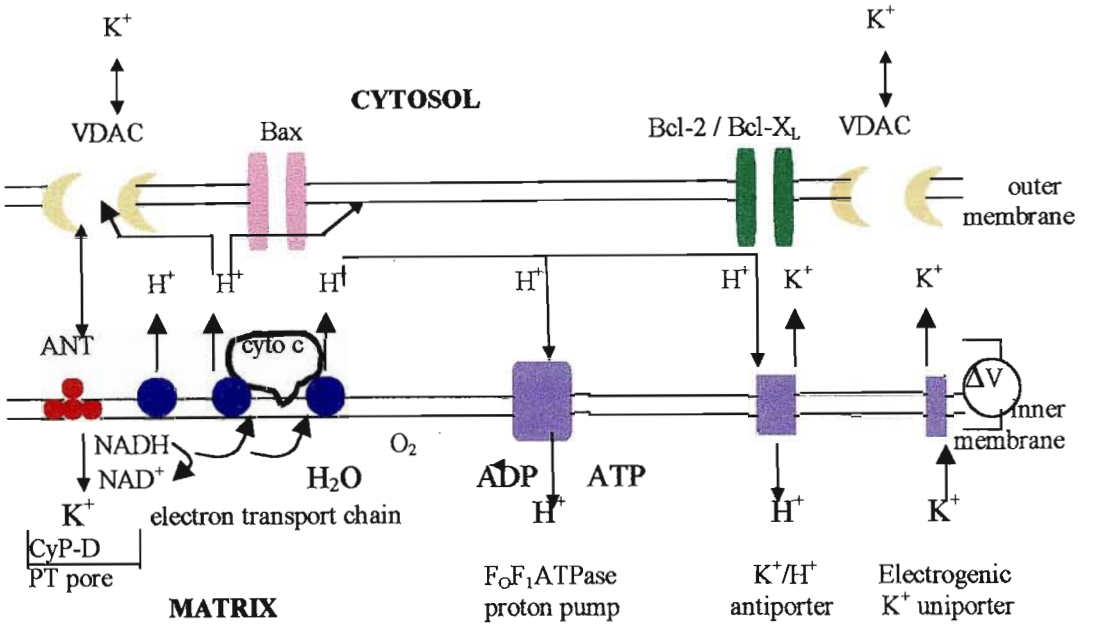

Figure 4.2 The regulation of membrane potential and volume in mitochondria.

The inner mitochondrial transmembrane potential is mainly a proton gradient, and depends on the respiratory chain components and the F_0F_1 ATPase proton pump to pump protons across the inner membrane. K^+ is the major determinant of mitochondrial matrix volume, and its transport across the inner membrane is controlled by several channels including a K^+/H^+ antiporter, an electrogenic K^+ uniporter, and perhaps the adenine nucleotide translocator (ANT), voltage-dependent anion channel (VDAC) and cyclophilin-D (CyP-D). Adapted from Reed (1997).

4.2.1.2 Bcl-2, Bcl-X_L, Bid and Bax proteins

It has been proposed that the complex interplay between the various Bcl-2 family members, Bcl-X_L, Bid, Bax and Bcl-2, and their relative proportions in the outer mitochondrial membrane, may influence the permeability and integrity of the mitochondrial membrane and the release of apoptogenic proteins which control cell death, either by opening pores, such as the PT pore, or producing breaks in the outer mitochondrial membrane (Green, 1998).

The outer membrane may contain the anti-apoptotic pore forming proteins of the Bcl-2 family, Bcl-2 and Bcl-X_L (Reed, 1994), whereas two other cytosolically located pro-apoptotic proteins, Bid and Bax, may be recruited from the cytoplasm to the mitochondrial

membrane during the induction of apoptosis, directly or indirectly resulting in the release of death-inducing factors (Li *et al.*, 1998; Luo *et al.*, 1998; Jurgensmeier *et al.*, 1998).

There are several mechanisms by which pro-apoptotic Bcl-2 family members might induce outer membrane permeability without affecting the inner membrane. These membrane-associated proteins may form channels large enough for the passage of soluble proteins (Reed, 1997) or cooperate with channels already present, such as the VDAC channel (Shimizu *et al.*, 1999). Alternate mechanisms might include a specific interaction with organellar membranes to cause visible changes (3-10 nm) in the lipid structure and permeability to high molecular mass, pro-apoptotic proteins (van Leyen *et al.*, 1998), or may be similar to the manner in which Bax causes instabilities in artificial membranes (Basanez *et al.*, 1999). Whether the pores created are large enough to admit fully folded apoptogenic proteins is another question altogether, however.

According to Crompton (1999), there is no direct evidence for pore-forming proteins in the outer membrane which could create pores large enough for the release of proteins from the intermembrane space (Crompton, 1999). Therefore, it is possible that pro-apoptotic protein release mainly occurs via a larger, multi-component PT pore, consisting of the VDAC channel and at least two other components (Fig. 4.1), which span the inner and outer membrane, and with which members of the Bcl-2 family may interact. The literature gives an incomplete and contradictory picture of this pore and only a few details are known.

It has also been suggested that cytochome c release may occur via mitochondrial swelling, but it is questionable whether such swelling occurs in most instances of apoptosis or whether it is required for cytochrome c release, as electron micrographs of apoptotic cells frequently contain apparently intact unswollen mitochondria. Further, it has also been reported that the pore-forming pro-apoptotic proteins Bid and Bax can release cytochrome c from isolated mitochondria in the absence of detectable mitochondrial swelling (Kluck *et al.*, 1999).

The Bcl-2 family has a number of conserved sequences termed BH (Bcl-2 homology) domains. The BH1, BH2, BH3, and BH4 domains have critical functions in determining the pro- and anti-apoptotic properties of the various family members, and are involved in mediating interactions between them (Gilmore *et al.*, 2000). Pro-apoptotic

Bid shares only the BH3 domain homology with other members of the family, although its structure shows striking similarity to Bcl-X_L, and hence, possibly the other Bcl-2 family members (Chou *et al.*, 1999).

The sequence homology between Bcl-X_L and other members of the Bcl-2 family suggests that these proteins exhibit a similar fold (Muchmore *et al.*, 1996). All of these proteins have a stretch of hydrophobic amino acids located at the carboxyl terminus, which presumably allows the proteins to post-translationally insert into membranes (Gilmore *et al.*, 2000). The Bcl-X_L structure is known to consist of two central, primarily hydrophobic α-helices (α5 and α6) arranged in an anti-parallel fashion, and surrounded by 5 amphipathic helices. Helices α1 and α2 are connected by a flexible 60-residue loop. BH1, BH2 and BH3 are in close proximity and form an elongated hydrophobic cleft that may represent the binding site for other Bcl-2 family members (Muchmore *et al.*, 1996).

The structure of Bcl-X_L, Bcl-2, Bid and Bax suggests a potential to form membrane pores, and Bcl-X_L, Bcl-2 and Bax have all been shown to form pores in artificial bilayers (Gilmore *et al.*, 2000). The channel-forming requirements and the properties of the channels differ between the anti- and pro-apoptotic proteins. The anti-apoptotic proteins Bcl-X_L and Bcl-2 form channels only at low pH and these channels are cation-selective, whereas the pro-apoptotic protein Bax can form channels, at neutral pH, that are anion-selective (Antonsson *et al.*, 2000).

The way in which Bcl-X_L is anti-apoptotic seems uncertain, although Bcl-X_L has been shown to modulate the osmotic and electrical homeostasis of the mitochondria (Vander Heiden *et al.*, 1997) and may, thereby, prevent the release of cytochrome c and other death-inducing factors, and hence, obviate apoptosis. It has been proposed that Bcl-2 acts at various levels (prevents cytochrome c release and caspase activation, regulates Ca^{2+} levels, and interacts with the pro-apoptotic Bcl-2 homologues to abrogate their apoptotic functions, as described in Section 1.4.2.2) to prevent apoptosis (Froesch *et al.*, 1999). The details of how this is achieved, however, have not been elucidated.

Pro-apoptotic Bax has been reported to be predominantly cytosolic in healthy cells, but it translocates to mitochondria in a number of cell types after receipt of a death signal (Wolter *et al.*, 1997), and can cause mitochondria to release cytochrome c (Jurgensmeier *et al.*, 1998). It has been proposed that Bax remains weakly attached to mitochondria in

the absence of apoptotic stimuli, and that only BH-3 proteins such as Bid may promote apoptosis by modifying the structure of Bax, leading to its insertion into mitochondrial membranes (Desagher *et al.*, 1999).

Full length Bid, also present in the cytosol, is inactive. Upon cleavage by caspase-8, the C-terminal fragment translocates to the mitochondria and is 100 times more efficient in inducing cytochrome c release compared to its full-length precursor (Li *et al.*, 1998; Luo *et al.*, 1998). Bid may either interact with pro-apoptotic members of the Bcl-2 family, such as Bax, through their respective BH3 domains, or on its own it is potentially able to form selective ion channels similar to those formed by Bax (Chou *et al.*, 1999). Translocation of Bid to mitochondria and binding to Bax leads to a change in conformation of Bax, and subsequent cytochrome c release from mitochondria. Caspase-induced Bid-cleavage is, however, not an essential requirement for its movement to mitochondria. Translocation of full-length Bid to the mitochondrial membrane may, therefore, occur in types of apoptosis in which activation of caspases is not a primary event in the apoptotic pathway (Desagher *et al.*, 1999).

Though the mechanism has not yet been elucidated, Bax can also functionally interact with the VDAC, as well as components of the mitochondrial inner membrane, including an adenine nucleotide transporter/translocase (ANT-which transports ADP and ATP between the matrix and intermembrane space and is part of the PT pore) and the F_0F_1 ATPase H^+ pump (which catalyses the synthesis of ATP) (Nourani *et al.*, 2000) (Fig. 4.1). Therefore, Bax may influence the behaviour of the PT pore, and thus, the efflux of apoptosis-inducing factors, and downstream events of the apoptotic cascade, as well as ATP metabolism. This, in turn, affects apoptosis, as ATP is required for this process.

Permeabilisation by Bid and Bax is greatly enhanced by a novel cytosolic factor, termed permeability enhancing factor (PEF). Preliminary characterisation showed that PEF is a large protein (>300 kDa) which is inactivated by caspases, and does not behave like Bid or Bax. The mechanism of action of PEF, in particular, how PEF is permitted to function only after a prior permeabilisation of the outer membrane by Bid and Bax, is unclear. One possibility is that PEF could interact with a target located on the lumenal side of the outer membrane. In this case PEF would only gain access to its sites of action when the outer membrane becomes permeable to some degree. Alternatively, PEF could

require the co-operation of a non-soluble factor that is located within the intermembrane space. A further possibility is that PEF interacts directly with channels produced by Bid or Bax (Kluck *et al.*, 1999) (by an unknown mechanism), resulting in cytochrome c release, and downstream apoptotic events.

While flow of metabolites across the outer membrane through pores may control apoptotic events and limit the rate of mitochondrial oxidation, and hence ATP levels, the inner membrane is the major permeability barrier between the cytosol and the mitochondrial matrix and houses important ATP-generating complexes (Lodish *et al.*, 1995).

4.2.2 Structure and function of components of the inner membrane

The inner membrane and the matrix are the sites of most reactions involved in the oxidation of fatty acids via β oxidation, the oxidation of pyruvate from glycolysis, via the tricarboxylic acid (TCA) cycle, and the coupled synthesis of ATP from ADP and P_i. These complex processes involve many steps but can be subdivided into three groups of reactions, each of which occurs in a discrete region of the inner membrane or matrix:

1. the oxidation of pyruvate or fatty acids to CO_2, coupled to the reduction of the electron carriers NAD^+ and FAD to NADH and $FADH_2$, respectively. These reactions occur in the matrix or on the inner-membrane proteins facing it (Fig. 4.1).
2. the electron transfer from NADH and $FADH_2$, via the electron transport chain, to O_2. These reactions occur in the inner membrane and are coupled to the generation of a proton-motive force across this membrane, as the reactions are used to pump protons across the membrane, out of the central matrix compartment (Figs 4.1, 4.2).
3. the harnessing of the energy stored in the electrochemical proton gradient for ATP synthesis by the F_0F_1 ATPase complex in the inner membrane (Figs 4.1, 4.2).

The last two groups of reactions involve multi-subunit proteins that are asymmetrically oriented in the inner mitochondrial membrane (Fig. 4.3). This membrane has highly convoluted inward foldings (cristae) that greatly expand the surface area of the inner membrane, enhancing its ability to generate ATP. These two groups of reactions will be discussed briefly because of the potential involvement of their components in the

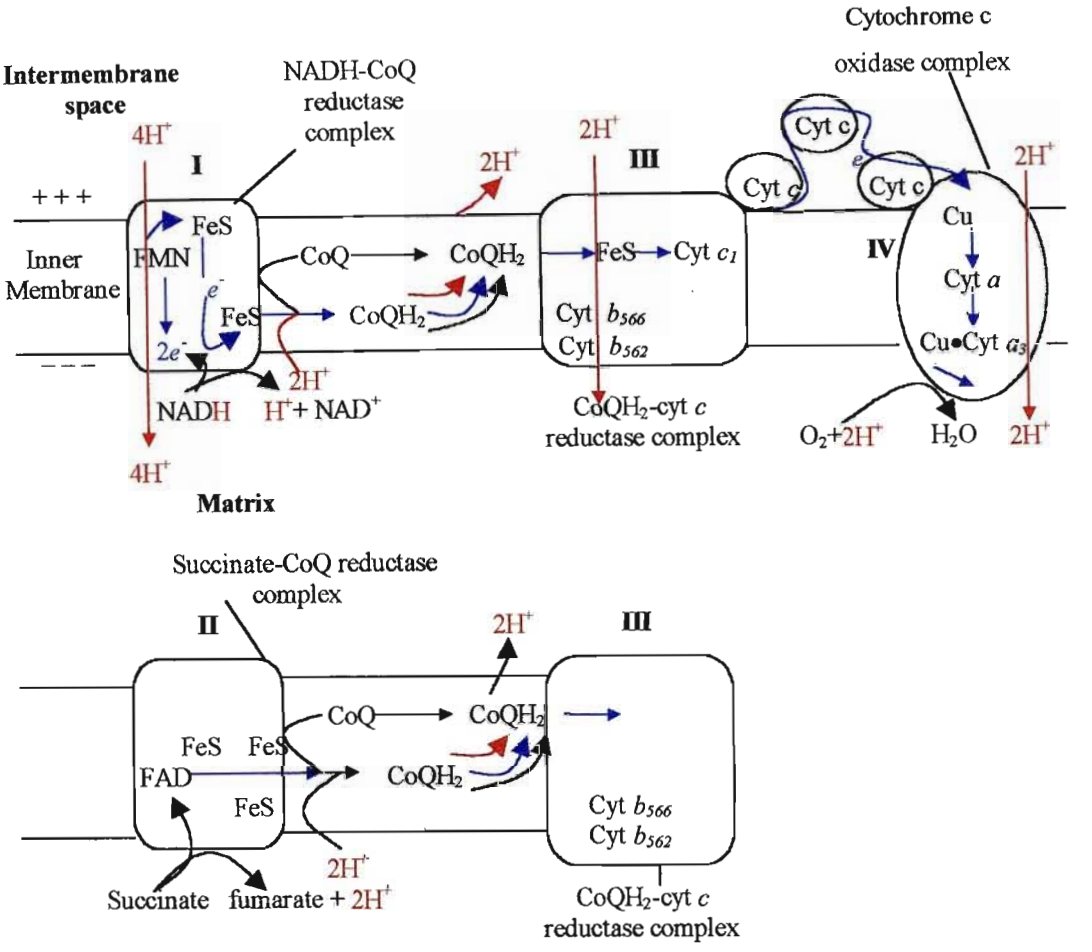

Figure 4.3 The pathway of electron transport (blue) and proton transport (red) in the inner mitochondrial membrane.

A pair of electrons is transported from one NADH to one CoQ molecule by the NADH-CoQ reductase complex (I), resulting in the transport of four electrons from the matrix to the intermembrane space. For every electron pair transported from CoQ through the $CoQH_2$-cytochrome c reductase complex (III), four protons are moved from the matrix to the intermembrane space. Finally, the peripheral protein cytochrome c diffuses in the intermembrane space, transporting (electrons one at a time) from the $CoQH_2$-cytochrome c reductase complex to the cytochrome c oxidase complex (IV). The transport of a pair of electrons through the latter complex, needed to reduce one oxygen atom, is accompanied by the translocation of two protons. The protons released into the matrix space by the oxidation of NADH are consumed in the formation of water from O_2, resulting in no net proton translocation from these reactions. Thus a total of 10 protons are translocated per pair of electrons moved from NADH to O_2.

The succinate-CoQ reductase complex (II) oxidises succinate to fumarate, reducing one CoQ to $CoQH_2$ which donates its electrons to the $CoQH_2$-cytochrome c reductase complex (III). No protons are translocated by the succinate-CoQ reductase complex. From Lodish *et al.* (1995).

apoptotic process.

The electron transport chain consists of four complexes, the NADH-CoQ reductase, succinate-CoQ reductase, $CoQH_2$-cytochrome c reductase, and cytochrome c oxidase complexes, which are composed of inorganic and organic molecules, as well as cofactors (Fig. 4.3). Electrons are shuttled between the complexes by coenzyme Q and cytochrome c. All the complexes, except the succinate-CoQ reductase, pump protons across the inner mitochondrial membrane, from the matrix into the intermembrane space (Lodish *et al.*, 1995), thereby generating an electrochemical gradient which has two components: a membrane potential (ψ_m – as protons are positively charged) and a pH gradient (protons determine acidity) (Chen and Rivers, 1990) (Figs 4.2, 4.3).

This gradient is used by the F_0F_1 ATPase complex (Lodish *et al.*, 1995) as the driving force for phosphorylation of ADP to form ATP (Chen and Rivers, 1990). The bipartite enzyme complex is composed of two oligomeric complexes, F_0 and F_1. The F_0 portion is an integral membrane protein, and consists of three subunits that form a proton conduction channel, while the F_1 portion contains nine subunits. Although it is not an integral membrane protein, F_1 probably forms the barrier that makes the inner membrane impermeable to protons. Proton movement through F_1, driven by the proton-motive force, promotes the catalytic synthesis of ATP by the F_1 portion (Lodish *et al.*, 1995). As previously mentioned, ATP is required for many cellular processes as well as for the execution phase of apoptosis (Leist *et al.*, 1997).

One of the complexes requiring ATP for regulation is the PT pore, spanning the inner and outer membrane, which appears to be the major channel involved in the release of apoptogenic factors during apoptosis. The point of regulation by ATP in this complex may be the inner membrane protein, adenine nucleotide translocase (ANT), which mediates ADP $\leftrightarrow$ ATP exchange and operates as a gated pore (Crompton, 1999).

4.2.3 The permeability transition (PT) pore – topology and regulation

The significance of the PT pore, the Ca^{2+}-dependent pore in the mitochondrial membranes, in the apoptotic process has only recently been discovered (Crompton, 1999). It seems to be involved in the release of apoptogenic proteins from the intermembrane

space under the influence of specific apoptogenic stimulae, and is ultimately responsible for the maintenance of ψ_m and ATP levels, as it regulates intramitochondrial Ca^{2+} levels, which, in turn, regulate the Ca^{2+}-sensitive enzymes of the TCA cycle. These enzymes regulate levels of succinate from the TCA cycle, which feeds into complex II of the electron transport chain, which maintains the H^+ gradient (Fig. 4.3) and ATP levels. The PT pore is, therefore, responsible for the ψ_m and control of ATP generation, and acts as a finely balanced sensor for apoptogenic signals (Fig. 4.5), such as those which will be described in Section 4.2.3.1.

The components of this pore are the outer membrane pore-forming protein voltage-dependent anion channel (VDAC), adenine nucleotide translocase (ANT) which, as mentioned above, is located on the inner mitochondrial membrane, and cyclophilin-D (CyP-D), a matrix component (Fig. 4.4). When occupied by transportable substrate (ADP, ATP), ANT alternates between two conformations in which the ADP/ATP-binding site is either on the matrix side of the inner membrane (m-state) or on the cytoplasmic side (c-state). ANT ligands that bind on the m-state inhibit the pore, whereas c-state ligands activate the pore, suggesting that the c-state conformation is required for PT pore opening. CyP-D is the mitochondrial isoform of a family of CyP proteins that catalyse *cis-trans* isomerisation of accessible Xaa-Pro peptide bonds in proteins. The catalytic activities of CyP point to a role for CyP-D in protein folding and/or conformational change, with a possible role in maintaining the conformation of ANT required for pore opening and closing (Crompton, 1999).

PT pores may establish contact between mitochondria in the formation of mitochondrial networks. Mitochondria have been reported to form tight intermitochondrial junctions, providing continuity between the matrix spaces of the apposed mitochondria, and allowing the thus-conjugated mitochondria to operate as a bioenergetic continuum. In this way potential energy in the form of the proton electrochemical gradient may be "wired" along conjugated mitochondria, permitting efficient energy transfer between different parts of the cell (Crompton, 1999). Though the PT pore appears to normally occur at contact sites between the mitochondria, it may form free non-mitochondria-linking pores in certain pathological circumstances (Crompton, 1999), although this is not clear from the literature.

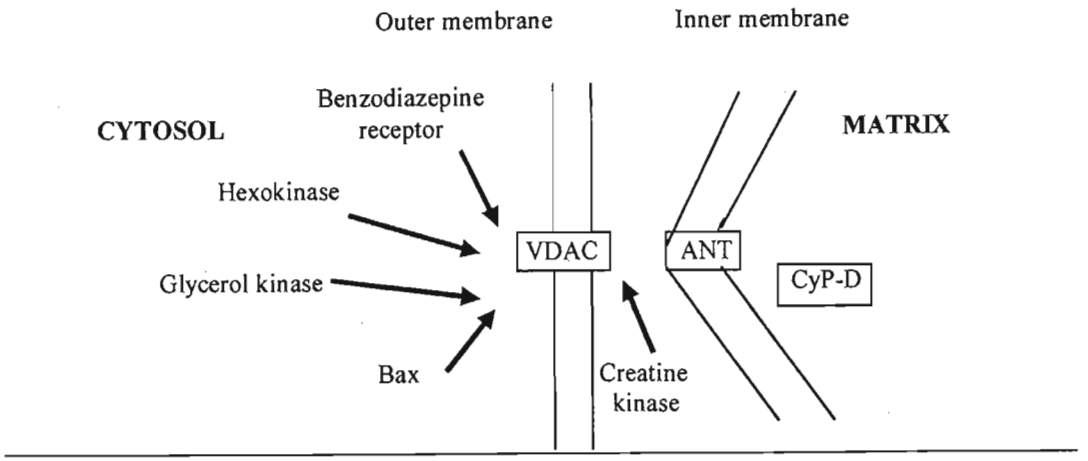

Figure 4.4 Permeability transition pore topology.

The basic unit of the permeability transition (PT) pore is the VDAC-ANT-CyP-D complex located at contact sites between the mitochondrial inner and outer membranes. Other proteins associate with the complex as indicated. ANT, adenine nucleotide translocase; CyP-D, cyclophilin-D; VDAC, voltage-dependent anion channel. From Crompton (1999).

The diameter of the closed PT pore has been estimated to be 1.0-1.3 nm, whereas that of the open pore is 2.0-2.6 nm. This possibly equates to an exclusion limit of 1.5 kDa (Crompton, 1999). As cytochrome c and AIF have molecular weights of 12.5 and 57 kDa, respectively, the PT pore does not have the potential to release these apoptogenic proteins from the intermembrane space (to facilitate the process of apoptosis), unless the recruited pro-apoptotic proteins Bid and Bax increase the size of the pore significantly, or pore opening eventually leads to outer membrane rupture.

The contact sites established by the VDAC-ANT-CyP-D complex between the inner and outer membranes has an important role in energy transduction. Certain kinases, e.g., hexokinase and glycerol kinase, are attracted to and associate with the VDAC-ANT complex (Fig. 4.4), thereby providing a conduit whereby ATP generated by oxidative phosphorylation is channelled directly to the kinases. The contact sites are also involved in the transfer of phosphatidylserine between the endoplasmic reticulum and the mitochondrial inner membrane. For this, other proteins, e.g kinases and benzodiazepine receptor (Fig. 4.4) are recruited to the sites for efficient phospholipid transfer (Crompton, 1999). The PT pore has several levels of fine regulation and hence, is a delicate sensor organelle which has great influence over cell well-being, being in control of the instruments of life (ATP and other metabolic products) and death (AIF, cytochrome c and

caspase release). The various ways in which mitochondria regulate this pore will now be discussed.

4.2.3.1 PT pore regulation under physiological conditions

Intramitochondrial Ca^{2+} is controlled by Ca^{2+} cycling (Fig. 4.5) and ultimately controls the ψ_m and ATP generation. Ca^{2+} enters mitochondria electrophoretically via the Ca^{2+} uniporter (Fig. 4.5), driven by respiratory-chain expulsion of H^+ and the ψ_m, and exits by exchange with Na^{2+} on the Na^{2+}/Ca^{2+} antiporter (Fig. 4.5). These two transport systems together with the Na^{2+}/H^+ antiporter establish a transport cycle that mediates slow, continuous cycling of Ca^{2+} across the inner membrane (Crompton, 1999).

4.2.3.2 PT pore regulation under pathological conditions

While high $[Ca^{2+}]$ and P_i causes the PT pore to open, high levels of ATP cause pore closure, either via ANT or by acting on attached hexokinases. Transient opening, which occurs at a frequency determined by matrix free $[Ca^{2+}]$, appears to be its normal mode of behaviour, whereas prolonged PT pore opening seems likely to occur only in pathological states (high Ca^{2+}, oxidative stress, Fig. 4.6). Rapid PT pore opening and closing ("flickering") may serve to regulate mitochondrial Ca^{2+} by allowing Ca^{2+} efflux, while prolonged opening may be the critical event leading to collapse of the ψ_m, which results in ATP depletion and cell death by necrosis. Similarly, ANT changes from a selective antiporter to a non-selective pore under high $[Ca^{2+}]$. The open pore is large enough to admit most metabolites as well as hydrated inorganic ions, including Ca^{2+}, and has a cut-off in permeability at 1.5 kDa (Crompton, 1999).

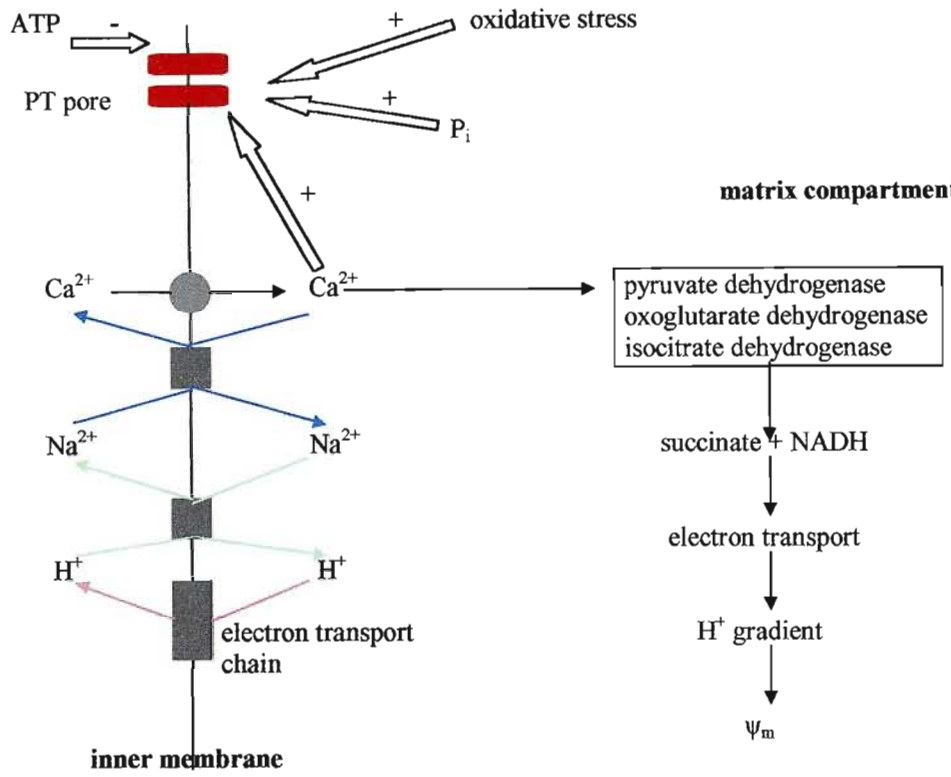

Figure 4.5 Physiological and pathological effects of mitochondrial Ca^{2+}.

Mitochondrial Ca^{2+} is controlled by a transport cycle driven by the proton pumps of the electron transport chain. The transport cycle is mediated by the Ca^{2+} uniporter, the Na^{2+}/Ca^{2+} antiporter and the Na^{2+}/H^+ antiporter of the inner membrane. Under physiological conditions, mitochondrial Ca^{2+} controls key regulatory dehydrogenases in the mitochondrial matrix. Under pathological conditions associated with cellular ATP depletion and oxidative stress, mitochondrial Ca^{2+} triggers opening of the PT pore, and ultimately affects ψ_m. Adapted from Crompton (1999).

In contrast with the normal behaviour of the mitochondrial Ca^{2+} transport cycle under normal conditions, a different response of the cycle emerges under pathological conditions, such as that illustrated in ischaemia and reperfusion, cardiac occlusion, stroke, etc., in which the effects of decreases in ATP and pH_i, and increases in $Na^{2+}{}_i$, all of which increase cytosolic Ca^{2+}, are seen (Fig. 4.6). Oxidative stress, which has a similar effect, brings about a slow, progressive increase in cytosolic resting (basal) free $[Ca^{2+}]$, in which the rates of Ca^{2+} influx and efflux across the inner membrane are equal. Each increment in resting cytosolic Ca^{2+} gives rise to a proportionally greater increase in mitochondrial $[Ca^{2+}]$ until, at about 1-3 μM cytosolic Ca^{2+}, mitochondrial Ca^{2+} overload occurs. In the

absence of ATP and in the presence of high P_i or peroxides, mitochondrial Ca^{2+} overload invariably leads to PT pore opening (Fig. 4.6), ψ_m collapse, and cell death by apoptosis or necrosis (Crompton, 1999). The form of cell death resulting from the death-inducing stimulus depends on the intensity of the insult, which influences Ca^{2+} levels. If the stimulus causes massive Ca^{2+} overload, cells become necrotic due to prolonged, wide-spread PT pore opening, resulting in rapid ATP depletion, immediate ψ_m collapse, and further PT pore opening. However, if the stimulus causes only moderate Ca^{2+} overload, only a limited number of PT pores open (ATP depletion and ψ_m collapse occur at a much lower rate), resulting in engagement of the apoptotic pathway through release of apoptogenic proteins, and delayed cell death (Crompton, 1999).

As the mitochondria lack catalase, H_2O_2 is reduced by GSH (glutathione peroxidase) (Crompton, 1999), a tripeptide which occurs in virtually all animal cells at high concentrations (0.1-10 mM). GSH has a number of important functions in metabolism, catalysis and transport. Its antioxidant functions are closely associated with its role in providing the cell with its reducing milieu which also arises from the reducing power of NADPH (Meister, 1995).

A model has been devised to explain PT pore opening during oxidative stress, e.g., that induced by H_2O_2. In this model, the oxidation to –S-S- and –S-As(OH)-S- linkages, in the ANT component of the pore structure yield pore opening, whereas reduction of these residues to $(-SH)_2$ and –SH, -S(NEM) produces pore closure. According to this model, the pore is maintained in the closed form by the normally highly reduced state of intramitochondrial GSH. It, therefore, appears that oxidative stress-induced pore opening, which is readily reversible, is probably mediated by oxidation of the GSH, NADPH or NADH pools through the sequential actions of glutathione peroxidase, glutathione reductase and pyridine nucleotide trans-hydrogenase, allowing dithiol formation and pore opening, and leading to the mitochondrial Ca^{2+} overload that is typically associated with peroxide-induced oxidative stress. Oxidative stress may, hence, cause PT pore opening by overriding inhibition by intramitochondrial ATP (Crompton, 1999). This may be explained by the above model, in which oxidation of ANT may cause a conformational change, and decreased ability to bind ATP, thus causing pore opening, even though ATP is present.

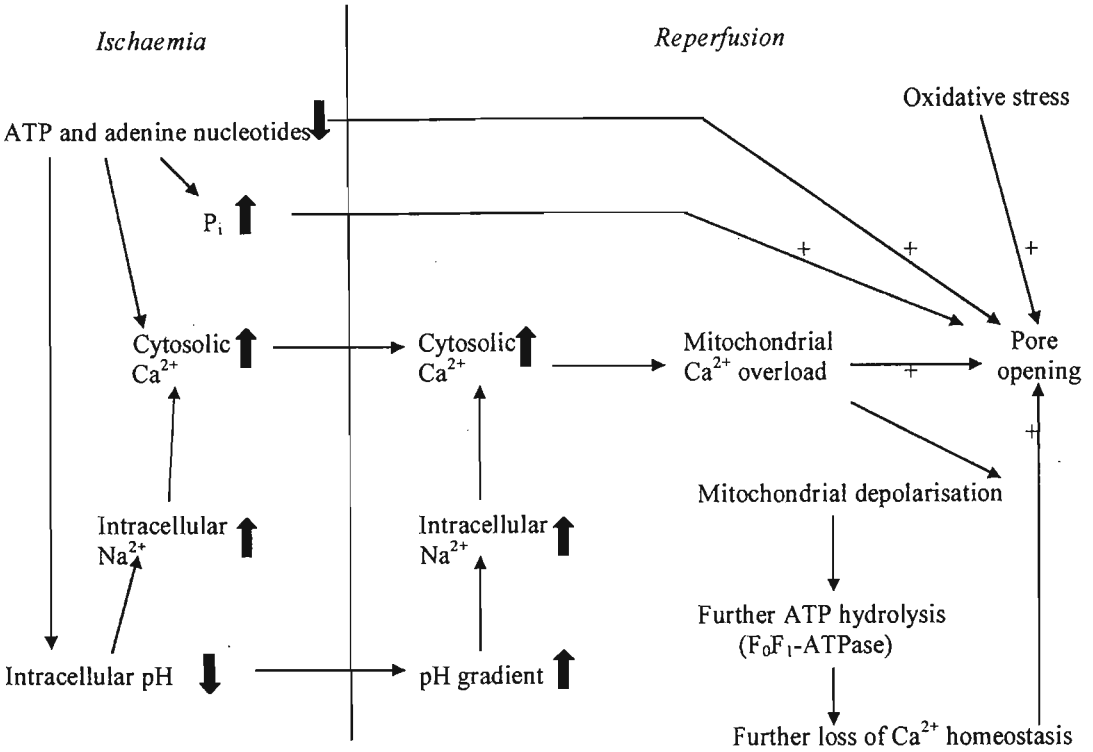

Figure 4.6 Involvement of the PT pore in ischaemia-reperfusion-induced cell death.

ATP dissipation during ischaemia leads to rises in resting cytosolic free [Ca^{2+}] and P_i. Reperfusion leads to excessive mitochondrial Ca^{2+} uptake. Mitochondrial Ca^{2+} overload, together with oxidative stress and the prevailing high P_i and low ATP, provoke PT pore opening. This initiates a vicious cycle i.e. inner membrane depolarisation, ATP hydrolysis by the mitochondrial ATP synthase, further increases in cytosolic Ca^{2+}, and so on, leading to cell death. From Crompton (1999).

Since PT pore opening leads to mitochondrial ATP hydrolysis, rather than synthesis, energy metabolism would be impaired, resulting in further Ca^{2+} increases, further PT pore opening and so on. ATP is needed to execute the apoptotic programme, however, and if ATP is not maintained, cells die by necrosis. If oxidative stress does actually bring about apoptosis by PT pore activation, then PT pore opening would need to occur without causing major ATP depletion, if necrosis is not to be induced. In principle, there are two ways in which this could take place: (i) a natural protein inhibitor of the F_0F_1-ATPase, "Inhibitor Protein", may limit ATP hydrolysis under conditions leading to apoptosis and, (ii) there may be transient and highly localised pore opening of a few mitochondria, so that only a few mitochondria are exposed to low ψ_m for brief intervals, and the impact on the energetic state of the cell is minimal (Crompton, 1999).

Mitochondrial depolarisation may facilitate PT pore opening, although depolarisation *per se* is insufficient to produce PT pore opening *in vivo*. Usually, a loss of ATP and high cytosolic [Ca^{2+}] is required. PT pore opening, however, increases with increased depolarisation. There does not appear to be a critical potential at which this occurs, there is rather an increasing propensity for pore opening as the mean ψ_m falls. The critical potential at which pore opening occurs would probably not be evident in experiments using cell populations, since mitochondria and potentials would possibly be out of phase in such populations. The observed range over which changes in potential affect the PT pore, 180-120 mV, would not be expected to lead to losses of mitochondrial Ca^{2+}, however, as the rate of Ca^{2+} influx via the uniporter increases with increasing ψ_m, but only up 110 mV or so, above which uniporter activity reaches a plateau (Crompton, 1999).

Mammalian mitochondria have been described to express their electrochemical gradient as a ψ_m of about 180 mV, and a pH gradient equivalent to about 60 mV (generating a total energy yield of approximately 240 mV) (Chen and Rivers, 1990). Regulation of the proton gradient may play a fundamental role in cellular programming, since the regulating proteins also affect the transport of metabolites, ions, precursor enzymes, and mitochondrial protein synthesis. Conceivably, the magnitude of the proton gradient and its expression, either as the pH gradient or ψ_m, may differ among cell types and change to meet the special needs (differentiation, changes in function, transformation) of individual cells (Chen and Rivers, 1990).

Observations of living cells, using the fluorescent dye Rhodamine 123, show that oncogenic transformation affects the mitochondria, but not in a consistent manner. Normal epithelial cells have low ψ_m. In contrast, studies of transformed cell lines/types (including bladder epithelial cells, human breast carcinoma) and surgical specimens showed that a great majority of adenocarcinomas, transitional cell carcinomas, squamous cell carcinomas and melanomas had high ψ_m. The difference in ψ_m between normal epithelial cells and carcinoma cells was at least 60 mV. High ψ_m was not detected in leukemias, lymphomas, neuroblastomas or osteosarcomas (Chen and Rivers, 1990).

This difference is potentially exploitable in cancer therapy. In apoptosis, changes in ψ_m have been reported. Cytochrome c is part of the respiratory chain and thus, in part,

responsible for maintaining the ψ_m. This suggests that cytochrome c may play an important role in ψ_m changes, and hence in normal cellular processes, disease states and cell death.

4.2.4 Cytochrome c structure and function

Cytochromes are haemoproteins that undergo one-electron oxidation-reduction changes in the iron of their haem prosthetic groups. Cytochromes of the *c* type are obligatory electron carriers of bacterial, plant and animal electron transfer chains. The prosthetic group of these cytochromes (Fig. 4.7) is a modified protohaem in which the vinyl side chain is covalently linked to the protein. Mammalian cytochrome c has a basic isoelectric point, consists of 103 amino acids, has a molecular weight of approximately 12.5 kDa, and is water-soluble because of the acidic and basic polar amino acid residues on the exterior of the protein. The tertiary structure of this cytochrome (Fig. 4.8) from different sources has been found to be quite similar. The haeme group is covalently tied to the protein by thioester bonds, with two cysteine residues at positions 14 and 17. The haeme is further stabilised by ligation of the fifth and sixth axial coordinates of the iron to histidine and methionine residues, and through hydrogen bonding of one of the propionic acid side chains with tryptophan and tyrosine. The structure appears to guarantee a high degree of immobilisation of the haeme. Although most of the haeme is buried in a hydrophobic crevice, one edge of the porphyrin ring and one of the propionic acid side chains are exposed to the solvent. A hydrophobic channel in the upper part of the crevice provides an alternate access to the haeme. The exposed porphyrin edge could accept electrons directly, or amino acids along the channel may act as electron conductors which transfer the electrons to the centrally located haeme (Tzagoloff, 1982). Cytochrome c mediates the transfer of electrons between complexes III and IV of the respiratory chain (Fig. 4.3). The interaction of cytochrome c with these enzymes seems to involve different parts of the molecule (Tzagoloff, 1982).

Like most mitochondrial proteins, cytochrome c is encoded by a nuclear gene and translated by cytosolic ribosomes as a cytoplasmic precursor molecule, apocytochrome c, which becomes selectively imported into the mitochondrial intermembrane space where a

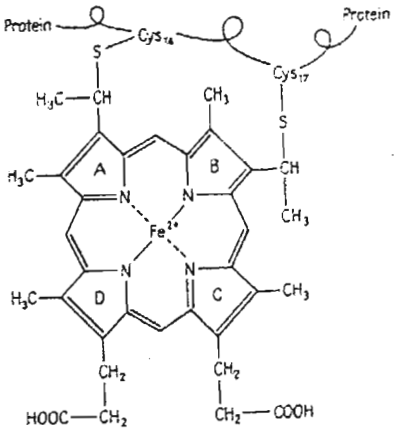

Figure 4.7 Prosthetic group of the type *c* cytochromes.

From Tzagoloff (1982).

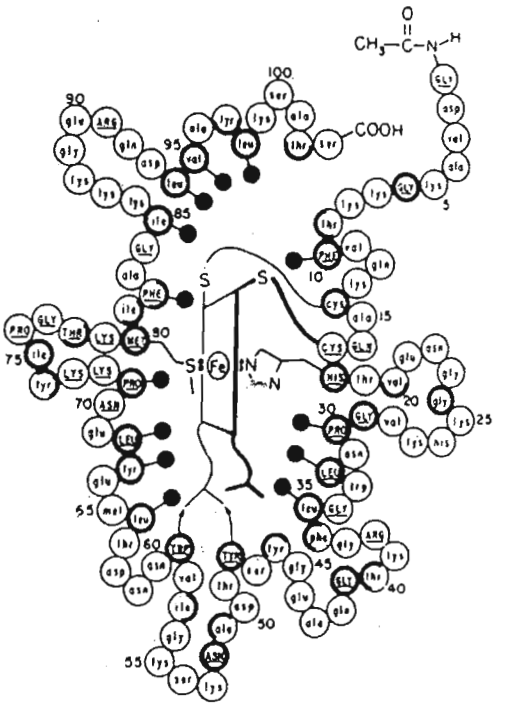

Figure 4.8 Tertiary structure of cytochrome c.

From Tzagoloff (1982).

haeme group is covalently attached via thioester linkages to cysteine residues, near the amino terminus of apocytochrome c by the haeme lyase. The uptake of apocytochrome c follows a unique import pathway into the mitochondrion, as it does not require an import receptor, proteolytic processing of a precursor sequence or high ψ_m (Drygas *et al.*, 1989). The covalent attachment of the haeme group promotes the import of apocytochrome c, and leads to its final protein folding which has been proposed to capture cytochrome c within the mitochondrion (Bossy-Wetzel *et al.*, 1998). Holocytochrome c is localised in the intermembrane space, and is loosely attached to the outer surface of the inner mitochondrial membrane (Hartl *et al.*, 1989).

4.2.4.1 Mechanism of cytochrome c release

Several mechanisms that may be responsible for cytochrome c release during apoptosis have been suggested: (a) outer mitochondrial membrane rupture occurring as a secondary consequence of prolonged mitochondrial PT pore opening and matrix swelling (Susin *et al.*, 1997); (b) physical disruption of the outer mitochondrial membrane early in apoptosis occurring as a result of inner mitochondrial membrane hyperpolarisation and matrix swelling, before permeability transition (Vander Heiden *et al.*, 1997); and (c) pore-forming pro-apoptotic proteins of the Bcl-2 family may directly interact with the outer mitochondrial membrane to allow efflux of cytochrome c (Kluck *et al.*, 1999).

Cytochrome c may also be released by ceramides. The apoptogenic properties of ceramides are, in part, mediated via their interaction with mitochondrial cytochrome c followed by its release. During such release, the redox state of cytochrome c influences its detachment from the inner mitochondrial membrane by ceramide. The release takes place when cytochrome c is oxidised but not when it is reduced. Ceramides also decrease the reducibility of cytochrome c and it is hypothesised that they directly interact with cytochrome c, with a higher affinity for the oxidised protein, and change the physico-chemical properties of cytochrome c, leading to its release from mitochondria. Release of cytochrome c by ceramide is not a consequence of a non-specific solubilisation of mitochondrial membranes due to the lipophilicity of ceramide, but rather is a specific event (Ghafourifar *et al.*, 1999). The mechanism of this event, however, remains to be revealed.

Much also remains unknown about the roles of various forms of cytochrome c. At the beginning of the present study, analysis of the form of cytochrome c present, as well as the release of cytochrome c, was seen as a promising novel avenue for detection of apoptosis.

4.2.4.2 Conformational changes and inactivation of cytochrome c

It has been inferred by some that cytochrome c can interact not only with its electron exchange partners but also with the inner mitochondrial membrane and, in the latter case, undergoes a conformational change. Jemmerson *et al.* (1999) demonstrated (via binding studies using epitope-specific antibodies) that a conformational change occurs in cytochrome c when the protein associates with synthetic anionic phospholipid vesicles. This change involves an opening of the haeme crevice resulting, in part, from the loss of both the iron-methionine 80 ligation, and H-bonds between amino acid side chains and one of the haeme propionates, as well as destabilisation of the tertiary structure of the polypeptide detected by the accessibility of the backbone amides to hydrogen-deuterium exchange. It has not been conclusively determined whether this conformational change has any biological significance, although cytochrome c-phospholipid interactions are considered to be a paradigm for the putative interaction of cytochrome c with the phospholipid-rich inner mitochondrial membrane (Jemmerson *et al.*, 1999).

The conformational change which occurs in cytochrome c bound to phospholipid vesicles cannot be detected in live cells. However, a conformational change in cytochrome c is reported to be an early event in apoptosis, which can be identified in pre-apoptotic cells that are negative for other indicators of apoptosis, and in necrosis. The change occurs in the omega loop region around amino acid residue 44, which is located to the right of and below the exposed haeme crevice on the native-like form of cytochrome c (Jemmerson *et al.*, 1999).

Loss of cytochrome c activity has also been reported in apoptosis. In Jurkat cells, the activity of cytochrome c was greatly diminished, and a death protease was found to participate in the events leading to the loss of cytochrome c activity. The death protease could have either of two effects: 1) the direct proteolytic inactivation of the cytochrome, or 2) the proteolytic release of a cytochrome c inhibitor. Extensive degradation of the

cytochrome is unlikely. Limited proteolysis, however, could alter one of the sites through which cytochrome c binds to other cytochromes, or could change the environment of the haeme, altering its redox potential (for example) so that it could no longer carry electrons between cytochrome c_1 and cytochrome oxidase. Such a proteolytic alteration could be accomplished by one of the death proteases, or by another protease released through the action of a death protease (Krippner *et al.*, 1996).

Adachi *et al.* (1997) proved that cytochrome c inactivation, in Fas-induced apoptosis in Jurkat cells, was mediated by a heat-labile cytosolic factor called cytochrome c-inactivating factor of apoptosis (CIFA). CIFA cannot penetrate the outer membrane of normal mitochondria, but the outer membrane of apoptotic mitochondria is permeable to CIFA. A potential mechanism for this penetration by CIFA is a Fas-dependent alteration in the membrane that causes its permeability to increase as the cytoplasm acidifies. Such permeability may also aid the release of cytochrome c release. It now also appears that release of cytochrome c from the mitochondria is not always required for caspase activation and apoptosis and that, in certain systems, the subcellular location of cytochrome c does not change during apoptosis (Adachi *et al.*, 1997). In such cases, analysis of the form of cytochrome c present may be useful.

4.2.4.3 Consequences of cytochrome c changes

Cytochrome c may initiate apoptosis by inducing the formation of the Apaf-1/caspase-9 complex. Cytosolic cytochrome c binds to Apaf-1; this complex requires dATP or ATP to bind and activate caspase-9 which then activates caspase-3, the executioner caspase, resulting in characteristic apoptotic morphology (Li *et al.*, 1997).

While cycling cells (including transformed cells) cannot survive the caspase-independent mitochondrial changes that contribute to apoptotic pathways, recent reports suggest that possibly other cells in the body can. Either mitochondrial function remains intact following the cytochrome c release, or new mitochondria are generated *de novo* in the surviving cells (Green, 1998). Apparent mitochondrial biogenesis in cells triggered to undergo apoptosis has been documented (Mancini *et al.*, 1997). Martinou *et al.* (1999) reported that mitochondria from neurons recovered their normal size and cytochrome c

content, by a process requiring *de novo* protein synthesis, suggesting that depletion of cytochrome c from mitochondria is a controlled process compatible with function recovery. This ability of mitochondria to recover fully their cytochrome c content and function, when homeostatic conditions are restored, may be specific for mitochondria from neurons, however.

Cytochrome c is required as an electron carrier in oxidative phosphorylation, a process which generates the majority of intracellular ATP. The electron transport between the complexes generates a proton gradient across the inner mitochondrial membrane, which maintains ψ_m (Bossy-Wetzel *et al.*, 1998). Although binding of cytochrome c to the inner mitochondrial membrane is not a function of ψ_m, the formation and the maintenance of ψ_m is dependent on the presence of a functional cytochrome c (Ghafourifar *et al.*, 1999). Thus, a long-term exclusion of cytochrome c from the electron transport chain can result in impairment of proton flow and a decrease in ψ_m, generation of ROS due to incomplete reduction of oxygen, and a cessation in ATP synthesis. However, some reports indicate that ψ_m and intracellular ATP levels are maintained for several hours after the appearance of cytosolic cytochrome c. Several explanations may account for this effect. First, not all mitochondrial cytochrome c may actively participate in the electron transport chain, i.e., the released cytochrome c might represent an excess not involved in electron transport. Second, maintenance of ψ_m may be accomplished by the import of cytosolic ATP through the ADP/ATP-translocator, generating a ψ_m by the oligomycin-sensitive proton pump (Bossy-Wetzel *et al.*, 1998). In contrast to reports of maintenance of ψ_m (Diaz *et al.*, 1999), even when cytochrome c is released (Kluck *et al.*, 1997), Ghafourifar *et al.* (1999) reported that, upon cytochrome c loss, mitochondrial oxygen consumption, ψ_m, and Ca^{2+} retention are diminished. Also, in apoptosis induced by some anti-cancer drugs, cytochrome c is released, ψ_m drops, ROS are produced, and the cell dies by a caspase-independent mechanism that resembles necrosis (Reed, 1997).

In cases of apoptosis where ψ_m is affected, it is unclear whether there is an early drop in ψ_m, associated with PT pore opening (Marchetti *et al.*, 1996; Zamzami *et al.*, 1996), or the ψ_m loss is only a conclusive event of apoptosis (Ferlini *et al.*, 1996) which requires functional mitochondria for its energy-dependent processes (Ankarcrona *et al.*,

1995). Other investigations suggest that apoptosis is, in fact, independent of mitochondrial ATP synthesis, but requires the integrity of the electron transport chain (Jia *et al.*, 1997). The permanent decay of ψ_m seen in many systems seems to be a consequence of downstream caspase activation, rather than an event leading to their activation (Crompton, 1999). Finucane *et al.* (1999) suggested the possibility that loss of ψ_m occurs in two stages, a minor caspase-independent stage loss followed by a more dramatic caspase-dependent loss. This might explain the discrepancies in reports of ψ_m loss or maintenance, the ψ_m decrease being detected only in caspase-dependent apoptosis (which is cell type- and inducer-specific) if the minor ψ_m decrease is too small for detection.

H_2O_2 (oxidative stress), which induces apoptosis, causes a dose-dependent reduction of ψ_m (Hoyt *et al.*, 1997) and cytochrome c efflux from mitochondria (Bossy-Wetzel *et al.*, 1998; Ghafourifar *et al.*, 1999). However, because of the cell type-specific nature of these events, it was considered a worthwhile exercise to determine whether these changes, and specifically cytochrome c release, occurred in the test cells used in the present investigation.

4.3 The effect of oxidative stress on mitochondria

Besides causing cellular damage by lipid peroxidation, oxidative stress may cause mitochondrial damage by affecting mitochondrial biochemical processes. Cell killing is correlated with a loss of mitochondrial energisation rather than with the depletion of ATP alone (Farber *et al.*, 1990). Mitochondria could be the main target for non-specific outer and inner membrane damage through oxidative stress (Buttke and Sandstrom, 1994). These membranes are disrupted by such stresses (Rapaport *et al.*, 1979), causing ψ_m dissipation (Niemenen *et al.*, 1995). A number of different lesions in mitochondrial DNA can also be produced by oxidising species. Reaction of the oxidizing species with deoxyribose may result in fragmentation with loss of bases and the appearance of a strand break. Alternatively, reactive species may react with thymine to produce a variety of lesions, which may be removed by repair enzymes but that similarly produce single-strand breaks (Farber *et al.*, 1990). Mitochondria have also been implicated as a source of ROS

during apoptosis (Mancini *et al.*, 1997), when cytochrome c is released and the ψ_m drops, as previously mentioned (Section 4.2.4.3).

Treatment of cells with H_2O_2 has been reported to cause cytochrome c efflux from mitochondria (Bossy-Wetzel *et al.*, 1998), and cytoplasmic cytochrome c may be detected immunologically using antibodies. Currently, most commercially available anti-cytochrome c antibodies are expensive monoclonal antibodies which may potentially have limited applications to either western blots or electron microscope immunocytochemistry, as these antibodies target a single epitope. In the experimental work in this chapter, attempts were made to produce universally applicable, multiple epitope-targeting polyclonal cytochrome c antibodies, thereby cutting costs by allowing a number of applications of the same antibody, and also verification of results using several techniques, where different epitopes may be destroyed or exposed. The antibodies produced were used to determine whether cytochrome c would be released in response to oxidative stress, in the test cells under investigation.

4.4 Determination of cytochrome c purity

The cytochrome c antigen used for antibody production had to be of high purity to prevent the simultaneous production of unwanted contaminating antibodies. To determine whether the commercially available cytochrome c was pure, it was electrophoresed on a sodium dodecyl sulfate polyacrylamide gel (SDS-PAGE). This was subsequently stained using an extremely sensitive silver stain method for the detection of proteins (Blum *et al.*, 1987). The tris-tricine gel system was chosen over the Laemmli system due to its superior resolution (Schägger and von Jagow, 1987).

4.4.1 Reagents

Solution A: 10% (m/v) SDS. SDS (10 g) was dissolved in dist.H_2O (100 ml) with gentle heating.

Solution B: [3 M Tris-HCl, 0.3% (m/v) SDS, pH 8.45]. Tris (72.7 g) was dissolved in approximately 180 ml of dist.H_2O, SDS [6 ml of a 10% (m/v) solution] added, adjusted to pH 8.45 with HCl, and made up to 250 ml.

Solution C: [48% (m/v) acrylamide, 3% (m/v) bis-acrylamide]. Acrylamide (48 g) and bis-acrylamide (3 g) were dissolved and made up to 100 ml with dist.H_2O and stored in an amber coloured bottle.

Solution D: [10% (m/v) ammonium persulfate]. Ammonium persulfate (0.05 g) was dissolved in dist.H_2O (500 µl) immediately before use.

Solution E: 4 x stacking gel buffer [500 mM Tris-HCl, pH 6.8]. Tris (3 g) was dissolved in dist.H_2O (40 ml), adjusted with HCl to pH 6.8 and made up to 50 ml.

Solution F: Reducing treatment buffer [125 mM Tris-HCl, 4% (m/v) SDS, 20% (v/v) glycerol, 10% (v/v) 2-mercaptoethanol, pH 6.8]. Buffer E (2.5 ml), solution A (4 ml), glycerol (2 ml) and 2-mercaptoethanol (1 ml) were made up to 10 ml with dist.H_2O. A few grains of bromophenol blue was added to the solution to serve as a tracker dye to enable protein migration through the gel to be monitored.

Running gel solution. Solution B (6 ml), solution C (3.6 ml), solution D (60 µl), TEMED (6 µl) and dist.H_2O (8.4 ml) were mixed together just before use.

Stacking gel solution. Solution B (1.5 ml), solution C (0.5 ml), solution D (30 µl), TEMED (12 µl) and dist.H_2O (4 ml) were mixed together immediately before use.

Anode buffer [200 mM Tris-HCl, pH 8.9]. Tris (24.22 g) was dissolved in dist.H_2O (~950 ml), adjusted to pH 8.9 with HCl and made up to 1 l.

Cathode buffer [100 mM Tris-HCl, 100 mM tricine, 0.1% (m/v) SDS, pH 8.25]. Tris (12.2 g) and tricine (17.9 g) were dissolved in dist.H_2O (~950 ml), SDS [10 ml of a 10% (m/v) solution] added, the pH adjusted to pH 8.25 with HCl, and made up to 1 l.

10 mg/ml Cytochrome c stock. Cytochrome c (0.8 mg, Sigma) was dissolved in dist.H_2O (80 µl).

Fixing solution [50% (v/v) methanol, 12% (v/v) acetic acid, 0.5% (v/v) formaldehyde. Methanol (100 ml), acetic acid (24 ml) and formaldehyde (100 µl of a 37% (m/v) solution) were diluted to 200 ml with dist.H_2O.

Washing solution [50% (v/v) ethanol]. Absolute ethanol (100 ml) was diluted to 200 ml with dist.H_2O.

Pretreatment solution [0.02% (m/v) $Na_2S_2O_3.5H_2O$]. $Na_2S_2O_3.5H_2O$ (40 mg) was dissolved in dist.H_2O (200 ml).

Impregnation solution [0.2% (m/v) $AgNO_3$, 0.75% (v/v) formaldehyde]. $AgNO_3$ (400 mg) was dissolved in dist.H_2O (200 ml) and formaldehyde [150 µl of a 37% (v/v) solution] was added.

Developing solution [60 g/l Na_2CO_3, 0.5% (v/v) formaldehyde, $Na_2S_2O_3.5H_2O$]. Na_2CO_3 (12 g) was dissolved in dist.H_2O (190 ml), $Na_2S_2O_3.5H_2O$ (4 ml of the pretreatment solution) and formaldehyde (100 µl of a 37% (v/v) solution) were added and the volume made up to 200 ml.

Stopping solution [50% (v/v) methanol, 12% (v/v) acetic acid]. Methanol (50 ml) and acetic acid (12 ml) were diluted to 100 ml with dist.H_2O.

4.4.2 Procedure

The Hoefer SE 250 Mighty Small II vertical slab electrophoresis unit was assembled prior to preparation of the gel mixtures. One notched aluminium plate and one glass plate was cleaned with ethanol for each of the two sides of the apparatus. These were clamped, with a 1.5 mm polyethylene spacer, separating the two plates at the edges of either side (into a gel caster). The running gel solution was run into the space between the plates to a depth of 3 cm from the top of the plate, and overlayed with dist.H_2O to allow for even polymerisation. Once the gel had set (evidenced by the appearance of the interface between gel solution and water, usually about 1 h), the water was removed with a syringe. Stacking gel solution was poured in, up to the notch of the aluminium plate, and a 15-well comb was inserted to form the sample application wells. Once this gel had set (about 30 min), the comb was removed and the wells were rinsed with dist.H_2O. The polymerised gels contained between the plates were then transferred to the Mighty Small apparatus to which they were clamped. The cathode buffer was placed in the top chamber and the anode buffer in the bottom chamber of the vertical slab gel electrophoresis unit. Samples (cytochrome c ranging in concentration from 5 to 150 μg per well) were combined with an equal volume of reducing treatment buffer (solution F), incubated in a boiling water bath for 1.5 min, and loaded onto the gels. The gel unit was connected to a power pack and run at 80 V, until the bromophenol blue tracker dye was about 0.5 cm from the bottom of the running gel. The apparatus was then disconnected from the power supply, the plates were removed and levered apart using a plastic spacer. The gel was removed using gloves and silver-stained for protein detection.

All the staining steps were carried out on an orbital shaker at room temperature, and in scrupulously clean glass containers in order to minimise background staining. The electrophoresis gel was soaked in fixing solution (50 ml, overnight), and incubated in washing solution (3 x 20 min), followed by soaking in pretreatment solution (1 min). The gel was rinsed in dist.H_2O (3 x 20 sec) and soaked in impregnation solution (20 min). Following rinsing in dist.H_2O (2 x 20 sec), the gel was incubated in developing solution until the protein bands became visible and the colour was sufficiently developed.

Development was stopped by briefly rinsing the gel in dist.H_2O followed by stopping solution (10 min), in which the gel was stored.

4.4.3 Results and discussion

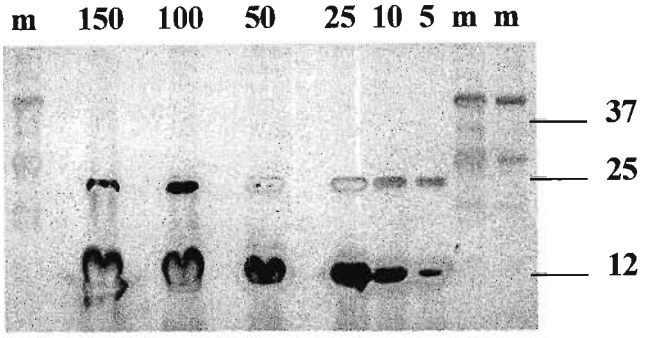

Figure 4.9 Silver-stained, 10% reducing SDS-PAGE gel for determination of cytochrome c purity.
Lanes m = MWM, lanes 150 - 5 = indicated amounts (μg) of cytochrome c.

Bands were visible at 13 and 26 kDa, and in lane 1, a very pale band at 39 kDa (Fig. 4.9, lane 150). The distortion of the 13 kDa bands in lanes 2-4 is possibly due to protein overloading. Samples were loaded in such a fashion, however, in order to detect protein contaminants that may be present in very small amounts in the cytochrome c preparation, but which may be highly immunogenic if simultaneously injected into the chickens along with the main immunogen. Because the commercial preparation of cytochrome c was 99% pure, the 26 kDa band was dismissed as a dimer, and the 39 kDa band (Fig. 4.9, lane 150) a trimer of cytochrome c. The commercial preparation did not seem to need further purification prior to injection and was, therefore, used as the immunogen in its purchased form.

4.5 Antibody production

Cytochrome c is a poor immunogen because it shows very little evolutionary divergence between mammalian and non-mammalian species (Fig. 4.10) (Mayer and Walker, 1987).

Chicken GDIEKGKKIF VQKCSQCHTV EKGGKHKTGP NLHGLFGRKT GQAEGFSYTD
Horse GDVEKGKKIF VQKCAQCHTV EKGGKHKTGP NLHGLFGRKT GQAPGFTYTD
Human GDVEKGKKIF IMKCSQCHTV EKGGKHKTGP NLHGLFGRKT GQAPGYSYTA

Chicken ANKNKGITWG EDTLMEYLEN PKKYIPGTKM IFAGIKKKSE RVDLIAYLKD ATSK
Horse ANKNKGITWK EETLMEYLEN PKKYIPGTKM IFAGIKKKTE REDLIAYLKK ATNE
Human ANKNKGIIWG EDTLMEYLEN PKKYIPGTKM IFVGIKKKEE RADLIAYLKK ATNE

Figure 4.10 Sequence homology between chicken, horse and human cytochrome c.
Red text represents the amino acids that vary between the three species. From SWISS PROT (http://expasy.nhri.org.tw/sprot/). Accession numbers P00016, P00004, and P00001, respectively.

Nevertheless, although antibodies generated were intended for use on human tissue, antibody production was attempted using horse cytochrome c because it is commercially available in a pure form at a low cost, sparing the time hazards and effort required to isolate cytochrome c from human sources. Due to the highly conserved nature of cytochrome c, the antibodies raised in chickens were expected to cross-react with human cytochrome c in tissues studied. Chickens were chosen for raising antibodies as chickens are available at a low cost and require little effort to house and feed, are easy to handle and may be easily sacrificed after use. The antibodies they produce are also easily purified, using polyethylene glycol precipitation. Most importantly, however, antibodies are concentrated in the egg yolks. This avoids the difficult bleeding procedure required to obtain antibody-containing blood from animals. For weakly immunogenic, highly conserved proteins (such as cytochrome c) isolated from mammalian sources, chickens provide a valuable test model for antibody production since epitopes of chicken cytochrome c would be most different from those of mammals, and hence, they should produce the best antibodies. This is shown to be the case in Figure 4.10.

Proteins are usually mixed with material that will increase the immunogenicity of the antigen preparation, i.e., adjuvants (Mayer and Walker, 1987). These are non-specific immune response stimulators which allow gradual release of antigen from the site of inoculation, thus ensuring maximal exposure of the antigen to MHC II antigen presenting cells (APC), which allows efficient antigen uptake by APCs, and thus, optimal antibody

response. The non-specific immune response is improved by including molecules of pathogenic origin since they stimulate lymphokine production and subsequent B cell proliferation. In addition, this provides a "depot" effect or deposit of bacteria which induces the infiltration of inflammatory APCs to the site. The "depot" action means that much smaller doses of antigen can be used and that antibody responses are more persistent (Harlow and Lane, 1988).

The most commonly used adjuvant for research work is Freund's adjuvant, which is a water-in-oil emulsion prepared with non-metabolisable oils. If the mixture contains heat-killed *Mycobacterium tuberculosis*, it is referred to as complete Freund's adjuvant (CFA). Without the bacteria it is known as incomplete Freund's adjuvant (IFA). To avoid side effects, the primary injection is given in CFA, while all boosts (which improve the titre and avidity of antibodies) are done in IFA (Harlow and Lane, 1988).

4.5.1 Reagents

Cytochrome c in saline solution. Cytochrome c (1 mg) was dissolved in PBS (1 ml, Section 2.3.1).

4.5.2 Procedure

Since no information was available on the immunogenicity of the antigen, 500 μg/ml of protein was chosen for immunisations. Intramuscular injection was used as the route of inoculation, to allow a slow release of the antigen.

The cytochrome c solution (1 mg/ml in PBS) was mixed with an equal volume of CFA (Sigma) for the first injection and with equal volumes of IFA (Sigma) for the subsequent four injections. The mixture was triturated (repeated, slow suctioning into a syringe and forceful ejection back into tube) for approximately 45 min, until a stable emulsion was obtained (evidenced by a droplet of emulsion which did not spread on a drop of 0.9% (m/v) NaCl). The mixture was divided equally into two syringes, and all air bubbles expelled. Each of two chickens was injected fortnightly, over a period of 10 weeks, with 500 μg of cytochrome c contained in a total volume of 1 ml. Due to the large

volume of the inoculum, it was delivered by injection into at least two sites, as large volumes injected into one site can cause severe granulomas (Harlow and Lane, 1988).

4.6 Antibody purification

The antibodies were isolated using a polyethyleneglycol (PEG) precipitation method, a very simple and efficient method in the purification of IgY (antibodies developed in chickens) (Polson *et al.*, 1985). PEG is a neutral, water-soluble, high-M_r polymer, and a mild precipitating agent used for the fractional precipitation of proteins, by a dehydration steric exclusion mechanism. Proteins become concentrated in the extrapolymer space as the increasing PEG concentration complexes more and more of the available solvating water, until proteins exceed their solubility limit.

4.6.1 Reagents

100 mM Na-phosphate buffer, 0.02% (m/v) NaN_3, pH 7.6. $NaH_2PO_4.H_2O$ (13.8 g) and NaN_3 (0.2 g) were dissolved in dist.H_2O (950 ml), titrated to pH 7.6 using NaOH, and made up to 1 l.

4.6.2 Procedure

Egg yolks were separated from the egg white and carefully washed under running water to remove all traces of albumin. The yolk sac was punctured and the yolk volume determined in a measuring cylinder. Two volumes of 100 mM Na-phosphate buffer, pH 7.6, were added and mixed thoroughly. Solid PEG (M_r 6000) was added to 3.5% (m/v) and dissolved by gentle stirring. The precipitated vitellin fraction was removed by centrifugation (4 420 x g, 30 min, RT), and the supernatant fluid was filtered through absorbent cotton wool (well moistened with water) to remove the lipid fraction. The PEG concentration was increased to 12% [i.e., 8.5% (m/v) was added], the solution was mixed thoroughly and centrifuged (12 000 x g, 10 min, RT). The supernatant was discarded and the pellet was dissolved in phosphate buffer, pH 7.6, in a volume equal to the volume

obtained after filtration. The final concentration of PEG was brought to 12% (m/v), the solution was stirred thoroughly and centrifuged (12 000 x g, 10 min, RT). The supernatant fluid was discarded and the final antibody pellet was dissolved in 1/6 of the original egg yolk volume, using phosphate buffer, pH 7.6, and stored at 4°C overnight. 0.02% (m/v) NaN_3 was added to the antibody solution which was then aliquoted, 50% (v/v) glycerol added, and stored at -20°C. The A_{280} of a 1 in 40 dilution of IgY in phosphate buffer was determined, and the concentration of IgY in the undiluted solution was calculated using the extinction coefficient of IgY, $E_{280}^{1\ mg/ml} = 1.25$.

4.7 Progress of immunisation procedure

The progress of polyclonal antibody production during immunisation procedures can be monitored using the ELISA (enzyme linked immunosorbent assay) technique. The high levels of sensitivity and specificity achieved with immunoassays result from the specific, high-affinity, reversible binding of antibodies to antigens, and from the existence of methods for attachment of sensitively detected labels (isotopes, fluorophores, enzymes) to antigens or antibodies. ELISAs are also accurate and reproducible, when identical amounts of antigen and antibody, and reaction conditions (temperature, incubation and development times, and the correct controls), are used (Clark and Engvall, 1980).

The antigen was adsorbed onto the ELISA plate, incubated with the test antibodies, which were incubated with an enzyme-linked secondary antibody (from a different species than the primary antibody), and subsequently a fluorescent substrate, to detect the amount of antibody-bound antigen. The detection system used was HRPO-linked secondary antibody, which requires the electron donating soluble substrate, ABTS, and the electron acceptor molecule, H_2O_2. HRPO-mediated oxidation of ABTS results in a colour shift from pale green to a dark green.

This technique complements Western blotting, which gives qualitative information on antibody specificity. ELISAs were used to plot the progress of immunisation and determine which weeks eggs contained the highest concentration of specific antibodies, so that these may be used for immunocytochemistry applications.

4.7.1 Reagents

Phosphate buffered saline (PBS), pH 7.2. See Section 2.3.1.

0.5% (m/v) Bovine serum albumin-PBS (BSA-PBS). BSA (0.5 g) was dissolved in PBS (100 ml).

0.1% (v/v) Tween-PBS. Tween-20 (1 ml) was made up to 1 l in PBS.

0.15 M Citrate-phosphate buffer, pH 5.0. A solution of citric acid (21 g/l) was titrated with a solution of $Na_2HPO_4.2H_2O$ (35.6 g/l) to pH 5.0.

Substrate solution [0.05% (m/v) ABTS and 0.0015% (v/v) H_2O_2 in citrate-phosphate buffer]. ABTS (7.5 mg) and H_2O_2 (7.5 µl) were dissolved in citrate-phosphate buffer, pH 5.0 (15 ml) for one ELISA plate.

Stopping buffer [citrate-phosphate-0.1% (m/v) NaN_3]. NaN_3 (0.1 g) was made up to 100 ml in citrate-phosphate buffer.

4.7.2 Procedure

Cytochrome c was coated at concentrations of 1, 5 and 10 µg/ml in PBS (150 µl, 16 h, RT). This was done using a checkerboard ELISA, varying antigen concentrations and antibody concentrations from eggs collected fortnightly, to determine which gave the most linear response over a range of serially diluted antibody and the greatest sensitivity. Non-specific binding of antibody was prevented by blocking the wells with 0.5% BSA-PBS (200 µl, 37°C, 1 h), and the plates were washed three times with Tween-PBS. Serial two-fold dilutions of IgY, starting from 1 mg/ml IgY, was prepared in 0.5% BSA-PBS and incubated (100 µl, 37°C, 2 h), the plates were washed three times with Tween-PBS, the HRPO-linked secondary antibody (rabbit anti-chicken, Sigma) was added to each well and incubated (120 µl of 1 in 20 000 in 0.5% BSA-PBS, 37°C, 1 h), and the plates were

washed three times with Tween-PBS. Substrate solution (150 µl) was added to each well and colour was allowed to develop (30 min) in the dark against the background of the controls (preimmune, no coat, no primary, no secondary, substrate only). The enzyme reaction was stopped by addition of citrate-phosphate-NaN_3 buffer (50 µl) and the A_{405} of each well was measured on a Titertek™ ELISA plate reader.

4.7.3 Results and discussion

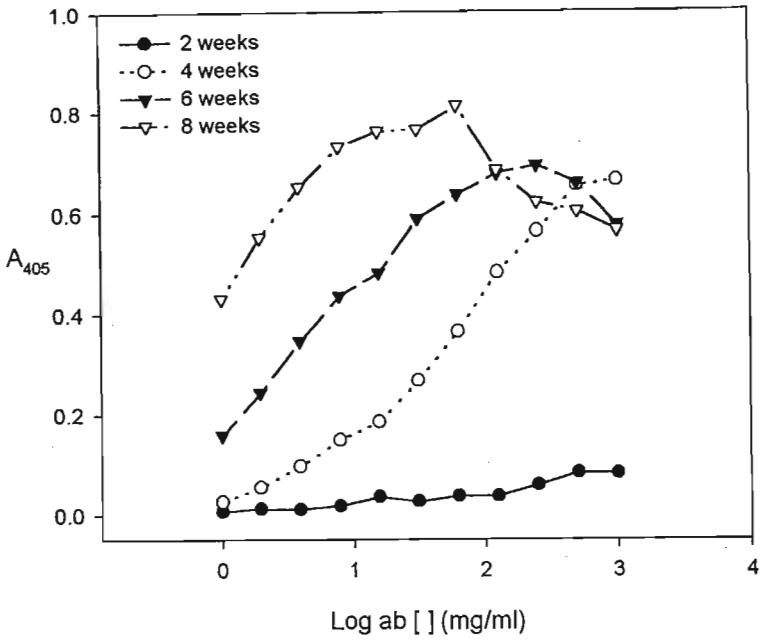

Figure 4.11 ELISA of IgY production against horse cytochrome c, at antigen coat concentration of 1 µg/ml.

Microtitre plates were coated with cytochrome c (1 µg/ml) and incubated with serial doubling dilutions (from 1 mg/ml to 2 µg/ml) of antibody collected at 2, 4, 6 and 8 weeks. Binding of antibodies was visualised by incubation with HRPO-linked rabbit anti-chicken IgY IgG, followed by ABTS/H_2O_2 substrate. Each point is the mean absorbance at 405 nm of duplicate samples. The absorbance values were blanked against control wells with substrate alone.

IgY from 4 weeks onwards showed a constant increase in the amount of cytochrome c-specific antibodies as time of exposure of the chicken to the antigen increased (Fig. 4.11), as evidenced by increased absorbance up till a dilution equivalent to 15 µg/ml of antibody, at 8 weeks. At higher antibody concentrations (at 8 weeks),

absorbance decreased due to the "prozone" effect, where steric hindrance from too many specific antibodies binding to the antigens caused decreased secondary antibody binding, and thus a less sensitive signal was obtained. This "prozone" effect was also seen at 6 weeks, but at a much higher antibody concentration, since there was a lower concentration of cytochrome c-specific antibodies at this time.

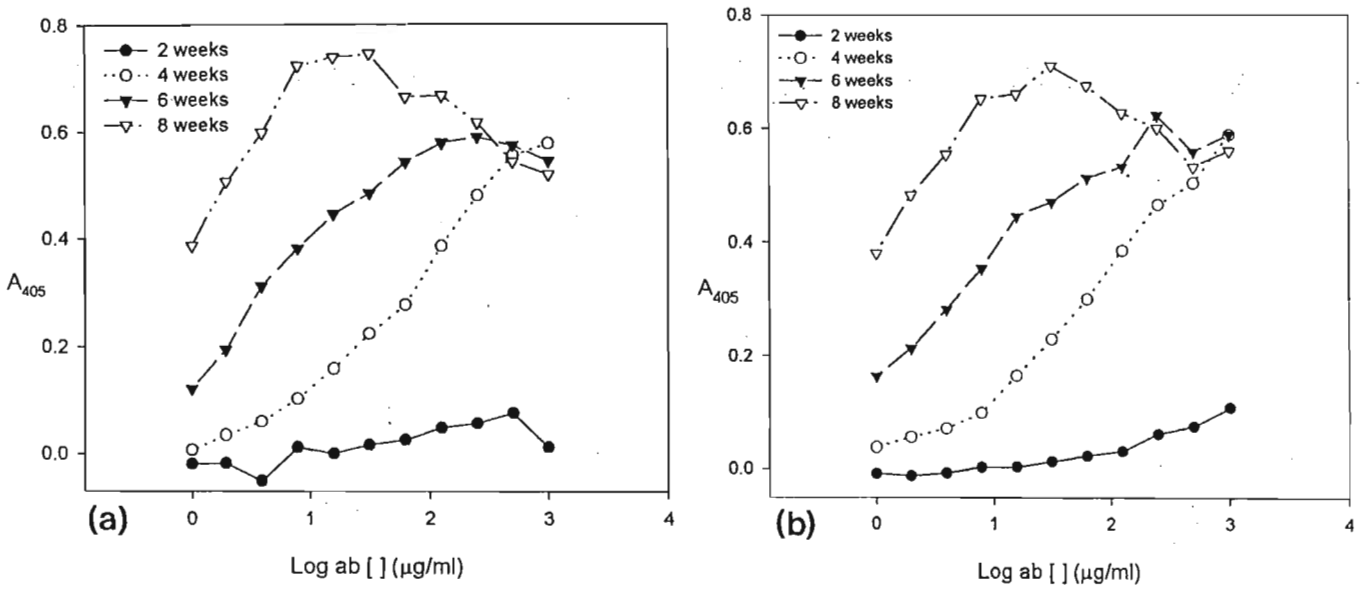

Figure 4.12 ELISA of IgY production against horse cytochrome c, at antigen coat concentrations of 5 and 10 µg/ml.

Microtitre plates were coated with (a) 5 and (b) 10 µg/ml cytochrome c, and incubated with serial doubling dilutions (from 1 mg/ml to 2 µg/ml) of antibody collected at 2, 4, 6 and 8 weeks. Binding of antibodies was visualised by incubation with HRPO-linked rabbit anti-chicken IgY IgG, followed by ABTS/H_2O_2 substrate. Each point is the mean absorbance at 405 nm of duplicate samples. The absorbance values were blanked against control wells with substrate alone.

The ELISA at 5 and 10 µg/ml coat concentration of cytochrome c (Fig. 4.12, a, b, respectively) yielded similar results to those of 1 µg/ml (Fig. 4.11) coat concentration. Therefore, in future experiments a low antigen coat concentration of 1 µg/ml can be used, thus minimising the use of the antigen and hence, the cost.

4.8 Antibody specificity/cross-reactivity and optimisation of homogenisation procedure

The testing of antibody specificity/cross-reactivity was done in several steps. Cell homogenates were fractionated to separate the mitochondrial fraction from the cytoplasmic fraction, assayed for protein content using the Bradford assay, separated by electrophoresis, western blotted and finally, probed with the anti-cytochrome c antibodies raised. This was a preliminary investigation to optimise the entire procedure which could be used to determine if cytochrome c is released from the mitochondria of these cells upon induction of apoptosis by oxidative stress (H_2O_2), and whether cytochrome c release may be used as a reliable marker for apoptosis.

4.8.1 Cell homogenisation and fractionation

Cells were homogenised and fractionated in order to separate the mitochondrial fraction from the cytoplasm. Cytochrome c is present only in the mitochondria, but may be translocated to the cytoplasm upon induction of apoptosis. The homogenisation procedure, therefore, had to be optimised since over-homogenising would rupture organelles, releasing their contents into the cytoplasm, thus giving a false result of cytochrome c release from mitochondria. In addition to optimisation of length of homogenisation, cell number was also optimised since a large amount of mitochondrial protein was required for loading so that detectable levels of cytochrome c would be present. The method used was essentially that of Tang *et al.* (1998), with the only modifications being the omission of protease inhibitors (PMSF, aprotinin, leupeptin, pepstatin A, chymostatin) from the lysis buffer, and replacement of the non-ionic detergent NP-40 with non-ionic Tween 20 in the TNC buffer (Section 4.8.1.1), due to the unavailability and high cost of NP-40. The supernatant remaining after the mitochondrial fraction was pelleted (10 000 x g) was used, instead of the conventional centrifugation at 100 000 x g to obtain the cytosolic fraction.

4.8.1.1 Reagents

Lysis buffer [20 mM HEPES, 10 mM KCl, 1.5 mM $MgCl_2$, 1 mM NaEDTA, 1 mM NaEGTA, 250 mM sucrose, pH 7.5]. HEPES (0.477 g), KCl (0.075 g), $MgCl_2$ (0.014 g), NaEDTA (0.037 g), NaEGTA (0.047 g) and sucrose (8.558 g) were dissolved in dist.H_2O (80 ml), the pH adjusted to pH 7.5 with KOH, and the volume made up to 100 ml.

TNC buffer [10 mM Tris-acetate, 5 mM $CaCl_2$, 0.5% (v/v) Tween-20, pH 8.0]. Tris (0.121 g) and $CaCl_2$ (0.074 g) were dissolved in dist.H_2O (80 ml) and the pH adjusted to pH 8.0 with acetic acid. Tween-20 (0.5 ml) was added and the volume made up to 100 ml.

4.8.1.2 Procedure

MCF10A cells were grown, seeded (3 x 10^6 and 4 x 10^6 cells/15 ml) (Section 2.4.1.2) and harvested (Section 2.4.2.2) as previously described, without treatment. Cells were subjected to subcellular fractionation immediately, without freezing, since freeze-thawing would disrupt membranes and result in the release of cytochrome c from mitochondria. Cells (3 x 10^6 or 4 x 10^6) were homogenised and the results assessed. Lysis buffer (300 µl) was added to a cell pellet, and the cells lysed using an Ultra-Turrax T8 homogeniser, fitted with a S8N-5G dispersing element. The times of homogenisation used were 1, 1.5, 2 and 2.5 min at the maximum setting on the homogeniser. The homogenates were centrifuged (1 000 x g, 4°C, 10 min) to remove insoluble material. The supernatant was then centrifuged (10 000 x g, 4°C, 20 min) to pellet the mitochondrial fraction, which was rinsed in lysis buffer, and solubilised in TNC buffer (25 µl, overnight, 4°C). The remaining supernatant was used as the cytoplasmic fraction. The mitochondrial and cytoplasmic fractions were stored at -80°C until required.

4.8.2 Bradford micro-assay for protein content

The Bradford dye-binding assay (Bradford, 1976) may be routinely used for protein determination, since it provides a very sensitive (microgram level) and rapid quantitative method. The assay is based on the binding of Coomasie brilliant blue G-250 dye to basic amino acid side chains, mainly arginine, and to a lesser extent to histidine, lysine, tyrosine, tryptophan and phenylalanine amino acid side chains. This binding causes a shift in the absorbance maximum of the dye from the cationic red form at 465 nm to the anionic blue form at 595 nm (Compton and Jones, 1985). The use of Serva blue G dye, instead of Coomassie brilliant blue G-250, decreases the level of protein-to-protein variability in dye binding and increases the sensitivity of the assay (Read and Northcote, 1981).

4.8.2.1 Reagents

Dye Reagent. Serva blue G dye (50 mg) was dissolved in 88% phosphoric acid (50 ml) and 99.5% ethanol (23.5 ml). The solution was made up to 500 ml with dist.H_2O, stirred for 30 min on a magnetic stirrer, filtered through Whatman No.1 filter paper and stored in a brown bottle.

Standard protein solution. A 1 mg/ml ovalbumin solution was made up in dist.H_2O. This was diluted to 100 µg/ml for the micro-assay.

4.8.2.2 Procedure

Protein standard (0-50 µl of the 100 µg/ml solution, i.e., 1-5 µg) or sample was diluted to 50 µl with dist.H_2O, or buffer, respectively, in 1.5 ml polyethylene microfuge tubes. Dye reagent (950 µl) was added, and the mixture was mixed by inversion of the tube. The colour was allowed to develop for 2 min after mixing, and the A_{595} was read, in 1 ml plastic micro-cuvettes. Assays for the standard curves were carried out in

quintuplicate at five concentrations of ovalbumin. Results for the assays were calculated from the equation generated by linear regression analysis of the standard curve.

4.8.2.3 Results

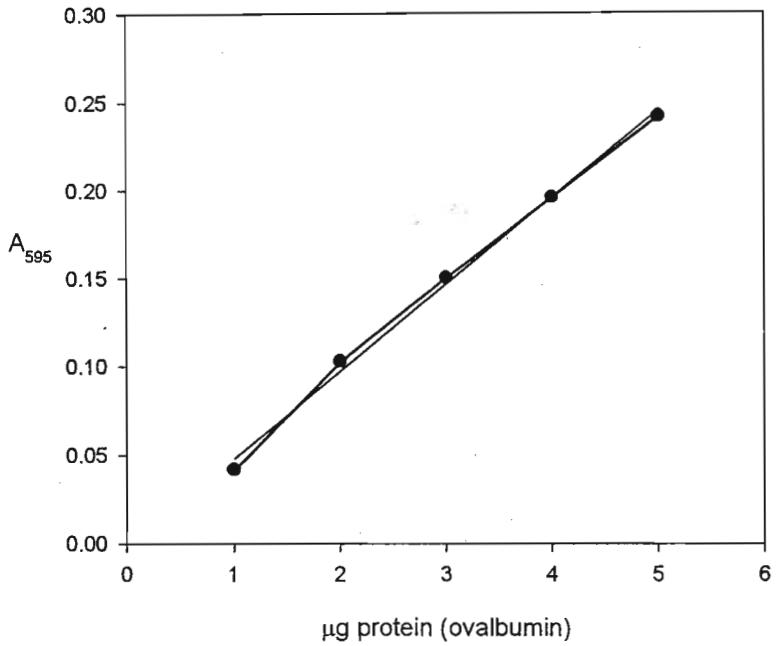

Figure 4.13 Calibration curve for Bradford microassay, for determination of protein content.

The standard solution produced a linear plot (Fig. 4.13) which was used to calculate the amount of protein, for loading in the western blot procedure.

4.8.3 Western blotting and development

Antibody specificity, as well as cross-species reactivity, may be determined by separation of proteins by SDS-PAGE and electrophoretically transferring the separated proteins to a matrix with a high protein binding capacity, such as nitrocellulose (Towbin *et al.*, 1979). This is known as western blotting. Following blocking of all the unoccupied sites on the membrane with an inert protein, the antigens are generally allowed to react sequentially with the primary antibody and a secondary antibody detection system, consisting of a secondary antibody directed against the primary antibody labelled with an

enzyme, such as alkaline phosphatase, which catalyses a reaction leading to the formation of a precipitating coloured product. The common alkaline phosphatase substrate is bromo-chloro-indolyl phosphate (BCIP). Cleavage of the phophodiester bond produces an indoxyl group that can undergo oxidation into an insoluble blue dimer called 5,5' dibromo 4,4' dichloro indigo. The colourless tetrazolium salt, nitro blue tetrazolium (NBT), is converted into an insoluble purple formazan upon reduction by the electrons liberated by this indoxyl group.

4.8.3.1 Reagents

Blotting buffer. Tris (3.03 g), glycine (14.4 g) and SDS (1 ml of a 10% (m/v) solution) were dissolved in dist.H_2O (900 ml). Methanol (10-20% (v/v)) was added just before use.

Ponceau S [0.1% (m/v) in 1% (v/v) acetic acid]. Ponceau S (0.1 g) was dissolved in 1% (v/v) acetic acid (1 ml acetic acid added to 99 ml dist.H_2O).

Tris buffered saline [TBS, 20 mM Tris, 200 mM NaCl, pH 7.4]. Tris (2.42 g) and NaCl (11.69 g) were dissolved in dist.H_2O (950 ml), adjusted to pH 7.4 with HCl, and made up to 1 l.

5% (m/v) fat-free milk-TBS. Fat-free milk powder (2.5 g) was dissolved in TBS (50 ml).

0.5% (m/v) BSA-TBS. BSA (0.5 g) was dissolved in TBS (100 ml).

Substrate buffer [50 mM Tris-HCl, 0.5 mM $MgCl_2$, pH 9.5]. Tris (0.606 g) and $MgCl_2$ (0.005 g) were dissolved in dist.H_2O (80 ml), the pH adjusted to pH 9.5 with HCl, and the volume made up to 100 ml.

Substrate solution. NBT (3 mg, Sigma) was dissolved in dimethyformamide (DMF, 70 µl, Fluka) and substrate buffer (30 µl). BCIP (1.5 mg, Sigma) was dissolved in DMF (100 µl) and the two solutions were added to substrate buffer (9.8 ml). This solution was made immediately before use.

4.8.3.2 Procedure

The mitochondrial and cytoplasmic fractions of the untreated MCF10A cells homogenised for various times (Section 4.8.1.2) were loaded with identical amounts of total protein, i.e., 25 µg, into each well and electrophoresed by SDS-PAGE as previously described (Section 4.4.2). Once gels were completely run, they were removed and soaked in blotting buffer with methanol (15 min), to improve the transfer of proteins to the nitrocellulose (Gershoni and Palade, 1982). For each gel to be blotted, six pieces of blotting paper, the same size as the gel, and one piece of nitrocellulose, slightly smaller than the gel, was saturated in blotting buffer. A mylar mask, slightly smaller than the gel, was placed at the bottom of the Hoefer Semi-Dry TE70 western blot apparatus. Three pieces of blotting paper were placed over this, followed by the nitrocellulose, the gel, and three more pieces of blotting paper. Care was taken at each layer to remove all air bubbles by rolling a glass pipette over the layers, to ensure even passage of current. Also, once the gel touches the nitrocellulose it must not be moved, since protein transfer starts immediately. The cover of the apparatus was placed on the top, and the two pieces connected by a cord to allow current flow. The apparatus was connected to a power-pack, and electrophoresed (28 mA, 8 V, 1 h 15 min). The nitrocellulose was removed, stained with Ponceau S so that the position of the molecular weight markers could be marked, to allow calculation of the molecular weights of protein bands detected in cell fractions, and then rinsed in dist.H_2O until the Ponceau stain was completely removed. The blot was stored overnight before development.

The nitrocellulose was blocked in 5% fat-free milk-TBS (1 h), washed in TBS (3 x 5 min) and incubated with primary antibody (10 µg/ml) in 0.5% BSA-TBS (2 h). Following washing in TBS (2 x 5 min), it was incubated in alkaline phosphatase-linked secondary antibody (rabbit anti-chicken, Sigma, diluted 1 in 5 000 in 0.5% BSA-TBS, 1 h)

and again washed in TBS (3 x 5 min). It was immersed in substrate solution and reacted in the dark until bands were clearly visible against a lightly-stained background. Finally, the strip was removed from the substrate solution, washed several times in dist.H_2O and dried between filter paper. This ensures good preservation of the bands.

4.8.3.3 Results and discussion

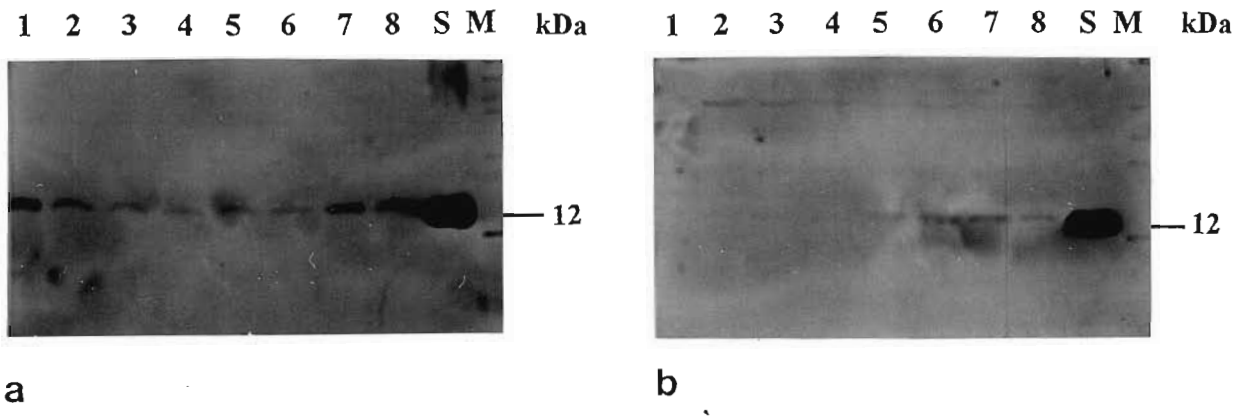

Figure 4.14 Western blot of mitochondrial and cytoplasmic fractions from untreated MCF10A cells. To optimise length of homogenisation and cell number for obtaining a detectable amount of mitochondrial cytochrome c, various times and cell numbers were tested. (a) Mitochondrial and (b) corresponding cytoplasmic fractions (25 µg protein per well) from untreated cells were electrophoresed on a tris-tricine SDS-PAGE, blotted, probed with chicken anti-cytochrome c primary antibody (10 µg/ml) and detected using the NBT/BCIP substrate. Lane 1 = 3 x 10^6 cells homogenised for 1 min; lane 2 = 4 x 10^6 cells, 1 min; lane 3 =3 x 10^6 cells, 1.5 min; lane 4 = 4 x 10^6 cells, 1.5 min; lane 5 = 3 x 10^6 cells, 2 min; lane 6 = 4 x 10^6 cells, 2 min; lane 7 = 3 x 10^6 cells, 2.5 min; lane 8 = 4 x 10^6 cells, 2.5 min; lane s = standard (1 µg horse cytochrome c); lane m = MWM.

Horse and human cytochrome c are known to be 12 kDa (SWISS PROT (http://expasy.nhri.org.tw/sprot/), accession numbers P00004, and P00001, respectively). However, they appear to migrate at approximately 15 kDa, relative to the molecular weight marker (MWM) on the blots. Although the tris-tricine gel system has been reported to give better resolution than the Laemmli system at lower M_r (Schägger and von

Jagow, 1987), it has recently been shown that other proteins of similar M_r (i.e., ~14 kDa) give anomalous results using this gel system (Meinesz, 1996). This may be due to the error obtained for very high or very low molecular mass proteins, as the migration (Rf values) of these proteins falls into the non-linear range of the standard curve which was plotted using the Rf values of the MWM, and which was used to calculate the M_r of the separated proteins in cell homogenates. In addition, cytochrome c is a very cationic protein (has a pI of 10) and may, therefore, migrate slower than other proteins, and hence, appears to be higher than the 14 kDa MWM. Since it has long been established that human and horse cytochrome c have M_r 12 kDa, the M_r of the cytochrome c bands were assumed to be 12 kDa.

Homogenisation of 3 x 10^6 cells for 1 min appeared to provide sufficient mitochondrial protein for clear detection of cytochrome c without the release of cytochrome c into the cytosolic fraction, due to over-homogenisation (Fig. 4.14, a, lane 1 was the darkest, the corresponding lane 1 in Fig. 4.14, b displayed no signal indicating that none of the cytochrome c had leaked into the cytoplasm through mitochondrial rupture). At 1.5 min there was very little cytochrome c present in the cytoplasmic fractions, whereas from 2 min of homogenisation and longer, there was an increasing amount of cytochrome c released into the cytoplasm. Therefore, increased mitochondrial rupture may have occurred during such extended periods of homogenisation.

From lane 2-7 (Fig. 4.14, b), there was a ~48 kDa band in the cytoplasm, whose intensity decreased until it disappeared, as the homogenisation time increased. This molecular weight corresponds to a polymer apocytochrome c, which has the same molecular weight as the holocytochrome c (Hartl *et al.*, 1989), but is normally present in the cytoplasm, where it is synthesised. The decrease in intensity of this ~48 kDa band corresponds with an increase in the intensity of a monomeric 12 kDa cytochrome c, thus, the 12 kDa bands in the cytoplasmic fraction may also represent apocytochrome c polymers which have been broken up during extra homogenisation, instead of cytochrome c which has been released by mitochondrial rupture resulting from over-homogenisation. However, this must be confirmed by testing whether the antibody raised is capable of recognising and binding to apocytochrome c. Apocytochrome c does not possess the haeme group present in holocytochrome c, nor has the same conformation as the mature

protein (Hartl *et al.*, 1989), so this may not be recognised by the antibody produced in this study.

There was no signal using the pre-immune antibody, indicating that there were no anti-cytochrome c antibodies present prior to immunisation (results not shown). Also, the results showed that there were no other non-specific antibodies present which might recognise other proteins present in the homogenate, even when the blot was developed for much longer than the blots used for the test anti-cytochrome c antibody (results not shown).

Although the antibodies were raised against horse cytochrome c, they cross-reacted well with the protein in human cell homogenates and are, therefore, applicable to studies on human tissues and, perhaps, other mammalian species as well. The single band detected amongst a variety of separated proteins indicates that the antibody is highly specific and that, with optimisation, may be applicable to electron microscopic immunocytochemistry for immunolocalisation of cytochrome c and its possible binding/co-localisation with other proteins involved in apoptosis.

4.9 Cytochrome c release in response to oxidative stress

At the commencement of this study, cytochrome c release, or cytochrome c conformational changes or inactivation, seemed to be the earliest detectable changes in the apoptotic process (Bossy-Wetzel *et al.*, 1998; Jemmerson *et al.*, 1999; Adachi *et al.*, 1997). Since variable cytochrome c release or changes is seen in different systems, using various apoptosis-inducers and cell types, cytochrome c release was assessed in our breast epithelial model system exposed to H_2O_2.

4.9.1 Reagents

See Sections 4.8.1.1, 4.8.2.1 and 4.8.3.1.

4.9.2 Procedure

Cells were grown, seeded (3 x 10^6 cells/15 ml), treated (Section 2.4.1.2) and harvested as previously described (Section 2.4.2.2). Harvested cells were homogenised (Section 4.8.1.2), and the protein content determined as previously described (Section 4.8.2.2). Homogenates were electrophoresed (Section 4.4.2), western blotted and developed as previously described (Section 4.8.3.2).

4.9.3 Results and discussion

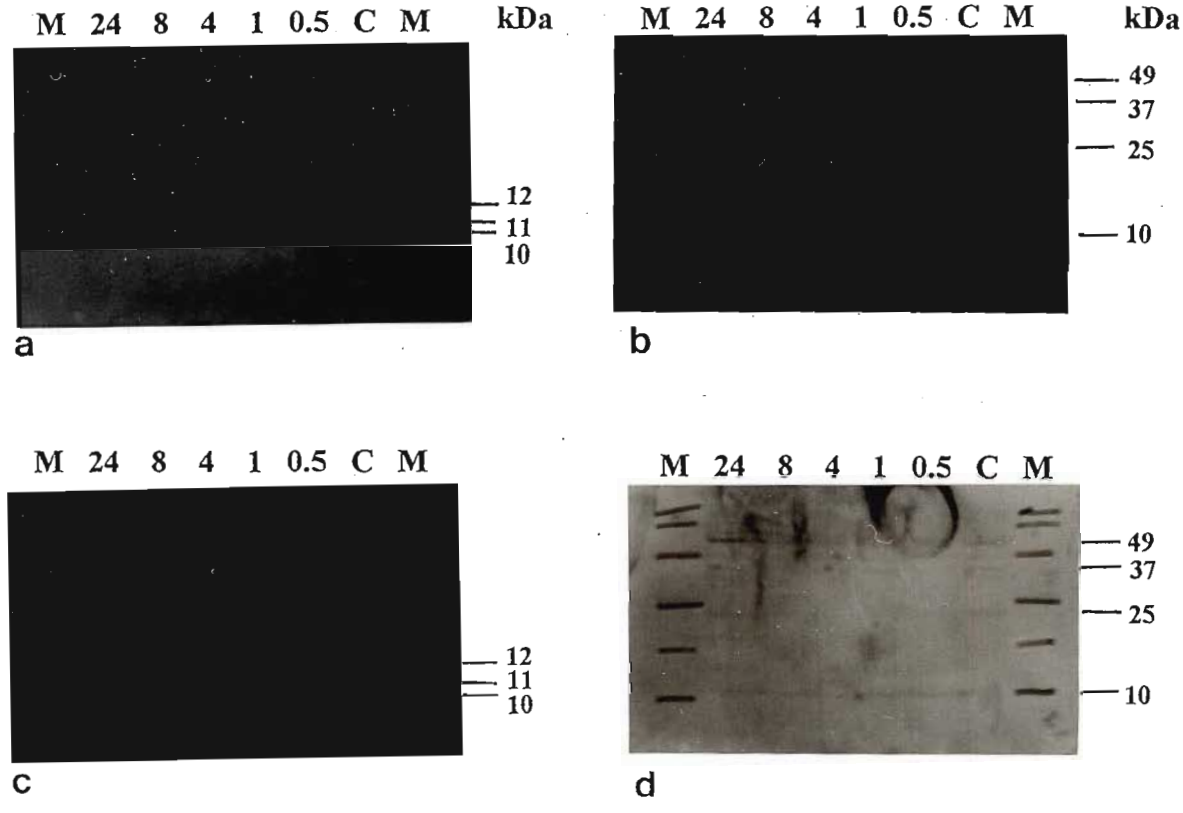

Figure 4.15 Western blots for determination of cytochrome c release by MCF10A cells in response to oxidative stress.

25 µg protein per well was electrophoresed on a tris-tricine SDS-PAGE, blotted, probed with chicken anti-cytochrome c primary antibody (10 µg/ml) and detected using the NBT/BCIP substrate. Samples were (a) mitochondrial and (b) cytoplasmic fractions from MCF10A cells treated with 100 µM H_2O_2 and 3 µM Fe^{2+} in serum free medium, (c) mitochondrial and (d) cytoplasmic fractions from MCF10A cells treated with 250 µM H_2O_2 and 3 µM Fe^{2+} in serum free medium. Lanes M = MWM, lanes 24 – 0.5 = indicated times of treatment in hours, lane C = control (untreated).

M_r values were calculated relative to the cytochrome c band in the control cells, which was assumed to be 12 kDa, as explained in Section 4.8.3.3. As a few of the paler bands present on the original blots (Figs 4.15, b, 4.16, d) were not well captured by photography, a representation of the bands seen on these blots is summarised (Table 4) to assist the interpretation of results.

Table 4. Summary of molecular weights of bands from western blotted, treated cell fractions.

MITOCHONDRIAL FRACTIONS							
Cells	**H_2O_2**	**C**	**0.5**	**1**	**4**	**8**	**24**
10 A	100	12, <10	12, 11	12, 11, 10	12, 11, 10	12, 11, 10	12, 11, 10
	250	12, <10	12, 11, 10	12, 11, 10	12, 11, 10	12, 11, 10	12, 11, 10
NeoT	100	12, <10	11	<11	<11	>11	>11
	250	12, <10	12, 10	12, 10	12, 10	12, <10	12, <10
CYTOPLASMIC FRACTIONS							
Cells	**H_2O_2**	**C**	**0.5**	**1**	**4**	**8**	**24**
10 A	100	-	10	10	<10	<10	<10
	250	-	>10	>10	>10	>10	>10
NeoT	100	-	-	-	-	-	-
	250	-	<10	<10	-	-	-
Present in all Cytoplasmic fractions				~25, 37, 49			

NB. <10 in the controls of mitochondrial fractions indicates that although there is an additional band at 10 kDa, it is at a much lower level than in the treated (test) cell fractions. < / > in test fractions indicates the intensity of the band relative to the previous band (i.e., the time immediately before).

There appeared to be modification of the original 12 kDa cytochrome c in mitochondria of 100- and 250 μM H_2O_2-treated cells (Fig. 4.15, a, c), as two other bands were visible at 10 and 11 kDa (and the antibody has been shown to be specific for

cytochrome c, Fig. 4.14). An increasing amount of the modified forms seemed evident with increased time of treatment (Fig. 4.15, a). The nature of these bands is uncertain, but is discussed below.

In 100 μM H_2O_2-treated cells, at 30 min only the 11 kDa band was visible, but from 1 h onwards the 11 and 10 kDa bands were present, with the samples at 24 h having the bands of greatest intensity (Fig. 4.15, a). At 250 μM H_2O_2, however, the 10 kDa band was visible from 30 min onwards (Fig. 4.15, c), possibly due to earlier damage because of the greater intensity of insult. Furthermore, at 250 μM the bands of mitochondrial cytochrome c decreased in intensity, possibly representing release of cytochrome c into the cytoplasm.

In addition to modification of mitochondrial cytochrome c in MCF10A cells, some cytochrome c was released (Fig. 4.15, b, d). The released protein was ~10 kDa, when calculated using criterion described above (Section 4.8.3.3), and may represent a release of an already modified form of the protein. Cytochrome c release was apparent from 30 min of treatment in both 100- and 250 μM-treated cells, but the cytoplasmic bands were of a much greater intensity at the higher H_2O_2 concentration, representating greater cytochrome c release. In the cytoplasmic fractions (Fig. 4.15, b, d) there were pale bands at ~25 and ~37 kDa, and more prominent ones at ~49 kDa. These are multiples of 12 kDa and may, therefore, represent dimers, trimers and tetramers of apocytochrome c which has been synthesised in the cytoplasm and which has not yet been imported into the mitochondria, as these bands were also present in the untreated control cells (while the 12 kDa band was not present in controls) (Fig. 4.15, b, d).

The nature of the additional 11 and 10 kDa bands is unknown, but some possible explanations to account for these forms of the cytochrome c protein are presented. The possibility that either the 10 or 11 kDa band was a result of reduction by mercaptoethanol during sample preparation was considered possible. Although there are no disulfide bonded fragments which could be lost by reduction, the haeme (0.6 kDa) is linked to the polypeptide via disulfide bonds, and forms of cytochrome c which have lost this group, therefore, may have been visible at ~11.4 kDa when the disulfide bonds were reduced. However, as the calculated M_r of the blotted proteins are estimations, and may not be very

accurate, these modified forms may represent a form of cytochrome c in which the haeme group has been removed by reduction of a disulfide bond. It is likely, however, that one of these forms occurs as a result of H_2O_2-treatment of the cells (i.e., the 11 kDa band), as this band is not present in the controls (Fig. 4.15, lanes C), but the 10 kDa band does occur in the mitochondria of control cells (at a lower level than in test cells).

Krippner *et al.* (1996) suggested that cytochrome c may be inactivated by a death protease through limited proteolysis and without extensive degradation. The possibility that the 10 kDa band in the controls (lanes C) may have resulted from intrinsic proteolysis cannot be ruled out, as the protease inhibitors were omitted from the lysis buffer during the isolation of mitochondrial fractions. In the treated cells, proteolysis may also occur, with 1 or 2 kDa being cleaved off the protein. These low molecular weight bands would not be detected on the gel used because of the limited resolution of peptides by the 10% acrylamide gel used here. Such proteolysis may result from the activation of a protease by oxidative signalling, or may occur because of increased susceptibility of the protein to proteolysis resulting from oxidative modification (Pacifici and Davies, 1990). However, whether this does occur in these cells remains to be determined.

Cytochrome c has not previously been reported to be glycosylated. However, a *b*-type cytochrome from a bacterium (*Sulfolobus acidocaldarius*) is glycosylated and is analogous, in structure and function, to *c*-type cytochromes with His/Met ligation in this species (Hettmann *et al.*, 1998). As cytochrome c is a highly conserved protein (Mayer and Walker, 1987), this may also occur in humans, although it has not been addressed. It may be possible that the lower M_r modified forms of cytochrome c represent a form of the protein which results from deglycosylation (resulting from oxidative stress), if the original 12 kDa protein is glycosylated.

A very recent report by von Ahsen *et al.* (2000) showed three forms of mitochondrial cytochrome c, a pre-cursor, an intermediate and a mature form. However, they do not give the M_r of these proteins. Whether these forms actually are a pre-cursor, intermediate and mature form is doubtful, however, as cytochrome c does not undergo proteolytic processing upon import into mitochondria (Hartl *et al.*, 1989). Furthermore, apocytochrome c and holocytochrome c in a mammalian species have identical M_r, i.e., 12 kDa (Hartl *et al.*, 1989). Therefore, it is our opinion that the 10 and 11 kDa bands

may, most likely, result from proteolytic cleavage as a consequence of oxidative signal transduction, or from increased proteolytic susceptibility after oxidative modification of the protein.

After it was established that cytochrome c can be both modified and released in response to oxidative stress in MCF10A cells, these results were compared with those obtained for MCF10AneoT cells, to see if there were differences between the normal and cancer cells at the molecular level.

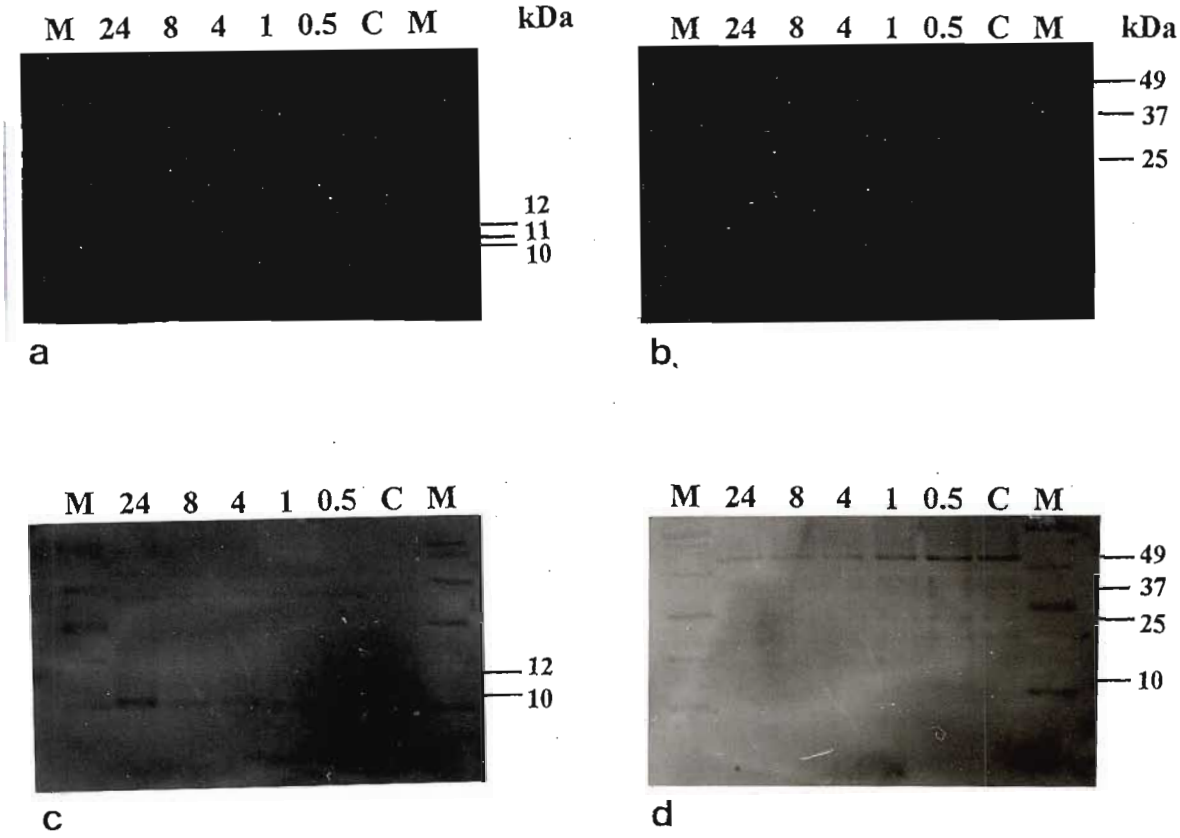

Figure 4.16 Western blots for determination of cytochrome c release by MCF10AneoT cells in response to oxidative stress.

25 μg protein per well was electrophoresed on a tris-tricine SDS-PAGE, blotted, probed with chicken anti-cytochrome c primary antibody (10 μg/ml) and detected using the NBT/BCIP substrate. Samples were (a) mitochondrial and (b) cytoplasmic fractions from MCF10AneoT cells treated with 100 μM H_2O_2 and 3 μM Fe^{2+} in serum free medium, (c) mitochondrial and (d) cytoplasmic fractions from MCF10AneoT cells treated with 250 μM H_2O_2 and 3 μM Fe^{2+} in serum free medium. Lanes M = MWM, lanes 24-0.5 = indicated times of treatment in hours, lane C = control (untreated).

Similar to the MCF10A cells, there appeared to be modification of mitochondrial cytochrome c from 30 min onwards in both 100- and 250 μM H_2O_2-treated cells (Fig. 4.16 a, c). However, from 1 h onwards in the 100 μM-treated cells (Fig. 4.16, a), the 12 and 10 kDa bands were no longer visible, and only the 11 kDa band was present. This may represent a modification of all the 12 kDa mitochondrial cytochrome c, compared to modification of only a proportion of the protein in the MCF10A cells (Fig. 4.15, a), and may be indicative of greater susceptibility of the MCF10AneoT cells to oxidative stress at the lower H_2O_2 concentrations, as shown in the morphological and caspase assays (in Chapters 2 and 3, respectively). There was a progressive decrease in intensity of the 11 kDa band at 1 and 4 h and a progressive increase in intensity at 8 and 24 h in 100 μM-treated cells (Fig. 4.16, a), possibly indicative of an attempt at recovery, by greater cytochrome c synthesis and import after longer treatment times, although these proteins subsequently still became modified (Fig. 4.16, a). The results obtained for 250 μM-treated cells (Fig. 4.16, c) are consistent with the possibility that the MCF10AneoT cells may recover after a certain level of damage, as the unmodified 12 kDa bands were present at all times of treatment (although decreasing in amount from 30 min to 24 h), while in the 100 μM-treated cells (Fig. 4.16, a), only the 11 kDa modified version was present from 1 h onwards.

In addition to the differences in modification of mitochondrial cytochrome c in the two cell lines tested, they also differed with regards to the release of cytochrome c into the cytoplasm. While cytochrome c release occurred in 100 μM-treated MCF10A cells (Fig. 4.15, b), the MCF10AneoT cells at the equivalent concentration (Fig. 4.16, b) did not release cytochrome c. However, there was cytochrome c release in 250 μM-treated MCF10AneoT cells (Fig 4.16, d) evidenced by the very pale bands at 30 min and 1 h, but there was no release at 4, 8 and 24 h, and this may also be indicative of recovery of the MCF10AneoT cells. There seems to be some non-specific binding of the anti-cytochrome c antibodies to high M_r cytoplasmic proteins in the 250 μM-treated cells (Fig. 4.16, d). These, however, developed only after blot development for an extended period of time relative to all the other blots, while trying to determine if cytochrome c was released by these cells. Cytochrome c release by these cells, therefore, may occur at a

very much lower level than the MCF10A cells, as over-development was required for the cytoplasmic bands to become visible.

The 49 kDa band (tetramer of cytochrome c), which was present in the cytoplasmic fractions of all the cells, whether treated or not (0 h controls) (Figs 4.15, b, c, 4.16, b,c,), was of a greater intensity in the cytoplasm of the 250 μM-treated MCF10AneoT cells and may represent increased apocytochrome c synthesis, as part of the recovery process, as has been previously reported (Martinou *et al.*, 1999). Although the extent of mitochondrial cytochrome c modification at 100 μM H_2O_2 was greater in the MCF10AneoT cells than in the MCF10A cells, there was cytochrome c release from mitochondria in MCF10A cells, but not in the MCF10AneoT cells at this concentration. There was very little cytochrome c release from mitochondria in the MCF10AneoT cells and possibly increased apocytochrome c synthesis at 250 μM H_2O_2, whereas the MCF10A cells released a larger amount of cytochrome c at this concentration. This implies that downstream apoptotic events, or the execution phase, could proceed in the MCF10A cells at the higher concentration of H_2O_2, but may be retarded in the MCF10AneoT cells, and that MCF10A cells may be committed to die, while the MCF10AneoT cells were possibly allowed a chance to recover. However, it must be remembered that cytochrome c release may be reversible, and may not necessarily reflect commitment to apoptosis (von Ahsen *et al.*, 2000). The results are consistent with the suggestion of a non-linear response to oxidative stress by the pre-malignant cells, and with the previous results of morphology and caspase activity assays (Chapters 2 and 3, respectively). However, the possibility of intrinsic molecular differences in the cytochrome c protein in the two cell lines, and resultant differences in susceptibility to oxidative stress, cannot be ruled out.

4.10 Discussion

The method for detection of cytochrome c release was relatively quick and simple, although very larger numbers of cells were required, making the pre-requisite use of cultured cells tedious and expensive. If more time was available for optimisation of a method such as the enhanced chemiluminescence (ECL) method, which involves electrophoresis and western blotting, but employs a very sensitive X-ray detection system,

the expense of the method could have been reduced considerably. Although raising antibodies takes several weeks, the actual procedure is relatively quick and can be done simultaneously while performing other experiments. Large amounts of antibody are obtained at a relatively low cost (compared to purchasing antibodies), and they can be used for several applications, such as western blots, cryoimmunocytochemistry, and also for fluorescent applications after conjugation of the antibody to a fluorescent molecule.

This method gave information at a molecular level, compared to the morphological and enzyme level given by the DNA laddering and caspase assays, as modifications of the cytochrome c protein were evident. However, the nature of the 10 and 11 kDa bands obtained in the mitochondrial fractions remains to be elucidated. Cytochrome c changes may occur earlier than 30 min, and may, therefore, be the earliest detectable apoptotic event in the system studied. The recovery of mitochondria in MCF10AneoT cells, proposed in Section 2.4.2.4, is reinforced by the results obtained in the western blots for detection of cytochrome c release

In the following chapter, the full sequence of apoptotic events that seem to be evident in the tests carried out on the cell systems examined will be proposed for the MCF10A cell system used, as the nature and sequence of events seems to be inducer- and cell-type specific.

CHAPTER 5

GENERAL DISCUSSION

Apoptosis is a physiological process which is highly regulated in normal cells, but may be dysregulated in tumour cells, leading to increased resistance to apoptosis in these cells (Cotgreave and Gerdes, 1998). However, though a particular apoptotic pathway may be dysfunctional in some cells, these cells may be induced to undergo apoptosis via alternate pathways (Wallace and Brodeur Lowe, 1999). Cells are usually able to cope with a certain level of oxidative stress, which, depending on the levels of oxidative stimuli and the cells anti-oxidative capacity, may lead to cell proliferation, apoptosis or necrosis.

The markers recommended for the early detection of apoptosis have changed over the years. Initially, morphological features such as membrane blebbing and DNA aggregation were used to identify the apoptotic form of cell death, by light and electron microscopy (Kerr *et al.*, 1994). Later, however, detection of biochemical events, such as DNA degradation (Marchetti *et al.*, 1996; Bossy-Wetzel *et al.*, 1998), phosphatidylserine (PS) exposure (Eisel *et al.*, 1998), caspase activity (Mancini *et al.*, 1998) and the most recent, cytochrome c changes (Bossy-Wetzel *et al.*, 1998), have become more prominently used. In a search for the best or most sensitive methods for detecting apoptosis, the focus has changed back to morphological examination, but has recently centred on the mitochondria (Mancini *et al.*, 1997; Green and Reed, 1998, Kluck *et al.*, 1999), due to the recent explosion of evidence of the involvement of mitochondria in damage-induced apoptosis (Coppola and Ghibelli, 2000).

Cancer therapy results in the generation of H_2O_2, which is usually the agent that induces cell death in treated cells (Cohen and d'Arcy Doherty, 1987). This mode of cell death may be induced via effects on the mitochondria and may be orchestrated via the mitochondrial response, as H_2O_2 may activate a ceramide signalling pathway which may result in the release of cytochrome c from mitochondria (Goldkorn *et al.*, 1999; Mathias *et al.*, 1998). It is clear from the literature that one pathway leading to apoptosis may be more dominant than others, in different cells types. Also, a number of paths can be working in combination at the same time (Mathias *et al.*, 1998). The general view in March 1999, at the commencement of this study, was that the sequence of events occurring via the mitochondrial pathway to the induction of apoptosis was initially, cytochrome c release either via mitochondrial swelling and

rupture (Susin *et al.*, 1997), or by the regulation of the PT pore, followed by caspase activation, and the subsequent execution phase (Crompton, 1999).

In this study, a "normal" breast epithelial cell line and its' pre-malignant derivative were treated with H_2O_2, as most anti-cancer drugs are metabolised to this ROI (Cohen and d'Arcy Doherty, 1987). The suitability of this system, and a few selected techniques for the detection of apoptosis, was tested as a model system for the future testing of the selectivity of anti-cancer drugs. As the study progressed, conflicting reports regarding the sequence of events in apoptotic pathways and mechanisms of the apoptotic process were observed in the literature. At the start of the study, we were aware of the variability of results obtained with different inducers of apoptosis on various cell types. Most of the research papers at the time of commencement of this study, however, advocated the line of investigation and markers of apoptotic events used in the current investigation. The results obtained in this study, which enable a model of the sequence of events in the progression of apoptosis to be suggested, does not fit the initial model of apoptotic events first proposed and described above, and is detailed in the next section.

5.1 A model of the apoptotic events in the MCF10A system

For the system studied (H_2O_2-treated breast epithelial cells), the methods chosen for detecting apoptosis were useful and seem appropriate, as they enabled a model for the sequence of events in the progression towards apoptotic death to be proposed (Fig. 5.1). The sequence of apoptotic events observed, however, does not correlate with the proposed conventional sequence, i.e., cytochrome c release, caspase activation, and subsequent activation of the execution phase (Fig. 5.1), resulting in the morphological features of apoptosis such as cell shrinkage, convolution of the nuclear membrane, DNA degradation, and plasma membrane blebbing (Bossy-Wetzel *et al.*, 1998).

The sequence of apoptotic events proposed for the model system under investigation is as follows (See Fig. 5.1 for details):

(1) cytochrome c release (30 min)

(2) nuclear convolution and DNA fragmentation (1 h)

(3) caspase activity (4-8 h).

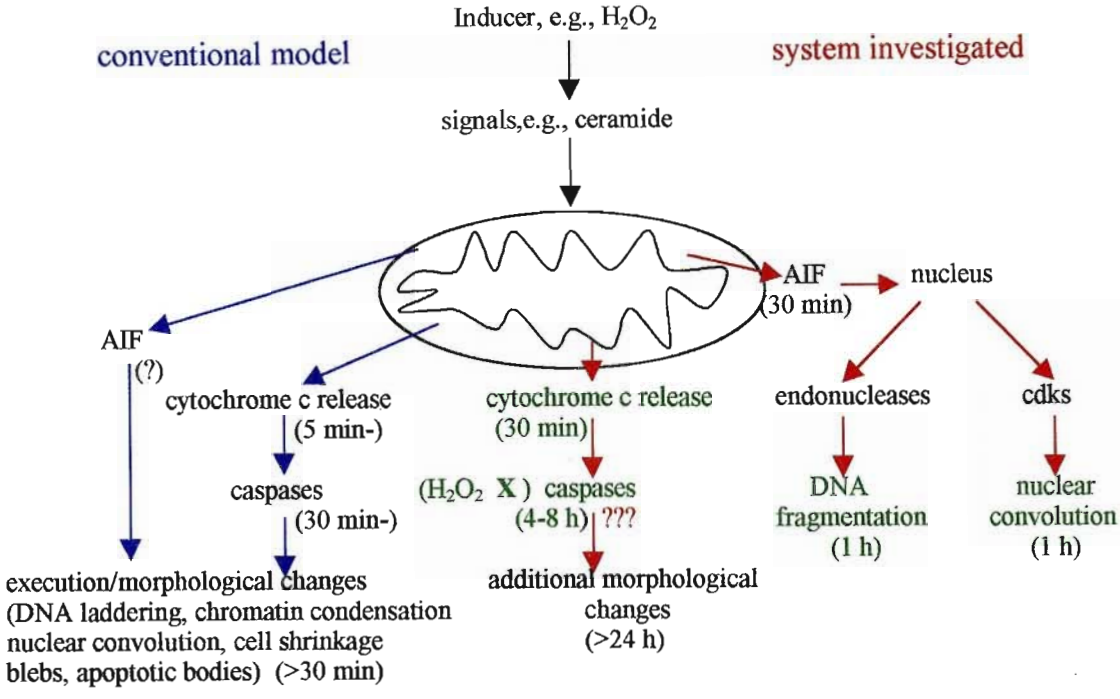

Figure 5.1 Model of apoptotic events.

A comparison of the sequence of apoptotic events that have been conventionally reported (blue arrows), and those determined in the system of H_2O_2-treated breast epithelial cells (red arrows), reveals that these cells may have a caspase-independent mechanism of apoptosis, or they may elicit the assistance of back-up suicide mechanisms involving cyclin dependent kinases (cdks) or apoptosis-inducing factor (AIF) until caspases become active. The key marker events are indicated by the green text.

Cytochrome c release seems to be an early event in agreement with recent reports of other investigators in other systems (Kluck *et al.*, 1997; Yang *et al.*, 1997; Zou *et al.*, 1997). In the model system used, caspase activity, however, was a relatively late event compared to other systems, and occurred after features such as convolution of the nuclear membrane and nuclear fragmentation, which have traditionally been reported to be a consequence of caspase cleavage (Duband-Goulet *et al.*, 1998), and a downstream event of caspase activation, respectively. This observation may, in part, be the result of caspase inhibition by H_2O_2, a phenomenon previously reported by Boggs *et al.* (1998). Some cells detoxify H_2O_2 via catalase or GSH. Once H_2O_2 is detoxified, inhibition of caspases is reversed. This may be the case here and thus, caspase activity may have been observed much later than may otherwise have been the case. Such activity would presumably occur after normal activation by the cytosolic complex of cytochrome c-Apaf-1-dATP, which binds to and activates caspase-9, and subsequently activates caspases-3, -6 and –7 (Coppola and Ghibelli, 2000). Caspases are responsible for lamin cleavage and chromatin

condensation. Therefore, in this system, other proteases must be responsible for such cleavage leading to collapse of the nuclear membrane, chromatin condensation and DNA fragmentation, as these phenomena were seen prior to caspase activation. Chromatin condensation and dissolution of the nuclear envelope, including solubilisation of the lamin meshwork that resides within the envelope, has also been reported to depend primarily on cyclin dependent kinases (cdks) (Harvey *et al.*, 2000), which may be activated by caspase-independent mechanisms (Heald *et al.*, 1993), and not on extranuclear caspases (Harvey *et al.*, 2000). Hence, an early cyclin-dependent kinase mechanism may be operating in the test system used. This is further supported by recent evidence that effector caspases may not be involved in early nuclear morphological changes, in chemical-induced apoptosis (Johnson *et al.*, 2000).

Apoptosis-inducing factor (AIF) which is released from mitochondria upon apoptotic stimuli, may mediate caspase-independent death in some cells (Deshmukh *et al.*, 2000), and this may also explain the early DNA fragmentation which occurred prior to caspase activity. Indeed, it has been suggested that vertebrate cells may have a caspase-independent death programme(s), which may serve as a back-up suicide mechanism (Weil *et al.*, 1998). In this study, some caspase activity was seen, but quite late, and the levels of activity and amounts of oxidative stress required for caspase activity induction differed between the MCF10A and MCF10AneoT cells. The normal MCF10A cells exhibited significant caspase activity after 8 h of treatment, and maximal activity was induced by 250 μM H_2O_2, higher levels of which induced necrosis in these cells. In contrast, the MCF10AneoT cells showed caspase activity after just 4 h of treatment, and maximal activity was induced by 500 μM H_2O_2. Levels of activity were also much higher in the MCF10AneoT cells, and these cells were able to cope better with the oxidative stress than the MCF10A cells, as they became necrotic, as evidenced by leakage of caspases out of the cell, at 1000 μM instead of at 500 μM. It seems likely that H_2O_2 inhibited the caspases until the H_2O_2 was detoxified. It also seems that the MCF10AneoT cells are able to tolerate higher levels of oxidative stress and possess more active caspases than the MCF10A cells. This may possibly be due to the higher GSH levels found in cancer cells, as higher GSH levels would confer a greater anti-oxidant capacity, and maintain redox-regulated caspases in a reduced, and thus activated, state. However, this has not been proven conclusively. Therefore, the possibility that other non-DEVD-specific

caspases may be cleaving and activating the DEVD-specific caspases, cannot be ruled out.

5.2 Theory of cytochrome c release

From the results of this study, it was seen that cytochrome c release was the earliest apoptotic event in the cells being studied. In the mitochondrial fractions of cells treated with 100 and 250 μM H_2O_2, two extra bands were seen at 10 and 11 kDa, in addition to the normal 12 kDa band of cytochrome c, and cytochrome c was also released into the cytoplasm. Our view of the mechanism of release and the form seen in the mitochondria will, therefore, be discussed in detail, as the mechanism by which cytochrome c release occurs is complex.

Cytochrome c is not easily released from mitochondria under normal circumstances. Though the mechanism of cytochrome c release has received considerable attention, to date, no unequivocal conclusions as to the mechanism of release have been drawn, partially due to the inducer- and cell-type specific nature of many apoptotic pathways and signals generated in different cell types. Various proteins and their properties need to be considered in order to devise a general model for the events leading to cytochrome c release and the effects of such release.

The VDAC channel is normally impermeable to cations (cytochrome c is cationic in nature). Although it does become cation-permeable at very low ψ_m (about 20 mV) (Dihanich, 1990), the size exclusion limit of 5 kDa at this ψ_m still excludes the possibility that the VDAC channel alone is responsible for cytochrome c release. (Also, at this low ψ_m there would be no need for cytochrome c release as cells become necrotic due to ATP depletion resulting from excessive ATP hydrolysis, which would occur in an attempt to maintain ψ_m) (Crompton, 1999). Therefore, VDAC, by itself, cannot release cytochrome c.

Pro-apoptotic Bid and Bax may form pores in the outer mitochondrial membrane (Chou *et al.*, 1999; Jurgensmeier *et al.*, 1998). However, pores formed by these proteins are anion-selective and occur at neutral pH (*in vitro*) (Antonsson *et al.*, 2000), therefore, they would not release cationic cytochrome c. There are reports that apoptosis requires slightly acidic intracellular conditions (Chen *et al.*, 1997; Gottlieb *et al.*, 1996; Barbiero *et al.*, 1995; Perez-Sala *et al.*, 1995). Intracellular acidification would not promote Bid/Bax pore formation and cytochrome c release, but may be required for downstream apoptotic events, such as activation of endonucleases

(Zhivotovsky, 1994). Therefore, cytochrome c release does not seem to occur via a ψ_m mechanism or via Bid/Bax at an acid pH.

Anti-apoptotic Bcl-2 and Bcl-X_L form channels at low pH and which are cation selective (*in vitro*) (Antonsson *et al.*, 2000). An acid pH, however, is apparently an ideal condition for apoptosis and cytochrome c release, as these processes require an acid pH. As Bcl-2 family members can interact with each other to control apoptosis (Chittenden *et al.*, 1995), Bax, which is translocated to mitochondria upon apoptotic stimulation, may interact with the already-present Bcl-2 pore to allow cytochrome c efflux. Alternately, mitochondrially-translocated Bid and Bax may also interact with the VDAC channels, as has been suggested by Nouraini *et al.* (2000) to release cytochrome c, if conditions do not favour pore formation by the individual proteins.

However, it must be kept in mind that intracellular acidification is not required for all types of apoptosis or all types of lethal stimuli, as exceptions have been described (Chen *et al.*, 1997). Therefore, Bax/Bid channels, which form under neutral conditions, may still form, and thereby release cytochrome c, without interacting with other proteins or channels, when acidification is not required for the apoptotic process. The exclusion limit formed by these proteins, either individually or as part of a pore-forming complex, is unknown. It was stated in 1999 that there is no direct evidence for pore-forming proteins in the outer membrane which could create pores large enough for the release of proteins from the intermembrane space (Crompton, 1999). A PEF protein which may facilitate the release of cytochrome c, and lead to cell death, was, however, discovered at about this time (Kluck *et al.*, 1999).

Even after cytochrome c release, however, cytosolic cytochrome c need not induce apoptosis (Coppola and Ghibelli, 2000). Cells can recover after the re-establishment of normal physiological conditions or factors. The integrity of the organelles is also apparently maintained during these events as indicated by electron microscopy (Martinou *et al.*, 1999). This insight contradicts the previous held popular hypothesis that states that cytochrome c release reflects irreversible damage to mitochondria and hence, commitment to cell death, and implies the existence of a specific channel that may control the reversible release of this process (Haycock, 1999). This fact makes cytochrome c release an unreliable marker of an early apoptotic event.

It has been suggested that cytochrome c release may also occur via mitochondrial swelling and outer membrane rupture, thus releasing cytochrome c

from the intermembrane space. Whether mitochondrial swelling occurs in most instances of apoptosis or is required for cytochrome c release is questionable, as electron micrographs of apoptotic cells frequently contain apparently intact unswollen mitochondria. Since it has been reported that the pro-apoptotic proteins Bid and Bax can release cytochrome c from isolated mitochondria in the absence of detectable mitochondrial swelling and in the presence of PEF (Kluck *et al.*, 1999), mitochondrial swelling is not likely to be required for cytochrome c release, as indicated by the current electron microscopic studies.

It is, therefore, our opinion that cytochrome c release occurs via the formation of Bax-VDAC pore complexes and with the assistance of PEF, as although there has been no direct evidence for a pore, Bid and Bax are a requirement for cytochrome c release. Therefore, Bid may also be involved in the Bax-VDAC-PEF pore formation.

It appears that release of cytochrome c from the mitochondria is not always required for caspase activation and apoptosis and that, in certain systems, the subcellular location of cytochrome c does not change during apoptosis (Adachi *et al.*, 1997). Hence, cytochrome c release may prove to be an unreliable marker of the apoptotic process, though a number of studies show that cytochrome c is released from mitochondria during apoptosis (Liu *et al.*, 1996; Yang *et al.*, 1997; Kluck *et al.*, 1997; Rosse *et al.*, 1998; Jurgensmeier *et al.*, 1998). Jemmerson *et al.* (1999) proved, however, that cytochrome c may also undergo a conformational change during apoptosis and may not be released and this is possibly what occurred in the current study, as very little cytochrome c was released. Although the cytochrome c in the mitochondrial fractions of treated cells exhibited the normal 12 kDa band, two additional forms at 10 and 11 kDa were present. These two forms may represent conformationally altered cytochrome c or processed forms (i.e. with some type of cleavage). Whether cytochrome c is released or undergoes a conformational change, in response to apoptotic stimuli, may be cell specific (Jemmerson *et al.*, 1999). It is evident now that even the mechanism of cytochrome c release may vary between cell types (Deshmukh *et al.*, 2000).

The possibility that other organelles, besides mitochondria, may harbour death-related proteins with a role like that of cytochrome c has not been addressed or ruled out.

5.3 *In vitro* vs *in vivo*

It must be remembered that the above scenario and model of how apoptosis occurs in the MCF10A and its *ras*-transfected pre-malignant derivative is specific to these cell lines. It must also be borne in mind that not all cultured cells *in vitro* may accurately reflect the processes occurring *in vivo*. Cell lines may be prevented from exhibiting certain apoptotic characteristics through the loss of hormone, cytokine and signal transduction pathways or other metabolic and cellular components present in the whole organism. The ultimate aim of this study is to set up an assay for assessing the selective toxicity of drugs, and the MCF10A and MCF10AneoT cell lines provide a very useful system for such preliminary studies, as there is an immortal "normal" cell line as well as the cancerous equivalent. In studies on chemotherapeutic agents, selective toxicity testing presents a problem as it is difficult to evaluate the effects of the drugs without a "normal" control, equivalent to those present *in vivo*. The MCF10 cell culture system, therefore, provides a valuable tool as it provides a near "normal" control, which is also immortal, allowing continuous culture of control cells.

Cell culture models have proven to be useful for studying oxidative stress in systems less complex than tissues, but still provide the opportunity to model events in living cells. Some of the complications in cell model systems can be reduced through selection of experimental conditions. For example, serum use may be eliminated for short-term experiments, such as those done on the order of hours, to reduce or eliminate multiple endogenous anti-oxidants in serum which would complicate the cellular system (Buxser *et al.*, 1999). Although this is done to obtain a more "accurate" result, i.e., the endogenous anti-oxidants would decrease the actual oxidative damage induced, such elements **are** present *in vivo*. This level of complexity must be taken into account, and it must be remembered that cell culture systems are in many ways artefactual model systems.

There are inaccuracies imposed due to the technical problems with cell culture assays, e.g., length of time of assays and concentrations of reagents compared to the equivalent required *in vivo*, e.g., in the cells where caspase activity continued to increase until 24 h, it is possible that apoptotic bodies were formed after this time but were not detected, as experiments were possibly terminated prior to this event. The inadequacies of certain assay procedures, e.g., the presence of apoptotic bodies in the cells being studied was not evident by light or electron microscopy, may also be a problem. Alternately, a loss of signal transduction from other cells which may be

present *in vivo* may lead to prolonged and non-progression of certain phases of the apoptotic process, i.e., the level of caspase activity required for cleavage of the cell into membrane-bound apoptotic bodies may not have been attained, due to the prolonging or non-progression of this apoptotic event.

Several other factors must also be considered, such as cell contact with normal ECM components which would alter the cellular signalling, and may lead to different cellular response from those obtained *in vitro*. Hence, although cell culture systems provide invaluable study tools, experiments should be repeated in whole tissue systems, as the majority of cancers grow as three-dimensional solid tumours and gene expression, and possibly function, can be significantly altered under such conditions (Rak *et al.*, 1995).

Such alterations in cancer cells may lead to further alteration of redox-state, and thus, further dysregulation of apoptosis, as the latter is a redox-regulated process (Haddad and Land, 2000). The redox-regulation of apoptosis is, however, a potential difference that may be exploited to selectively kill cancer cells.

5.4 Redox regulation of apoptosis

It is now widely accepted that the process of apoptosis is redox-modulated (Haddad and Land, 2000). The ability of cells to undergo or initiate apoptosis has been found to be dependent on intracellular levels of the redox buffer, GSH (Boggs *et al.*, 1998). GSH depletion is an important trigger of the apoptotic pathway (Haddad and Land, 2000), and is necessary, but not sufficient, for apoptosis (Coppola and Ghibelli, 2000). Glutathione is found in two redox forms, GSH (reduced) and GSSG (oxidised). Under conditions of oxidative stress, GSSG is formed and may either recycle back to GSH or exit from the cells via physiological carriers, leading to overall glutathione depletion, or may have an increased GSSG/GSH ratio. However, GSH extrusion may not necessarily be a consequence of oxidative stress, i.e., non-oxidative apoptogenic agents may also cause GSH extrusion (Coppola and Ghibelli, 2000). This may, in itself, lead to oxidative stress in the cell either by allowing formation of ROIs (Haddad and Land, 2000) or by lowering the cells' defence against ROIs (Coppola and Ghibelli, 2000).

GSH depletion and efflux occur at a very early stage of apoptosis, concomitant with upregulation of Bax, whose transcription is mediated by p53 (Haddad and Land, 2000). The proapoptotic effects of p53, which is itself a redox-regulated protein

(Hainaut and Milner, 1993), are associated with transcription of genes particularly involved in modulating the response of the cell to oxidative stress. Therefore, alteration in redox equilibrium may have pleiotropic effects on susceptibility to DNA damage, gene transcription and nuclear signal transduction in response to an apoptotic stimulus (Haddad and Land, 2000). Additional proteins, such as caspases, are regulated by redox proteins like thioredoxin and GSH (Baker *et al.*, 2000).

Mitochondrial function is particularly sensitive to oxidative stress, in association with mixed disulfide formation on mitochondrial proteins. Increased membrane permeability and loss of ψ_m, common apoptotic events, have been coupled to alterations of protein redox balance (Cotgreave and Gerdes, 1998), implicating the involvement of GSH. In addition, redox alterations are involved in both models of cytochrome c export from mitochondria, by facilitating PT pore opening on the one hand, or by promoting disulfide bond formation, leading to Bax homodimerisation, on the other. The release of cytochrome c from mitochondria is a cellular response to GSH depletion, independent of the destiny of the cells, i.e., apoptosis or survival. The mere translocation of cytochrome c into the cytosol may not be a terminal event leading cells to apoptosis, as previously indicated, but rather may be the consequence of a redox disequilibrium which, under certain circumstances (e.g., binding of cytochrome c to Apaf-1 and caspase-9), may lead to caspase activation and apoptosis (Coppola and Ghibelli, 2000).

Several events/components of the apoptotic pathway are thus redox-modulated: initiation of apoptosis via p53 and Bax, cytochrome c release, and the activation of key proteases, e.g., caspases. In addition, the redox status of a cell will strongly influence the function of mitochondria, which is central to damage-induced apoptosis, as well as the "powerhouse" of the cell. Therefore, regulation of redox state is an important cellular function, and its dysregulation can have dire consequences in organisms, as is seen in cancer cells, which, as previously mentioned, are reported to have a non-linear reaction to redox stress (Allen, 1991).

5.5 Normal vs cancer cells

Cancer cells have an altered redox-state (Chiao *et al.*, 1995) and thus, dysregulated apoptotic pathways. The increased amounts of oxidative stress required to induce apoptosis in the MCF10AneoT cells relative to the MCF10A cells may be due to several factors, or perhaps a combination of these factors.

Cell cycle arrest and induction of apoptosis may be diminished in the MCF10AneoT cell line compared to the normal MCF10A cells, as a proportion of the p53 proteins in the MCF10AneoT cells is conformationally altered (Shekhar *et al.*, 1997), and therefore, the induction of p53 in response to oxidative stress may be altered.

GSH levels are also increased in some tumour cells (Mitchell and Russo, 1987). Such alterations in GSH should confer greater anti-oxidant resistance to these cells, although cancer cells are also reported to have a non-linear response to oxidative stress (Allen, 1991). In addition, since GSH can control the closing of the mitochondrial PT pore, by reduction of the disulfide bond in the ANT component (Crompton, 1999), higher GSH levels would delay the release of cytochrome c. In the current study a higher amount of H_2O_2 (i.e., oxidative stress) was required for cytochrome c release from the transformed, pre-malignant MCF10AneoT cells compared to the normal MCF10A cells. This may be explained by an inducible GSH response, or the non-linear response of cancer cells to oxidative stress. Cells in which a reduced intracellular environment is maintained would be anticipated to be able to activate cysteine proteases, like caspases, and be able to partake in apoptosis (Boggs *et al.*, 1998). However, as previously reported, higher GSH levels lead to increases in resistance to apoptosis (Cotgreave and Gerdes, 1998). Most such studies increased GSH (by extracellular addition) beyond basal levels, however, thereby increasing the anti-oxidants. This procedure may impede initial apoptosis signalling especially with respect to oxidation-sensitive pathways (Boggs *et al.*, 1998). In the system investigated, however, although caspase activity was much higher in the MCF10AneoT cells than in the normal cells and hence, more rapid apoptosis was anticipated, the results correlated with the literature which states that increased GSH levels lead to apoptosis-resistance, as the MCF10AneoT cells were more resistant to oxidative stress and the effects of high caspase activity than the normal cells. This supports the hypothesis of a caspase-independent mechanism of cell death in these cells as proposed in the model (Fig. 5.1), because morphological features of apoptosis were apparent much earlier than caspase activity. The reason that caspase activity is higher in the MCF10AneoT cells may be that these cells are still able to cope with the oxidative stress, due to the high levels of GSH which detoxify H_2O_2, thus allowing caspases to be activated, while the insult to the normal cells is overwhelming and caspase activation is inhibited, and they become necrotic.

It seems that the *ras* mutation in cancer cells may be a source of resistance to oxidative stress, as Ras signalling may have led to the increased GSH levels proposed and the Ras pathway to apoptosis seems to be altered when just one additional mutations is present. This may even affect the p53 activity. Although p53 in the MCF10AneoT cells is not mutated, conformational alteration does prevent its normal functioning. This too may be a result of the high GSH levels causing alteration of the p53 conformation.

Altered sphingolipid composition, both increases and decreases, have also been reported in cancer cells. Changes in the expression/function of enzymes which synthesise, utilise, degrade or modify ceramide could potentially impact on therapeutic responses through the alteration of total or relative levels of ceramide and hence, ceramide signalling which leads to apoptosis (Fig. 1.1). Altered sphingolipid metabolism, therefore, could lead to reduced sensitivity to anti-cancer therapies (Modrak *et al.*, 2000). This may also explain why the MCF10AneoT cells require higher levels of oxidative stress to release cytochrome c.

There may also be higher levels of Bcl-2 in the MCF10AneoT cells. Bcl-2 exerts its anti-apoptotic effect by acting on different steps of apoptotic signalling, e.g., radical scavenging, regulation of intracellular Ca^{2+} fluxes, inhibition of cytochrome c release, and inhibition of caspase-9 relocalisation, i.e., it affects the mitochondrial pathway to apoptosis (Coppola and Ghibelli, 2000). Cancer cells also have higher membrane potentials than their normal counterparts (Chen and Rivers, 1990). Therefore, it is likely that the cancer cells will be able to maintain ATP levels required for the apoptotic process, while the normal cells will become depleted of ATP and switch to necrotic cell death instead.

The question we are left with, then, is which are the best methods for detecting apoptosis.

5.6 Which are the best methods for detecting apoptosis?

Cytochrome c has recently been shown to be released from mitochondria simply by addition of redox active stimuli to cells (Coppola and Ghibelli, 2000). Therefore, for the system investigated, although cytochrome c release was observed earliest, i.e., by 30 min, it may not necessarily reflect induction of apoptosis, as cytochrome c may not have interacted with Apaf-1 and caspase-9 to allow downstream events (caspase activation and execution) to continue. In addition,

cytochrome c release may be reversible, and may not always occur, making detection of cytochrome c release an unreliable marker of the apoptotic process. Cytochrome c conformational changes (as evidenced by the two additional forms) may not be used independently as an indicator of cell death, as such changes may simply be a response to oxidative stimuli, and may not lead to apoptotic death.

Caspase activity also cannot be used as a marker for apoptosis in a system such as described, as caspase-independent mechanisms of cell death may occur. It seems that in such a system as was used, a combination of morphological and biochemical assays must be conducted in tandem, as no method seems to be reliable if used individually. Morphological examination by light microscopy and DNA laddering would be the best methods to simply detect apoptotic death, as these were considerably quicker than the time-consuming observation of cellular ultrastructure by electron microscopy, which also may be subjective. However, if a complete model of the sequence of events leading to progression of apoptosis is required, to explore possible differences between normal and cancer cells for therapy, additional tests, such as those for caspase activity and cytochrome c release, should be done. Results from tests of this type may yield additional valuable information and provoke thoughts on the order of apoptotic events (as indicated by the assay of certain "executioner" proteins and enzymes and downstream effects) and of further differences in the normal and cancer cells, possibly revealing potential targets for therapy or exploitable physiological differences, such as GSH and ceramide levels.

If there was a limited number of samples, the use of annexin v, to detect phosphatidylserine (PS) exposure on the cytoplasmic face of the outer leaflet of the plasma membrane might be useful. This would be a much quicker and easier method than examination of morphology and DNA degradation. However, annexin v should be used in conjunction with propidium iodide, to distinguish between live and dead cells as PS exposure might also occur in necrotic cells.

Though the MCF10A cell line is reported to have a functional p53 protein and, hence, be competent to undergo apoptosis, there is always the possibility that, under the redox stimulus used, both cell lines may be blocked or delayed from proceeding to apoptosis due to some peculiarity of the p53 protein, and hence, we did not see the advanced stages of apoptosis, i.e., cellular blebbing and release of membrane-bound apoptotic bodies.

5.7 Future work

In future experiments, it would be very interesting to extend assay times to see if the cells progress to "true" apoptosis (i.e., the formation of apoptotic bodies), and whether such characteristics would be exhibited if the H_2O_2 was replaced after 24 h, as cells may have already detoxified the previously added amount. Also, determination of the total anti-oxidative capacity and the redox potential of the normal cells compared to the cancerous ones, as well as differences in the levels of GSH and ceramide, both before and during the various treatment concentrations and times, to ascertain if these may be potential therapeutic targets, may yield interesting results. Assays for proteinases other than caspases, such as matrix metalloproteinases and cathepsins, which are both upregulated in apoptosis (Sympson *et al.*, 1994; Nitatori *et al.*, 1995) might give information about cleavage by non-caspase proteases, which has previously barely been addressed. The nature of the 10 and 11 kDa bands, obtained on the western blots for cytochrome c, should also be determined, as they may represent just an oxidatively modified version of the protein or they may be important to downstream apoptotic events. Cytochrome c analysis should also be conducted on 500- and 1000 μM-treated cells, to ascertain whether the lower M_r bands are also obtained in necrotic cell death.

REFERENCES

Adachi, S., Cross, A. R., Babior, B. M. and Gottlieb, R. A. (1997) Bcl-2 and the outer mitochondrial membrane in the inactivation of cytochrome c during Fas-mediated apoptosis, J. Biol. Chem. **272**, 21878-21882.

Allen, R. G. (1991) Oxygen-reactive species and anti-oxidant responses during development : the metabolic paradox of cellular differentiation, P.S.E.B.M., **196**, 117-129.

Allen, R. T., Cluck, M. W. and Agrawal, D. K. (1998) Mechanisms controlling cellular suicide : role of Bcl-2 and caspases, Cell Mol. Life Sci. **54**, 427-445.

Ankarcrona, M., Dypbukt, J. M., Bonfoco, E., Zhivotovsky, B., Orrenius, S., Lipton, S. A. and Nicotera, P. (1995) Glutamate-induced neuronal death : succession of necrosis or apoptosis depending on mitochondrial function, Neuron, **15**, 961-973.

Antonsson, B., Montessuit, S., Lauper, S., Eskes, R. and Martinou, J. C. (2000) Bax oligomerisation is required for channel-forming activity in liposomes and to trigger cytochrome c release from mitochondria, Biochem. J. **345**, 271-278.

Aragane, Y., Kulms, D., Metze, D., Wilkes, G., Poppelmann, B., Luger, T. A. and Schwarz, T. (1998) Ultraviolet light induces apoptosis via direct activation of CD95 independently of its ligand CD95L, J. Cell Biol. **140**, 171-182.

Arends, M. J., Moris, R. G. and Wyllie, A. H. (1990) Apoptosis : the role of the endonuclease, Am. J. Pathol. **136**, 593-608.

Ashwell, J. D., Berger, N. A., Cidlowski, J. A., Lane, D. P. and Korsmeyer, S. J. (1994) Coming to terms with death : apoptosis in cancer and immune development, Immunol. Today, **15**, 147-151.

Baker, A., Dos Santos, B. and Powis, G. (2000) Redox control of caspase-3 activity by thioredoxin and other reduced proteins, Biochem. Biophys. Res. Comm. **268**, 78-81.

Bannerman, D. D., Sathyamoorthy, M. and Goldblum, S. E. (1998) Bacterial lipopolysaccharide disrupts endothelial monolayer integrity and survival signalling events through caspase cleavage of adherens junction proteins, J. Biol. Chem. **273**, 35371-35380.

Barbacid, M. (1987) *ras* Genes, Annu. Rev. Biochem. **56**, 779-827.

Barbiero, G. Duranti, F., Bonelli, G., Amenta, J. S. and Baccino, F. M. (1995) Intracellular ionic variations in the apoptotic death of cells by inhibitor of cell cycle progression, Exp. Cell Res. **217**, 410-418.

Basanez, G., Nechushtan, A., Drozhinin, O., Chanturiya, A., Choe, E., Tutt, S., Wood, K. A., Hsu, Y., Zimmerberg, J. and Youle, R. J. (1999) Bax, but not Bcl-X_L, decreases the lifetime of planar phospholipid bilayer membranes at subnanomolar concentrations, Proc. Natl. Acad. Sci. USA, **96**, 5492-5497.

Basolo, F., Elliott, J., Tait, L., Chen, X. Q., Maloney, T., Russo, I. H., Pauley, R., Momiki, S., Caamano, J., Klein-Szanto, A. J. P., Koszalka, M. and Russo, J. (1991) Transformation of human breast epithelial cells by c-Ha-*ras* oncogene, Mol. Carcinogen. **4**, 25-35.

Bates, S. and Vousden, K. H. (1999) Mechanisms of p53-mediated apoptosis, Cell Mol. Life Sci. **55**, 28-37.

Beere, H. M. and Hickman, J. A. (1993) Differentiation : a suitable strategy for cancer chemotherapy?, Anti-cancer drug Des. **8**, 299-322.

Bissonnette, N., Wasylyk, B. and Hunting, D. J. (1997) The apoptotic and transcriptional transactivation activities of p53 can be dissociated, Biochem. Cell Biol. **75**, 351.

Blum, H., Beier, H. and Gross, H. G. (1987) Improved silver staining of plant proteins, RNA and DNA in polyacrylamide gels, Electrophoresis, **8**, 93-99.

Boggs, S. E., McCormick, T. S. and Lapetina, E. G. (1998) Glutathione levels determine apoptosis in macrophages, Biochem. Biophys. Res. Comm. **247**, 229-233.

Bollag, G., Adler, F., elMasry, N., McCabe, P. C., Conner, E., Thompson, P., McCormick, F. and Shannon, K. (1996) Biochemical characterisation of a novel *KRAS* insertion mutation from a human leukemia, J. Biol. Chem. **271**, 32491-32494.

Borner, C. (1996) Diminished cell proliferation associated with the death-protective activity of bcl-2, J. Biol. Chem. **271**, 12695-12698.

Borner, C., Martinou, I., Mattmann, C., Irmler, M., Schaerer, E., Martinou, J. C. and Tschopp, J. (1994) The protein Bcl-2α does not require membrane attachment, but two conserved domains to suppress apoptosis, J. Cell Biol. **126**, 1059-1068.

Bortner, C. D., Oldenburg, N. B. E. and Cidlowski, J. A. (1995) The role of DNA fragmentation in apoptosis, Trends in Cell Biol. **5**, 21-26.

Bossy-Wetzel, E., Newmeyer, D. D. and Green, D. R. (1998) Mitochondrial cytochrome c release in apoptosis occurs upstream of DEVD-specific caspase activation and independently of mitochondrial transmembrane potential, EMBO J. **17**, 37-49.

Boudreau, N., Sympson, C. J., Werb, Z. and Bissell, M. J. (1995) Suppression if ICE and apoptosis in mammary epithelial cells by extracellular matrix, Science, **267**, 891-893.

Bradford, M. M. (1976) A rapid and sensitive method for the quantitation of microgram quantities of protein utilising the principle of protein-dye binding, Anal. Biochem. **72**, 248-254.

Brancolini, C., Lazarevic, D., Rodrigquez, J. and Schneider, C. (1997) Dismantling cell-cell contacts during apoptosis is coupled to a caspase-dependent proteolytic cleavage of β-catenin, J. Cell Biol. **139**, 759-771.

Brown, G. I. (1974) "Introduction to inorganic chemistry", Longman Group Limited, London, pp 250-261.

Buttke, T. M. and Sandstrom, P. A. (1994) Oxidative stress as a mediator of apoptosis, Immunol. Today, **15**, 7-10.

Buxser, S. E., Sawada, G. and Raub, T. J. (1999) Analytical and numerical techniques for evaluation of free radical damage in cultured cells using image cytometry and fluorescent indicators, Methods Enzymol. **300**, 256-274.

Cejna, M., Fritsch, G., Printz, D., Schulte-Hermann, R. and Bursch, W. (1994) Kinetics of apoptosis and secondary necrosis in cultured rat thymocytes and S.49 mouse lymphoma and CEM human leukemia cells, Biochem. Cell Biol. **72**, 677-685.

Chen, Q., Benson, R. S. P., Whetton, A. D., Brant, S. R., Onowitz, M., Montrose, M.H., Dive, C. and Watson, A. M. J. (1997) Role of acid/base homeostasis in the suppression of apoptosis in haemopoietic cells by v-Abl protein tyrosine kinase, J. Cell Sci. **110**, 379-387.

Chen, C. Y. and Faller, D. V. (1995) Direction of $p21^{ras}$-generated signals towards cell growth or apoptosis is determined by protein kinase C and Bcl-2, Oncogene, **11**, 1487-1498.

Chen, L. B. and Rivers, E. N. (1990) Mitochondria in cancer cells In "Genes and Cancer" (Ed. D. Carney and K. Sikora), John Wiley and Sons, Chichester, England, pp 127-135.

Chiao, C., Carothers, A. M., Grunberger, D., Solomon, G., Preston, G. A. and Barrett, J. C. (1995) Apoptosis and altered redox state induced by caffeic phenethyl ester (CAPE) in transformed rat fibroblasts, Can. Res. **55**, 3576-3583.

Chinnaiyan, A. M. and Dixit, V. M. (1997) Portrait of an executioner : the molecular mechanism of FAS/APO-1-induced apoptosis, Semin Immunol. **9**, 69-76.

Chittenden, T., Harrington, E. A., O' Connor, R., Flemington, C., Lutz, R. J., Evan, G. I. and Guild B. C. (1995) Induction of apoptosis by the Bcl-2 homologue Bak, Nature, **372**, 733-736.

Chou, J. J., Li, H., Salvesen, G. S., Yuan, J. and Wagner, G. (1999) Solution structure of BID, an intracellular amplifier of apoptotic signalling, Cell, **96**, 615-624.

Clark, B. R. and Engvall, E. (1980) Enzyme-linked immunosorbent assay (ELISA) : theoretical and practical aspects In "Enzyme immunoassay" (Ed. E. T. Maggio), CRC Press, Florida, pp 167-179.

Clark, G. J., Kinch, M. S., Gilmer, T. M., Burridge, K. and Der, C. J. (1996) Overexpression of the Ras-related TC21/R-Ras2 protein may contribute to the development of human breast cancers, Oncogene, **12**, 169-176.

Cohen, G. M. and d'Arcy Doherty, M. (1987) Free radical mediated cell toxicity by redox cycling chemicals, Br. J. Cancer, **55**, 46-52.

Coopersmith, C. M., Chandrasekaran, C., McNevin, M. S. and Gordon, J. I. (1997) Bi-transgenic mice reveal that K-rasVal^{12} augments a p53-independent apoptosis when small intestinal villus enterocytes reenter the cell cycle, J. Cell Biol. **138**, 167-179.

Compton, S. J. and Jones, C. G. (1985) Mechanism of dye response and interference in the Bradford protein assay, Anal. Biochem. **151**, 369-374.

Coppola, S. and Ghibelli, L. (2000) GSH extrusion and the mitochondrial pathway of apoptotic signalling, Biochem. Soc. Trans. **28**, 56-61.

Cotgreave, I. A. and Gerdes, R. G. (1998) Recent trends in glutathione biochemistry, Biochem. Biophys. Res. Comm. **242**, 1-9.

Cotter, T. G., Lennon, S. V., Glynn, J. M. and Green, D. R. (1992) cited in **Vanags, D. M., Porn-Ares, M. A., Coppola, S., Burgess, D. H. and Orrenius, S.** (1996) Protease involvement in fodrin cleavage and phophatidylserine exposure in apoptosis, J. Biol. Chem. **271**, 31075-31085.

Crompton, M. (1999) The mitochondrial permeability transition pore and its role in cell death, Biochem. J. **341**, 233-249.

Cui, S., Reichner, J. S., Mateo, R. B. and Albina, J. E. (1994) Activated murine macrophages induce apoptosis in tumour cells through nitric oxide-dependent or – independent mechanisms, Cancer Res. **54**, 2462-2467.

Dallaporta, B., Marchetti, P., de Pablo, M. A., Maisse, Duc, H. T., Metivier, D., Zamzami, N., Geuskens, M. and Kroemer, G. (1999) Plasma membrane potential in thymocyte apoptosis, J. Immunol. **162**, 6534-6542.

Denis, F., Rheaume, E., Aouad, S. M., Alam, A., Sekaly, R. P. and Cohen, L. Y. (1998) The role of caspases in T cell development and the control of immune responses, Cell Mol. Life Sci. **54**, 1005-1019.

Desagher, S., Osen-Sand, A., Nichols, A., Eskes, R., Montessuit, S., Lauper, S., Maundrell, K., Antonsson, B. and Martinou, J. C. (1999) Bid-induced conformational change of Bax is responsible for mitochondrial cytochrome c release during apoptosis, J. Cell Biol. **144**, 891-901.

Deshmukh, M., Kuida, K. and Johnson, E. M. (2000) Caspase inhibition extends the commitment to neuronal death beyond cytochrome c release to the point of mitochondrial depolarisation, J. Cell Biol. **150**, 131-143.

Diaz, G., Setzu, M. D., Zucca, A., Isola, R., Diana, A., Murru, R., Sogos, V., Gremo, F. (1999) Subcellular heterogeneity of mitochondrial membrane potential : relationship with organelle distribution and intercellular contacts in normal, hypoxic and apoptotic cells J. Cell Sci. **112**, 1077-1084.

Dihanich, M. (1990) Pore-forming proteins of biological membranes, Experientia, **46**, 131-145.

Dillard, C. J. and Tappel, A. L. (1984) Fluorescent damage products of lipid peroxidation, Methods Enzymol. **105**, 337-340.

Douglas, A. M., Georgalis, A. M., Benton, L. R., Canavan, K. L. and Atchison, B. A. (1992) Purification of human leucocyte DNA : proteinase K is not necessary, Anal. Biochem. **201**, 362-365.

Drygas, M. E., Lambowitz, A. M. and Nargang, F. E. (1989) Cloning and analysis of the *Neurospora crassa* gene for cytochrome c haeme lyase, J. Biol. Chem. **264**, 17897-17906.

Duband-Goulet, I., Courvalin, J. C. and Buendia, B. (1998) LBR, a chromatin and lamin binding protein from the inner nuclear membrane, is proteolysed at late stages of apoptosis, J. Cell Sci. **111**, 1441-1451.

Dypbukt, J. M., Ankarcrona, M., Burkitt, M., Sjoholm, A., Strom, K., Orrenius, S. and Nicotera, P. (1994) Different pro-oxidant levels stimulate growth, trigger apoptosis, or produce necrosis of insulin-secreting RINm5F cells, J. Biol. Chem. **269**, 30553-30560.

Eisel, D., Fertig, G., Fischer, B., Manzow, S. and Schmelig, K. (1998) "Apoptosis and cell proliferation" (2nd ed.), Boehringer Mannheim, Germany, p31.

Enari, M., Sakahira, H., Yokoyama, H., Okawa, K., Iwamatsu, A. and Nagata, S. (1998) A caspase-activated DNase that degrades DNA during apoptosis, and its inhibitor ICAD, Nature, **391**, 43-50.

Eskes, R., Antonsson, B., Osen-Sand, A., Montessuit, S., Richter, C., Sadoul, R., Mazzei, G., Nichols, A. and Martinou, J. C. (1998) Bax-induced cytochrome c release from mitochondria is independent of the permeability transition pore but highly dependent on Mg^{2+} ions, J. Cell Biol. **143**, 217-224.

Evans, C. W. (1991) "The Metastatic Cell : Behaviour and Biochemistry", Chapman and Hall, London, p38.

Evan, G. I., Brown, L., Whyte, M. and Harrington, E. (1995) Apoptosis and the cell cycle, Curr. Opin. Cell Biol. 7, 825-834.

Evans, E. K., Kuwana, T., Strum, S. L., Smith, J. J., Newmeyer, D. D. and Kornbluth, S. (1997) Reaper-induced apoptosis in a vertebrate system, EMBO J. **16**, 7372-7381.

Fadok, V. A., McDonald, P. P., Bratton, D. L. and Henson, P. M. (1998) Regulation of macrophage cytokine production by phagocytosis of apoptotic and post-apoptotic cells, Biochem. Soc. Trans. **26**, 653-656.

Farber, J. L., Kyle, M. E. and Coleman, J. B. (1990) Biology of disease : mechanisms of cell injury by activated oxygen species, Lab. Invest. **62**, 670-679.

Farrelly, N., Lee, Y. J., Oliver, J., Dive, C. and Streuli, C. H. (1999) Extracellular matrix regulates apoptosis in mammary epithelium through a control on insulin signalling, J. Cell Biol. **144**, 1337-1347.

Ferlini, C., Di Cesare, S., Rainaldi, G., Malorni, W., Samoggia, P., Biselli, R. and Fattorossi, A. (1996) Flow cytometric analysis of early phases of apoptosis by cellular and nuclear techniques, Cytometry, **24**, 106-115.

Fesus, L. (1993) Biochemical events in naturally occurring forms of cell death, FEBS Lett. **328**, 1-5.

Finucane, D. M., Bossy-Wetzel, E., Waterhouse, N. J., Cotter, T. G. and Green, D. R. (1999) Bax-induced caspase activation and apoptosis via cytochrome c release from mitochondria is inhibitable by Bcl-X_L, J. Biol. Chem. **274**, 2225-2233.

Fisher, D. E. (1994) Apoptosis in cancer therapy : crossing the threshold, Cell, **78**, 539-542.

Foote, C. S., Shook, F. C. and Abakerli, R. B. (1984) Characterisation of singlet oxygen, Methods Enzymol. **105**, 36-56.

Fraser, A. and Evan, G. (1996) A licence to kill, Cell, **85**, 781-784.

Frisch, S., Vuori, K., Ruoslahti, E. and Chan-Hui, P. Y. (1996) Control of adhesion-dependent cell survival by focal adhesion kinase, J. Cell Biol. **134**, 793-799.

Froelich, C. J., Orth, K., Turbov, J., Seth, P., Gottlieb, R., Babior, B., Shah, G. M., Bleackley, R. C., Dixit, V. M. and Hanna, W. (1996) New paradigm for lymphocyte granule-mediated cytotoxicity, J. Biol. Chem. **271**, 29073-29079.

Froesch, B. A., Aime-Sempe, C., Leber, B., Andrews, D. and Reed, J. C. (1999) Inhibition of p53 transcriptional activity by Bcl-2 requires its membrane-anchoring domain, J. Biol. Chem. **274**, 6469-6475.

Garland, J. M. and Halestrap, A. (1997) Energy metabolism during apoptosis, J. Biol. Chem. **272**, 4680-4688.

Gershoni, J. M. and Palade, G. E. (1982) Electrophoretic transfer of proteins from sodium dodecyl sulfate polyacrylamide gels to a positively charged membrane filter, Anal. Biochem. **131**, 1-15.

Ghafourifar, P., Klein, S. D., Schuch, O., Schenk, U., Pruschy, M., Rocha, S. and Richter, C. (1999) Ceramide induces cytochrome c release from isolated mitochondria, J. Biol. Chem. **274**, 6080-6084.

Ghibelli, L., Meraseca, V., Coppola, S. and Gualandi, G. (1995) Protease inhibitors block apoptosis at intermediate stages : a compared analysis of DNA fragmentation and apoptotic nuclear morphology, FEBS Lett. **377**, 9-14.

Gidrol, X., Sabelli, P. A., Fern, Y. S. and Kush, A. K. (1996) Annexin-like protein from *Arabidopsis thaliana* that rescues *ΔoxyR* mutant of *Escherichia coli* from H_2O_2 stress, Proc. Natl. Acad. Sci. USA, **93**, 11268-11273.

Gilbert, H. F. (1995) Thiol / disulfide exchange equilibria and disulfide bond stability, Methods Enzymol. **251**, 8-28.

Gilmore, A. P., Metcalfe, A. D., Romer, L. H. and Streuli, C. H. (2000) Integrin-mediated survival signals regulate the apoptotic function of Bax through its conformation and subcellular localisation, J. Cell Biol. **149**, 431-445.

Goldkorn, T., Balaban, N., Chea, V., Matsukuma, K., Gilchrist, D., Wang, H. and Chan, C. (1998) H_2O_2 acts on cellular membranes to generate ceramide signalling and initiate apoptosis in tracheobronchial epithelial cells, J. Cell Sci. **111**, 3209-3220.

Goping, G., Wood, K. A., Sei, Y. and Pollard, H. B. (1999) Detection of fragmented DNA in apoptotic cells embedded in LR White : a combined histochemical (LM) and ultrastructural (EM) study, J. Histochem. Cytochem. **47**, 561-568.

Gottlieb, R. A., Nordberg, J., Skowronski, E. and Babior, B. M. (1996) Apoptosis induced in Jurkat cells by several agents is preceded by intracellular acidification, Proc. Natl. Acad. Sci. USA, **93**, 654-658.

Graeber, T. G., Osmanian, C., Jacks, T., Housman, D. E., Koch, C. J., Lowe, S. W. and Giaccia, A. J. (1996) Hypoxia-mediated selection of cells with diminished apoptotic potential in solid tumours, Nature, **379**, 88-91.

Green, D. R. (1998) Apoptotic pathways : the roads to ruin, Cell, **94**, 695-698.

Green, D. R. and Reed, J. C. (1998) Mitochondria and apoptosis, Science, **281**, 1309-1312.

Gregory, C. D., Devitt, A. and Moffatt, O. (1998) Roles of ICAM-3 and CD14 in the recognition and phagocytosis of apoptotic cells by macrophages, Biochem Soc. Trans. **26**, 644-649.

Ha, H., Hajek, P., Bedwell, D. M. and Burrows, P. D. (1993) A mitochondrial porin cDNA predicts the existence of multiple human porins, J. Biol. Chem. **268**, 12143-12149.

Haber, D. A. (1999) Using genes to cure cancer, Cell, **98**, 728-730.

Haddad, J. J. E. and Land, S. C. (2000) The differential expression of apoptosis factors in the alveolar epithelium is redox sensitive and requires NF-κB (RelA)-selective targeting, Biochem. Biophys. Res. Comm. **271**, 257-267.

Hainaut, P. and Milner, J. (1993) Redox modulation of p53 conformation and sequence-specific DNA binding *in vitro*, Cancer Res. **53**, 4469-4473.

Hakem, R., Hakem, A., Duncan, G. S., Henderson, J. T., Woo, M., Soengas, M. S., Elia, A., de la Poma, J. L., Kagi, D., Khoo, W., Potter, J., Yoshida, R., Kaufman, F. A., Lowe, S. W., Penninger, J. M. and Mak, T. W. (1998) Differential requirement for caspase-9 in apoptotic pathways in vivo, Cell, **94**, 339-352.

Halliwell, B. and Gutteridge, J. M. C. (1990) Role of free radicals and catalytic metal ions in human disease : an overview, Methods Enzymol. **186**, 1-85.

Harlow, E. and Lane, D. (1988) "Antibodies : a laboratory manual", Cold Spring Harbour, New York, pp 1-116.

Harris, A. S. and Morrow, J. S. (1990) Calmodulin and calcium-dependent protease 1 coordinately regulate the interaction of fodrin with actin, Proc. Natl. Acad. Sci. USA, **87**, 3009-3013.

Hartl, F. U., Pfanner, N., Nicholson, D. W. and Neupert, W. (1989) Mitochondrial protein import, Biochimica et Biophysica Acta, **988**, 1-45.

Harvey, K. J., Lukovic, D. and Ucker, D. S. (2000) Caspase-dependent Cdk activity is a requisite effector of apoptotic death events, J. Cell Biol. **148**, 59-72.

Haycock, D. A. (1999) Integration of damage signals before commitment to death, J. Cell Biol. **144**, 803.

Heald, R., McLoughlin, M. and McKeon, F. (1993) Human Wee1 maintains mitotic timing by protecting the nucleus from cytoplasmically activated Cdc2 kinase, Cell, **74**, 463-474.

Henkart, P. A. and Grinstein, S. (1996) Apoptosis : mitochondria resurrected?, J. Exp. Med. **183**, 1293-1295.

Hettmann, T., Schmidt, C. L., Anemuller, S., Zahringer., U., Moll, H., Petersen, A. and Schaefer, G. (1998) Cytochrome $b_{558/566}$ from the Archaeon *Sulfolobus acidocaldarius*, J. Biol. Chem. **273**, 12032-12040.

Hickman, J. A. (1996) Apoptosis and chemotherapy resistance, Eur. J. Cancer A. **32**, 921-926.

Hockenbery, D. M., Zutter, M., Hickey, W., Nahm, M. and Korsmeyer, S. J. (1991) Bcl-2 protein is topographically restricted in tissues characterised by apoptotic cell death, Proc. Natl. Acad. Sci. USA, **88**, 6961-6965.

Hoyt, K. R., Gallagher, A. J., Hastings, T. G. and Reynolds, I. J. (1997) Characterisation of hydrogen peroxide toxicity in cultured rat forebrain neurons, Neurochem. Res. **22**, 333-340.

Hozak, P., Sasseville, M. J., Raymond, Y. and Cook, P. R. (1995) Lamin proteins form an internal nucleoskeleton as well as a peripheral lamina in human cells, J. Cell Sci. **108**, 635-644.

Hunter, T. (1997) Oncoprotein networks, Cell, **88**, 333-346.

Hwang, C., Lodish, H. F. and Sinskey, A. J. (1995) Measurement of glutathione redox state in cytosol and secretory pathway of cultured cells, Methods Enzymol. **251**, 212-221.

Huot, J., Houle, F., Rousseau, S., Deschenes, R. G., Shah, G. M. and Landry, L. (1998) SAPK2/p38-dependent F-actin reorganisation regulates early membrane blebbing during stress-induced apoptosis, J. Biol. Chem. **143**, 1361-1373.

Hupp, T. R. (1999) Regulation of p53 protein function through alterations in protein-folding pathways, Cell Mol. Life Sci., **55**, 88-95.

Ilic, D., Almeida, A. C., Schlaepfer, D. D., Dazin, P., Aizawa, S. and Damsky, C. H. (1998) Extracellular matrix survival signals transduced by focal adhesion kinase suppress p53-mediated apoptosis, J. Cell Biol. **143**, 547-560.

Jia, L., Allen, P. D., Macey, M. G., Grahn, M. F., Newland, A. C. and Kelsey, S. M. (1997) Mitochondrial electron transport chain activity, but not ATP synthesis is required for drug-induced apoptosis in human leukemic cells : a possible novel mechanism of regulating drug resistance, Brit. J. Haematol. **98**, 686-698.

Jemmerson, R., Liu, J., Hausauer, D., Lam, K. P., Mondino, A and Nelson, R. D. (1999) A conformational change in cytochrome c of apoptotic and necrotic cells is detected by monoclonal antibody binding and mimicked by association of the native antigen with synthetic phospholipid vesicles, Biochemistry, **38**, 3599-3609.

Johnson, V. L., Ko, S. C. W., Holmstrom, T. H., Eriksson, J. E. and Chow, S. C. (2000) Effector caspases are dispensible for the early nuclear morphological changes during chemical-induced apoptosis, J. Cell Sci. **113**, 2941-2953.

Jurgensmeier, J. M., Xie, Z., Deveraux, Q., Ellerby, L., Bredesen, D. and Reed, J. C. (1998) Bax directly induces release of cytochrome c from isolated mitochondria, Proc. Natl. Acad. Sci. USA, **95**, 4997-5002.

Kass, G. E. N., Eriksson, J. E., Weis, M., Orrenius, S. and Chow, S. C. (1996) Chromatin condensation during apoptosis requires ATP, Biochem. J. **318**, 749-752.

Kerr, J. F. R., Winterford, C. M. and Harmon, B. V. (1994) Apoptosis : its significance in cancer and cancer therapy, Cancer, **73**, 2013-2026.

Kinoshita, T., Yokota, T., Arai, K. and Miyajima, A. (1995) Regulation of Bcl-2 expression by oncogenic Ras protein in haematopoietic cells, Oncogene, **10**, 2207-2212.

Kinzler, K. W. and Vogelstein, B. (1996) Lessons from herediatry colorectal cancer, Cell, **87**, 159-170.

Kluck, R. M., Bossy-Wetzel, E., Green, D. R. and Mewmeyer, D. D. (1997) The release of cytochrome c from mitochondria : a primary site for Bcl-2 regulation of apoptosis, Science, **275**, 1132-1136.

Kluck, R. M., Degli Esposti, M., Perkins, G., Renken, C., Kuwana, T., Bossy-Wetzel, E., Goldberg, M., Allen, T., Barber, M. J., Green, D. R. and Newmeyer, D. D. (1999) The pro-apoptotic proteins, Bid and Bax, cause a limited permeabilisation of the mitochondrial outer membrane that is enhanced by cytosol, J. Cell Biol. **147**, 809-822.

Kneppler-Nicolai, B., Savill, J. and Brown, S. B. (1998) Constitutive apoptosis in human neutrophils requires synergy between calpains and the proteasome downstream of caspases, J. Biol. Chem. **273**, 30530-30536.

Kondo, T., Takeuchi, K., Doi, Y., Yonemura, S., Nagat, S. and Tsukita, S. (1997) ERM (ezrin / radixin / moesin)-based molecular mechanism of microvilla breakdown at an early stage of apoptosis, J. Cell Biol. **149**, 749-758.

Kothakota, S., Azuma, T., Reinhard, C., Klippel, A., Tang, J., Chu, K., McGarry, T. J., Kirschner, M. W., Koths, K., Kwiatkowski, D. J. and Williams, L. T. (1997) Caspase-3-generated fragment of gelsolin : effector of morphological change in apoptosis, Science, **278**, 294-298.

Krippner, A., Matsuno-Yagi, A., Gottlieb, R. A. and Babior, B. M. (1996) Loss of function of cytochrome c in Jurkat cells undergoing Fas-mediated apoptosis, J. Biol. Chem. **271**, 21629-21636.

Kroemer, G. C. (1997) The proto-oncogene Bcl-2 and its role in regulating apoptosis, Nat. Med. **3**, 614-620.

Kumar, S. and Colussi, P. A. (1999) Prodomains-adaptors-oligomerisation : the pursuit of caspase activation in apoptosis, TIBS, **24**, 1-4.

Laemmli, U. K., Kas, E., Polijak, E. and Adachi, Y. (1992) Scaffold-associated regions : *cis*-acting determinants of chromatin structural loops and functional domains, Curr. Opin. Genet. Dev. **2**, 275-285.

Lee, Y. J., Galoforo, S. S., Berns, C. M., Tong, W. P., Kim, H. R. C. and Corry, P. M. (1997) Glucose deprivation-induced cytotoxicity in drug resistant human breast carcinoma MCF-7/ADR cells : role of c-myc and Bcl-2 in apoptotic cell death, J. Cell Sci. **110**, 681-686.

Leist, M., Single, B., Castoldi, A. F., Kuhnle, S. and Nicotera, P. (1997) Intracellular adenosine triphosphate (ATP) concentration : a switch in the decision between apoptosis and necrosis, J. Exp. Med. **185**, 1481-1486.

Levine, A. J. (1997) p53, the cellular gatekeeper for growth and division, Cell, **88**, 323-331.

Li, H., Zhu, H., Xu, C. and Juan, J. (1998) Cleavage of BID by caspase-8 mediates the mitochondrial damage in the Fas pathway of apoptosis, Cell, **94**, 491-501.

Li, P., Nijhawan, D., Budihardjo, I., Srinivasula, S. M., Ahmad, M., Alnemri, E. S. and Wang, X. (1997) Cytochrome c and dATP-dependent formation of Apaf-1/caspase-9 complex initiates an apoptotic protease cascade, Cell, **91**, 479-489.

Lindsay, G. S. and Wallace, H. M. (1999) Changes in polyamine catabolism in HL-60 human promyelogenous leukemia cells in response to etoposide-induced apoptosis, Biochem. J. **337**, 83-87.

Liu, B., Andrieu-Abadie, N., Levade, T., Zhang, P., Obeid, L. M. and Hannun, Y. A. (1998) Glutathione regulation of neutral sphingomyelinase in tumour necrosis factor-α-induced cell death, J. Biol. Chem. **273**, 11313-11320.

Liu, X., Kim, C. N., Yang, J., Jemmerson, R. and Wang, X. (1996) Induction of apoptotic program in cell-free extracts : requirement for dATP and cytochrome c, Cell, **86**, 147-157.

Lodish, H., Baltimore, D., Berk, A., Zipursky, S. L., Matsudaira, P. and Darnell, J. (1995) "Molecular Cell Biology", Scientific American Books, New York, USA, pp 739-776; 810-829.

Lowe, S. W., Ruley, H. E., Jacks, T. and Housman, D. E. (1993) p53-dependent apoptosis modulates the cytotoxicity of anti-cancer agents, Cell, **74**, 957-967.

Luo, X., Budihardjo, I., Zou, H., Slaughter, C. and Wang, X. (1998) Bid, a Bcl-2-interacting protein, mediates cytochrome c release from mitochondria in response to activation of cell surface death receptors, Cell, **94**, 481-490.

Maly, K., Uberall, F., Loferer, H., Doppler, W., Oberhuber, H., Groner, B. and Grunicke, H. H. (1989) Ha-*ras* activates the Na^+/H^+ antiporter by a protein kinase c-independent mechanism, J. Biol. Chem. **264**, 11839-11842.

Mancini, M., Anderson, B. O., Caldwell, C., Sedghinasab, M., Paty, P. B. and Hockenbery, D. M. (1997) Mitochondrial proliferation and paradoxical membrane depolarisation during terminal differentiation and apoptosis in a human colon carcinoma cell line, J. Cell Biol. **138**, 449-469.

Mancini, M., Nicholson, D. W., Roy, S., Thornberry, N. A., Peterson, E. P., Casciola-Rosen, L. A. and Rosen, A. (1998) The caspase-3 precursor has a cytosolic and

mitochondrial distribution : implications for apoptotic signalling, J. Cell Biol. **140**, 1485-1495.

Marchetti, P., Susin, S. A., Decaudin, D., Gamen, S., Castedo, M., Hirsch, T., Zamzami, N., Naval, J., Senik, A. and Kroemer, G. (1996) Apoptosis-associated derangement of mitochondrial function in cells lacking mitochondrial DNA, Cancer Res. **56**, 2033-2038.

Martin, S. and Green, D. (1995) Protease activation during apoptosis : death by a thousand cuts?, Cell, **82**, 349-352.

Martin, S. J., Green, D. R. and Cotter, T. G. (1994) Dicing with death : dissecting the components of the apoptosis machinery, TIBS, **19**, 26-30.

Martin, S. J., O'Brien, G. A., Nishioka, W. K., McGahon, A. J., Mahboubi, A., Saido, T. C. and Green, D. R. (1995) Proteolysis of fodrin (non-erythroid spectrin) during apoptosis, J. Biol. Chem. **270**, 6425-6428.

Martinou, I., Dasagher, S., Eskes, R., Antonsson, B., Andre, E., Fakan, S. and Martinou, J. C. (1999) The release of cytochrome c from mitochondria during apoptosis of NGF-deprived sympathetic neurons is a reversible event, J. Cell Biol. **144**, 883-889.

Mathias, S., Pena, L. A. and Kolesnick, R. N. (1998) Signal transduction of stress via ceramide, Biochem. J. **335**, 465-480.

Mayer, R. J. and Walker, J. H. (1987) "Immunochemical methods in cell and molecular biology", Academic Press, London, pp 1-10.

McCarthy, N. J., Whyte, M. K. B., Gilbert, C. S. and Evan, G. I. (1997) Inhibition of Ced-3 / ICE-related proteases does not prevent cell death induced by oncogenes, DNA damage, or the Bcl-2 homologue Bak, J. Cell Biol. **136**, 215-227.

McKeon, F. (1991) Nuclear lamin proteins : domains required for nuclear targeting, assembly, and cell cycle-regulated dynamics, Curr. Opin. Cell Biol. **3**, 82-86.

Meier, P. and Evan, G. (1998) Dying like flies, Cell, **95**, 295-298.

Meinesz, R. E. (1996) A study of the role of redox potential in lysosomal function, MSc Thesis, University of Natal, Pietermaritzburg, 38.

Meister, A. (1983) Selective modification of glutathione metabolism, Science, **220**, 472-477.

Meister, A. (1994) Glutathione-ascorbic acid anti-oxidant system in animals, J. Biol. Chem. **269**, 9397-9400.

Meister, A. (1995) Glutathione metabolism, Methods Enzymol. **251**, 3-7.

Miller, T. M., Moulder, K. L., Knudson, C. M., Creedon, D. J., Deshmukh, M., Korsmeyer, S. J. and Johnson, E. M. (1997) Bax deletion further orders the cell death pathway in cerebellar granule cells and suggests a caspase-independent pathway to cell death, J. Cell Biol. **139**, 205-217.

Mills, J. C., Lee, V. M. Y. and Pittman, R. M. (1998a) Activation of a PP2A-like phosphatase and dephosphorylation of τ protein characterise onset of the execution phase of apoptosis, J. Cell Sci. **111**, 625-636.

Mills, J. C., Stone, N. L., Erhardt, J. and Pittman, R. N. (1998b) Apoptic membrane blebbing is regulated by myosin light chain phosphorylation, J. Cell Biol. **140**, 627-636.

Mills, J. C., Stone, N. L. and Pittman, R. N. (1999) Extranuclear apoptosis : the role of the cytoplasm in the execution phase, J. Cell Biol. **146**, 703-707.

Mitchell, J. B. and Russo, A. (1987) The role of glutathione in radiation and drug induced cytotoxocity, Br. J. Cancer, **55**, 96-104.

Miyashita, T. and Reed, J. C. (1995) Tumour suppressor p53 is a direct transcriptional activator of the human *bax* gene, Cell, **80**, 293-299.

Modrak, D. E., Lew, W., Goldenberg, D. M. and Blumenthal, R. (2000) Sphingomyelin potentiates chemotherapy of human cancer xenografts, Biochem. Biophys. Res. Comm. **268**, 603-606

Morel, Y. and Barouki, R. (1999) Repression of gene expression by oxidative stress, Biochem J. **342**, 481-496.

Muchmore, S. W., Sattler, M., Liang, H., Meadows, R. P., Harlan, J. P., Yoon, H. S., Nettesheim, D., Chang, B. S., Thompson, C. B., Wong, S. L., Ng, S. C. and Fesik, S. W. (1996) X-ray and NMR structure of human Bcl-X_L, an inhibitor of programmed cell death, Nature, **381**, 335-341.

Muller, J. M., Rupec, R. A. and Baeuerle, P. A. (1997) Study of gene regulation by NF-κB and AP-1 in response to reactive oxygen intermediates, Methods : a companion to Methods Enzymol. **11**, 301-312.

Murphy, J. N., Bredesen, D. E., Cortopassi, G., Wang, E. and Fiskum, G. (1996) Bcl-2 potentiates the maximal calcium uptake capacity of neural cell mitochondria, Proc. Natl. Acad. Sci. USA, **93**, 9893-9898.

Nagata, S. and Golstein, P. (1995) The fas death factor, Science, **267**, 1449-1456.

Negoescu, A., Guillermet, C. H., Lorimier, P. H., Robert, C., Lantuejoul, S., Brambilla, E. and Labat-Moleur, F. (1998) TUNEL apoptotic cell detection in archived paraffin-embedded tissues, Biochemica no. 3 (Roche Molecular Biochemicals), 36-41.

Newmeyer, D. D., Farschon, D. N. and Reed, J. C. (1994) Cell-free apoptosis in *Xenopus* egg extracts : inhibition by Bcl-2 and requiremnt for an organelle fraction rich in mitochondria, Cell, **79**, 353-364.

Nicholson, D. W. and Thornberry, N. A. (1997) Caspases : killer proteases, TIBS, **22**, 299-308.

Nicotera, P. and Leist, M. (1997) Energy supply and the shape of death in neurons and lymphoid cells, Cell Death Diff. **4**, 435-442.

Niemenen, A. L., Saylor, A. K., Tesfai, S. A., Herman, B. and Lemasters, J. J. (1995) Contribution of the mitochondrial permeability transition to lethal injury after exposure of hepatocytes to t-butylhydroperoxide, Biochem J. **307**, 99-106.

Nitatori, T., Sato, N., Waguri, S., Karasawa, Y., Araki, H., Shibanai, K., Kominami, E. and Uchiyama, Y. (1995) Delayed neuronal death in the CA1 pyramidal cell layer of the gerbil hoppocampus following transient ischaemia is apoptosis, J. Neurosci. **15**, 1001-1011.

Nouraini, S., Six, E., Matsuyama, S., Krajewski, S. and Reed, J. C. (2000) The putative pore-forming domain of Bax regulates mitochondrial localisation and interaction with Bcl-X_L, Mol. Cell Biol. **20**, 1604-1615.

Oltvai, Z. N. and Korsmeyer, S. J. (1994) Checkpoints of dueling dimers foil death wishes, Cell, **79**, 189-192.

Ozawa, K., Kuwubara, K., Tamatani, M., Takasuji, K., Tsukamoto, Y., Kaneda, S., Yanagi, H., Stern, D. M., Eguchi, Y., Tsujimoto, Y., Ogawa, S. and Tohyama, M. (1999) 150-kDa oxygen-regulated protein (ORP150) suppresses hypoxia-induced apoptotic cell death, J. Biol. Chem. **274**, 6397-6404.

Pacifici, R. E. and Davies, K. J. A. (1990) Protein degradation as an index of oxidative stress, Methods Enzymol. **186**, 485-502.

Petit, P. X., Lecoeur, H., Zorn, E., Dauguet, C., Mignotte, B. and Gougeon, M. L. (1995) Alterations of mitochondrial structure and function are early events of dexamethasone-induced thymocyte apoptosis, J. Cell Biol. **130**, 157-167.

Perez-Sala, D., Collado-Escobar, D. and Mollinedo, F. (1995) Intracellular alkalinisation suppresses lovastatin-induced apoptosis in HL-60 cell line through the inactivation of a pH dependent endonuclease, J. Biol. Chem. **270**, 6235-6242.

Piperakis, S. M., Visvardis, E. E. and Tassiou, A. M. (1999) Comet assay for nuclear DNA damage, Methods Enzymol. **300**, 184-194.

Platt, N., da Silva, R. P. and Gordon, S. (1998) Class A scavenger receptors and the phagocytosis of apoptotic cells, Biochem. Soc. Trans. **26**, 639-640.

Podak, E. R. (1999) How to induce involuntary suicide : the need for dipeptidyl peptidase I, Proc. Natl. Acad. Sci. USA, **96**, 8312-8314.

Polson, A., Coetzer, T., Kruger, J., von Maltzen, E. and van der Merwe, K. J. (1985) Improvement in the isolation of IgY from the yolks of eggs laid by immunised hens, Immunol. Invest. **14**, 323-327.

Popov, I. and Lewin, G. (1999) Anti-oxidative homeostasis : characterisation by means of chemiluminescent technique, Methods Enzymol. **300**, 437-456.

Popp, B., Court, D. A., Benz, R., Neupert, W. and Lill, R. (1996) The role of the N and C termini of recombinant *Neurospora* mitochondrial porin in channel formation and voltage-dependent gating, J. Biol. Chem. **271**, 13593-13599.

Porter, N. A. (1984) Chemistry of lipid peroxidation, Methods Enzymol. **105**, 273-282.

Raff, M. C. (1992) Social controls on cell survival and cell death, Nature, **356**, 397-400.

Rak, J., Mitsuhashi, Y., Erdos, V., Huang, S. N., Filmus, J. and Kerbel, R. S. (1995) Massive programmed cell death in intestinal epithelial cells induced by three-dimensional growth conditions : suppression by mutant c-H-*ras* oncogene expression, J. Cell Biol. **131**, 1587-1598.

Rao, L., Perez, D. and White, E. (1996) Lamin proteolysis facilitates nuclear events during apoptosis, J. Cell Biol. **135**, 1441-1455.

Rapaport, S. M., Schewe, T., Wiesner, R., Halangk, W., Ludwig, P., Janick-Hohne, M., Tannert, C., Hiebsch, C. and Klatt, D. (1979) The lipoxygenase of reticulocytes. Purification, characterisation, and biological dynamics of the lipoxygenase : its identity with the respiratory inhibitors of the reticulocyte, Eur. J. Biochem. **96**, 545-561.

Read, S.M. and Northcote, D. H. (1981) Minimisation of variation in the response to different proteins of the Coomassie Blue dye-binding assay for protein, Anal. Biochem. **116**, 53-64.

Reed, J. C. (1994) Bcl-2 and the regulation of programmed cell death, J. Cell Biol. **124**, 1-6.

Reed, J. C. (1997) Cytochrome c : can't live with it – can't live without it, Cell, **91**, 559-562.

Reszka, A., Bulinski, J., Drebs, E. G. and Fischer, E. H. (1997) Mitogen-activated protein kinase / extracellular signal-regulated kinase 2 regulates cytoskeletal organisation and chemotaxis via catalytic and microtubule-specific interactions, Mol. Biol. Cell, **8**, 1219-1232.

Rice, G. C., Hoy, C. and Schimke, R. T. (1986) Transient hypoxia enhances the frequency of dihydrofolate reductase gene amplification in chinese hamster ovary cells, Proc. Natl. Acad. Sci. USA, **83**, 5978-5982.

Rosse, T., Olivier, R., Monney, L., Rager, M., Conus, S., Fellay, I., Jansen, B. and Borner, C. (1998) Bcl-2 prolongs cell survival after Bax-induced release of cytochrome c, Nature, **391**, 496-499.

Ruoslahti, E. and Reed, J. C. (1994) Anchorage dependence, integrins, and apoptosis, Cell, 77, 477-478.

Rusnak, J. M., Calmels, T. P. G., Hoyt, D. G., Kondo, Y., Yalowich, J. C. and Lazo, J. S. (1996) Genesis of discrete higher order DNA fragments in apoptotic human prostatic carcinoma cells, Mol. Pharmacol. **49**, 244-252.

Russo, J., Tait, L. and Russo, I. H. (1991) Morphological expression of cell transformation induced by c-Ha-*ras* oncogene in human breast epithelial cells, J. Cell Science, **99**, 453-463.

Sager, R., Gadi, I. K., Stephens, L. and Grabowy, C. T. (1985) Gene amplification : an example of accelerated evolution in tumourigenic cells, Proc. Natl. Acad. Sci. USA, **82**, 7015-7019.

Salvesen, G. S. and Dixit, V. M. (1997) Caspases : intracellular signalling by proteolysis, Cell, **91**, 443-446.

Salvesen, G. S. and Dixit, V. M. (1999) Caspase activation : the induced-proximity model, Proc. Natl. Acad. Sci. USA, **96**, 10964-10967.

Samuel, S. K., Minish, T. M. and Davie, J. R. (1997) Altered nuclear matrix profiles in oncogene-transformed mouse fibroblasts exhibiting high metastatic potential, Cancer Res. **57**, 147-151.

Sato, N., Iwata, S., Nakamura, K., Hori, T., Mori, K. and Yodoi, J. (1995) Thiol-mediated redox regulation of apoptosis, J. Immunol., **154**, 3194-3203.

Schägger, H. and von Jagow, G. (1987) Tricine sodium dodecyl sulfate polyacrylamidegels for the separation of proteins in the range from 1 to 100 kDa, Anal. Biochem. **166**, 368-379.

Schmaltz, C., Hardenbergh, P. H., Wells, A. and Fisher, D. E. (1998) Regulation of proliferation-survival decisions during tumour cell hypoxia, Mol. Cell Biol. **18**, 2845-2854.

Schmitt, E., Sane, A. T., Steyaert, A., Cimoli, G. and Bertrand, R. (1997) The Bcl-X_L and Bax-α control points : modulation of apoptosis induced by cancer chemotherapy and relation to TPCK-sensitive protease and caspase activation, Biochem. Cell Biol. **75**, 301-314.

Schreck, R. and Baeuerle, P. A. (1994) Assessing oxygen radicals as mediators in activation of inducible eukaryotic transcription factor NF-κB, Methods Enzymol. **234**, 151-163.

Scott, P. A. E., Gleadle, J. M., Bicknell, R. and Harris, A. L. (1998) Role of the hypoxia sensing system, acidity and reproductive hormones in the variability of vascular endothelial growth factor induction in human breast carcinoma cell lines, Int. J. Cancer, **75**, 706-712.

Sgonc, R. and Wick, G. (1994) Methods for the detection of apoptosis, Int. Arch. Allergy Immunol. **105**, 327-332.

Shekhar, P. V. M., Welte, R., Christman, J. K., Wang, H. and Werdell, J. (1997) Altered p53 conformation : a novel mechanism of wild-type p53 functional inactivation in a model for early human breast cancer, Int. J. Onco. **11**, 1087-1094.

Shibata, M. A., Maroulakou, I. G., Jorcyk, C. L., Gold, L. G., Ward, J. M. and Green, J. E. (1996) p53-independent apoptosis during mammary tumour progression in C3(1)/SV40 large T antigen transgenic mice : suppression of apoptosis during the transition from preneoplasia to carcinoma, Cancer Res. **56**, 2998-3003.

Shim, H., Dolde, C., Lewis, B. C., Wu, C. S., Dang, G., Jungmann, R. A., Dalla-Favera, R. and Dang, C. V. (1997) c-myc transactivation of *LDH-A* : implications for tumour metabolism and growth, Proc. Natl. Acad. Sci. USA, **94**, 6658-6663.

Shimizu, Y., Narita, M. and Tsujimoto, Y. (1999) Bcl-2 family proteins regulate the release of apoptogenic cytochrome c by the mitochondrial channel VDAC, Nature, **399**, 483-487.

Siegel, R. M., Martin, D. A., Zheng, L., Ng, S. Y., Bertin, J., Cohen, J. and Lenardo, M. J. (1998) Death-effector filaments : novel cytoplasmic structures that recruit caspases and trigger apoptosis, J. Cell Biol. **141**, 1243-1253.

Simm, A., Bertsch, G., Frank, H., Zimmermann, U. and Hoppe, J. (1997) Cell death of AKR-2B fibroblasts after serum removal : a process between apoptosis and necrosis, J. Cell Sci. **110**, 819-827.

Slee, E. A., Harte, M. T., Kluck, R. M., Wolf, B. B., Casiano, C. C., Newmeyer, D. D., Wang, H. G., Reed, J. C., Nicholson, D. W., Alnemri, E. S., Green, D. R. and Martin, S. J. (1999) Ordering the cytochrome c-initiated caspase cascade, J. Cell Biol. **144**, 281-292.

Sloane, B. F., Sameni, M., Cao, L., Berquin, I., Rozhin, J., Ziegler, G., Moin, K. and Day, N. (1994) Alterations in processing and trafficking of cathepsin B during malignant progression In "Biological function of proteases and inhibitors" (N. Katanuma, K. Suzuki, J. Travis, H. Fritz, S. Karger and A. G. Basel, eds.), Japan Scientific Societies Press, Tokyo, Japan, 131-141.

Soule, H. D., Maloney, T. M., Wolman, S. R., Peterson, W. D., Brenz, R., McGrath, C. M., Russo, J., Pauley, R. J., Jones, R. F. and Brooks, S. C. (1990) Isolation and characterisation of a spontaneously immortalised human breast epithelial cell line, MCF10, Cancer Res, **50**, 6075-6086.

Soullam, B. and Worman, H. J. (1993) The amino-terminal domain of the lamin B receptor is a nuclear envelope targeting signal, J. Cell Biol. **120**, 1093-1100.

Srinivasula, S. M., Ahmad, M., Fernandes-Alnemri, T. and Alnemri, E. S. (1998), Mol. Cell, **1**, 949-957 cited in **Kumar, S. and Colussi, P. A.** (1999) Prodomains-adaptors-oligomerisation : the pursuit of caspase activation in apoptosis, TIBS, **24**, 1-4.

Staal, F. J. T., Anderson, M. T., Staal, G. E. J., Herzenberg, L. A., Gitler, C. and Herzenberg, L. A. (1993) Redox regulation of signal transduction : tyrosine phosphorylation and calcium influx, Proc. Natl. Acad. Sci. USA, **91**, 3619-3622.

Steller, H. (1995) Mechanisms and genes of cellular suicide, Science, **267**, 1445-1449.

Stennicke, H. R. and Salvesen, G. S. (1997) Biochemical characteristics of caspases-3, -6, -7 and –8, J. Biol. Chem. **272**, 25719-25723.

Sun, J. S., Tsuang, Y. H., Huang, W. C., Chen, L. T., Hang, Y. S. and Lu, F. J. (1997) Menadione-induced cytotoxicity to rat osteoblasts, Cell Mol. Life Sci. **53**, 967-976.

Susin, S. A., Zamzami, N., Castedo, M., Daugas, E., Wang, H. G., Geley, S., Fassy, F., Reed, J. C. and Kroemer, G. (1997) The central executioner of apoptosis : multiple connections between protease activation and mitochondria in Fas/APO-1?CD-95- and ceramide-induced apoptosis, J. Exp. Med. **186**, 25-37.

Sympson, T. J., Talhouk, R. S., Alexander, C. M., Chin, J. R., Clift, S. M., Bissell, M. J. and Werb, Z. (1994) Targeted expression of stromelysin-1 in mammary gland provides evidence for a role of proteinases in brancing morphogenesis and the requirement for an intact basement membrane for tissue-specific gene expression, J. Cell Biol. **125**, 681-693.

Szatrowski, T. P. and Nathan, C. F. (1991) Production of large amounts of hydrogen peroxide by human tumour cells, Cancer Res. **51**, 794-798.

Tait, L., Soule, H. D. and Russo, J. (1990) Ultrastructural and immunocytochemical characterisation of an immortalised human breast epithelial cell line, MCF10, Cancer Res., **50**, 6087-6094.

Tan, X. and Wang, J. Y. J. (1998) The caspase-RB connection in cell death, Trends Cell Biol. **8**, 116-120.

Tang, D. G., Li, L., Zhu, Z. and Joshi, B. (1998) Apoptosis in the absence of cytochrome c accumulation in the cytosol, Biochem. Biophys. Res. Comm. **242**, 380-384.

Thompson, C. B. (1995) Apoptosis in the pathogenesis and treatment of disease, Science, **267**, 1456-1462.

Thornberry, N. A. and Lazebnik, Y. (1998) Caspases : enemies within, Science, **281**, 312-316.

Tokayasu, K. T. (1980) Immunocytochemistry on ultrathin frozen sections, Histochem. J. **12**, 281-303.

Towbin, H., Staehlin, T. and Gordon, J. (1979) Electrophoretic transfer of proteins from polyacrylamide gels to nitrocellulose sheets : procedure and some applications, Proc. Natl. Acad. Sci. USA, **76**, 4350-4353.

Tzagaloff, A. (1982) "Mitochondria", Plenum Press, New York, USA. pp 67-75.

Ulukaya, E. and Wood, E. J. (1998) The anti-proliferative and cell death-inducing effect of H_2O_2 on squamous cell carcinoma cells, Biochem. Soc. Trans. **26**, S347.

van de Water, B., Nagelkerke, J. F. and Stevens, J. L. (1999) Dephosphorylation of focal adhesion kinase (FAK) and loss of focal contacts precede caspase-mediated cleavage of FAK during apoptosis in renal epithelial cells, J. Biol. Chem. **274**, 13328-13337.

van Leyen, K., Duvoisin, R. M., Engelhardt, H. and Wiedmann, M. (1998) A function for lipoxygenase in programmed organelle degradation, Nature, **395**, 395-395.

Vander Heiden, M. G., Chandel, N. S., Williamson, E. K., Schumacker, P. T. and Thompson, C. B. (1997) Bcl-X_L regulates the membrane potential and volume homeostasis of mitochondria, Cell, **91**, 627-637.

Vanags, D. M., Porn-Ares, M. A., Coppola, S., Burgess, D. H. and Orrenius, S. (1996) Protease involvement in fodrin cleavage and phophatidylserine exposure in apoptosis, J. Biol. Chem., **271**, 31075-31085.

Vaux, D. L., Wilhelm, S. and Hacker, G. (1997) Requirements for proteolysis during apoptosis, Mol. Cell Biol. **17**, 6502-6507.

Villa, P. G., Henzel, W. J., Sensenbrenner, M., Henderson, C. E. and Pettmann, B. (1998) Calpain inhibitors, but not caspase inhibitors, prevent actin proteolysis and DNA fragmentation during apoptosis, J. Cell Sci. **111**, 713-722.

von Ahsen, O., Renken, C., Perkins, G., Kluck, R. M., Bossy-Wetzel, E. and Newmeyer, D. D. (2000) Preservation of mitochondrial structure and function after Bid- or Bax-mediated cytochrome c release, J. Cell Biol. **150**, 1027-1036.

Walker, P. R. and Sikorska, M. (1994) Endonuclease activities, chromatin structure and DNA degradation in apoptosis, Biochem. Cell Biol. **72**, 615-623.

Walker, P. R. and Sikorska, M. (1997) New aspects of the mechanism of DNA fragmentation in apoptosis, Biochem. Cell Biol. **75**, 287-299.

Wallace, S. S. (1997) Recognition and processing of oxidative DNA lesions, Biochem. Cell Biol. 75, 477.

Wallace-Brodeur, R. R and Lowe, S. W. (1999) Clinical implications of *p53* mutations, Cell Mol. Life Sci. **54**, 64-75.

Weaver, V. M., Lach, B., Walker, P. R. and Sikorska, M. (1993) Role of proteolysis in apoptosis : involvement of serine proteases in internucleosomal DNA fragmentation in immature thymocytes, Biochem. Cell Biol. **71**, 488.

Weil, M., Jacobson, M. D. and Raff, M. C. (1998) Are caspases involved in the death of cells with a transcriptionally inactive nucleus? Sperm and chicken erythrocytes, J. Cell Sci. **111**, 2707-2715.

Weinhouse, S. (1972) Glycolysis, respiration, and anomalous gene expression in experimental hepatomas: G. H. A. Clowes Memorial Lecture, Can. Res. **32**, 2007-2016.

Welsh, J. (1994) Induction of apoptosis in breast cancer cells in response to vitamin D and anti-oestrogens, Biochem. Cell Biol. **72**, 537-545.

Wertz, I. E. and Hanley, M. R. (1996) Diverse molecular provocation of programmed cell death, TIBS, **21**, 359-364.

Williams, G. T., Smith, C. A., McCarthy, M. J. and Grimes, E. A. (1992) Apoptosis : final control point in cell biology, Trends Cell Biol. **2**, 263-266.

Wilson, M. R. (1998) Apoptotic signal transduction : emerging pathways, Biochem. Cell Biol. **76**, 573-582.

Wolter, K. G., Hsu, Y. T., Smith, C. L., Nechushtan, A., Xi, X. G. and Youle, R. J. (1997) Movement of Bax from the cytosol to the mitochondria during apoptosis, J. Cell Biol. **139**, 1281-1292.

Wu, X. and Levine, A. J. (1994) p53 and E2F-1 cooperate to mediate apoptosis, Proc. Natl. Acad. Sci. USA, **91**, 3602-3606.

Yakes, F. M. and van Houten, B. (1997) Mitochondrial DNA damage is more extensive and persists longer than nuclear DNA damage in human cells following oxidative stress, Proc. Natl. Acad. Sci. USA, **94**, 514-519.

Yang, E. and Korsmeyer, S. J. (1996) Molecular thanatopsis : a discourse on the Bcl-2 family and cell death, Blood, **88**, 386-401.

Yang, J., Liu, X., Bhalla, K., Kim, C. N., Ibrado, A. M., Cai, J., Pend, T. I., Jones, D. P. and Wang, X. (1997) Prevention of apoptosis by Bcl-2 : release of cytochrome c from mitochondria blocked, Science, **275**, 1129-1132.

Young, S. D. and Hill, R. P. (1990) Effects of reoxygenation on cells from hypoxic regions of solid tumours : analysis of transplanted murine tumours for evidence of DNA overreplication, Can. Res. **50**, 5031-5038.

Zamzami, N., Susin, S. A., Marchetti, P., Hirsch, T., Gomez-Monterrey, I., Castedo, M. and Kroemer, G. (1996) Mitochondrial control of nuclear apoptosis, J. Exp. Med. **183**, 1533-1544.

Zhivotovsky, D., Wade, D., Nicotera, P. and Orrenius, S. (1994) Role of nucleases in apoptosis, Int. Arch. Allergy Immunol. **105**, 333-338.

Zhu, N. and Wang, Z. (1997) An assay for DNA fragmentation in apoptosis without phenol/chloroform extraction and ethanol precipitation, Anal. Biochem. **246**, 155-158.

Zou, H., Henzel, W. J., Liu, X. S., Lutschg, A. and Wang, X. D. (1997) Apaf-1, a human protein homologous to c-elegans ced-4, participates in cytochrome c-dependent activation of caspase-3, Cell, **90**, 405-413.